



HELLENIC
MEDITERRANEAN
UNIVERSITY



universit 
BORDEAUX



UNIVERSITY
of York



Queen's University
Belfast



Erasmus+

The European Commission support for the production of this publication does not constitute an endorsement of the contents which reflects the views only of the authors, and the Commission cannot be held responsible for any use which may be made of the information contained therein.

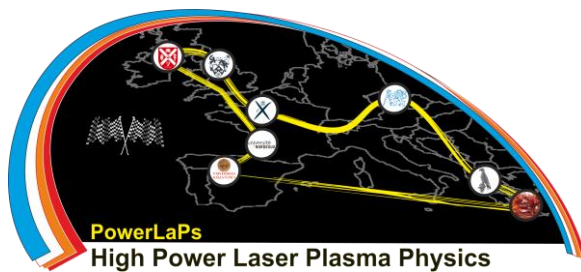
Co-funded by the
Erasmus+ Programme
of the European Union



PowerLaPs

Innovative Education & Training in High Power Laser Plasmas

Plasma Physics - Theory and Experiments



Erasmus+

Output Identification: O1

Output Title: Plasma Physics - Theory and Experiments



O1 - Plasma physics

O1 - Theory

1. What is a plasma?.....6-22

D. Batani, E. d'Humières, J.J. Santos, V.T. Tikhonchuk

- 1.1 Plasma: the fourth state of matter
- 1.2 Natural plasmas and laboratory plasmas
- 1.3 Collective phenomena in plasmas
- 1.4 Characteristic quantities of plasmas
- 1.5 Debye's length
- 1.6 Collisions of particles. Mean free path and collisional frequency
- 1.7 Plasma oscillations. Electronic plasma frequency
- 1.8 Velocity distribution function
- 1.9 Mean macroscopic quantities
- 1.10 Problems

2. Movement of particles in magnetic and electric fields.....23-39

D. Batani, E. d'Humières, J.J. Santos, V.T. Tikhonchuk

- 2.1 Uniform and continuous magnetic field
- 2.2 Movement in uniform magnetic and electric fields
- 2.3 Alternating and non-uniform electric field
- 2.4 Non-uniform magnetic field
- 2.5 Problems

3. Coulombian collisions.....40-46

D. Batani, E. d'Humières, J.J. Santos, V.T. Tikhonchuk

- 3.1 Collisions between charged particles
- 3.2 Elastic collisional cross section
- 3.3 Momentum transfer cross section
- 3.4 Mean free path and collisional frequency
- 3.5 Problems

4. Hydrodynamic description of a plasma.....47-55

D. Batani, E. d'Humières, J.J. Santos, V.T. Tikhonchuk

- 4.1 Equations
- 4.2 Electromagnetic properties of plasma
- 4.3 Linear theory
- 4.4 Problems

5. Waves in non-magnetised plasmas.....56-64

D. Batani, E. d'Humières, J.J. Santos, V.T. Tikhonchuk

- 5.1 Propagation of an electromagnetic wave in a plasma
- 5.2 Electrostatic plasma waves in hot plasma
- 5.3 Problems



6. Electromagnetic waves into magnetised plasmas.....65-83

M. Tatarakis

- 6.1 Magnetised plasma
- 6.2 Isotropic plasma
- 6.3 Propagation normal to the magnetic field
- 6.4 Parallel propagation
- 6.5 Faraday rotation
- 6.6 Rotation for propagation at a general angle θ
- 6.7 Nonuniform media and the WKB approximation

7. Kinetic description of a plasma.....84-91

D. Batani, E. d'Humières, J.J. Santos, V.T. Tikhonchuk

- 7.1 Distribution function of particles
- 7.2 Klimontovich equation
- 7.3 Vlasov kinetic equation
- 7.4 Collision integral
- 7.5 Macroscopic field, Maxwell's equations
- 7.6 Macroscopic quantities in a plasma
- 7.7 Problems

8. Equilibrium solutions to the Vlasov kinetic equation.....92-99

D. Batani, E. d'Humières, J.J. Santos, V.T. Tikhonchuk

- 8.1 Equilibrium of a homogeneous plasma
- 8.2 Plasma in an external electric potential
- 8.3 Plasma in a capacitor
- 8.4 Plasma in an external magnetic field
- 8.5 Problems

9. Electromagnetic properties of an isotropic plasma.....100-118

D. Batani, E. d'Humières, J.J. Santos, V.T. Tikhonchuk

- 9.1 Dispersion equation of electromagnetic waves
- 9.2 General properties of the dielectric permittivity
- 9.3 General solution of the dispersion equation
- 9.4 Linearized Vlasov equation
- 9.5 Kinetics of electromagnetic waves
- 9.6 Langmuir waves
- 9.7 Ion acoustic waves
- 9.8 Imaginary part of the dielectric permittivity
- 9.9 Landau damping of plasma waves
- 9.10 Qualitative interpretation of Landau damping
- 9.11 Problems

10. Instabilities of a non-equilibrium plasma.....119-128

D. Batani, E. d'Humières, J.J. Santos, V.T. Tikhonchuk

- 10.1 Radiative losses of a charged particle in plasma
- 10.2 Instability of an electron beam in plasma



- 10.3 Instability of a mono-energetic beam
- 10.4 Nonlinear saturation of instabilities
- 10.5 Problems

11. Plasmas and Radiation.....129-169

D. Batani

- 11.1 Radiative properties of plasmas
- 11.2 Laser-Plasma profile in the ns regime
- 11.3 Equilibrium (and types of equilibrium) in a plasma
- 11.4 Equation of radiation transfer
- 11.5 Radiation emission from plasmas
- 11.6 Radiative hydrodynamics

O1 - Experiments

1. EXP 1. FLYCHK code.....171-176

D. Batani, J. Trela

- 1. The FLYCHK code
- 2. FLYCHK exercises

2. EXP 2. Plasma focus.....177-198

A. Skoulakis, G. Andrianaki, G. Tazes

- 1. Laboratory project aim
- 2. Theoretical background
- 3. Operation Principle
- 4. The miniature plasma focus device
- 5. Experimental procedure
- 6. Experimental results analysis

3. EXP 3. Plasma pinch.....199-228

A. Skoulakis, G. Andrianaki, G. Tazes

- 1. Laboratory project aim
- 2. Theoretical background
- 3. X-pinch system (apparatus & diagnostics)
- 4. Experimental procedure
- 5. Experimental results analysis

O1 – Annex

Supplementary educational material.....229

- **O1-A1-Plasma Physics** (*M. Tatarakis*)



HELLENIC
MEDITERRANEAN
UNIVERSITY



UNIVERSITÉ
BORDEAUX



Erasmus+

O1 – Theory



HELLENIC
MEDITERRANEAN
UNIVERSITY



université
BORDEAUX



Erasmus+

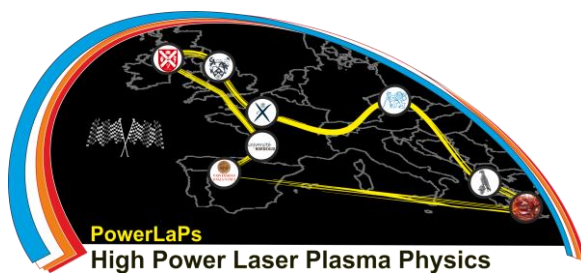
PowerLaPs

Innovative Education & Training in High Power Laser Plasmas

Plasma Physics - Theory and Experiments

Chapter 1: What is Plasma?

D. Batani, E. d'Humières, J.J. Santos, V.T. Tikhonchuk



université
de BORDEAUX



1 What is a plasma?

The term plasma was introduced for the first time in 1922 by the American physicist Irvin Langmuir, who was studying electrical discharges in weakly ionised gases. The word “plasma” has a Greek etymological root which literally means “something that has no use”. Irvin Langmuir and his compatriot Lewis Tonks gave this name to a gas containing charged particles, whose movement is governed by electromagnetic forces. These two researchers were the first to discover the collective electronic oscillations in a plasma. Langmuir waves or electronic plasma waves constitute the fundamental (eigen) modes of a plasma.

The specificity of a plasma resides in its *self-consistent* behaviour: the charged particles themselves create the fields and are therefore subjected to the action of these fields in return. This causes the particles to move collectively, sometimes in the form of waves. This coherent movement of the particles, which recurs periodically in space and time, is what causes the natural oscillations of plasma.

In this course, we will be studying the basic physical models and the numerical modelling methods that can be employed to account for the collective behaviour of plasmas. In general, all plasma models feature two combined systems: the first consists of particle movement equations and the second describes the changes in the electrical and magnetic fields. The connection between the movement of the electrical charges and the generation of electromagnetic and electrostatic fields is a source of both richness and complexity in the description of plasmas and in their modelling.

1.1 Plasma: the fourth state of matter

When the temperature is increased, matter first changes from a solid state to a liquid state by melting, and then to a gaseous state by vaporisation. The molecules, subjected to repeated collisions, are split into atoms at between 5,000 and 10,000 K. At temperatures exceeding 10,000 K the atoms themselves are split into electrons and positive ions. In this way, plasma constitutes a fourth state of matter. The phenomenon of *thermal ionisation* of a gas is a consequence of impacts (collisions) between particles. It becomes more pronounced as the temperature of the gas rises.

Conversely, when the temperature falls, the free electrons are recombined with the ions to recreate atoms. This recombination may be *radiative*, if it is accompanied by the emission of radiation, or a *three-body* recombination if a third particle participates in this process. Optical, ultra-violet and X radiations also contribute to the ionisation of gases by the process of *photoionisation* or *multiphoton ionisation*.

The ionised gases can be roughly divided into three major families:

- *Weakly ionised* gases: a few electrons move around in an ocean of neutral molecules or atoms. The binary collisions between an electron or an ion and an atom determine the dynamics of the charged particles (electric arcs, discharge tubes, the ionosphere, intergalactic molecular clouds).
- *Highly ionised and weakly collisional* gases: including dilute plasmas and hot plasmas whose particle trajectories are mainly determined by electrical fields or external magnetic fields (stars, fusion plasmas).
- *Highly ionised and highly collisional* gases: which include dense plasmas and cold plasmas in which the collisions determine the behaviour of the plasma (centres of stars, metals and semi-conductors).

1.2 Natural plasmas and laboratory plasmas

Plasmas are found everywhere: over 99.9% of the universe is composed of matter in the plasma state. Consequently, plasmas make up most of the matter of the sun, the stars, interstellar and intergalactic space, white dwarfs, etc.

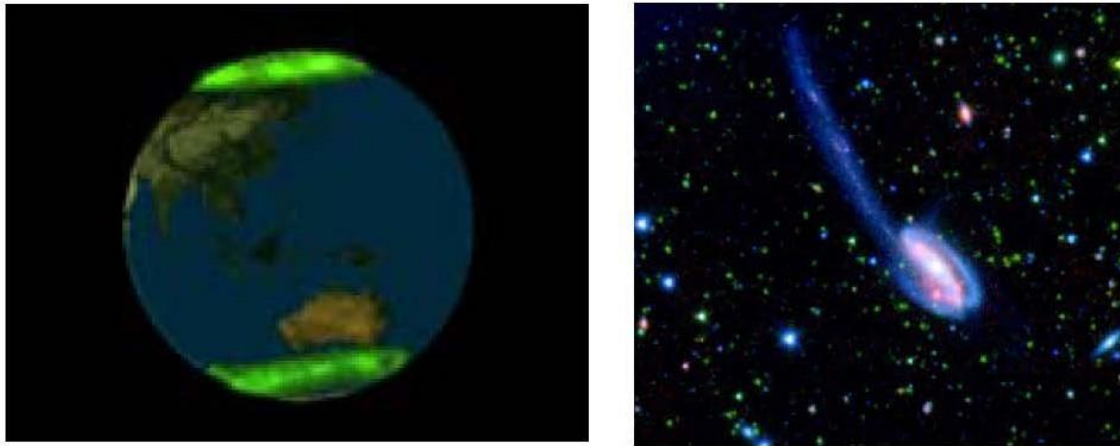


Figure 1: On the left: satellite photograph of the aurorae boreales appearing around both magnetic poles of the Earth. On the right: photograph of the Tadpole galaxy: light emissions produced by excited ions and molecules. Photography by NASA.

The aurorae boreales, which can be observed around the Earth's magnetic poles, are a spectacular manifestation of the existence of electrons and protons, emitted by the sun (the solar wind) and trapped within the Van Allen belts of the magnetosphere. As they pass through the atmosphere, the energetic electrons excite the atoms which, as they are de-excited, emit the light observed during the course of an aurora borealis. Since the electrons are trapped in the Earth's magnetic field lines, the aurorae appear simultaneously at the two magnetic poles (see figure 1-a).

The galaxies are made up of stars and inter-stellar gases. Their electromagnetic emissions enable us to observe them. In particular, the emissions in the optical and infra-red fields are caused by excited ions and molecules in the gases (see figure 1-b). The ionosphere consists of a layer of ionised gas situated at an altitude of around 120 to 400 km above the Earth. Because of its ability to reflect certain electromagnetic waves, the ionosphere plays a key role in shortwave telecommunications around the Earth. Knowledge of the ionosphere's properties is very important for satellite communications and for the navigation systems of ships, aircraft and motor vehicles.

Plasmas are frequently encountered in our daily lives: a candle flame is a very weakly ionised plasma, light sources contain weakly ionised plasma discharges of rare gases; Ne, Kr or Xe. The same discharges are found in plasma screens, but at very low levels. Plasmas are produced in metal-welding and cutting processes that use electric arcs. Many laser processes use or produce plasmas.

Plasmas play an important role in research on energy production issues. The fusion of light nuclei of deuterium and tritium represents an inexhaustible source of energy that could satisfy all of humanity's needs for several millennia. The synthesis of light nuclei is the biggest source of energy in the universe. All stars burn light elements for billions of years, but these nuclear fusion reactions are only efficient at very high temperatures exceeding one hundred million degrees Kelvin.

Laboratory research on thermonuclear fusion began around fifty years ago. The main problem

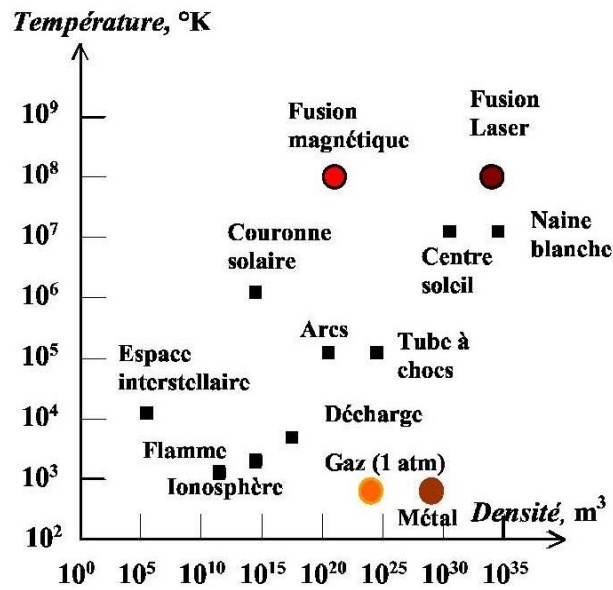


Figure 2: Characteristic parameters of plasmas in nature and in the laboratory.

is to heat the plasma up to these very high temperatures and to maintain (confine) it for the time required for combustion. Two approaches are currently being studied: magnetic confinement fusion (MCF) in which plasma is confined in a magnetic field, and inertial confinement fusion (ICF). In the first case, a low-density plasma at approximately $10^{20} m^{-3}$ is confined in a high magnetic field of approximately 5–10 T. This is carried out in *tokamak* or *stellarator* types of machines. Figure 3-a shows a photograph of the biggest tokamak device in existence: the Joint European Torus (JET). The characteristic dimension of its chamber is approximately 5 m. The new ITER (International Thermonuclear Experimental Reactor) machine designed for the demonstration of thermonuclear energy production is currently being built in France, on the Cadarache site near Aix en Provence.



Figure 3: On the left: photograph of the interior of the JET tokamak chamber. On the right: photograph of the laser-irradiated target for inertial confinement fusion.

Inertial confinement fusion is carried out by the compression and heating of small capsules of a mixture of deuterium and tritium by the radiation from intense lasers. The target, of millimetric size, (see figure 3-b) is compressed to $100 \mu m$ and the fusion reaction is produced for a fraction

of a nanosecond. Very high-energy lasers are required to produce these conditions. They must be capable of attaining and exceeding 1 MJ and very high power levels of above 10 TW. Two laser chains on this scale are currently under construction. An NIF (National Ignition Facility) laser has been built at the Livermore laboratory in California in the United States. The other laser, the LMJ (Laser MégaJoule), is under construction at CEA/CESTA in Le Barp near Bordeaux.

The density of electrons, n_e , and ions, n_i , within a plasma may vary significantly. From the level of around 1 particle per m^3 in the interstellar environment, it can exceed 10^{12} particles per m^3 in the Earth's ionosphere, and while there are 10^{14} particles per m^3 in the solar corona and 10^{20} particles per m^3 in a magnetic fusion plasma, there are around 10^{32} particles per m^3 at the centre of the sun or in an inertial confinement fusion plasma. Nevertheless, all of these systems can be considered in the same manner if the characteristic spatial scale of the process that interests us, L , far exceeds the mean distance between the particles, $n^{-1/3}$.

In comparison, a high vacuum contains approximately 10 particles per m^3 , whereas a gas at atmospheric pressure under normal temperature conditions has 3×10^{25} per m^3 . The electron density in a metal is around 10^{29} particles per m^3 .

As is the case for density, the plasma state covers a vast range of temperatures. In *cold plasmas* (flash tubes, electric arcs, plasma torches, etc.), the temperature T barely exceeds 10,000 K. In these cases, the mean thermal agitation energy, $k_B T$, is insufficient to ensure complete ionisation, and these plasmas are often weakly ionised. In *hot plasmas* produced in thermonuclear fusion by magnetic confinement or inertial confinement, the temperature approaches 100 million degrees Kelvin. In comparison, the temperature at the centre of the sun is approximately 10 million degrees Kelvin. The plasmas exhibit a collective behaviour if the mean thermal agitation energy exceeds the mean interaction energy between the particles, $e^2 n^{1/3} / 4\pi\epsilon_0$. Here, $k_B = 1.38 \times 10^{-23}$ J/K is the Boltzmann constant, $e = 1.6 \times 10^{-19}$ C is the elementary charge and $\epsilon_0 = (1/36\pi) \times 10^{-9}$ F/m is the dielectric constant.

The conditions

$$\ln^{1/3} \gg 1 \quad \text{and} \quad g_p = e^2 n^{1/3} / 4\pi\epsilon_0 k_B T \ll 1 \quad (1.1)$$

define the range of parameters in which the matter is in a plasma state. The quantity g_p is what is referred to as the plasma parameter. Figure 2, shows several examples of natural and artificial plasmas in a density and temperature diagram (n, T).

A weakly ionised plasma consists of a *mixture of electrons and ions* in equilibrium with neutral molecules and atoms. A totally ionised plasma consists primarily of electrons and ions. The *degree of ionisation* of an ionised gas is the ratio of the density of ionised atoms to the total density of atoms (ionised and neutral). Depending on the creation process, the degree of ionisation of a plasma can vary between 10^{-10} (weakly ionized plasma) and 1 (totally ionized plasma).

Several different species of ions may exist within a single type of plasma, and there may be several different ionisation states for a single species. For example:

- a plasma created by laser breakdown in a gas like helium may contain He^+ ions and He^{++} ions, as well as helium atoms in the fundamental state or in excited states;
- a solid material, such as polyethylene $(\text{CH})_n$, that is irradiated by laser will produce a plasma consisting of hydrogen H^+ ions, and carbon C^+ , C^{2+} , C^{3+} , \dots , C^{6+} ions, in addition to H and C atoms.

1.3 Collective phenomena in plasmas

In a gas in which the particles are not charged, the forces acting between the particles are forces that have a very small radius of action of a quantum nature. However, in a plasma, the interaction

forces between charged particles are *Coulomb electric forces* with a large radius of action. The Coulomb potential created by a charge q at the distance r , in a vacuum is expressed by:

$$\Phi(r) = \frac{q}{4\pi\epsilon_0 r}. \quad (1.2)$$

Any charged particle in a plasma interacts in this way, via the attractive and repulsive Coulomb forces, with a large number of other charged particles.

In this way, any excess charge at the local level, resulting from the disorderly thermal movement of the electrons or a separation of charges, immediately becomes a source of intense magnetic fields and electric currents. These fields act, in turn, on all of the other particles in the plasma. As a result of multiple electrostatic interactions, the trajectory of an electron will be subjected to both small disturbances due to the action of distant charges, and to occasionally strong deviations caused by local collisions with an atom, an ion or an electron.

Therefore, a plasma, because of its sensitivity to any disturbance, can only tolerate small deviations from electrical neutrality. In this way, all of these forces contribute to maintaining, in equilibrium, the *electrical quasi-neutrality of the plasma* which is expressed by the relationship:

$$n_e q_e + \sum_i n_i q_i = 0 \quad (1.3)$$

in which n_e and n_i , $q_e = -e$ and $q_i = Ze$ respectively represent the electronic and ionic densities and the charges of the electrons and ions. The sum concerns all ionic species and, for each species, all states of charge that exist in the plasma. In the case of a mixture of ionic species with different states of charge, the problem is simplified by limiting ourselves to a single ionic species whose mean state of charge $\langle Z \rangle$ and mean mass $\langle m_i \rangle$, depend on the respective concentrations of each species that makes up the mixture. There may therefore be several definitions of $\langle Z \rangle$ and $\langle m_i \rangle$ according to the physical quantity in question.

1.4 Characteristic quantities of plasmas

The mass of a proton is 1,837 times greater than that of an electron. Therefore, due to the high inertia of the ions ($m_e/m_i \ll 1$), we can expect the behaviour of the two components of a plasma to be very different. In a simplified model, the ions can therefore be considered to be almost stationary and to form a neutralising background.

Consequently, in a similar type of approach to that used for studying a gas, the plasma can be considered to consist of two perfect fluids: electrons and ions, which are characterised by macroscopic quantities such as density, mean velocity, temperature and pressure. In a fluid model, therefore, a plasma is characterised by:

- the density $n_{e,i}$, the mean velocity $\vec{v}_{e,i}$ and the temperature $T_{e,i}$ of the electrons (ions);
- the density n_0 , the speed \vec{u}_0 and the temperature T_0 of the neutral particles (for a plasma that is not totally ionised).

Four characteristic lengths can be defined for a plasma, namely:

- the mean distance between particles, $d_{e,i}$;
- Landau's length, or the minimum approach distance between two particles, r_0 ;
- Debye's length or the charge screening length, λ_D ;

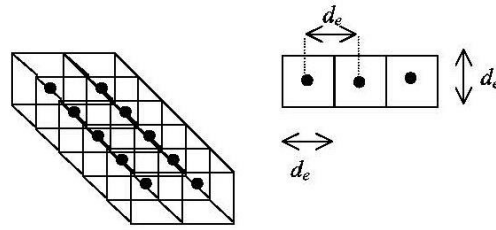


Figure 4: Regular distribution of the particles in space.

- the mean range of a particle between two consecutive collisions, $\lambda_{e,i}$.

In the same way, we define the time scale by introducing the characteristic frequencies for a plasma. These are:

- the electron oscillation frequency or the electronic plasma frequency, ω_{pe} ;
- the ion oscillation frequency or the ionic plasma frequency, ω_{pi} ;
- the rotation frequency of the electrons and ions in the magnetic field, or the Larmor frequencies, $\omega_{ce,i}$;
- the frequency between two consecutive collisions of the particles, $\nu_{e,i}$.

1.4.1 Mean distance between particles. Landau's length

If we presume that the electrons (ions) are evenly distributed throughout the plasma (1 electron per cubic cell, of dimension d_e , see diagram in figure 4), we can define the mean distance between the electrons (ions):

$$d_{e,i} = n_{e,i}^{-1/3}. \quad (1.4)$$

Landau's length r_0 is the minimum approach distance between two electrons. It corresponds to the distance at which the mean kinetic energy of an electron is equal to the potential interaction energy:

$$\frac{1}{2}m_e v_e^2 = k_B T_e = \frac{e^2}{4\pi\epsilon_0 r_0}$$

where v_e is the most probable speed for the electron. Landau's length is therefore expressed as:

$$r_0 = \frac{e^2}{4\pi\epsilon_0 k_B T_e}. \quad (1.5)$$

Comparing these two characteristic lengths enables us to introduce the plasma parameter, $g_p = r_0/d_e$ (1.1) and to distinguish between two types of plasmas:

- standard kinetic plasmas which correspond to the condition $d_e \gg r_0$ (the kinetic energy is much higher than the potential energy)
- strongly correlated plasmas in the case of the inverse condition $d_e \lesssim r_0$ (the potential energy is higher than the kinetic energy).

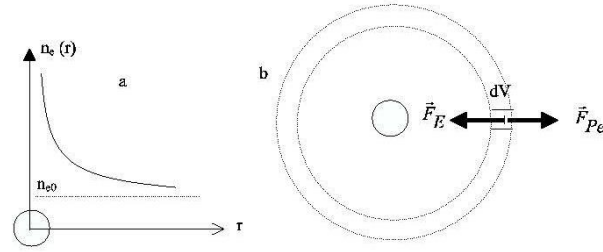


Figure 5: a) Distribution of the electronic density in proximity to an ion. b) The forces that apply to an elementary volume of electrons.

1.5 Debye's length

The Debye-Hückel effect was first observed in electrolytes by the physicists Peter Debye and Erich Hückel in 1923. It corresponds to the charge-screening phenomenon that exists in an ionised environment. To evaluate this effect, let us consider an ion with the charge q_i in the plasma. The ion, by attracting the electrons, contributes to modifying the distribution of the electronic density n_e in close proximity to it, around the equilibrium density n_{e0} within the plasma (see figure 5-a), and consequently, the effective potential of the ion $\Phi(r)$ compared to the potential the ion would have had if it were isolated.

1.5.1 Distribution of the electronic density

We are considering a plasma that is uniform in temperature, $T_e = \text{cste}$. However, the electron density is not constant, because they are attracted by the ion due to the Coulomb force. The element with a unit volume dV (see figure 5b) is subjected to the electrical attractive force

$$\vec{F}_E = n_e q_e \vec{E} = -n_e q_e \vec{\nabla} \Phi(r)$$

and to the pressure force that results from the electronic density gradient in proximity to the ion

$$\vec{F}_{Pe} = -\vec{\nabla} n_e k_B T_e = -k_B T_e \vec{\nabla} n_e.$$

These two forces oppose each other and in equilibrium, we have:

$$-n_e q_e \vec{\nabla} \Phi(r) - k_B T_e \vec{\nabla} n_e = 0.$$

Because of the spherical symmetry of the problem (radial forces), this gives us:

$$\frac{1}{n_e} \frac{dn_e}{dr} = -\frac{q_e}{k_B T_e} \frac{d\Phi}{dr}.$$

After integration, and based on the fact that at a large distance from the ion, the electronic density tends toward equilibrium density n_{e0} , *Boltzmann's Law* can be inferred:

$$n_e(r) = n_{e0} \exp\left(-\frac{q_e \Phi(r)}{k_B T_e}\right). \quad (1.6)$$

When the terms in the exponential function before the 1 are small, i.e. when there is a high level of kinetic energy in relation to the potential energy (standard kinetic plasma) $k_B T_e \gg e\Phi$, we can expand the Taylor series equation (1.6):

$$n_e(r) = n_{e0} \left(1 - \frac{q_e \Phi(r)}{k_B T_e}\right). \quad (1.7)$$

1.5.2 Distribution of potential

From the preceding results, we can derive the form of the potential Φ by using Poisson's equation:

$$\vec{\nabla} \cdot \vec{E} = \rho/\epsilon_0 = -\Delta\Phi(r)$$

or:

$$-\epsilon_0\nabla^2\Phi(r) = n_e q_e + n_{i0} q_i = (n_e - n_{e0})q_e + (n_{e0}q_e + n_{i0}q_i). \quad (1.8)$$

with the condition of quasi-neutrality and the formula (1.7), this ultimately gives us:

$$\Delta\Phi(r) = \frac{n_{e0}q_e^2}{\epsilon_0 k_B T_e} \Phi(r) = \frac{\Phi(r)}{\lambda_{De}^2}. \quad (1.9)$$

Here λ_{De} represents the Debye electron length, expressed by:

$$\lambda_{De} = \sqrt{\epsilon_0 k_B T_e / n_e e^2}. \quad (1.10)$$

In spherical coordinates, the Laplacian is expressed as: $\Delta = r^{-2}(\partial/\partial r)(r^2\partial/\partial r)$. Integration (1.9) leads to the following expression of the Debye potential of a charge q :

$$\Phi(r) = \frac{q}{4\pi\epsilon_0 r} \exp\left(-\frac{r}{\lambda_{De}}\right).$$

The Coulomb potential (potential of an isolated charge) is therefore replaced in a plasma by the Debye potential $\Phi(r)$, and the length λ_{De} represents the characteristic scale of the decrease in potential, associated with the screening effect. In the most general case, all of the particles participate in the screening phenomenon. These contributions are added together in the right-hand part of the equation (1.9). Consequently, the Debye radius in an electron-ion plasma is expressed as:

$$\frac{1}{\lambda_D^2} = \frac{1}{\lambda_{De}^2} + \frac{1}{\lambda_{Di}^2} = \frac{n_{e0}q_e^2}{\epsilon_0 k_B T_e} + \frac{n_{i0}q_i^2}{\epsilon_0 k_B T_i}. \quad (1.11)$$

In ionospheric plasmas, the Debye length is a few millimetres whereas it measures a few tens of microns in fusion plasmas. On scales above these values, the plasma tends to maintain its neutrality with regard to any local disruption.

There is a simple explanation for the fact that the Debye length is dependent on the temperature. In fact, this screening effect is carried out *dynamically*. The trajectories of the electrons, when they pass close to an ion, are slightly deviated and therefore tend to move slightly closer together, whereas the ions move away from each another.

If the temperature is very high, the excited high-speed particles undergo smaller deflections and the screening effect is therefore less effective (greater Debye length), whereas a higher particle density will strengthen the screening effect (smaller Debye length).

1.5.3 Number of electrons in the Debye sphere

The sphere with a radius λ_{De} around an ion is called the Debye sphere. The Debye sheath notion is only valid if there is a large number of electrons in the charge cloud, which ensures the validity of the Boltzmann distribution. In practice, this means that there is a large number of electrons N_{De} in the Debye sphere. The number of electrons in the Debye sphere is expressed by:

$$N_{De} = \frac{4}{3}\pi n_e \lambda_{De}^3 \quad (1.12)$$

for $N_{De} \gg 1$, the screening is strong and the individual effects are dominant. The electrons behave in almost the same way as a gas in relation to the ions. Conversely, for $N_{De} \ll 1$, the screening is weak and the collective effects are dominant. The plasma is said to be strongly correlated. Ultimately, the plasma is degenerated.

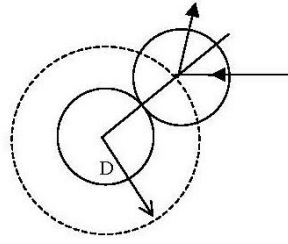


Figure 6: Diagram of a collision between two molecules.

1.6 Collisions of particles. Mean free path and collisional frequency

A molecule in a neutral gas follows a rectilinear trajectory between two collisions, whose length is called the *free path*. The free path can have any value. We will subsequently focus on the mean value of the free path, which is referred to as the *mean free path*. Insofar as there is no distant interaction, which is not the case for plasmas, the mean free path and the frequency of molecular collisions can easily be estimated using a simple method.

Let us liken the molecules to hard, impenetrable spheres (billiard balls) and let D be the distance between the centres of two molecules when they come into contact (see figure 6). The sphere shown by a dotted line represents the Debye sphere of a molecule. When a collision takes place, the centre of one molecule is situated on the Debye screening sphere of another molecule. Between two collisions, one molecule moves in a straight line, while the others remain stationary. Let us consider that the movement of this molecule corresponds to the length L . It will have come into contact with all of the molecules contained in the volume $\pi D^2 L$. For a molecular density equal to n , it will have undergone $N_c = n \pi D^2 L$ collisions. The mean distance between two collisions is called the *mean free path*, which is expressed by: $\lambda_c = L/N_c = 1/n\pi D^2$. In reality, the movement of the other molecules must be taken into account, which gives us:

$$\lambda_c = \frac{1}{\sqrt{2}n\pi D^2}. \quad (1.13)$$

The number of impacts per second is the *collision frequency*, ν_c , which is the quotient of the mean velocity \bar{v} by the mean free path λ_c :

$$\nu_c = n \pi D^2 \bar{v}. \quad (1.14)$$

The preceding description actually applies to a binary collision between two molecules. In a plasma, the electron-ion collisions prove to be a more complex phenomenon due to the long range of the shielded Coulomb potential of the ion, whose characteristic length is equal to the Debye length. To estimate the mean free path in a plasma, we can use the formulae (1.13) and (1.14) in which the diameter of the molecule must be replaced by the Landau length (1.5). In addition, we must take account of nearby interactions at distances below r_0 , as well as collisions at long distances, approaching the Debye length. These distant collisions lead to the additional logarithmic factor, $\ln \Lambda = \ln(\lambda_D/r_0) \simeq \ln N_{De}$. This factor is called the *Coulombian logarithm*.

More detailed calculations give the following formula for the frequency of electron-ion collisions:

$$\nu_{ei} = \frac{Z^2 e^4 n_i \ln \Lambda}{3 \epsilon_0^2 m_e^{1/2} (2\pi k_B T_e)^{3/2}}. \quad (1.15)$$

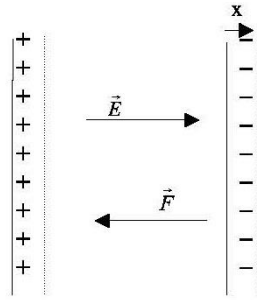


Figure 7: Separation of charges in a plasma oscillation.

The mean free path of an electron is $\lambda_{ei} = v_{Te}/\nu_{ei}$, where $\sqrt{k_B T_e/m_e} = v_{Te}$ is the thermal electron speed. A plasma is considered to be highly collisional if the mean free path is much smaller than the characteristic length of the problem, $\lambda_{ei} \ll L$. However, a plasma will be in a weakly collisional state, or in the Knudsen mode, if there is a long mean free path $\lambda_{ei} \gg L$. In ideal plasmas, the mean free path is very long compared to the Debye length. Consequently, the collisional effects are of the second order and in the following chapters, we will be focusing exclusively on non-collisional plasmas.

1.7 Plasma oscillations. Electronic plasma frequency

Let us consider a section of plasma of length L , consisting of stationary ions and electrons. Plasma is neutral: the electron density n_e is equal to the density of the ions. Imagine that the electrons are pulled toward the right-hand side for a distance of x . In the left-hand part, there is a surplus of ions and in the right-hand part a surplus of electrons. The system is therefore equivalent to a charged parallel-plate capacitor. The electric field \vec{E} resulting from the separation of charges is expressed by:

$$E = \sigma_s / \epsilon_0$$

where $\sigma_s = n_e q_e x$ is the surface charge density. The electrons are therefore subjected to a restoring force, $F = q_e E$, and the equation for their movement is expressed as:

$$\frac{dx}{dt} = v_x, \quad m_e \frac{dv_x}{dt} = -\frac{n_e q_e^2 x}{\epsilon_0}.$$

These two equations can be reduced to an oscillator equation: $d^2x/dt^2 = -\omega_{pe}^2 x$. Therefore, the electrons oscillate at a specific angular frequency ω_{pe} given by:

$$\omega_{pe} = \sqrt{n_e e^2 / m_e \epsilon_0}. \quad (1.16)$$

This angular frequency is called the *electronic plasma frequency*, (which is actually an angular frequency). As we shall see, the electronic plasma frequency plays a fundamental role in plasma physics. Its inverse, ω_{pe}^{-1} corresponds to the characteristic response time of the electrons to the external disruption. There is a simple relationship between the three electronic parameters in a Maxwellian plasma: the product of the Debye length (1.10) by the plasma frequency (1.16) corresponds to the electronic thermal velocity:

$$\lambda_{De} \omega_{pe} = \sqrt{k_B T_e / m_e} = v_{Te}.$$

1.8 Velocity distribution function

Here, we will provide a reminder of several aspects of the kinetic theory of gases that are essential to understanding the plasma physics course.

In gases, or in ionised gases in equilibrium, the interaction forces between molecules are extremely weak and only become apparent when two of them collide. The molecules are widely spaced and can move around almost freely. At a given moment, the velocities may be of any possible magnitude and move in direction.

The density of atoms or molecules in a gas, or of the charged particles in a plasma, may vary from 10^{10} to 10^{22} particles per cm^3 . It is easy to convince oneself that it would be completely impossible to calculate the trajectory of each particle. We must therefore adopt a statistical approach to the problem, and for this purpose, we must introduce the particle distribution function.

If we take an elementary volume of the medium in question, and we consider the number dn of particles whose respective velocity components are between \vec{v} and $\vec{v} + d\vec{v}$, i.e. those whose speed components are respectively situated between v_x and $v_x + dv_x$, v_y and $v_y + dv_y$, v_z and $v_z + dv_z$, is given by:

$$dn = f(x, y, z, v_x, v_y, v_z, t) dv_x dv_y dv_z = f d^3v$$

where the function f , called the *velocity distribution function*, represents the number of molecules at each velocity in the elementary volume of the gas. If the medium is not homogeneous and not stationary, the distribution function will also depend on the position (x, y, z) in question, and the time t . This function may also be isotropic or anisotropic in the velocity space. The function will be referred to as *isotropic* if it does not depend on the direction of the velocity vector, in other terms, if it only depends on the velocity modulus. In this case, the velocities of the molecules are randomly oriented in all directions. Otherwise, it will be referred to as *anisotropic*.

For example, a gas jet whose *directed velocity* is oriented in any direction is anisotropic. In a chamber filled with a gas that is static and in equilibrium, the velocity distribution function is isotropic. Statistically, for a given direction, there are as many molecules moving in one direction as there are moving in the opposite direction. In general, a velocity distribution function that is anisotropic will, due to the collisions between molecules or with the walls of a chamber, naturally tend towards a homogeneous, isotropic and stationary distribution function, i.e. towards a *state of equilibrium*. The velocity distribution function in equilibrium is a *Maxwell distribution function*, expressed as:

$$f_M(v) = n \left(\frac{m}{2\pi k_B T} \right)^{3/2} \exp \left(-\frac{mv^2}{2k_B T} \right) \quad (1.17)$$

where n represents the density of the gas (number of molecules or atoms per elementary volume), m – the mass of the molecules (atoms) and k_B is Boltzmann's constant. The $m/2\pi k_B T$ coefficient is chosen in such a manner that the distribution function is *normalised* by the particle density: $n = \int f(v) d^3v$.

As the Maxwellian distribution is isotropic (it does not depend on v_x , v_y , or v_z but only on $v = \sqrt{v_x^2 + v_y^2 + v_z^2}$ this gives us:

$$dn = n \left(\frac{m}{2\pi k_B T} \right)^{3/2} \exp \left(-\frac{mv^2}{2k_B T} \right) d^3v = n \left(\frac{m}{2\pi k_B T} \right)^{3/2} \exp \left(-\frac{mv^2}{2k_B T} \right) 4\pi v^2 dv = f_1(v) dv$$

where $f_1(v) = 4\pi v^2 f_M(v)$ represents the *velocity modulus distribution function* in three-dimensional space. The shape of the function $f_1(v)$ is shown in figure 8. It reaches a peak at the speed $v_0 = \sqrt{2k_B T/m}$. We refer to this as the *most probable speed*.

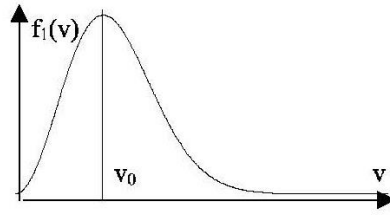


Figure 8: Velocity (modulus) distribution function $f_1(v)$, for a gas in equilibrium.

1.9 Mean macroscopic quantities

1.9.1 Density and mean velocities

Knowing the particle distribution function, we can then, for any *microscopic* $A(\vec{v})$ quantity (scalar, vectorial or tensorial), define a mean (*macroscopic*) value:

$$\langle A(\vec{r}, t) \rangle = \frac{1}{n} \int A(\vec{v}) f(\vec{r}, \vec{v}, t) d^3v. \quad (1.18)$$

For example, the mean velocity \vec{u} is in this way defined by

$$\vec{u}(\vec{r}, t) = \langle \vec{v} \rangle = \frac{1}{n} \int \vec{v} f(\vec{r}, \vec{v}, t) d^3v.$$

By replacing f with a Maxwell function, we obtain: $\langle \vec{v} \rangle = 0$. This is understandable insofar as this distribution function is isotropic. The mean velocity modulus can also be determined:

$$v_m = \langle v \rangle = \frac{1}{n} \int v f_1(v) dv = \sqrt{\frac{8k_B T}{\pi m}}.$$

At the moment a collision occurs, the velocity of a molecule varies in magnitude and direction. To avoid the difficulty of changes in direction, we will focus mainly on either the mean velocity modulus, or the mean kinetic energy:

$$\varepsilon_m = \frac{1}{2} m \langle v^2 \rangle = \frac{m}{2n} \int v^2 f_1(v) dv = \frac{3}{2} k_B T. \quad (1.19)$$

On the basis of this formula, we can define the thermal velocity:

$$v_T = \sqrt{k_B T / m}. \quad (1.20)$$

The mean kinetic energy in one direction, $\varepsilon_{mx} = \frac{1}{2} m \langle v_x^2 \rangle$, is therefore expressed as: $\varepsilon_{mx} = \frac{1}{2} k_B T$. It can be concluded that the mean kinetic energy relating to the direction x is proportional to the temperature. Analogous relationships can also be expressed with the components according to axes y and z . More generally, a degree of freedom is the name given to a parameter that can be used to determine the system, and the kinetic energy associated with any degree of freedom i is given by

$$\varepsilon_{mi} = \frac{1}{2} k_B T.$$

This term constitutes the *equipartition of energy* principle.

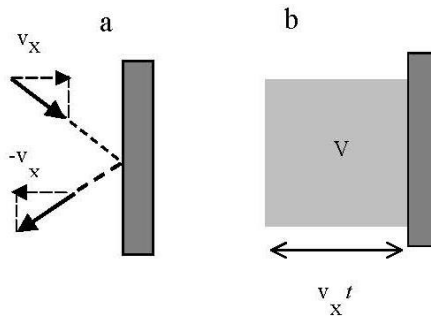


Figure 9: Diagram showing the collision of a molecule with a wall.

Monoatomic gas. For a monoatomic molecule, there are 3 degrees of freedom for translational motion. The mean kinetic energy ε_m of the molecule is given by:

$$\varepsilon_m = \sum_{i=x,y,z} \frac{1}{2} m \langle v_i^2 \rangle = \frac{3}{2} k_B T.$$

Diatomic gas. A molecule of a diatomic gas has a fixed position in space, and we know the position of its centre of gravity and the direction of its axis. A molecule like oxygen, which has a stretched form (shaped like a dumbbell) simultaneously performs three translational movements in addition to two rotational movements around its centre of gravity. This gives us 5 degrees of freedom and the kinetic energy is due to 5 terms: 3 for the translational movements and 2 for the rotational. The kinetic energy $\frac{1}{2} k_B T$ is associated with each of these degrees of freedom and the energy of a molecule at 5 degrees of freedom is $\frac{5}{2} k_B T$. While the distance between molecules may vary, we must also add the vibrational movement of the two atoms: one in relation to the other. This adds two additional degrees of freedom; therefore, the mean energy is $3k_B T$.

1.9.2 Pressure of a gas

If we consider a molecule of mass m colliding with a wall at a velocity of \vec{v} , whose component perpendicular to the wall is v_x , and we accept that the collision is *elastic* and that the wall is *stationary*, the component of velocity after reflection on the wall changes sign (see figure 9a). The variation in the amount of movement of the molecule during the collision is therefore given by:

$$i_x = 2m v_x = \tilde{F} \Delta t.$$

It corresponds to the impulse given by the wall: \tilde{F} represents the force exerted by the wall at the moment of the impact and Δt is the duration of the impact. The collisional frequency shall be referred to as ν , corresponding to the number of molecules that strike the wall during a period of unit time. If $q = \nu S t$ molecules strike a surface S over a given period of time t , the variation in the total amount of movement will be:

$$I_x = \langle q i_x \rangle = 2 S m \langle \nu t v_x \rangle = F t.$$

The magnitude $F = 2 S m \langle \nu v_x \rangle$ represents the total force provided by the wall. It is proportional to the surface and the pressure (force per surface unit) and is therefore expressed by:

$$p = 2 \nu m \langle v_x \rangle.$$

Let us suppose that all of the molecules have the same velocity v_{x0} . Half of them move towards the wall, while the other half move away from it. Therefore, the number of molecules that strike the wall over the time t corresponds to half of the molecules contained in the volume $V = S v_{x0} t$. With n referring to the molecular density, this gives us: $\nu = \frac{1}{2} n v_{x0}$. Considering the expression of $p = F/S$, it follows that, $p = n m v_{x0}^2$.

To generalise the application of this result to the Maxwellian distribution of molecules, we must take the mean over the distribution function, therefore $p = n m \langle v_x^2 \rangle$. Since the particle distribution function is isotropic, the means of the velocity squared are the same for all three directions, $\langle v_x^2 \rangle = \frac{1}{3} \langle v^2 \rangle$. Using this formula and the expression (1.19) for the mean energy, we obtain:

$$p = \frac{1}{3} n m \langle v^2 \rangle = \frac{2}{3} n \varepsilon_m = n k_B T. \quad (1.21)$$

The pressure of a gas is therefore proportional to the temperature.

Table 1: Several orders of magnitude for hydrogen and oxygen.

Gas	H ₂	O ₂
Molecule diameter (nm)	0.24	0.3
T (K)	300	300
p (torr)	760	760 7.6×10^{-4}
n (cm ⁻³)	2.5×10^{19}	2.5×10^{19} 2.5×10^{13}
Mean distance (nm)	3.4	3.4 340
v_m (m/s)	1930	480 480
λ_c (nm)	150	100 10 ⁸
ν_c (s ⁻¹)	10^{10}	4.4×10^9 4.4×10^3

The characteristic parameters for molecular oxygen and hydrogen are presented in table 1. A gas is considered to be highly collisional if the mean free path (1.13) is very small compared to the characteristic length of the problem, $\lambda_c \ll L$. A gas, however, is in a weakly collisional state, or in the Knudsen mode, if the mean free path is long, $\lambda_c \gg L$. Table 1 shows us that under normal conditions, the gases are highly collisional and the mean free path is less than one micron. At low pressures, however, the mean free path becomes long and the collisional effects can be ignored.

1.10 Problems

1. Calculate the value of the plasma parameter (1.1) for the plasmas presented in figure 2: magnetic fusion, solar corona, arc and flame. On the graph (n, T) , plot the line $g_p = 1$ separating the ideal plasmas, $g_p \ll 1$ from the non-ideal plasmas, $g_p \geq 1$.
2. Show that the inequality $r_0 \ll d_e$ also leads to $d_e \ll \lambda_{De}$ and $N_{De} \gg 1$. Find the relationship between the Debye number N_{De} and the plasma parameter g_p .
3. Calculate the Landau length (1.5), the Debye length (1.10) and the plasma frequency (1.16) for the plasmas presented in figure 2: laser fusion, centre of the sun, ionosphere.
4. For two typical laboratory plasmas, with
 - (a) $T_e = 10,000 \text{ }^\circ\text{C}$, $T_i = 1,000 \text{ }^\circ\text{C}$, $n = 10^{12} \text{ cm}^{-3}$;
 - (b) $k_B T_e = k_B T_i = 1 \text{ keV}$, $n = 10^{12} \text{ m}^{-3}$
 calculate the temperatures in eV and in degrees K, the thermal velocities of the electrons and

ions ($Z = 1$), the plasma parameter $\Lambda = 4\pi n\lambda_{De}^3$, the electronic Debye length λ_{De} , the mean distance between the particles $d_e = n_e^{-1/3}$, and the electronic pressure p_e .

On a diagram $n_e - T_e$, plot the lines corresponding to $d_e = r_0$ and $r_0 = \lambda_{de}$, where $r_0 = e^2/(4\pi\epsilon_0 k_B T)$ is the minimum approach distance. Identify the characteristics of the plasmas in the spaces delimited by such lines.

5. Find the solution to the Poisson's equation (1.9) for $r \neq 0$, with the knowledge that it has the form $\Phi(r) = u(r)/r$. Based on the solution obtained, show the state in which the weak coupling approximation is valid.
6. Calculate the value of the electric field produced during plasma oscillations with the electron displacement amplitude equal to the Debye length in a laser fusion plasma. Compare it to the value of the electric field in the hydrogen atom.
7. The plasma is treated as a classical system. The classical approximation, for a particle of velocity v , is valid if the de Broglie length, $\lambda_{DB} = h/mv$, is shorter than the mean distance between the particles, and shorter than the minimum approach distance for a gas of charged particles, i.e. $\lambda_{DB} < n_e^{-1/3}$ and $\lambda_{DB} < e^2/k_B T$. This approximation is no longer valid if the temperature is very high or very low. Calculate the temperature interval (in eV) for which the classical approximation is valid for three plasmas with respective densities of: 10^5 cm^{-3} (ionospheric plasma), 10^{14} cm^{-3} (magnetic fusion plasma) and 10^{21} cm^{-3} (inertial fusion plasma).
8. An ideal plasma consists of a mixture of two perfect gases of ions and electrons. Let us consider a situation of thermodynamic equilibrium in which the particle density $n_{e,i}$ in the presence of an electrostatic field of potential ϕ locally follows a Boltzmann distribution:

$$n_{e,i} = n_{e,i}^0 \exp\left(-\frac{q_{e,i}\phi}{k_B T}\right).$$

We want to obtain the form of the potential around the nucleus of an ion with the charge Ze in the plasma. To this end, we seek to resolve (in spherical geometry) the Poisson's equation for $\phi(r)$, with the densities $n_{e,i}$ plus a point charge. We will use the weak coupling approximation, $e\phi \ll k_B T$.

- (a) Write the Poisson's equation, considering the nucleus as a point source placed at the origin of the coordinate system.
 - (b) Linearise the non-linear terms in ϕ .
 - (c) Express the Laplace operator while assuming spherical symmetry.
 - (d) Find the solution to the Poisson's equation for $r \neq 0$, with the knowledge that it has the form $\Phi(r) = u(r)/r$.
 - (e) Impose the continuity of the potential found for $r \rightarrow \infty$ and $r = 0$.
 - (f) Based on the solution obtained, show the state in which the weak coupling approximation is valid.
9. Let us consider nitrogen in thermodynamic equilibrium in a large chamber with an absolute temperature T . n refers to the mean number of molecules per elementary volume. Calculate the velocity v and the mean free path λ_e of diatomic nitrogen at the temperature $T = 300 \text{ K}$, under the pressure $p = 1 \text{ atm}$, using the perfect gas approach.
A.N. : molecular diameter of nitrogen $\sigma = 0.47 \text{ nm}$ and the molar mass $M = 28 \text{ g/mol}$. Molar constant of perfect gases $R = 8.135 \text{ J/K/mol}$. Avogrados number $N_A = 6.02 \times 10^{23} \text{ mol}^{-1}$.

10. In a gas in thermal equilibrium, the number of molecules whose velocity vectors are situated in a solid angle $d\Omega$ and have a modulus of between v and $v + dv$ is:

$$dn(v) dv = A \frac{d\Omega}{4\pi} v^2 \exp\left(-\frac{mv^2}{2k_B T}\right).$$

With the knowledge that the volume V of the chamber contains N molecules at the temperature T , calculate the constant A .

A.N. To calculate the integrals: $I_n = \int_0^\infty x^n \exp(-ax^2) dx$ we will use: $I_0 = \frac{1}{2}\sqrt{\pi/a}$, $I_1 = 1/(2a)$ and the relation: $I_n = \frac{1}{2}I_{n-2}(n-1)/a$.

11. Calculate the mean value of the quantities $\sqrt{v_x^2}$, $\frac{1}{2}mv^2$, $|\vec{v}|$, in relation to the thermal velocity, defined as $v_T = \sqrt{k_B T/m}$, for a Maxwellian distribution (1.17).
12. Let us consider a chamber with a volume V containing N molecules of helium in thermodynamic equilibrium. Numerically calculate, for $T = 300$ K:
- the most probable velocity v_0 for the gas molecules,
 - the mean velocity v_m ,
 - the mean quadratic velocity v_q .
- A.N. : Molar mass of helium: $M = 4$ g/mol.
13. A small hole in the chamber with a section of s , allows the helium to escape into the vacuum. Demonstrate that the expression $f(v) dv$ of the number of molecules which are among those escaping per second, have velocity vectors situated in a small solid angle around the normal and a velocity of between v and $v + dv$. In the molecular beam emitted in this way, and for a temperature $T = 300$ K, calculate:
- the most probable molecular velocity v'_0 ,
 - the mean velocity v'_q ,
 - the mean quadratic velocity v'_q .



HELLENIC
MEDITERRANEAN
UNIVERSITY



université
BORDEAUX



Erasmus+

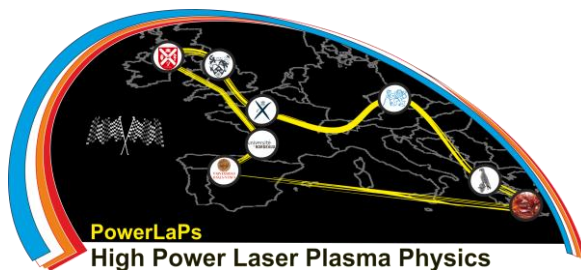
PowerLaPs

Innovative Education & Training in High Power Laser Plasmas

Plasma Physics - Theory and Experiments

Chapter 2: Movement of particles in magnetic and electric fields

D. Batani, E. d'Humières, J.J. Santos, V.T. Tikhonchuk



université
de BORDEAUX

2 Movement of particles in magnetic and electric fields

Collective effects in a plasma are the result of long-range interactions that interlink the charged particles via Coulombian interactions. The dynamics of electrons and ions in the presence of electromagnetic fields play a key role in determining the behaviour of a plasma and its practical uses. The simplest way to consider a plasma is to assume that the electric and magnetic fields are predefined and to focus on the movement of the charged particles in these fields. This will then enable the calculation of the current and charges so that the electromagnetic fields can be recalculated using Maxwell's equations. This procedure, involving successive iterations concerning the positions of the particles and the values of the fields, leads to a self-consistent description of the behaviour of a plasma.

Consequently, to describe the influence of magnetic and electric fields on the movement of charged particles, we ignore the macroscopic fields created by the electrons and ions within the plasma and only take account of the applied fields created by external sources. In the presence of an electric field \vec{E} and a magnetic field \vec{B} , the movement of a particle of the species $\alpha = e, i$ mass m_α and charge q_α is governed by the Lorentz force:

$$\frac{d\vec{x}}{dt} = \vec{v}, \quad \frac{d\vec{v}}{dt} = \frac{q_\alpha}{m_\alpha} (\vec{E} + \vec{v} \wedge \vec{B}). \quad (2.1)$$

We are considering non-relativistic particles, and under these conditions, the equations of motion (2.1) are linear, acceleration $d\vec{v}/dt$ is therefore a linear function of velocity. Nevertheless, the equation for velocity becomes quite complicated if the field values vary along the orbit of the particle, $\vec{r}(t)$. We shall first consider uniform and stationary magnetic fields and then those that vary slightly in space and time.

2.1 Uniform and continuous magnetic field

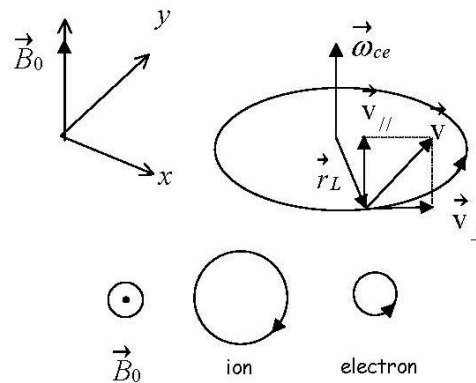


Figure 10: Representation of the trajectory of an electron and an ion in a uniform magnetic field. The field \vec{B} is directed from the back towards the front of the plane of the figure.

In a uniform and continuous magnetic field, and in the absence of an electric field, the equation of motion (2.1) is reduced to:

$$\frac{d\vec{v}}{dt} = \frac{q_\alpha}{m_\alpha} \vec{v} \wedge \vec{B} = -\omega_{c\alpha} \vec{b} \wedge \vec{v} \quad (2.2)$$

where $\omega_{c\alpha} = q_{\alpha}B/m_{\alpha}$ represents the angular frequency of gyromagnetic rotation and $\vec{b} = \vec{B}/B$ is the unit vector in the direction of the magnetic field. According to (2.1), we obtain two equations. The equation of motion parallel to the magnetic field

$$d\vec{v}_{\parallel}/dt = 0 \quad (2.3)$$

corresponds to the equation for a uniform rectilinear motion, $z = z_0 + v_{\parallel}t$. The equation of motion, in a perpendicular plane to the magnetic field is expressed as:

$$d\vec{v}_{\perp}/dt = -\omega_{c\alpha}\vec{b} \wedge \vec{v}_{\perp} \quad (2.4)$$

which describes the rotation of particles around the lines of induction of the magnetic field. The direction of rotation depends on the sign of the charge:

$$dv_x/dt = \omega_{c\alpha}v_y, \quad dv_y/dt = -\omega_{c\alpha}v_x.$$

Electrons and ions have opposite charges and rotate in opposite directions: electrons are negatively charged and rotate in the positive direction; ions are positively charged and rotate in the negative direction. After derivation in relation to time, the equation (2.4) leads to the equation for a uniform, circular motion with the angular frequency $\omega_{c\alpha}$:

$$\frac{d^2\vec{v}_{\perp}}{dt^2} = -\omega_{c\alpha}^2\vec{v}_{\perp}. \quad (2.5)$$

From this, we can infer that:

$$v_x = v_{\perp} \cos(\omega_{c\alpha}t + \phi), \quad v_y = -v_{\perp} \sin(\omega_{c\alpha}t + \phi) \quad (2.6)$$

where ϕ is an arbitrary phase defined by the initial conditions. The trajectory of the electron at a given instant is therefore a helix whose pitch is defined by the velocity v_{\parallel} , and the radius of gyration by the velocity v_{\perp} (see figure 11). The coordinates of the current point on the helix are:

$$x = x_0 + \frac{v_{\perp}}{\omega_{c\alpha}} \sin(\omega_{c\alpha}t + \phi), \quad y = y_0 + \frac{v_{\perp}}{\omega_{c\alpha}} \cos(\omega_{c\alpha}t + \phi), \quad z = z_0 + v_{\parallel}t. \quad (2.7)$$

The radius of gyration or the Larmor radius, $r_{L\alpha}$, is established by the following relation: $r_{L\alpha} = v_{\perp}/|\omega_{c\alpha}|$. Consequently, it is expressed by:

$$r_{L\alpha} = \frac{m_{\alpha}v_{\perp}}{|q_{\alpha}|B_0}. \quad (2.8)$$

If we add the vector of the particle's coordinates to the perpendicular plane, $\vec{r}_{L\alpha}$, we can show the trajectory in vector form:

$$\vec{v}_{\perp} = \omega_{c\alpha}\vec{r}_{L\alpha} \wedge \vec{b}, \quad \text{ou} \quad \vec{r}_{L\alpha} = \omega_{c\alpha}^{-1}\vec{b} \wedge \vec{v}_{\perp} \quad (2.9)$$

and the velocity of the particle is expressed by

$$\vec{v} = \vec{v}_{\parallel} + \vec{v}_{\perp} = \vec{v}_{\parallel} + \omega_{c\alpha}\vec{r}_{L\alpha} \wedge \vec{b}.$$

The particle's position results from the composition of a circular movement of the particle around a centre of rotation - the guiding centre - which itself moves at a constant velocity parallel to the direction of the magnetic field, which is therefore expressed in the following manner:

$$\vec{r} = \vec{r}_{\parallel} + \vec{r}_{L\alpha} = \vec{r}_{\parallel} + \omega_{c\alpha}^{-1}\vec{b} \wedge \vec{v}_{\perp}.$$

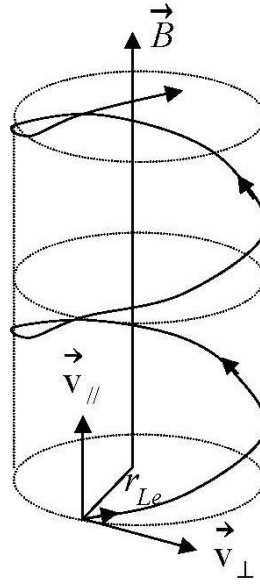


Figure 11: Representation of the trajectory of an electron in a uniform magnetic field.

The first term $\vec{r}_{||}$ on the right-hand side represents the trajectory of the guiding centre and the second term, which we shall designate as $\vec{r}_{L\alpha}$ is the radius vector representing the particle position over the gyration circle as shown on figure 12.

The transverse kinetic energy of a charged particle of the α species is expressed by $W_{\alpha\perp} = \frac{1}{2}m_{\alpha}v_{\perp}^2$. In this way, we can determine the expression of the Larmor radius of the particle according to its transverse kinetic energy $W_{\alpha\perp}$:

$$r_{L\alpha} = \frac{(2m_{\alpha}W_{\alpha\perp})^{1/2}}{|q_{\alpha}|B}.$$

The value of $\vec{v}_{||}$, the position of the axis of rotation x_0, y_0 , and the radius of gyration $\vec{r}_{L\alpha}$ are integration constants of the movement that vary from one particle to another. Consequently, the number of particles with a given radius and helix pitch are determined by the ion and electron velocity distribution functions.

A particle performing a rotation can be considered to be a current loop. The magnetic field produced by this current is characterised by the magnetic moment, $\vec{\mu} = \frac{1}{2} \int \vec{r}' \wedge \vec{j} d\vec{r}'$. In our case $\vec{j}_{\alpha} = q_{\alpha} \vec{v}_{\perp} \delta(\vec{r}' - \vec{r}_{L\alpha}(t))$. Therefore, by using the formula (2.9) for the Larmor radius, the magnetic moment induced by the gyration of the particles in the magnetic field is expressed as:

$$\vec{\mu}_{\alpha} = -\vec{b} \frac{q_{\alpha} v_{\perp}^2}{2\omega_{c\alpha}} = -\vec{b} \frac{m_{\alpha} v_{\perp}^2}{2B_0}. \quad (2.10)$$

This magnetic field opposes the external magnetic field, which it therefore tends to diminish. Plasma is a *diamagnetic medium*, the self-consistent reaction of the plasma is directed in such a manner as to eliminate the external disturbance.

In this case, the plasma is assumed to be collisionless. This description is valid provided that the effective collision frequency ν remains well below the cyclotron angular frequency ($\nu \ll \omega_{c\alpha}$).

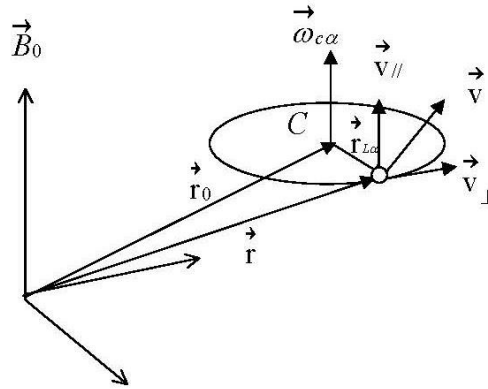


Figure 12: Guiding centre C of the particle.

In this case, the particles will be said to be “magnetised” and their trajectory can be schematically represented as a sequence of helices interrupted by occasional collisions. After the collision, the particle’s velocity changes and, as a consequence, the radius and the pitch of the helix are modified. However, the direction of the helix axis does not change. One species (electrons) may also be magnetised whereas the other may not. This will be the case, for example, if $\omega_{ci} \leq \nu \ll \omega_{c\alpha}$.

2.2 Movement in uniform magnetic and electric fields

2.2.1 Stationary electric field. Electric drift

We will now consider the case of a uniform and continuous magnetic field and of an electric field that is also uniform and continuous (static field). The acceleration of a charged particle is described by the equation (2.1). The component of the electric field $\vec{E}_{||}$ directed along \vec{B} produces a rectilinear and uniformly accelerated movement in the direction of the magnetic field. As they have opposite electric charges, the electrons and the ions move in opposite directions.

Let us now turn our attention towards the component \vec{E}_{\perp} of the electric field perpendicular to the magnetic field. To simplify, we shall suppose that $\vec{E}_{||} = 0$ and $\vec{v}_{||} = 0$. Hence:

$$\frac{d\vec{v}_{\perp}}{dt} = -\omega_{c\alpha} \vec{b} \wedge \vec{v}_{\perp} + \frac{q_{\alpha}}{m_{\alpha}} \vec{E}_{\perp}. \quad (2.11)$$

This equation can be simplified by derivation in relation to time. This gives us:

$$\frac{d^2\vec{v}_{\perp}}{dt^2} = -\omega_{c\alpha}^2 \vec{v}_{\perp} - \frac{q_{\alpha}}{m_{\alpha}} \omega_{c\alpha} \vec{b} \wedge \vec{E}_{\perp}.$$

This is the same type of equation as (2.5) but in this case, it contains an additional constant term. It can be compared to the form (2.5) with the velocity expressed as $\vec{v}_0 = \vec{v}_{\perp} - \vec{v}_E$, where

$$\vec{v}_E = \frac{q_{\alpha}}{m_{\alpha} \omega_{c\alpha}} \vec{E} \wedge \vec{b} = \frac{\vec{E} \wedge \vec{B}}{B^2}. \quad (2.12)$$

Therefore, \vec{v}_0 is now the gyration velocity and \vec{v}_E is the guiding centre velocity. It is perpendicular to both the electric force and the magnetic field, and it is independent of the charge and mass

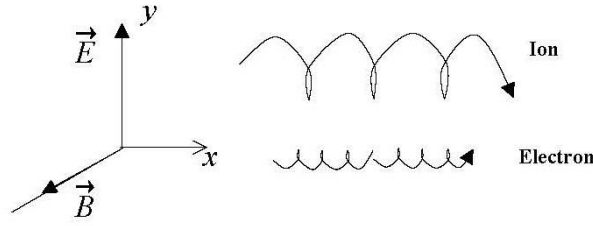


Figure 13: Trajectories of an electron and an ion whose initial velocity was zero.

of the particle in question (electron, ion). Consequently, it represents an overall movement of the plasma. It is called the *electric drift velocity*.

The trajectory of the particle propelled in a perpendicular plane to the magnetic field is the sum of a rectilinear movement at a velocity of \vec{v}_E and a rotational movement at the cyclotron frequency and with a radius of $v_0/\omega_{c\alpha}$. It is a cycloid. Figure 13 represents the trajectories of an electron and an ion with zero initial velocity. The ion starts out in the direction of the electric field \vec{E}_\perp , and then, under the effect of the magnetic field, its trajectory describes cycloid arcs. The electron starts out in the opposite direction but the curvature of the arcs is also inverted. That is why its movement takes place in the same sense as the ion. Due to the great difference in mass, an electron describes much smaller arcs than an ion, but it performs a much higher number of them per second, with the result that in the end, the drift velocities of the electrons and ions are equal.

2.2.2 Alternating electric field. Cyclotron resonance

Let us now consider a uniform magnetic field \vec{B} , and a uniform and alternating electric field $\vec{E} = \vec{E}_0 \sin \omega t$ with an angular frequency ω . The latter has a projection of $E_{0\parallel}$ over \vec{B} and a component in the perpendicular plane $\vec{E}_{0\perp}$. As we have seen above, the movement equation (2.1) is split in two: one for the movement along the axis of the magnetic field and the other in the perpendicular plane. Let us now consider the parallel movement. The equation is similar to (2.3) but with the oscillating external force:

$$\frac{d\vec{v}_\parallel}{dt} = \frac{q_\alpha}{m_\alpha} \vec{E}_{0\parallel} \sin \omega t. \quad (2.13)$$

Here, the magnetic field does not intervene and for the trajectory of the particle, we have:

$$v_\parallel(t) = v_{0\parallel} - \frac{q_\alpha}{m_\alpha \omega} \vec{E}_{0\parallel} \cos \omega t, \quad z(t) = z_0 + v_{0\parallel} t - \frac{q_\alpha}{m_\alpha \omega^2} \vec{E}_{0\parallel} \sin \omega t. \quad (2.14)$$

These equations describe an oscillating rectilinear trajectory with an amplitude of $r_\alpha = |q_\alpha E_{0\parallel}|/m_\alpha \omega^2$.

For the movement in the perpendicular plane, the equation (2.1) takes the form

$$\frac{d\vec{v}_\perp}{dt} = -\omega_{c\alpha} \vec{b} \wedge \vec{v}_\perp + \frac{q_\alpha}{m_\alpha} \vec{E}_{0\perp} \sin \omega t. \quad (2.15)$$

By calculating the temporal derivative of this equation, we obtain a similar equation to (2.5) but which includes the oscillating external force:

$$\frac{d^2\vec{v}_\perp}{dt^2} = -\omega_{c\alpha}^2 \vec{v}_\perp + \omega \frac{q_\alpha}{m_\alpha} \vec{E}_{0\perp} \cos \omega t - \frac{q_\alpha}{m_\alpha} \omega_{c\alpha} \vec{b} \wedge \vec{E}_{0\perp} \sin \omega t. \quad (2.16)$$

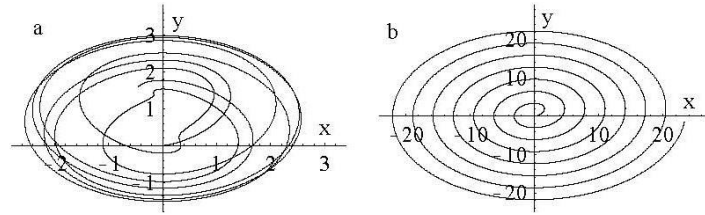


Figure 14: Trajectory of a particle in a uniform magnetic field and an oscillating electric field: a) the ratio of the irrational frequencies $\omega/\omega_{c\alpha} = 1.39$, b) the case of cyclotron resonance $\omega/\omega_{c\alpha} = 1$. Note the difference in scales.

This is a second-order differential equation with a periodic excitation. We seek the solution in the form of a sum of the oscillations at the eigen frequency and at the excitation frequency:

$$\vec{v}_{\perp}(t) = \vec{v}_1 \cos \omega_{c\alpha} t - \vec{v}_2 \sin \omega_{c\alpha} t + \vec{v}_3 \cos \omega t - \vec{v}_4 \sin \omega t. \quad (2.17)$$

By adding this form to the preceding equation (2.15), we obtain the amplitudes of the oscillations generated:

$$\vec{v}_2 = \vec{b} \wedge \vec{v}_1, \quad \vec{v}_3 = \frac{q_{\alpha}}{m_{\alpha}} \frac{\omega \vec{E}_{0\perp}}{\omega_{c\alpha}^2 - \omega^2}, \quad \vec{v}_4 = \frac{q_{\alpha}}{m_{\alpha}} \frac{\omega_{c\alpha} \vec{b} \wedge \vec{E}_{0\perp}}{\omega_{c\alpha}^2 - \omega^2}. \quad (2.18)$$

The two other constants are defined by the initial conditions.

$$\vec{v}_1 + \vec{v}_3 = \vec{v}_{0\perp} \quad \text{et} \quad \omega_{c\alpha} \vec{v}_2 + \omega \vec{v}_4 = \omega_{c\alpha} \vec{b} \wedge \vec{v}_{0\perp}.$$

This enables us to obtain the formula that describes the particle's orbit in the perpendicular plane:

$$\vec{r}_{\perp}(t) = \vec{r}_{0\perp} + \frac{\vec{v}_1}{\omega_{c\alpha}} \sin \omega_{c\alpha} t - \frac{\vec{v}_2}{\omega_{c\alpha}} (1 - \cos \omega_{c\alpha} t) + \frac{\vec{v}_3}{\omega} \sin \omega t - \frac{\vec{v}_4}{\omega} (1 - \cos \omega t). \quad (2.19)$$

The orbit of each particle is quite complex and consists of two elliptical movements. The first movement is produced at the eigen rotational frequency $\omega_{c\alpha}$ and with a radius of rotation $r_{B\alpha}$ depending on the initial conditions and the electric field. In the case $v_{0\perp} = 0$, the cyclotronic radius of rotation is

$$r_{B\alpha} = \frac{q_{\alpha}}{m_{\alpha}} \frac{\omega}{\omega_{c\alpha}} \frac{E_{\perp}}{\omega_{c\alpha}^2 - \omega^2}.$$

The second movement is forced by the electric field acting on the elliptical orbit. The rotational frequency is ω and the radii of this ellipse are $r_{B\alpha} \omega_{c\alpha} / \omega$ and $r_{B\alpha} (\omega_{c\alpha} / \omega)^2$. Since the amplitudes of the velocities in the formula (2.17) do not change, the mean energy of the movement in the perpendicular plane is constant. The energy gain of the particle is mainly due to the work carried out by the component of the parallel electric field. An example of a trajectory is presented in figure 14a for the case $\vec{r}_0 = 0$ and $\vec{v}_{0\perp} = 0$. In the specific case of a rational frequency ratio, $\omega/\omega_{c\alpha} = n/m$, the orbit therefore takes on a relatively simple form.

It is easily seen that the preceding formulae are not valid in the specific case in which the excitation frequency is equal to the cyclotron frequency. This is the cyclotron resonance. In this very specific case, the particle can gain energy in the perpendicular plane. In the resonant case, the formula (2.17) is incorrect and so we must take account of the secular terms with a linear time dependence:

$$\vec{v}_{\perp}(t) = (\vec{v}_1 + \vec{a}_1 t) \cos \omega_{c\alpha} t - (\vec{v}_2 + \vec{a}_2 t) \sin \omega_{c\alpha} t. \quad (2.20)$$

The new terms $\vec{a}_{1,2}$ take account of the acceleration of the particle. By adding this form to the basic equation (2.15) for $\omega = \omega_{c\alpha}$, we obtain the velocities and the amplitudes of the accelerations:

$$\vec{a}_1 = -\vec{b} \wedge \vec{a}_2, \quad \vec{a}_2 = -\frac{q\alpha}{2m_\alpha} \vec{E}_{0\perp}, \quad \vec{v}_2 = \frac{\vec{a}_1}{\omega_{c\alpha}} + \vec{b} \wedge \vec{v}_1. \quad (2.21)$$

The final constant is determined by the initial condition: $\vec{v}_1 = \vec{v}_{0\perp}$. This enables us to write the formula for the particle's orbit in the perpendicular plane in the following form:

$$\vec{r}_\perp(t) = \vec{r}_{0\perp} - \frac{\vec{v}_2}{\omega_{c\alpha}} - \frac{\vec{a}_1}{\omega_{c\alpha}^2} + \left(\frac{\vec{v}_2}{\omega_{c\alpha}} + \frac{\vec{a}_1}{\omega_{c\alpha}^2} + \frac{\vec{a}_2 t}{\omega_{c\alpha}} \right) \cos \omega_{c\alpha} t + \left(\frac{\vec{v}_{0\perp}}{\omega_{c\alpha}} - \frac{\vec{a}_2}{\omega_{c\alpha}^2} + \frac{\vec{a}_1 t}{\omega_{c\alpha}} \right) \sin \omega_{c\alpha} t. \quad (2.22)$$

The radius of rotation increases in a linear manner over time (see figure 14) and the energy of the particle increases as t^2 . Cyclotron resonance is therefore an efficient method of heating particles in natural and laboratory plasmas.

2.3 Alternating and non-uniform electric field

2.3.1 Ponderomotive force

Let us consider an alternating electric field and assume that its amplitude is not constant, but that it varies along the direction of the field, $E_x(x, t) = E_0(x) \sin \omega t$. To simplify the analysis, we consider the characteristic length of the amplitude variation,

$$l_E = E_0 \left(\frac{dE_0}{dx} \right)^{-1}, \quad (2.23)$$

and we assume that it is large compared to the amplitude of the electron's oscillation in this alternating field, $r_e = eE_0/m_e\omega^2$. In this case, the electron movement equation (2.1) is expressed as:

$$\frac{dx}{dt} = v_x, \quad \frac{dv_x}{dt} = \frac{q_e}{m_e} E_0(x) \cos \omega t \quad (2.24)$$

It can be solved in an approximate manner by considering $r_e/l_E \ll 1$ as the development parameter. Consequently, the electron's orbit, $x(t) = x^{(0)}(t) + x^{(1)}(t)$, and its velocity, $v_x(t) = v_x^{(0)}(t) + v_x^{(1)}(t)$ are developed in zero-order terms (homogeneous field) and small first-order corrections in r_e/l_E . At zero order, E_0 is constant and the equations (2.24) are solved as follows:

$$v_x^{(0)} = \frac{q_e E_0}{m_e \omega} \sin \omega t, \quad x^{(0)} = \frac{q_e E_0}{m_e \omega^2} (1 - \cos \omega t). \quad (2.25)$$

Here, the electron oscillates at an amplitude r_e around the position, $x = r_e$ and $v_x = 0$. To obtain the first-order equations, we expand the field amplitude on a Taylor series by taking account of the first two terms:

$$E_0(x) \approx E_0 + x^{(0)}(t) \frac{dE_0}{dx} = E_0 \left[1 + \frac{r_e}{l_E} (1 - \cos \omega t) \right].$$

Therefore, the first-order equations are set out in the following manner:

$$\frac{dx^{(1)}}{dt} = v_x^{(1)}, \quad \frac{dv_x^{(1)}}{dt} = \frac{q_e^2 E_0}{m_e^2 \omega^2} \frac{dE_0}{dx} (1 - \cos \omega t) \cos \omega t. \quad (2.26)$$

Considering the second equation, it can be seen that the velocity $v_x^{(1)}$ contains three different terms. Firstly, there is one term oscillating at the frequency ω . This is clearly a slight correction of the zero-order term, and is of little interest. Then there is the term containing $\cos^2 \omega t = \frac{1}{2}(1 + \cos 2\omega t)$ which

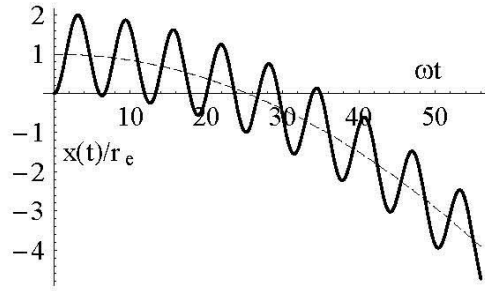


Figure 15: Movement of a particle in an alternating and non-uniform electric field. The field has a positive gradient and it is 160 times greater than the amplitude of the oscillations. The displacement of the oscillation centre is shown by a dotted line.

gives rise to oscillations at the second harmonic and finally, there is one secular term, which never oscillates and is actually of the greatest interest, because it describes a permanent displacement of the electron's oscillation centre in relation to its initial position.

To obtain a better view of the secular term's effect, we derive the equation for velocity $\bar{v}_x^{(1)}$, averaged over the field oscillation period $2\pi/\omega$:

$$m_e \frac{d\bar{v}_x^{(1)}}{dt} = -\frac{q_e E_0}{2m_e \omega^2} \frac{dE_0}{dx} = -\frac{d}{dx} \frac{q_e^2 E_0^2}{4m_e \omega^2}. \quad (2.27)$$

The left-hand part is the mean acceleration of the electron. Consequently, the right-hand part is a force, which is called the *ponderomotive force*, F_p . It can be seen that this force results from the gradient of the *ponderomotive potential*,

$$\vec{F}_p = -\vec{\nabla} \frac{q_e^2 E_0^2}{4m_e \omega^2} \equiv -\vec{\nabla} U_p. \quad (2.28)$$

The ponderomotive force and the ponderomotive potential represent the mean effect of an inhomogeneous alternating electric field on a particle. The force is directed in the opposite direction to the intensity gradient, E_0^2 , of the oscillating electric field. Consequently, the particle is ejected from the area in which the field is the strongest. Note that this *drift* effect does not depend on the charge of the sign: all particles - electrons and ions - are driven out by the field. Nevertheless, the lighter electrons are subjected to a much higher force than that exerted on the heavier ions. Figure 15 shows a particle's orbit in the oscillating field for the parameter $r_e/l_E = 1/160$. Six oscillations are required to displace the particle over a distance equal to the amplitude of its oscillations.

2.3.2 Electrostatic waves and particle trapping

Consider a wave whose electric field, $E_x(t, x) = E_0 \sin(\omega t - kx)$, travels in the direction x at the phase velocity, $v_{ph} = \omega/k$. The movement equations for a particle with mass m and charge q in this wave are:

$$\frac{dx}{dt} = v, \quad m \frac{dv}{dt} = q E_0 \sin(\omega t - kx). \quad (2.29)$$

In fact, it is easier to solve this system if we position ourselves in the reference frame of the wave, which is displaced at the phase velocity:

$$x = v_{ph} t + X, \quad v = v_{ph} + V.$$

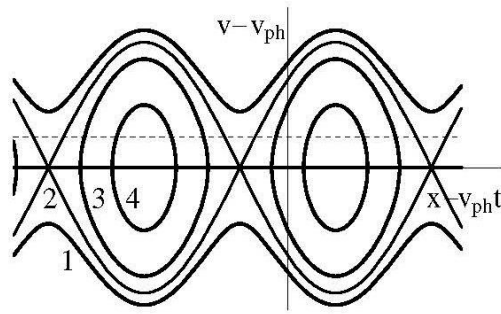


Figure 16: Orbits of resonating particles in the phase velocity coordinate system: 1 – a free particle, 2 – the separator, 3, 4 – the trapped particles. The particles with positive velocities travel towards the right-hand side and those with negative velocities move towards the left.

Let us accept that at a given moment $t = 0$, the particle is in the position $X = X_0$ with the velocity $V = V_0$. The dynamics equations are expressed as:

$$\frac{dX}{dt} = V, \quad m \frac{dV}{dt} = -qE_0 \sin kX.$$

In this coordinate system, the time is no longer clearly shown and we can calculate the first integral of this system:

$$\frac{1}{2}mV^2 - \frac{q}{k}E_0 \cos kX = \frac{1}{2}mV_0^2 - \frac{q}{k}E_0 \cos kX_0. \quad (2.30)$$

This is the energy conservation law. The particle may take energy from the field, or otherwise it may transfer energy to it, but the total amount of energy remains the same. In addition, if we calculate the mean for the initial coordinate of the particle, its energy remains unchanged. It is instructive to plot a phase graph, representing the dependence of particle's velocity according to its abscissa, $V(X)$. According to the equation (9.53), all particles have a periodic motion, but the trajectory of each particle depends on the value of the parameter $2qE_0/kmV_0^2$, which is the ratio of the potential energy in the wave qE_0/k to the kinetic energy of the particle. If this parameter is small, the particle is almost free, its velocity hardly varies and the oscillation frequency is high, $\omega_b \approx kV_0$. It increases when the particles move away from the resonance.

However, if the parameter is $2qE_0/kmV_0^2 > 1$, the particle's trajectory has ended, and we say that this particle is trapped in the wave. It performs oscillations around the minimum potential, $kX_m = 0, 2\pi, \dots$. The frequency of these oscillations is independent of the velocity, $\omega_b \approx \sqrt{qkE_0/m}$, but depends on the amplitude E_0 . This fact is essential to our analysis: when the amplitude of the field is very low, the oscillation period of the trapped particles is infinitely long. The typical trajectories of the particles near the resonance are plotted in figure 38. Curve 2 constitutes the separator between the free particles and the trapped particles.

2.4 Non-uniform magnetic field

In the case of non-uniform magnetic fields \vec{B} that vary over time, the problem cannot be resolved as easily as for a uniform and continuous field. The particle is not completely attached to the field line, and performs a much more complex movement. To simplify the analysis, in this case we assume that the magnetic field \vec{B} varies slowly in space (and possibly in time). This means

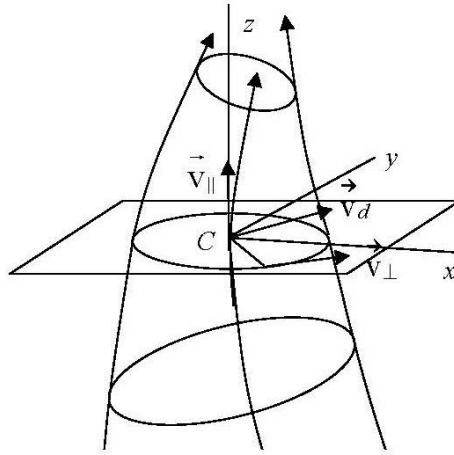


Figure 17: Movement of a particle in a non-uniform magnetic field.

redefining the characteristic times and lengths of magnetic field variation by the relations:

$$\tau_c = \left(\frac{1}{B} \left| \frac{\partial B}{\partial t} \right| \right)^{-1}, \quad l_{\perp} = \left(\frac{|\vec{\nabla}_{\perp} B|}{B} \right)^{-1}, \quad l_{\parallel} = \left(\frac{|\vec{\nabla}_{\parallel} B|}{B} \right)^{-1} \quad (2.31)$$

and considering that we have:

$$\tau_c \gg \frac{2\pi}{\omega_c}, \quad l_{\perp} \gg r_L, \quad l_{\parallel} \gg \frac{2\pi v_{\parallel}}{\omega_c}. \quad (2.32)$$

When these conditions have been met, we can assume that at all times, the particle's trajectory remains a helix which is progressively deformed. This is an *adiabatic* approximation similar to the approach presented in the preceding paragraph 2.3.

This enables us to study the mechanisms by which inhomogeneous static magnetic fields interact with the charged particles. The non-uniformity of the magnetic field (gradient of the magnetic field and curvature of the induction lines) in this way contributes to the *drift* of particles in the magnetic field and to their *reflection* due to a *magnetic mirror* effect. The latter effect is the cause of the aurorae boreales that can be observed in the magnetosphere. The *magnetic confinement of thermonuclear plasmas* by a complex magnetic configuration is one of the key aspects of the studies carried out in magnetic confinement fusion.

We then consider that the magnetic field intensity is constant over time. We shall consider a zero, continuous and oscillating electric field in turn. We assume that the induction lines, which are mainly directed towards z , are slightly curved in the direction of x . Figure 17 shows the appearance of the induction lines of a non-uniform magnetic field. The induction lines draw closer together as the field intensity increases. The velocity of a charged particle (electron, ion) can be broken down into three components:

$$\vec{v} = \vec{v}_{\parallel} + \vec{v}_{\perp} + \vec{v}_d.$$

The first two represent the almost helical movement around the lines of force. The particle rotates around the guiding centre C in a perpendicular plane to \vec{B} with the velocity v_{\perp} . The guiding centre of the particle moves along the field's induction line at the velocity v_{\parallel} . The final component v_d

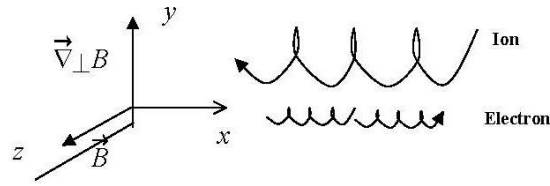


Figure 18: Movement of a particle in the magnetic field gradient.

represents the drifting motion of the guiding centre, perpendicularly to the induction lines, which as we shall see, is due to the non-uniformity of the magnetic field.

This drift velocity can itself be broken down into two terms: $\vec{v}_d = \vec{v}_g + \vec{v}_c$. Here, \vec{v}_g is the *gradient drift velocity* and \vec{v}_c is the *curvature drift velocity* of the magnetic field. For a magnetic field that varies slightly in space, we can use a Taylor series expansion to express the field in proximity to a point \vec{r}_0 in the form:

$$\vec{B}(\vec{r}) \approx \vec{B}(\vec{r}_0) + (\vec{\rho} \cdot \vec{\nabla}) \vec{B}(\vec{r}_0) \quad (2.33)$$

with $\vec{\rho} = \vec{r} - \vec{r}_0$. Positioning ourselves at a point \vec{r}_0 assumed to be the origin, we consider $\vec{B}_0 = \vec{B}(\vec{r}_0)$. We will now examine different magnetic field geometries.

2.4.1 Gradient perpendicular to the magnetic field. Gradient drift

Here, we assume that the magnetic field \vec{B} is directed towards z ($B_x = B_y = 0$) and that it varies in the perpendicular direction y , $B_z(y)$. Under these conditions, the variation in a particle's radius and gyration period will be manifested by a slow drift of the guiding centre. The particle movement diagram for the particles in the magnetic field gradient is presented in figure 18. Here, the characteristic dimension of the gradient in proximity to this point according to (2.32) can be defined by:

$$l_c = \left(\frac{1}{B_0} \left| \frac{\partial B_z}{\partial y} \right| \right)^{-1}.$$

In proximity to point $\vec{r}_0 = \vec{0}$, considered to be the origin, the magnetic field is expressed as: $B_z \approx B_0(1 + y/l_c)$, up to the limit of $l_c \gg r_L$, which gives us $y/l_c \ll 1$. For an α particle, the force exerted in perpendicular plane to the magnetic field is expressed by: $\vec{F}_\perp = q_\alpha \vec{v}_\perp \wedge \vec{B}$. From this, we determine the acceleration components using the equations (2.1):

$$\frac{dv_x}{dt} = \omega_{c\alpha} \left(1 + \frac{y}{l_c} \right) v_y, \quad \frac{dv_y}{dt} = -\omega_{c\alpha} \left(1 + \frac{y}{l_c} \right) v_x. \quad (2.34)$$

These equations are solved in a similar manner to that described in paragraph 2.3.1. Since the nonlinear terms to the right-hand side of the equations (2.34) are second-order equations, we develop the particle velocities and coordinates according to the small parameter, $r_L/l_c \ll 1$. Ignoring the nonlinear terms in (2.34), proportional to y/l_c , the movement equations, $dx/dt = v_x$ and $dy/dt = v_y$ give us the rotation of the particle at the cyclotronic frequency, at the point of origin, see the equations (2.6) and (2.7). Then, for the nonlinear terms in (2.34), we obtain the following expressions:

$$y v_y = -\frac{v_\perp^2}{2\omega_{c\alpha}} \sin 2(\omega_{c\alpha} t + \phi), \quad y v_x = \frac{v_\perp^2}{2\omega_{c\alpha}} [1 + \cos 2(\omega_{c\alpha} t + \phi)].$$

The term $y v_y$ oscillates at twice the frequency of the cyclotron frequency. This produces a corresponding movement on the x axis at the second $\omega_{c\alpha}$ harmonic, which is not very important because of the $r_\alpha/l_c \ll 1$ parameter. However, in addition to an oscillating term, the term $y v_x$ also contains a secular component that is independent of time. The particle is therefore subjected to a constant acceleration along the y axis. By calculating the mean \bar{v}_y over a rotation period, we obtain the acceleration of the slow movement:

$$d\bar{v}_y/dt = -v_\perp^2/2l_c. \quad (2.35)$$

This acceleration is constant; it is not dependent on y and it follows the direction of the field gradient. This action is similar to the action of the uniform electric field, perpendicular to the magnetic field, considered in the previous paragraph 2.2.1. By transferring this acceleration (2.35) into the relation (2.12) instead of the electric acceleration, $(q_\alpha/m_\alpha) \vec{E}_\perp$, we ultimately obtain the expression of the drift velocity (2.12), associated with any transverse gradient $\vec{\nabla}_\perp B$ of the magnetic field:

$$\vec{v}_g = -\frac{v_\perp^2}{2B\omega_{c\alpha}} \vec{\nabla}_\perp B \wedge \vec{b} = \frac{W_{\alpha\perp}}{q_\alpha B^2} \vec{b} \wedge \vec{\nabla}_\perp B. \quad (2.36)$$

It can be seen that the drift velocity is perpendicular to both the direction of the magnetic field and the direction of its gradient. The direction of drift is opposite for the electrons and ions and its amplitude is proportional to the energy of the particle $W_{\alpha\perp}$ in the perpendicular plane. Consequently, a polarisation current is created. Therefore, this differs from the case of electric field drift, considered in paragraph 2.2.1, in which the electrons and ions move in the same direction and sense.

2.4.2 Curvature of magnetic field lines. Curvature drift

When the magnetic induction lines are curved (see figure 17), the movement following these lines is also curved. Due to the curvature of the trajectory, there is a centrifugal acceleration whose modulus $g_c = v_\parallel^2/R_c$, where v_\parallel is the velocity of the guiding centre of the particle along the line of force and R_c is the local radius of curvature of the induction line. Let us suppose that the magnetic field is mainly directed along the z axis but that it has a small component B_x related to the local curvature, $\kappa_c = 1/R_c$, along the x axis (figure 17). The local radius of curvature is therefore given by:

$$R_c = \left(\frac{1}{B_z} \left| \frac{\partial B_x}{\partial z} \right| \right)^{-1}.$$

In a more general manner, the local curvature of the field line is a vector, $\vec{\kappa}_c$, defined by the following relation:

$$\vec{\kappa}_c = (\vec{b} \cdot \vec{\nabla}) \vec{b}.$$

Consequently, the centrifugal acceleration is also a vector, $-\vec{\kappa}_c v_\parallel^2/m_\alpha$, situated in the perpendicular plane to the field vector. By transferring this acceleration into the relation (2.5), instead of the electric acceleration, we obtain a drift velocity due to the centripetal force. This is the curvature drift velocity which is expressed by:

$$\vec{v}_d = -\frac{v_\parallel^2}{m_\alpha \omega_{c\alpha}} \vec{\kappa}_c \wedge \vec{b} = \frac{2W_{\alpha\parallel}}{q_\alpha B} \vec{b} \wedge \vec{\kappa}_c.$$

The drift velocity is therefore perpendicular to the plane defined by the magnetic field and the local radius of curvature, in an identical manner to the gradient drift, but in this case, it is proportional to the energy of the parallel movement, $W_{\alpha\parallel}$.

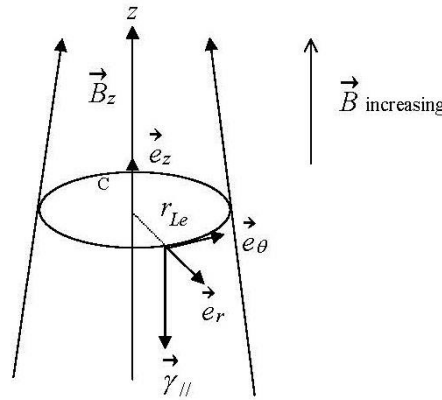


Figure 19: Movement of an electron in the magnetic field increasing in the direction of the z axis.

2.4.3 Gradient parallel to the magnetic field. Magnetic mirror

We shall again consider that the magnetic field is directed along z ($B_z \neq 0$). It is always constant over time, but now it is only supposed to vary in the z direction and to be increasing ($\partial B_z / \partial z > 0$). The appearance of the induction lines is shown in figure 19.

As the magnetic field satisfies the Maxwell's equation $\vec{\nabla} \cdot \vec{B} = 0$, there is therefore a radial field component B_r which induces a force in the z direction that will now be expressed in the following way. The divergence of the magnetic field in cylindrical coordinates taking account of the symmetry of revolution around z , is expressed as:

$$\frac{1}{r} \frac{\partial}{\partial r} (r B_r) + \frac{\partial B_z}{\partial z} = 0.$$

Assuming that the derivative of B_z does not depend on r , the radial component B_r is therefore a linear function of r :

$$B_r(r) = -\frac{r}{2} \frac{\partial B_z}{\partial z}.$$

By considering the radius r of the electron's trajectory to be equal to the Larmor radius r_{Le} , we can determine the expression of the force exerted on an electron along the direction z :

$$\vec{F} = -e v_{\perp} \vec{e}_{\theta} \wedge \vec{e}_r B_r = -\frac{m_e v_{\perp}^2}{2} \frac{1}{B_z} \frac{\partial B_z}{\partial z} \vec{e}_z$$

where \vec{e}_r , \vec{e}_{θ} and \vec{e}_z are the unit vectors in cylindrical coordinates. The direction of the acceleration is independent of the sign of the charge (electron, ion). The longitudinal movement of the electrons and ions is slowed down due to the increase in the magnetic field in the direction of z .

The magnetic moment of a charged particle rotating in a magnetic field is given by the expression (2.10):

$$\mu_{\alpha} = m_{\alpha} v_{\perp}^2 / 2 B_z. \quad (2.37)$$

From this, we can establish that the force exerted along z is proportional to the magnetic moment and moves in the same sense for the electrons and ions:

$$F_z = -\mu_e \partial B_z / \partial z.$$

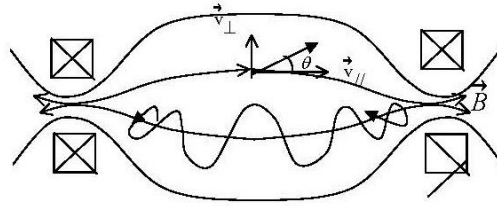


Figure 20: Magnetic mirror in a Helmholtz configuration. The crossed squares represent two coils that create the magnetic field, which is stronger in the plane of the coils and decreases elsewhere. The particle is trapped between the coils, where the magnetic field is at its minimum level.

The movement equation for the particle according to the z axis is: $m_e dv_{\parallel}/dt = F_z$. Using the definition of parallel velocity, $dz/dt = v_{\parallel}$, we obtain:

$$m_e \frac{dv_{\parallel}}{dt} = m_e v_{\parallel} \frac{dv_{\parallel}}{dz} = \frac{d}{dz} \frac{m_e v_{\parallel}^2}{2} = -\mu_e \frac{\partial B_z}{\partial z}. \quad (2.38)$$

As the diamagnetic force is of purely magnetic origin, it does not contribute to modifying the total kinetic energy, but it changes the distribution of the parallel and perpendicular movements of the field. The conservation of the total kinetic energy of the particle can be presented in the following form:

$$\frac{d}{dz} \left(\frac{1}{2} m_e v^2 \right) = \frac{d}{dz} \left(\frac{1}{2} m_e v_{\parallel}^2 + \frac{1}{2} m_e v_{\perp}^2 \right) = 0.$$

In this way, by using the definition of the magnetic moment (2.37), we obtain:

$$\frac{d}{dz} \left(\frac{1}{2} m_e v_{\parallel}^2 + \mu_e B_z \right) = 0.$$

In addition, according to (2.38): $-\mu_e dB_z/dt + d(\mu_e B_z)/dt = 0$. We ultimately obtain the magnetic moment conservation law:

$$d\mu_e/dz = 0. \quad (2.39)$$

We can demonstrate that the magnetic moment is an adiabatic invariant: it does not change even if the magnetic field varies over time and if the energy of the particle is not conserved. The only important criterion for the conservation of the magnetic moment is for the characteristic field variation time to be much greater than the cyclotron rotation period.

According to (2.38), we can observe that the longitudinal kinetic energy of the electron $\frac{1}{2} m_e v_{\parallel}^2$ decreases when it moves up towards the ascending values of the magnetic field. Consequently, its velocity v_{\parallel} decreases. At the same time, the transverse velocity v_{\perp} of the particle increases in order to maintain its constant magnetic moment μ_e (2.37). The longitudinal energy is therefore transformed into transversal energy. In this way, if the magnetic field increases sufficiently, the particle may then be reflected towards areas with a weaker magnetic field. This corresponds to a *magnetic mirror* effect.

2.4.4 Magnetic confinement. Loss cone

The magnetic mirror is used to confine the charged particles. A ‘‘Helmholtz’’ magnetic configuration is shown in figure 20. The field is at its minimum level in the middle and its maximum level at the

narrowest points. The particles that are not reflected can escape through the narrow openings. We shall now determine the loss angle in this magnetic geometry. We consider a particle with a velocity of v_0 at a point at which the magnetic induction has a minimum value of B_0 . The maximum value of the magnetic induction is B_m . The particle will be reflected ($v_{\parallel} = 0$) at the point at which the magnetic field is such that:

$$\frac{1}{2}m_{\alpha}v_{\perp 0}^2 = \frac{1}{2}m_{\alpha}v_{\perp}^2,$$

hence $v_{\perp} = v_0$. Magnetic moment conservation links the field and velocity values:

$$\frac{B_0}{B} = \frac{v_{\perp 0}^2}{v_0^2} = \sin^2 \theta.$$

Here, θ represents the angle of the orbit cone in the area in which the field is equal to B . If this angle is too small, B may be higher than B_m and the particle will leave the system. Otherwise, it will be reflected. The angle θ_m of the loss cone is given by the expression $\sin^2 \theta_m = B_0/B_m$.

2.5 Problems

- Express the ratio of the Larmor radius of an ion of mass M and charge Z to that of an electron with the same transverse energy W_{\perp} . Determine the expression of the magnetic moment of an electron in a rotational movement in a uniform magnetic field \vec{B} according to its transverse kinetic energy W_{\perp} and \vec{B} . Calculate the value of the Larmor radius in the magnetic field at the Earth's surface ($B = 50 \mu\text{T}$).
- Calculate the cyclotronic frequencies of the electrons and ions in a magnetic fusion plasma ($B = 5 \text{ T}$). Compare them with the corresponding plasma frequencies. (Use the data in figure 2 for the density and temperature values.)
- Show that the expression (2.12) of the drift velocity can be obtained simply by making an appropriate change of coordinate system. What is the trajectory of the particle in this coordinate system?
- Calculate the movement of a charged particle placed in a homogeneous magnetic field directed along the z axis and an electric field created by a line with the electric loading of charges λ parallel to the magnetic field. Schematically plot the particle's orbit in the plane perpendicular to the magnetic field.
- Ionospheric plasma is situated in intersecting magnetic and gravitational fields. Estimate the value of the drift velocity in this configuration and plot the orbits of the electrons and ions in these fields. The magnetic field on the Earth's surface is $50 \mu\text{T}$, and the gravitational acceleration is 10 m/s^2 .
- Let us consider an electric wire through which a 1 kA current is flowing. Calculate the orbit of an electron with 10 eV of energy in the magnetic field created by this current at a distance of $R = 10 \text{ cm}$.
- We shall presume that the magnetic field in the magnetic mirror in figure 20 varies according to the axis of the coil in the following manner: $B_z = B_0(1 + z^2/L^2)$. Calculate the oscillation period of a particle trapped in this coil. Schematically plot the particle's orbit. How is this orbit modified if the field B_0 is inhomogeneous in the radial direction?



8. Schematically describe the movement of particles in the Van Allen belts. We will assume that the Earth's magnetic field is a magnetic dipole. Plot the orbits in the meridian and equatorial planes.
9. A laser beam has a hollow intensity profile with the minimum level on the axis. Calculate the oscillation frequency of a charged particle trapped in the laser field. Propose a trapping criterion.



HELLENIC
MEDITERRANEAN
UNIVERSITY



université
BORDEAUX



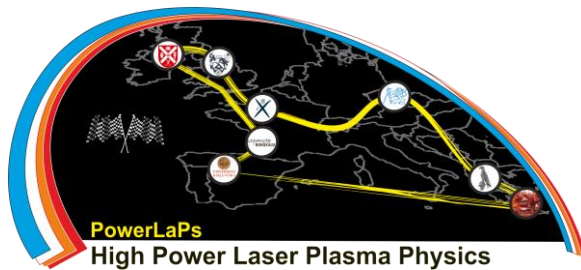
PowerLaPs

Innovative Education & Training in High Power Laser Plasmas

Plasma Physics - Theory and Experiments

Chapter 3: Coulombian collisions

D. Batani, E. d'Humières, J.J. Santos, V.T. Tikhonchuk



université
de BORDEAUX

3 Coulombian collisions

In a collision between an electron and an ion (or between two electrons or two ions), the potential for long-range interaction is the Coulomb potential. At short range, the interaction takes place via repulsive forces of a quantum nature that vary much more quickly than the Coulomb potential.

Here, we shall be covering elastic electron-ion collisions (in addition to electron-electron and ion-ion collisions) in the traditional sense. Although this description is not wholly satisfactory, it does enable us to specify certain parameters and the fundamental physical quantities associated with collisions in plasmas.

3.1 Collisions between charged particles

Collisions between two particles play a very important role in the kinetic theory of ionised gases. A distinction is made between two types of collisions:

- an elastic collision between two particles, in which there is no change in the internal energy of the particles;
- an inelastic collision, in which the internal electronic state of the atom or ion is modified. These collisions therefore contribute to changing the excitation or ionisation state of the molecules, atoms and ions in the plasma.

3.1.1 Elastic electron-ion collisions (traditional approach)

Let us consider an elastic collision between an electron and an ion (see Figure 21). We will ignore the electron-electron interactions and will assume that the ion is stationary in the collision. The electron's trajectory in the mass centre system of the colliding particles is a *hyperbola*, characterised by the parameters a' , b' and c' :

$$c'^2 = a'^2 + b'^2, \quad \text{and} \quad a' = c' \cos \Psi$$

where θ is the angle of deflection, linked to the angle Ψ by the relation $\theta + 2\Psi = \pi$, and b is the impact parameter in the collision: $b = c' \sin \Psi$. We also introduce b_{\min} , which is the minimum approach distance: $b_{\min} = c' - a' = c'(1 - \cos \Psi)$. From this, we therefore establish that:

$$b_{\min} = b \frac{1 - \cos \Psi}{\sin \Psi}.$$

In an elastic collision, two conservation laws are validated:

1. Conservation of total energy:

$$\frac{1}{2}m_e v^2 = \frac{1}{2}m_e v'^2 - \frac{Ze^2}{4\pi\epsilon_0 b_{\min}} \quad (3.1)$$

The left-hand term represents the kinetic energy of the electron at infinity, because its potential energy at infinity is zero; the right-hand term represents the sum of the kinetic and potential energies of the electron at the minimum approach distance.

2. Kinetic moment conservation:

$$m_e v b = m_e v' b_{\min} \quad (3.2)$$

which is valid for the central interaction forces.

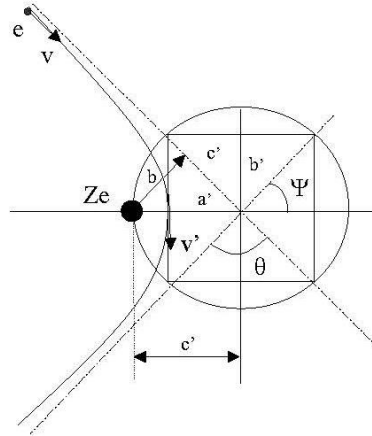


Figure 21: Trajectory of an electron during a collision with a stationary ion.

On the basis of conservation equations (3.1) and (3.2), we obtain:

$$\frac{v'^2}{v^2} = \frac{b^2}{b_{\min}^2} \quad \text{et} \quad \frac{b^2}{b_{\min}^2} = 1 - \frac{2Ze^2}{4\pi\epsilon_0 b^2 m v^2}.$$

Based on these two equations, we establish that

$$b = \frac{Ze^2}{4\pi\epsilon_0 m_e v^2} \cot \frac{\theta}{2}.$$

We ultimately obtain an expression that associates the impact parameter b , with the angle of deflection θ :

$$b = b_c \cot \frac{\theta}{2} \quad (3.3)$$

where b_c is the critical impact parameter, which is expressed by:

$$b_c = \frac{Ze^2}{4\pi\epsilon_0 m_e v^2}. \quad (3.4)$$

The critical impact parameter corresponds to the impact parameter value for a deviation of 90° . If, in the expression (3.4) of the critical impact parameter, we take $v^2 = v_{Te}^2 = k_B T_e / m_e$, then the critical impact parameter will be expressed in the following way:

$$b_0 = \frac{Ze^2}{4\pi\epsilon_0 k_B T_e} \quad (3.5)$$

that corresponds to Z times the Landau's distance r_0 (1.5), which represents the minimum approach distance of two electrons.

3.2 Elastic collisional cross section

Let us consider a homogeneous flow Φ of mono-kinetic electrons (see figure 22a). This electron beam makes contact with a target ion which acts like a stationary scattering centre. For an isotropic interaction potential (corresponding to the central forces), the number of electrons scattered, per

unit of time, in a solid angle $d\Omega = \sin\theta d\theta d\varphi$ corresponding to a deflection of between θ and $\theta + d\theta$ and φ and $\varphi + d\varphi$ is therefore given by:

$$\frac{dN}{dt} = \Phi \frac{d\sigma(\theta)}{d\Omega} d\Omega$$

where $d\sigma/d\Omega$ is the differential collisional cross section. To convince oneself that σ does indeed have the dimensions of a surface, one simply has to consider the equation with dimensions relating to the number of particles scattered: $T^{-1} = L^{-2} \times T^{-1}$.

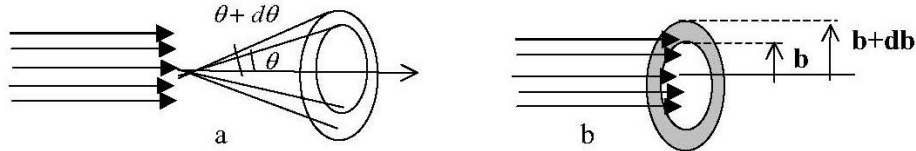


Figure 22: a) Scattering of an electron beam by an ion. b) Definition of the impact parameter.

The electrons deflected between the angle cones θ and $\theta + d\theta$ have impact parameters of between b and $b + db$ (see figure 22b). As the cross section does not depend on φ , we obtain:

$$\Phi 2\pi b db = \Phi 2\pi \frac{d\sigma(\theta)}{d\Omega} \sin\theta d\theta$$

From this, we therefore establish that:

$$\frac{d\sigma(\theta)}{d\Omega} = \frac{b db}{\sin\theta d\theta}. \quad (3.6)$$

the basis of (3.3), we obtain the *Rutherford cross section* :

$$\frac{d\sigma(\theta)}{d\Omega} = \frac{b_c^2}{4 \sin^4(\theta/2)}. \quad (3.7)$$

This formula was devised by Professor Ernest Rutherford in 1911 in order to explain the results of his experiments on the scattering of α particles in a thin layer of gold leaf. By measuring the angular scattering diagram, he successfully estimated the minimum approach distance b_c and showed that it was much smaller than the radius of an atom.

3.3 Momentum transfer cross section

Several physical quantities can be defined on the basis of the differential cross section. The most important are the total cross section, characterising the total number of collisions produced per unit of time, and the transport cross section, characterising the slowing-down of a particle due to the collisions with the other particles in the environment.

The total cross section for a Coulomb potential is obtained by integrating the Rutherford cross section for all scattering angles:

$$\sigma_0 = 2\pi \int \frac{d\sigma(\theta)}{d\Omega} \sin\theta d\theta.$$

It is easy to see that this integral is strongly divergent and that σ_0 tends towards infinity. These are small-angle collisions, i.e. for high impact parameters b , which correspond to distant collisions

that are the cause of the divergence. Here, the calculation is performed for a Coulomb potential. In fact, we have seen that the shielding phenomenon around an ion, resulting from an accumulation of electrons in close proximity to it, leads to a shielded Debye potential, which decreases exponentially with a characteristic decay length that equals the Debye electron length. Here, due to the Debye sheath, it is therefore necessary to introduce a break by introducing a maximum impact parameter, b_{\max} , corresponding to a minimum angle of deflection, θ_{\min} . This maximum impact parameter can be considered to be equal to the Debye length, λ_{De} . According to (3.3), and on the basis of the fact that θ_{\min} is a small angle, it follows that:

$$\frac{b_{\max}}{b_c} = \cot \frac{\theta_{\min}}{2} \approx \frac{2}{\theta_{\min}}. \quad (3.8)$$

It must be understood that the cross section itself is not a measurable physical quantity. We can only measure the result of the passage of a given particle through the plasma. Consequently, there are three different definitions of the mean cross section.

- The measurement of slowing down, relating to the momentum transfer cross section.
- The measurement of angular deflection relating to the transverse scattering cross section.
- The measurement of energy losses relating to the energy loss cross section.

Each of these definitions gives specific expressions for the cross section, the collisional frequency and the mean free path of the particle. All of these definitions will be considered in detail in the second part of the plasma course. Here, we shall consider the most frequent phenomenon – momentum transfer.

Let us consider the slowing down of an electron of velocity v_e , during its propagation through a plasma. In a collision of this electron with an ion of very high mass, $m_i \gg m_e$, it undergoes a deflection θ , without the modulus of the velocity being modified. Consequently, the variation in the amount of movement projected in the initial direction of its trajectory is $\Delta v_{\parallel} = m_e v_e (1 - \cos \theta)$. The angle of deflection θ , corresponds to the impact parameter b given by the formula (3.3). For a period of time Δt , the number of collisions of this type, with an impact parameter of between b and $b + db$, is: $n_i v_e \Delta t 2\pi b db$. According to the definition (3.6), this number of collisions leading to the deflection of the angle θ is expressed as:

$$n_i v_e \Delta t 2\pi \frac{d\sigma(\theta)}{d\Omega} \sin \theta d\theta.$$

To obtain the slowing down of the electron per unit of time, we must therefore calculate the integral for all possible scattering angles:

$$\frac{dm_e v_e}{dt} = - \int m_e v_e (1 - \cos \theta) n_i v_e 2\pi \frac{d\sigma(\theta)}{d\Omega} \sin \theta d\theta = -m_e n_i v_e^2 \sigma_t. \quad (3.9)$$

We therefore introduce the momentum transfer cross section, which will be defined by the following formula:

$$\sigma_t = 2\pi \int_{\theta_{\min}}^{\pi} \frac{d\sigma(\theta)}{d\Omega} (1 - \cos \theta) \sin \theta d\theta = 2\pi b_c^2 \ln \frac{2}{1 - \cos \theta_{\min}}.$$

As $\theta_{\min} \ll 1$, according to the equation (3.8) we ultimately obtain

$$\sigma_t(v) = 4\pi b_c^2 \ln \frac{b_{\max}}{b_c}. \quad (3.10)$$

We can see that the cross section of the Coulombian collisions is a function that is highly sensitive to the electron velocity. The minimum approach distance is proportional to v_e^{-2} , and the cross section therefore decreases in the form of $1/v_e^4$. In contrast to neutral gases, the fastest particles generate fewer collisions in a plasma, because the minimum approach distance diminishes with velocity.

The cross section (3.10) is the product of the surface area of the disc with a radius of the minimum approach distance, and a logarithm. In ideal plasmas, this *Coulombian logarithm* is high, around 10 or more. The most significant contribution therefore results from collisions with a high impact parameter of approximately the Debye length. However, collisions with low impact parameters, of approximately b_c , do not play an important role. This means that in ideal plasmas, collisions only contribute to small deflections. In this way, the particle must undergo several collisions before a significant change in its direction of propagation occurs.

3.4 Mean free path and collisional frequency

The characteristic slowing-down time of an electron is expressed by $\tau_{ei} = 1/n_i v_e \sigma_t$. The inverse of this time defines the collisional frequency, $\nu_{ei} = n_i v_e \sigma_t$. By considering distributed electrons according to a Maxwellian velocity distribution function, we can replace the electron velocity in this relation with the thermal electron velocity, $v_e \simeq v_{Te}$. In this way, we ultimately obtain the expression of the mean electron-ion collisional frequency:

$$\nu_{ei} = \frac{n_i Z^2 e^4 \ln \Lambda}{4\pi \epsilon_0^2 m_e^{1/2} (k_B T_e)^{3/2}}$$

where the quantity $\ln \Lambda = \ln(\lambda_{De}/b_0)$ is called the *Coulombian logarithm*. Kinetic theory leads to a similar expression of the electron-ion collisional frequency that is close, by a small factor, to the following form:

$$\nu_{ei} = \frac{n_i Z^2 e^4 \ln \Lambda}{3(2\pi)^{3/2} \epsilon_0^2 m_e^{1/2} (k_B T_e)^{3/2}}. \quad (3.11)$$

We define the mean free path, which represents the mean distance travelled by the electron during the time $1/\nu_{ei}$ by: $\lambda_{ei} = v_{Te}/\nu_{ei}$. It increases in the form of T_e^2 and this is the reason why hot plasmas are only very slightly collisional.

The electron-electron and ion-ion collisional frequencies are obtained in the same manner. Kinetic theory leads to the following formula:

$$\nu_{\alpha\alpha} = \frac{n_\alpha q_\alpha^4 \ln \Lambda}{12\pi^{3/2} \epsilon_0^2 m_\alpha^{1/2} (k_B T_\alpha)^{3/2}}. \quad (3.12)$$

By comparing these expressions, it can be noted that in a quasi-neutral plasma, the ratio of the electron-ion and electron-electron collisional frequencies is equal to Z . It follows that in plasmas with multi-charged ions, the electron-ion collisions are dominant. For plasmas in equilibrium, where $T_e \simeq T_i$, the ion-ion collisional frequency is lower due to the high mass of the ions in relation to the electron mass, $\nu_{ii}/\nu_{ee} \sim Z^3 \sqrt{m_e/m_i}$. On the other hand, the mean free paths of the electrons and ions do not depend on the masses and they are therefore of the same order of magnitude. The mean free path of the ions is shorter for multi-charged ions.

3.5 Problems

1. Let us consider a collision between two hard, impenetrable spheres of diameter D (like billiard balls). The sphere shown in dotted lines in figure 6 represents the Debye sphere. Show that:



$b db = \frac{1}{4} D^2 \sin \theta d\theta$. Using (3.6), establish that the cross section σ is isotropic, i.e. that it is independent of θ .

2. If we could treat ions as rigid spheres of radius R , and electrons as point features entering into elastic collisions with the ions, what would be the cross section of the collisions between the two species for a given angle? Choose a possible value of R to estimate the Coulombian collisions.
3. Now let us turn our attention to electron-electron collisions. Using the Rutherford cross section, determine the differential cross section σ for an angle of deflection of 90° , with the free path between two collisions at 90° being defined by $\lambda_{ee} = 1/n_e\sigma$. Show that for a conventional kinetic plasma, we have: $r_0 \ll d_e \ll \lambda_{De} \ll \lambda_{ee}$.
4. We obtained the collisional frequency ν_{ei} by considering the amount of electron movement following collisions with ions. What is the value of the collisional frequency relating to the variation in the movement of the ions after collisions with the electrons, ν_{ie} ? Compare ν_{ei} with ν_{ie} . Comment.
5. Calculate the mean electron-ion collisional frequency in a plasma containing several species of ions. State the expression of the mean charge of the ions under these conditions.



HELLENIC
MEDITERRANEAN
UNIVERSITY



université
BORDEAUX



Erasmus+

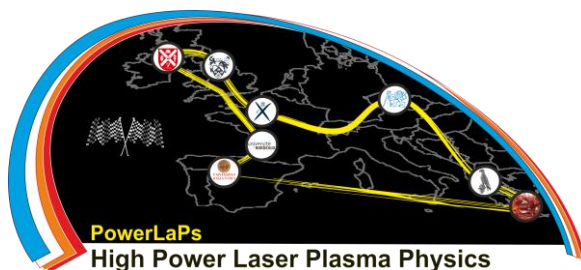
PowerLaPs

Innovative Education & Training in High Power Laser Plasmas

Plasma Physics - Theory and Experiments

Chapter 4: Hydrodynamic description of a plasma

D. Batani, E. d'Humières, J.J. Santos, V.T. Tikhonchuk



Erasmus+

université
de BORDEAUX

4 Hydrodynamic description of a plasma

There are two main approaches to describing a plasma. The *microscopic (kinetic)* approach describes the evolution of the distribution function of the plasma particles. Kinetic theory provides a detailed description, but kinetic equations are very complicated to solve because the distribution function evolves over the course of phases which have three spatial coordinates and three velocity components. The *macroscopic (hydrodynamic)* approach describes the evolution of the plasma's average values: density, average velocity and temperature. Fluid theory gives a limited description of plasma, assuming that the velocity distribution function is always close to a Gaussian. Fluid theory produces results more rapidly and with sufficient precision on a large scale - far superior to the Debye length.

We will look at kinetic theory in the second part of this lecture. Let's begin by looking at the fluid theory of plasma.

4.1 Equations

Fluid equations are determined from the Boltzmann equation with the Lorentz force and the collision term. A demonstration is given in the second part of this lecture. It involves calculating the successive moments of the distribution function. For now we will simply give the expressions of the hydrodynamic equations in their final form, supposing that the plasma is isotropic and the pressure scalar. We categorise the different species of particles based on their density n_α , average velocity \vec{u}_α and temperature T_α .

Particle conservation equation

$$\frac{\partial n_\alpha}{\partial t} + \vec{\nabla} \cdot (n_\alpha \vec{u}_\alpha) = 0. \quad (4.1)$$

Momentum transfer equation (Euler equation)

$$n_\alpha m_\alpha \left(\frac{\partial}{\partial t} + \vec{u}_\alpha \cdot \vec{\nabla} \right) \vec{u}_\alpha = n_\alpha q_\alpha \left(\vec{E} + \vec{u}_\alpha \wedge \vec{B} \right) - \vec{\nabla} p_\alpha + \sum_\beta \vec{R}_{\alpha\beta} \quad (4.2)$$

where $p_\alpha = n_\alpha k_B T_\alpha$ is the kinetic pressure and $\vec{R}_{\alpha\beta}$ represents the friction force. The quantity $d/dt \equiv \partial/\partial t + \vec{u}_\alpha \cdot \vec{\nabla}$ represents drift in relation to time, following the movement of the fluid. This is relevant for the highly mobile electrons whose movement is affected by binary collisions with the ions. For those ions considered to be virtually static, in light of their inertial force, the friction term is often disregarded.

Energy conservation equation

$$\frac{3}{2} n_\alpha k_B \left(\frac{\partial}{\partial t} + \vec{u}_\alpha \cdot \vec{\nabla} \right) T_\alpha + p_\alpha \vec{\nabla} \cdot \vec{u}_\alpha = -\vec{\nabla} \cdot \vec{q}_\alpha + \sum_\beta Q_{\alpha\beta} \quad (4.3)$$

where $Q_{\alpha\beta}$ represents the heat acquired by α species particles as a result of friction with β species particles and \vec{q} is the flow of heat transported by α species particles. In the absence of a magnetic field (applied or self-generated), the thermal conductivity is given by Fourier's theory:

$$\vec{q}_\alpha = -\kappa_\alpha \vec{\nabla} T_\alpha$$

where κ_α is the thermal conductivity of the α species. Due to their high level of mobility, electrons dominate thermal conductivity. In the presence of a magnetic field the heat flow is a tensor quantity, the direction of vector \vec{q}_α is not parallel to the direction of the temperature gradient $\vec{\nabla}T_\alpha$. It is restricted in the direction perpendicular to the magnetic field by the gyration movement around the magnetic field.

The heat flow and energy exchange between particle species are second-order effects. For a simplified approach, we can disregard them and use the equation (4.3) to represent energy conservation:

$$\frac{3}{2} \frac{dT_\alpha}{dt} + T_\alpha \vec{\nabla} \cdot \vec{u}_\alpha = 0.$$

Velocity \vec{u}_α can be eliminated by using the continuity equation (4.1) which is similar in form:

$$\frac{dn_\alpha}{dt} + n_\alpha \vec{\nabla} \cdot \vec{u}_\alpha = 0.$$

Using these two equations, we can determine that there is a simple relationship between density and temperature. This relationship can be expressed in the form:

$$T_\alpha/n_\alpha^{\gamma_\alpha-1} = \text{const} \quad \text{ou} \quad p_\alpha/n_\alpha^{\gamma_\alpha} = \text{const}. \quad (4.4)$$

This is the adiabatic condition, and with the preceding equations we arrive at $\gamma_\alpha = \frac{5}{3}$. This value is the same as that obtained for perfect neutral monatomic gases. For plasmas, it is applicable to three-dimensional flows. We will see later on that, depending on the type of problem, the constant γ_α is 3 for uni-dimensional flows and 1 for isothermal flows.

Plasma can be considered to be a mixture of two fluids, conforming to macroscopic equations: a fluid composed of electrons whose density is n_e and average velocity \vec{u}_e , and a fluid of ions with a density of n_i and average velocity \vec{u}_i . Using the general equations (4.1) and (4.2), we can obtain the equations for the electrons ($q_e = -e$):

$$\frac{\partial n_e}{\partial t} + \vec{\nabla} \cdot (n_e \vec{u}_e) = 0, \quad (4.5)$$

$$\frac{\partial \vec{u}_e}{\partial t} + \vec{u}_e \cdot \vec{\nabla} \vec{u}_e = -\frac{e}{m_e} (\vec{E} + \vec{u}_e \wedge \vec{B}) - \frac{1}{n_e m_e} \vec{\nabla} p_e - \nu_{ei} (\vec{u}_e - \vec{u}_i) \quad (4.6)$$

and for the ions ($q_i = Ze$):

$$\frac{\partial n_i}{\partial t} + \vec{\nabla} \cdot (n_i \vec{u}_i) = 0, \quad (4.7)$$

$$\frac{\partial \vec{u}_i}{\partial t} + \vec{u}_i \cdot \vec{\nabla} \vec{u}_i = \frac{Ze}{m_i} (\vec{E} + \vec{u}_i \wedge \vec{B}) - \frac{1}{n_i m_i} \vec{\nabla} p_i. \quad (4.8)$$

We have ignored the friction force in the equation representing the movement of the ions (4.8) because ions have greater mass and electron collisions have a very minimal effect on ionic velocity. We will see later on that $\nu_{ie} \sim \nu_{ei} m_e/m_i \ll \nu_{ei}$. However we cannot afford to neglect the importance of friction in the electron movement equation (4.6) where ν_{ei} represents the frequency of the effective collisions between electrons and ions (3.11).

To complete this system of equations, we need equations of state which make the connection between pressure values $p_e = n_e k_B T_e$ and $p_i = n_i k_B T_i$ and the other physical quantities. In this case we will use the simple model provided by the equations (4.4):

$$p_e/n_e^{\gamma_e} = \text{const} \quad \text{and} \quad p_i/n_i^{\gamma_i} = \text{const}. \quad (4.9)$$

The γ_e factor of the electron gas is 3 for one-dimensional adiabatic compression and 1 for isothermal compression. We will also assume $\gamma_i = 3$ for the ions because they behave in an adiabatic manner in one dimension. This will be explained later on by kinetic theory.

The hydrodynamic equations are combined with Maxwell's equations

$$\vec{\nabla} \cdot \vec{E} = \rho / \epsilon_0 \quad (4.10)$$

$$\vec{\nabla} \wedge \vec{E} = -\partial_t \vec{B} \quad (4.11)$$

$$\vec{\nabla} \cdot \vec{B} = 0 \quad (4.12)$$

$$\vec{\nabla} \wedge \vec{B} = \mu_0 \vec{j} + \epsilon_0 \mu_0 \partial_t \vec{E} \quad (4.13)$$

via the electrical and magnetic fields, and the charge and current densities. The charge density ρ and current density \vec{j} are self-consistent quantities produced by the plasma itself:

$$\rho = \rho_e + \rho_i = -en_e + Zen_i \quad \text{the total density of the electrical charge,} \quad (4.14)$$

$$\vec{j} = \vec{j}_e + \vec{j}_i = -en_e \vec{u}_e + Zen_i \vec{u}_i \quad \text{total current density} \quad (4.15)$$

4.2 Electromagnetic properties of plasma

Our next objective is to solve the fluid equations, considering the fields \vec{E} and \vec{B} to be known quantities. This will allow us to express the charge and current densities with reference to the electric and magnetic fields and then use them in the Maxwell's equations.

Plasma is an example of a dielectric field, and in this respect possesses a specific property. Plasma sustains electromagnetic waves, it is an undulating movement that appears in the propagation of electric and magnetic fields, coupled with disturbances in the current and electric charge of the plasma. Different types of waves may exist within a plasma, and in this course we will focus on the most simple example: *linear waves* spreading through a homogeneous plasma. We will look at low-amplitude waves which can be considered to act as a slight disturbance to the initial state. These waves can be described by linear equations, and can then be processed using a Fourier analysis. Generally speaking, an external electric field applied to a dielectric medium will be modified by the polarisation of the molecules, which create their own electric field. Consequently, this field will be added to the external field, creating the total field. Using the general electrodynamic formulation, electric displacement $\vec{D} = \epsilon_0 \vec{E} + \vec{P}$ is the sum of the external induction $\epsilon_0 \vec{E}$ and the polarisation of the medium, \vec{P} . The linear polarisation of a dielectric medium is proportional to the applied field:

$$\vec{P} = \epsilon_0 \chi * \vec{E}, \quad (4.16)$$

where χ is the dielectric susceptibility. We can thus determine the electric displacement field \vec{D} :

$$\vec{D} = \epsilon_0 \vec{E} + \vec{P} = \epsilon_0 (1 + \chi) * \vec{E} = \epsilon_0 \epsilon * \vec{E} \quad (4.17)$$

where $\epsilon = 1 + \chi$ is the relative dielectric permittivity. In neutral media these quantities, χ and ϵ , are often considered as constants, but in plasma they depend upon space and time. For example, the polarisation at a given moment t depends upon the values of the field in previous moments, $t' < t$. As a result, the relationships (4.16) and (4.17) are convolution integrals, such as

$$\vec{P}(t) = \epsilon_0 \int_{-\infty}^t \chi(t-t') \vec{E}(t') dt.$$

This is a very common situation, even in neutral media. It is useful to recall that electrical circuits with an alternating current containing condensers and inductors create the same type of relationships.

As a general rule, it is easier to use a Fourier transform, where the convolution relationship (4.17) can be expressed in a simple multiplication:

$$\vec{P}(\omega, \vec{k}) = \epsilon_0 \chi(\omega, \vec{k}) \vec{E}(\omega, \vec{k}), \quad \vec{D}(\omega, \vec{k}) = \epsilon_0 \epsilon(\omega, \vec{k}) \vec{E}(\omega, \vec{k}). \quad (4.18)$$

The same type of relation can be calculated for the density of the electric current. Using a Fourier transform, it can be linked to the electric field:

$$\vec{j}(\omega, \vec{k}) = \sigma(\omega, \vec{k}) \vec{E}(\omega, \vec{k}) \quad (4.19)$$

where $\sigma(\omega, \vec{k})$ is the electrical conductivity. This is Ohm's law. The relation between permittivity and conductivity is simple. Current density is linked to polarisation by the relation: $\vec{j} = \partial \vec{P} / \partial t$, or the Fourier transform

$$\vec{j}(\omega, \vec{k}) = -i\omega \epsilon_0 \chi(\omega, \vec{k}) \vec{E}(\omega, \vec{k}),$$

therefore

$$\sigma = -i\omega \epsilon_0 \chi \quad \text{and} \quad \epsilon = 1 + i\sigma / \epsilon_0 \omega. \quad (4.20)$$

The values of the functions ϵ , σ and χ will be determined from the fluid equations in the next section.

4.3 Linear theory

Hydrodynamic equations, which describe the movement of particles, enable us to calculate the currents and polarisations induced by electric and magnetic fields within plasma. They represent a system of equations whose unknowns are n_e , n_i , \vec{u}_e , \vec{u}_i , p_e , p_i , and whose sources are the fields \vec{E} and \vec{B} . Furthermore, we can discount the non-linear terms which exist within these equations by assuming that the disturbances to the quantities remain very small in relation to the equilibrium quantities. As a result, the differential equations for the unknown quantities are linear, and we can solve them using the Fourier method. All scalar quantities of the plasma, vectorial or tensorial $a(\vec{r}, t)$, will be expressed in the form:

$$a(\vec{r}, t) = a_0 + a^{(1)} \exp(-i\omega t + i\vec{k} \cdot \vec{r})$$

where a_0 represents the quantity without disturbance, homogeneous and time-independent, and $a^{(1)}$ is a first-order disturbance. We can assume that the first-order disturbance is very weak: $|a^{(1)}| \ll |a_0|$.

4.3.1 Linearisation of the equations

Let us consider a plasma in a state of equilibrium: homogeneous, isotropic and stationary, with zero velocity $\vec{u}_{\alpha 0} = 0$, and constant densities $n_{\alpha 0}$ bound by their condition of quasi-neutrality (1.3): $n_{e0} = Z n_{i0}$. By applying the equations (4.5) – (4.8), we can take this homogeneous, stationary plasma and add a non-zero external magnetic field, \vec{B}_0 , while still supposing that the external electric field applied is null, $\vec{E}_0 = 0$.

Now let us suppose that the fields \vec{E} and \vec{B} represent disturbances, $\vec{E}^{(1)}$ and $\vec{B}^{(1)}$. This obviously leads to disturbances in the hydrodynamic quantities: $n_{\alpha}^{(1)}$, $\vec{u}_{\alpha}^{(1)}$ and $p_{\alpha}^{(1)}$. The equations of state (4.9) thus give:

$$\frac{p_{\alpha 0} + p_{\alpha}^{(1)}}{p_{\alpha 0}} = \left(\frac{n_{\alpha 0} + n_{\alpha}^{(1)}}{n_{\alpha 0}} \right)^{\gamma_{\alpha}}.$$

This is the equation of state for the gas. We can determine that

$$\frac{\vec{\nabla} p_{\alpha}^{(1)}}{p_{\alpha 0}} = \gamma_{\alpha} \frac{\vec{\nabla} n_{\alpha}^{(1)}}{n_{\alpha 0}}$$

and as $p_{\alpha 0} = n_{\alpha 0} k_B T_{\alpha 0}$ we are left with: $\vec{\nabla} p_{\alpha}^{(1)} = \gamma_{\alpha} k_B T_{\alpha 0} \vec{\nabla} n_{\alpha}^{(1)}$.

The linearised equations (4.5) - (4.8) for the electrons and ions can be written as follows:

$$\frac{\partial n_e^{(1)}}{\partial t} + n_{e0} \vec{\nabla} \cdot \vec{u}_e^{(1)} = 0, \quad (4.21)$$

$$\frac{\partial \vec{u}_e^{(1)}}{\partial t} = -\frac{e}{m_e} (\vec{E}^{(1)} + \vec{u}_e^{(1)} \wedge \vec{B}_0) - \gamma_e \frac{k_B T_{e0}}{n_{e0} m_e} \vec{\nabla} n_e^{(1)} - \nu_{ei} (\vec{u}_e^{(1)} - \vec{u}_i^{(1)}), \quad (4.22)$$

$$\frac{\partial n_i^{(1)}}{\partial t} + n_{i0} \vec{\nabla} \cdot \vec{u}_i^{(1)} = 0, \quad (4.23)$$

$$\frac{\partial \vec{u}_i^{(1)}}{\partial t} = \frac{Ze}{m_i} (\vec{E}^{(1)} + \vec{u}_i^{(1)} \wedge \vec{B}_0) - \gamma_i \frac{k_B T_{i0}}{n_{i0} m_i} \vec{\nabla} n_i^{(1)}. \quad (4.24)$$

It should be noted that the disturbance in the magnetic field does not appear in these equations. In the linear approach only the electric field solicits a response from the plasma; the disturbance associated with the magnetic field is a second-order term which can be ignored here. Here, the same equations used in the Fourier transform are reduced to the following algebraic equations:

$$-i\omega n_e^{(1)} + in_{e0} \vec{k} \cdot \vec{u}_e^{(1)} = 0, \quad (4.25)$$

$$-i\omega \vec{u}_e^{(1)} = -\frac{e}{m_e} (\vec{E}^{(1)} + \vec{u}_e^{(1)} \wedge \vec{B}_0) - i\vec{k} \gamma_e n_e^{(1)} \frac{k_B T_{e0}}{n_{e0} m_e} - \nu_{ei} (\vec{u}_e^{(1)} - \vec{u}_i^{(1)}), \quad (4.26)$$

$$-i\omega n_i^{(1)} + in_{i0} \vec{k} \cdot \vec{u}_i^{(1)} = 0, \quad (4.27)$$

$$-i\omega \vec{u}_i^{(1)} = \frac{Ze}{m_i} (\vec{E}^{(1)} + \vec{u}_i^{(1)} \wedge \vec{B}_0) - i\vec{k} \gamma_i n_i^{(1)} \frac{k_B T_{i0}}{n_{i0} m_i}. \quad (4.28)$$

We can use this system to calculate fluid velocities, and thus determine the density of total current (4.14):

$$\vec{j}^{(1)} = -en_{e0} \vec{u}_e^{(1)} + Zen_{i0} \vec{u}_i^{(1)} = en_{e0} (\vec{u}_i^{(1)} - \vec{u}_e^{(1)}) \quad (4.29)$$

and, by extension, the electrical conductivity σ .

4.3.2 Electrical conductivity of non-magnetised plasma

Let us start by considering the case of a plasma without an external magnetic field, $\vec{B}_0 = 0$. The equations shown above are linear and contain two vectors: the \vec{k} -vector and the \vec{E} vector. The plasma response will thus depend on the orientation of these two vectors. Generally speaking, we can break down the electric field into two components: one parallel to the wave vector and one perpendicular: $\vec{E} = \vec{E}_l + \vec{E}_{tr}$. We thus end up with two different systems: one for longitudinal movement (parallel to the vector \vec{k}) and the other for the perpendicular movement.

For the perpendicular movement, the velocities are also perpendicular to the \vec{k} -vector, so $\vec{k} \cdot \vec{u}_{\alpha tr}^{(1)} = 0$, and the continuity equations (4.25) and (4.27) predict that the disturbances to density will be zero: $n_{\alpha tr}^{(1)} = 0$. Meanwhile, the movement equations (4.26) and (4.28) give us the fluid velocities:

$$-i\omega \vec{u}_{etr}^{(1)} = -\frac{e}{m_e} \vec{E}_{tr}^{(1)} - \nu_{ei} (\vec{u}_{etr}^{(1)} - \vec{u}_{itr}^{(1)}), \quad (4.30)$$

$$-i\omega \vec{u}_{itr}^{(1)} = \frac{Ze}{m_i} \vec{E}_{tr}^{(1)}. \quad (4.31)$$

As you can see, pressure disturbances are not included in these equations. This is easy to explain when we recall that a pressure disturbance can only be produced by a density disturbance, which is zero in this case. By subtracting these two equations and using the formula (4.29) for the density of the electric current, we finally obtain a clear expression of electrical conductivity in the perpendicular plane:

$$\sigma = \frac{e^2 n_{e0}}{\nu_e - i\omega} \left(\frac{1}{m_e} + \frac{Z}{m_i} \right). \quad (4.32)$$

It contains two contributions: from the electrons and the ions. The former is always dominant, because $Zm_e/m_i \ll 1$. We often ignore the ionic contribution and assume that conductivity comes primarily from the electrons.

Electronic conductivity (4.32) conforms to the standard Drude model; it is proportional to the electron density and depends on the collisional frequency and the electric field frequency. It does not, however, depend on the wave vector. In cases in which we can ignore collisions and the ionic contribution, using the formulae (4.20) and (4.32) we can calculate the dielectric permittivity at high frequencies:

$$\epsilon = 1 - \omega_{pe}^2/\omega^2. \quad (4.33)$$

Let us now return to the longitudinal movement induced by the parallel component of the electric field $\vec{E}_l = E_l \vec{k}/k$. In this case the continuity equations (4.25) and (4.27) give us the relations which connect the density disturbances and the corresponding velocity: $n_{\alpha l}^{(1)} = (k/\omega) n_{\alpha 0} u_{\alpha l}^{(1)}$. By adding these values to the movement equations (4.26) and (4.28) we obtain:

$$-i\omega u_{el}^{(1)} = -\frac{e}{m_e} E_l^{(1)} - i\gamma_e u_{e,l}^{(1)} \frac{k^2}{\omega} \frac{k_B T_{e0}}{m_e} - \nu_{ei} (u_{el}^{(1)} - u_{il}^{(1)}), \quad (4.34)$$

$$-i\omega u_{il}^{(1)} = \frac{Ze}{m_i} E_l^{(1)} - i\gamma_i u_{i,l}^{(1)} \frac{k^2}{\omega} \frac{k_B T_{i0}}{m_i}. \quad (4.35)$$

It is more convenient to write these equations for the electronic $j_{el}^{(1)} = -en_{e0}u_{el}^{(1)}$, and ionic $j_{il}^{(1)} = Zen_{i0}u_{il}^{(1)}$ currents. This gives us:

$$j_{el}^{(1)} = in_{e0} \frac{e^2}{m_e} \frac{\omega}{\omega^2 - \gamma_e k^2 v_{Te}^2} E_l^{(1)} - i \frac{\nu_{ei}\omega}{\omega^2 - \gamma_e k^2 v_{Te}^2} j_{il}^{(1)}.$$

At this point we have introduced the thermal velocity $v_{T\alpha} = \sqrt{k_B T_{\alpha 0}/m_\alpha}$ as per the definition (1.20). Similarly, for the ionic current density:

$$j_{il}^{(1)} = in_{e0} \frac{Ze^2}{m_i} \frac{\omega}{\omega^2 - \gamma_i k^2 v_{Ti}^2} E_l^{(1)}.$$

Adding these two currents together gives us a the expression of the total current density (4.29):

$$j_l^{(1)} = j_{e,l}^{(1)} + j_{i,l}^{(1)} = i\epsilon_0 \omega \sum_{\alpha=e,i} \frac{\omega_{p\alpha}^2}{\omega^2 - \gamma_\alpha k^2 v_{T\alpha}^2} E_l^{(1)} - i \frac{\nu_{ei}\omega}{\omega^2 - \gamma_e k^2 v_{Te}^2} j_{il}^{(1)}$$

where $\omega_{p\alpha}$ is the plasma frequency of the α species. Finally, as $j_l = \sigma_l E_l$ (4.19), as per (4.20), we arrive at a figure for longitudinal dielectric permittivity.

$$\epsilon_l = 1 - \sum_{\alpha=e,i} \frac{\omega_{p\alpha}^2}{\omega^2 - \gamma_\alpha k^2 v_{T\alpha}^2} \left(1 + i \frac{\nu_{ei}\omega}{\omega^2 - \gamma_e k^2 v_{Te}^2} \right)^{-1}. \quad (4.36)$$

This expression is more complex than perpendicular conductivity. First of all, it depends on the frequency ω and the wave vector \vec{k} , and there are also contributions from both particle species, electrons and ions. We can use this expression to determine the longitudinal normal modes of non-magnetised plasma.

4.3.3 Electrical conductivity of plasma in a homogeneous magnetic field

Let us now consider the electrical conductivity of a homogeneous plasma subjected to a uniform magnetic field. To simplify this analysis, we will consider the example of a cool, non-collisional plasma. According to section 4.3.1, plasma disturbances are induced by an alternating electric field. Let us suppose that the latter has a projection of E_{\parallel} in the direction of the external field $\vec{b} = \vec{B}_0/B_0$, and a component in the perpendicular plane, E_{\perp} :

$$\vec{E}^{(1)} = (E_{\parallel}\vec{b} + E_{\perp}\vec{e}_{\perp}) e^{-i\omega t + i\vec{k}\cdot\vec{r}}$$

where \vec{e}_{\perp} is the unit vector in the direction of the electrical field in the perpendicular plane \vec{b} .

As we saw in chapter 2, here, the velocity of the guiding centre \vec{v}_0 of a particle, which represents the overall movements for each species of particle, includes three velocity components: \vec{v}_{\parallel} , \vec{v}_{\perp} , \vec{v}_{\wedge} respectively, following the direction of the magnetic field \vec{b} , the direction of the electric field in the perpendicular plane, \vec{e}_{\perp} and, in the cross-cutting direction, $\vec{b} \wedge \vec{e}_{\perp}$. To solve the disturbance equations (4.25) – (4.28), we break down velocity $\vec{u}_{\alpha}^{(1)}$ into three terms:

$$\vec{u}_{\alpha}^{(1)} = u_{\alpha\parallel}\vec{b} + u_{\alpha\perp}\vec{e}_{\perp} + u_{\alpha\wedge}\vec{b} \wedge \vec{e}_{\perp}.$$

According to this equation (4.26), the movement of a particle in a cold plasma ($T = 0$) can be expressed as follows:

$$-i\omega\vec{u}_{\alpha}^{(1)} = \frac{q_{\alpha}}{m_{\alpha}}\vec{E}^{(1)} - \omega_{c\alpha}\vec{b} \wedge \vec{u}_{\alpha}^{(1)} \quad (4.37)$$

where $\omega_{c\alpha} = q_{\alpha}B_0/m_{\alpha}$ is the cyclotron frequency. This equation can be divided into three components:

$$-i\omega u_{\alpha\parallel} = \frac{q_{\alpha}}{m_{\alpha}}E_{\parallel}, \quad -i\omega u_{\alpha\perp} = \frac{q_{\alpha}}{m_{\alpha}}E_{\perp} + \omega_{c\alpha}u_{\alpha\wedge}, \quad -i\omega u_{\alpha\wedge} = -\omega_{c\alpha}u_{\alpha\perp}.$$

Solving the second and third equations leaves us with:

$$u_{\alpha\parallel} = i\frac{q_{\alpha}}{m_{\alpha}\omega}E_{\parallel}, \quad u_{\alpha\perp} = -i\frac{q_{\alpha}}{m_{\alpha}}\frac{\omega}{\omega_{c\alpha}^2 - \omega^2}E_{\perp}, \quad u_{\alpha\wedge} = -\frac{q_{\alpha}}{m_{\alpha}}\frac{\omega_{c\alpha}}{\omega_{c\alpha}^2 - \omega^2}E_{\perp}. \quad (4.38)$$

For each particle species, we then specify the macroscopic current density: $\vec{j}_{\alpha} = q_{\alpha}n_{\alpha 0}\vec{u}_{\alpha}^{(1)}$, and since this current is proportional to the electric field, we are left with the electrical conductivity of α -species particles as per the formula (4.19). The total electric current density is the sum of all electronic and ionic currents, and as such the total conductivity is the sum of the electronic and ionic conductivities.

Now that we know the conductivity, we can calculate the dielectric permittivity using the formula (4.20). The magnetic field induces anisotropy in the plasma, and as a result dielectric permittivity is a tensor. If we suppose that the magnetic field follows the z axis ($b_z = 1$), the

dielectric permittivity can be expressed as:

$$\begin{aligned}
 \epsilon_{xx} = \epsilon_{yy} \equiv \epsilon_{\perp} &= 1 - \sum_{\alpha=e,i} \frac{\omega_{p\alpha}^2}{\omega^2 - \omega_{c\alpha}^2}; \\
 \epsilon_{zz} \equiv \epsilon_{\parallel} &= 1 - \sum_{\alpha=e,i} \frac{\omega_{p\alpha}^2}{\omega^2}; \quad \epsilon_{xz} = \epsilon_{yz} = 0; \quad \epsilon_{zx} = \epsilon_{zy} = 0; \\
 \epsilon_{xy} = -\epsilon_{yx} \equiv ig &= -i \sum_{\alpha=e,i} \frac{\omega_{p\alpha}^2 \omega_{c\alpha}}{\omega(\omega^2 - \omega_{c\alpha}^2)}.
 \end{aligned} \tag{4.39}$$

We can also present this tensor in matrix form:

$$\epsilon = \begin{vmatrix} \epsilon_{\perp} & ig & 0 \\ -ig & \epsilon_{\perp} & 0 \\ 0 & 0 & \epsilon_{\parallel} \end{vmatrix}. \tag{4.40}$$

The first two diagonal terms are different from the third. Within the limits of the weak magnetic field, $\omega_c \ll \omega$, this difference is a correction, and second-order in ω_c/ω . It represents the *magneto-resistance* of the plasma in the directions perpendicular to the magnetic field. The non-diagonal terms $\pm ig$, which are first-order in ω_c/ω , can be attributed to the current component which is perpendicular to both \vec{E}_0 and \vec{B} . This creates a *Hall effect* which corresponds to the creation of an electric current in the direction perpendicular to the electric field.

Note that the g contributions of the electrons and ions are opposing signs, and the values of the permittivity components depend heavily on the relation between frequency ω , cyclotron frequency, $\omega_{c\alpha}$, and plasma frequency, $\omega_{p\alpha}$. We should also note that the relation between the cyclotron frequencies of the ions and electrons, $\omega_{ci}/|\omega_{ce}| = Zm_e/m_i$ is much smaller than the relation between the plasma frequencies, $\omega_{pi}/\omega_{pe} = (Zm_e/m_i)^{1/2}$. For this reason, the magnetic effects on the ions will be visible at very low frequencies. The zz component of the tensor is not affected by the magnetic field, and can be compared with the formula (4.33).

4.4 Problems

1. Deduce the Maxwell's equations for the following cases:

$$\vec{\nabla} \wedge (\vec{\nabla} \wedge \vec{E}) + \frac{1}{c^2} \frac{\partial^2 \vec{E}}{\partial t^2} = -\mu_0 \frac{\partial \vec{j}}{\partial t}, \tag{4.41}$$

$$\frac{1}{\mu_0} \vec{\nabla} \wedge (\vec{E} \wedge \vec{B}) + \frac{\partial}{\partial t} \left(\frac{1}{2\mu_0} B^2 + \frac{1}{2} \epsilon_0 E^2 \right) = -\vec{j} \cdot \vec{E}. \tag{4.42}$$

What do the different terms in the equation (4.42) stand for?

2. Consider an electromagnetic planewave moving through a plasma. The electric field of the wave can be expressed as follows: $\vec{E} = \text{Re} \vec{E}_0 e^{i\vec{k} \cdot \vec{r} - i\omega t}$. Determine the relations (4.16) – (4.19) the relation (4.20), between dielectric permittivity ϵ and electrical conductivity σ .
3. In order to calculate plasma frequency, we can assume there is a slight disturbance in the electronic density $n_e^{(1)}$ with $n_e^{(1)} \ll n_{e0}$. Using the Poisson's equation $\vec{\nabla} \cdot \vec{E} = \rho/\epsilon_0$, the continuity equation for the electrons (4.21) and the equation for the movement of the electrons in the electric field (4.22) created by the disturbance in density, deduce the temporal oscillation equation for the disturbance in electronic density $n_e^{(1)}$. Consider the example of a cold plasma, $T_e = 0$.



HELLENIC
MEDITERRANEAN
UNIVERSITY



universit 
BORDEAUX



Erasmus+

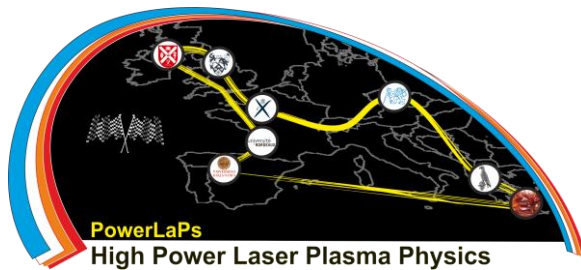
PowerLaPs

Innovative Education & Training in High Power Laser Plasmas

Plasma Physics - Theory and Experiments

Chapter 5: Waves in non-magnetised plasmas

D. Batani, E. d'Humi res, J.J. Santos, V.T. Tikhonchuk



Erasmus+

universit 
de
BORDEAUX

5 Waves in non-magnetised plasmas

Different types of waves exist within plasma, and in this lecture we will be looking at the most straightforward case: linear waves in homogeneous plasma. These are low-amplitude waves which can be likened to a slight disturbance in the initial state of the plasma.

Each of these waves is defined by two major properties: its *dispersion*, the relation between the wave frequency ω and the wave vector \vec{k} , and its *polarisation*, which represents the direction of the wave's electric field in relation to the wave vector and the magnetic field in the plasma. The nature of the electrostatic waves means that the polarisation is longitudinal. In a non-magnetised plasma there are two types of electrostatic waves: high-frequency electronic plasma waves, and low-frequency ionic acoustic waves. Electromagnetic waves are transverse waves, whose polarisation is perpendicular to the wave vector. In a non-magnetised plasma, they exist in the high frequency range, higher than the electronic plasma oscillation.

5.1 Propagation of an electromagnetic wave in a plasma

Here, we are seeking to identify the conditions in which an electromagnetic wave exists in a homogeneous plasma with no external magnetic field. Let us consider the example of a transversal electromagnetic plane wave whose electric and magnetic fields can be expressed in the following manner:

$$\vec{E} = \text{Re } \vec{E}_0 e^{i\vec{k}\cdot\vec{r}-i\omega t}, \quad \vec{B} = \text{Re } \vec{B}_0 e^{i\vec{k}\cdot\vec{r}-i\omega t} \quad (5.1)$$

the polarisation of the field E_0 is perpendicular to the wave vector, $\vec{k} \cdot \vec{E}_0 = 0$. The spatial and temporal evolutions of the electromagnetic fields are described by Maxwell's equations (7.16) – (7.19). In the Fourier transform, they take the following forms:

$$i\epsilon_0 \vec{k} \cdot \vec{E} = \rho; \quad \vec{k} \cdot \vec{B} = 0; \quad (5.2)$$

$$\omega \vec{B} = \vec{k} \wedge \vec{E}; \quad -\frac{\omega}{c^2} \vec{E} = i\mu_0 \vec{j} + \vec{k} \wedge \vec{B}. \quad (5.3)$$

The two first equations are satisfied for a transversal wave, as the density of the charges ρ is necessarily zero, because as we saw in section 4.3.2, a perpendicular electric field does not induce disturbances in the particle density and, as a result, the charge density can only be zero. Now let us consider the equations (5.3). The first expresses the relation between the magnetic and electric fields, and as a closing condition in the second equation, we will use Ohm's Law (4.19) with perpendicular electrical conductivity.

The equation for the electric field is therefore expressed as:

$$-\frac{\omega^2}{c^2} \vec{E} = i\mu_0 \omega \sigma_{\perp} \vec{E} + \vec{k} \wedge \vec{k} \wedge \vec{E}. \quad (5.4)$$

The final term can be simplified using the vectorial identity $\vec{k} \wedge \vec{k} \wedge \vec{E} = \vec{k}(\vec{k} \cdot \vec{E}) - k^2 \vec{E} = -k^2 \vec{E}$. For conductivity, we use the formula (4.32). The electromagnetic field propagation equation is therefore expressed as:

$$\left(c^2 k^2 + \frac{\omega_{pe}^2 \omega}{\omega + i\nu_e} - \omega^2 \right) \vec{E} = 0. \quad (5.5)$$

For this equation to function, as the electric field is non-zero, the term in brackets must be zero. This gives us: *the dispersion equation* for an electromagnetic wave in a plasma:

$$\omega^2 = \omega_{pe}^2 \frac{\omega}{\omega + i\nu_e} + k^2 c^2. \quad (5.6)$$

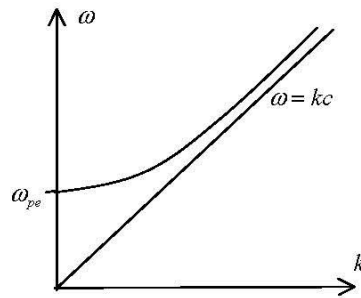


Figure 23: Dispersion curve for an electromagnetic plane wave: the linear asymptote $\omega = kc$ corresponds to the electromagnetic wave in a vacuum.

Assuming that the collisional frequency is low, $\nu_e \ll \omega_{pe}$, we can obtain the frequency of an electromagnetic wave in a plasma:

$$\omega_{em}(k) = \pm \sqrt{\omega_{pe}^2 + k^2 c^2}. \quad (5.7)$$

The dispersion curve $\omega_{em}(k)$ is shown in figure 23. The two signs correspond to the two waves which travel in opposite directions. Both waves have two orthogonal linear polarisations between them in the plane perpendicular to the wave vector.

The presence of the plasma modifies the dispersion of electromagnetic waves. In a vacuum, $\omega_{pe} = 0$, all frequencies are allowed. In a plasma, however, only electromagnetic waves with a frequency that is greater than the plasma frequency can propagate. In a dispersive medium, i.e. when the dielectric permittivity depends on the frequency, $\epsilon(\omega)$, we can define two characteristic wave velocities: phase velocity $v_{ph} = \omega/k$, and group velocity $v_g = \partial\omega/\partial k = kc^2/\omega$. Using the dispersion equation (5.7), we begin by checking that the product of these two speeds for our electromagnetic wave is: $v_{ph}v_g = c^2$. Therefore, v_{ph} is always higher than c , however, $v_g < c$. This latter relation defines the velocity of energy transmission in the wave.

5.1.1 Energy in electromagnetic waves

The energy of electromagnetic waves can be broken down into three terms: the energy of the electric field, the energy of the magnetic field and the energy of the electrons moving in these fields. Assuming that the wave is linearly polarised, the electric field of the wave can be calculated using the formula:

$$E_y(t, x) = E_0 \cos(\omega_{em}t - kx)$$

where $\omega_{em}(k)$ is given by the formula (5.7) and the electric field E_y is perpendicular to the wave vector \vec{k} parallel to the x axis. The expression for the magnetic field can be expressed using the Faraday equation:

$$B_z(t, x) = \frac{k}{\omega_{em}} E_0 \cos(\omega_{em}t - kx).$$

By calculating the mean for the wave period $2\pi/\omega_{em}$, we can obtain the density of electric and magnetic energy:

$$W_E = \frac{1}{2} \epsilon_0 \langle E_y^2 \rangle = \frac{1}{4} \epsilon_0 E_0^2, \quad W_B = \frac{1}{2\mu_0} \langle B_z^2 \rangle = \frac{1}{4} \epsilon_0 \frac{k^2 c^2}{\omega_{em}^2} E_0^2.$$

Using the dispersion equation, we can see that the magnetic energy is weaker than the electric energy, by a factor of $k^2 c^2 / \omega_{em}^2 = 1 - \omega_{pe}^2 / \omega_{em}^2$.

We also need to take the energy of the plasma's electrons into account. Using the linearised electron movement equation (4.30), $\partial_t \vec{v}_e = -(e/m_e) \vec{E}$, the average velocity of the electrons can be expressed as:

$$u_{e,y}(t, x) = -\frac{eE_0}{m_e \omega_{em}} \sin(\omega_{em} t - kx).$$

Therefore, the mean kinetic energy of the electron fluid is

$$W_e = \frac{1}{2} n_{e0} m_e \langle u_{e,y}^2 \rangle = \frac{1}{4} \frac{e^2 n_e}{m_e \omega_{em}^2} E_0^2 = \frac{1}{4} \frac{\omega_{pe}^2}{\omega_{em}^2} \epsilon_0 E_0^2.$$

The presence of the plasma has no effect on the total energy of the electromagnetic wave $W_{em} = W_E + W_B + W_e = \frac{1}{2} \epsilon_0 E_0^2$. It remains the same as it was in the vacuum, but this energy is distributed differently. The energy of the electric field does not change, but some of the magnetic field energy is converted into plasma current energy.

The energy W_{tot} is transported in the plasma at the group velocity $\vec{v}_g = \vec{k} c^2 / \omega_{em}$. The flow of wave energy is given by the Poynting vector, $\vec{S} = \vec{v}_g W_{em}$

$$W_{em} = \frac{\epsilon_0}{2} |E_0|^2, \quad \vec{S} = \frac{c^2 \vec{k}}{\omega} W_{em}, \quad (5.8)$$

so the wave energy is transmitted in the direction of propagation. This is a property of isotropic media. As we shall see in section 6, this is not the case for a magnetised plasma.

5.1.2 Collisional absorption of electromagnetic waves

In the presence of electron-ion collisions, the dispersion equation (5.5) requires complex solutions. The imaginary parts of the frequency and the wave vector correspond to the collisional damping of the electromagnetic wave as it is propagated through the plasma.

Two potential physical situations can be envisaged. One situation consists of considering the problem in its initial condition, i.e. we impose an electric field with the spatial period $2\pi/k$ at the starting point, $t = 0$, throughout the entire space, and we examine its development over time. In this case, we are obliged to consider the wave number k as a real quantity and the solution to the equation (5.6), which within the limits of $\nu_e \ll \omega$ gives us:

$$\omega_{em}(k) = \pm \sqrt{\omega_{pe}^2 + k^2 c^2} - i \frac{\omega_{pe}^2}{2\omega^2} \nu_e \equiv \pm \omega'_{em} - i \gamma_{em}. \quad (5.9)$$

According to our definition (5.1) of the temporal dependency of the fields, the negative part of the frequency corresponds to its decay over time, and thus to the damping of the initial field. This damping is proportional to the collisional frequency and the plasma frequency, so it is proportional to the square of the electronic density. Damping also decreases if the wave frequency increases, so those waves with frequencies close to the plasma frequency experience a stronger damping effect.

As the wave has a complex frequency, its energy becomes a function of time,

$$W_{em}(t) = \frac{\epsilon_0}{2} |E_0|^2 e^{-2\gamma_{em} t}.$$

It is more convenient to express this dependency in the form of a differential equation:

$$\partial_t W_{em} = -2\gamma_{em} W_{em}, \quad (5.10)$$

which represents the energy conservation law for electromagnetic waves in a homogeneous, dissipative medium.

The second option is to consider the problem in spatial terms. Let us suppose that at a given location, $x = 0$, a generator produces an electric field E_y which oscillates at frequency ω . We can now examine the spatial distribution of this field. In this example, we are obliged to consider the frequency ω as a real quantity, and the solution to the equation (5.6) within the limits of $\nu_e \ll \omega$ gives us a complex k value. Supposing that $k = k' + ik''$ and $k' \gg k''$, we obtain:

$$k'_{em} = \pm \frac{1}{c} \sqrt{\omega^2 - \omega_{pe}^2} \quad k''_{em} = \frac{\omega_{pe}^2}{c^2} \frac{\nu_e}{2k'\omega} \equiv \frac{\gamma_{em}}{v_g}. \quad (5.11)$$

The two k' signs correspond to the propagation of the wave in the positive and negative directions along the x axis. The sign of k'' is always the same as $k = k'$. This corresponds to the attenuation of the wave in the direction of propagation. For a plane wave which is propagated along the x axis, this gives us $\vec{E} = \text{Re } \vec{E}_0 e^{ik'x - k''x - i\omega t}$, and as $k'' > 0$, the wave is attenuated exponentially. This is collisional absorption. The energy of this electromagnetic wave diminishes in space:

$$W_{em}(x) = \frac{\epsilon_0}{2} |E_0|^2 e^{-2\gamma_{em}x/v_g}.$$

This dependency, as with the equation (5.10), can be expressed as a differential equation: $\partial_x W_{em} = -2(\gamma_{em}/v_g) W_{em}$. In a more general example in which the wave varies in space and time, this energy conservation equation will take the following form:

$$\partial_t W_{em} + \vec{v}_g \cdot \vec{\nabla} W_{em} = -2\gamma_{em} W_{em}. \quad (5.12)$$

This clearly shows that energy is transmitted at the group velocity, establishing the link between spatial and temporal damping.

We should also note that a real solution for $k = k'$ only exists at high frequencies, $\omega > \omega_{pe}$. For frequencies below the plasma frequency, the equation (5.6) gives us an imaginary solution for $k = k' = \pm(i/c) \sqrt{\omega_{pe}^2 - \omega^2}$, even if there are no collisions. But this solution does not correspond to absorption. This is *non-propagation*, the electric field created by the generator cannot penetrate the plasma, but it is attenuated exponentially over the distance $1/|k| = c/\sqrt{\omega_{pe}^2 - \omega^2}$. This is the *skin effect*. It arises because the external electric field is shielded by the current of free electrons induced in the plasma.

5.2 Electrostatic plasma waves in hot plasma

An electrostatic wave is a *longitudinal wave* (its electric field $\vec{E} = \text{Re } \vec{E}_0 e^{-i\omega t + i\vec{k} \cdot \vec{r}}$ is parallel to the wave vector \vec{k}). The propagation of this wave contributes to a compression (as with sound waves in gas), and thus to a disturbance in density and pressure. Moreover, the electrostatic wave does not contain a magnetic field. This can be seen in the Maxwell's equations (5.2) et (5.2). Bearing in mind that $\vec{k} \wedge \vec{E}_0 = 0$, we can determine from the equations (5.2) that $\vec{B} = 0$ and

$$\epsilon_0 \omega \vec{E} + i \vec{j} = 0. \quad (5.13)$$

This is equivalent to the Poisson's equation $i \epsilon_0 \vec{k} \cdot \vec{E} = \rho$, due to the fact that charge density and current density are linked by the continuity equation (4.1), $\omega \rho = \vec{k} \cdot \vec{j}$.

In addition, by using the relation between current density and polarisation, $\vec{j} = -i\omega \vec{P}$ and the definition of dielectric permittivity, we obtain the following equation for longitudinal waves $\epsilon_l E = 0$, i.e.

$$\epsilon_l(\omega, \vec{k}) = 0. \quad (5.14)$$

The solutions to this equation represent the eigen modes of plasmas. We can define two different frequency domains. For high-frequency waves, $\omega \gg kv_{Te}$, compression is adiabatic and one-dimensional, and as such we can use $\gamma_e = 3$. At lower frequencies, however, where $\omega \ll kv_{Te}$, compression is isothermal and gives us $\gamma_e = 1$.

5.2.1 Plasma oscillation

In high frequencies and in the example $\nu_e \ll \omega$, the general formula for parallel dielectric permittivity (4.36) takes on a simpler form:

$$\epsilon_l = 1 - \sum_{\alpha=e,i} \frac{\omega_{p\alpha}^2}{\omega^2} \left(1 + \frac{3k^2 v_{T\alpha}^2}{\omega^2} - i \frac{\nu_{e\alpha}}{\omega} \right). \quad (5.15)$$

One can clearly see that in a cold plasma $T_e = T_i = 0$ with no collisions $\nu_{ei} = 0$, the equation (5.14) would have a simple solution:

$$\omega^2 = \omega_{pe}^2 + \omega_{pi}^2 \approx \omega_{pe}^2.$$

These are essentially electronic oscillations, as the contribution made by the ions is negligible on account of their inertia. The dispersion curve $\omega(k)$ is shown in figure 34.

The difference in a hot plasma comes from the thermal correction term for the plasma's characteristic frequency. The high-frequency solution corresponds to the condition $\omega \approx \omega_{pe} \gg kv_{Te}, \nu_{ei}$. We can therefore ignore the ionic contribution in (5.15), which gives us:

$$\omega_{es}(k) = \pm \omega_{pe} \left(1 + \frac{3}{2} k^2 v_{Te}^2 \right) - \frac{i}{2} \nu_{ei}. \quad (5.16)$$

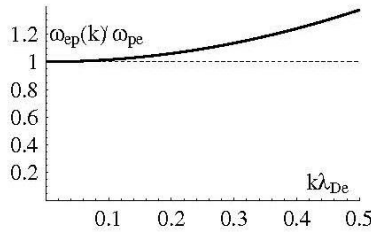


Figure 24: Dispersion curve for the Langmuir wave. The dotted line represents the electronic plasma frequency.

This is the dispersion equation for plasma oscillations in hot plasma. These oscillations are also known as Langmuir waves, they represent the oscillations in an electric charge caused by the oscillation of electrons around immobile ions, as we saw in section 1.7. The damping of these waves is caused by electron collisions.

Kinetic theory tells us that these waves exist in the case of $k\lambda_{De} \ll 1$. In the opposite scenario $k\lambda_{De} \gtrsim 1$, the adiabatic compression hypothesis does not apply. The oscillation is heavily damped by its interaction with the electrons.

5.2.2 Electronic plasma wave oscillation

Let us suppose that a Langmuir wave of amplitude E_0 is excited. Using the Poisson's equation for the electric field $E_x = E_0 \cos(\omega_{es}t - kx)$, we can calculate the disturbance in electronic density $n_e^{(1)}$ caused by the electric field:

$$en_e^{(1)} = -\epsilon_0 k E_0 \sin(\omega_{es}t - kx).$$

The maximum density is delayed by a quarter-period in space in relation to the field maximum. We can use the continuity equation to determine the electron velocity: $ku_e^{(1)} = \omega_{es}n_e^{(1)}$. This value has the same phase as the density disturbance.

The energy of the Langmuir waves is divided between the electric field and the kinetic energy of the electrons, $\frac{1}{2}\epsilon_0 E^2 + \frac{1}{2}n_e m_e (u_e^{(1)})^2$. By adding these two terms together, we can see that

electrostatic energy oscillates in the form of $\cos^2(\omega t - kx)$ and the kinetic energy of the electrons in the form of $\sin^2(\omega t - kx)$, although the coefficients are identical $\frac{1}{2}\epsilon_0 E_0^2 = \frac{1}{2}n_e m_e (\epsilon_0^2 \omega_{es}^2 / e^2) E_0^2$, if we take account of the dispersion equation: $\omega_{es}^2 \simeq \omega_{pe}^2$. As a result, the plasma waves correspond to the oscillation in energy between the energy of the electric field and the kinetic energy of the electrons. By calculating the mean for the plasma wave period, we find that half of the energy is stored in the form of kinetic energy in the electrons and the other half as energy in the electric field.

According to the formula (5.16), the group velocity of the plasma oscillations $\vec{v}_g = 3\vec{k}v_{Te}^2/\omega$ is very weak, below the thermal velocity of the electrons and, of course, the velocity of light. Therefore the Poynting vector is small, $\vec{S}_{es} = \vec{v}_g W_{es}$ and these waves do not transmit much energy, although the energy density W_{es} may be substantial.

5.2.3 Ionic acoustic waves

There is also a solution to the low-frequency equation (5.14), $kv_{Te} \gg \omega \gg kv_{Ti}$. This branch is called the ionic acoustic wave. The phase velocity of this wave falls between the electron and ion thermal velocities. This allows us to take $\gamma_e = 1$ and $\gamma_i = 3$ and ignore ω^2 and ωv_{ei} in front of $k^2 v_{Te}^2$ in the electronic part of the formula (4.36). The dielectric permittivity (4.36) is thus:

$$\epsilon_l = 1 + \frac{1}{k^2 \lambda_{De}^2} - \frac{\omega_{pi}^2}{\omega^2 - 3k^2 v_{Ti}^2}$$

using the relation $\lambda_{De} = v_{Te}/\omega_{pe}$ for the Debye length of the electrons. We can see that, in this domain, the electrons and the ions behave completely differently. The contribution of the electrons in $\epsilon_{||}$ does not depend on the frequency, but on the number of waves k . This tells us that the electrons are more or less static, shielding the electric field created by the ions, in a process similar to the Debye shielding of static ions 1.4.1. However, the ions contribute dynamically, like electrons in high-frequency conditions.

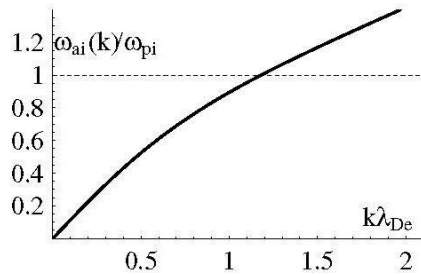


Figure 25: Dispersion curve for the ionic acoustic wave of $ZT_e/T_i = 10$. The dotted line represents the ionic plasma frequency.

The general solution to the dispersion equation (5.14) in the low-frequency field is shown in figure 35. The frequency of this wave is of the same order as the ionic plasma frequency and depends heavily upon k :

$$\omega_{ai}^2 = \frac{k^2 c_s^2}{1 + k^2 \lambda_{De}^2} + 3k^2 v_{Ti}^2. \quad (5.17)$$

In this equation, $c_s = \omega_{pi} \lambda_{De} = \sqrt{Zk_B T_e / m_i}$ represents the speed of sound in the plasma.

There are two important limits to this dispersion. The long wavelength limit, $k^2 \lambda_{De}^2 \ll 1$, which corresponds to the quasi-linear dispersion,

$$\omega_{ai}(k) \approx \pm |k| v_s \left(1 - k^2 \lambda_{De}^2 \frac{c_s^2}{2v_s^2} \right) \quad (5.18)$$

where $v_s = \sqrt{c_s^2 + 3v_{Ti}^2}$. This dispersion is reminiscent of the dispersion of an acoustic wave in a gaseous medium, and the velocity v_s acts as the speed of sound. This is also known as a pseudo-sound wave. The analogy goes further still. Ionic acoustic waves up to $k^2 \lambda_{De}^2 \ll 1$ are quasi-neutral density oscillations, because up to this limit electrons and ions oscillate in phase $n_e^{(1)} \simeq Z n_i^{(1)}$, and the electric field is weak.

Nonetheless, there is a difference between neutral sound waves and ionic acoustic waves. The condition required for the latter to exist is $v_s \gg v_{Ti}$. This condition can only be satisfied in a non-isothermal plasma where $ZT_e \gg 3T_i$. Kinetic theory tells us that ionic acoustic waves cannot exist in a plasma in thermal equilibrium where $T_i = T_e$ because the damping effect is too strong.

The mode (5.17) in the field of shorter wavelengths, $k^2 \lambda_{De}^2 \gtrsim 1$, is known as an ionic plasma wave. Up to this limit its dispersion is:

$$\omega_{ai}(k) = \pm \omega_{pi} \left(1 + \frac{3}{2} k^2 \lambda_{Di}^2 - \frac{1}{2k^2 \lambda_{De}^2} \right). \quad (5.19)$$

The dispersion of this wave is similar to the dispersion of Langmuir waves (5.16). Since the wavelength is shorter than the Debye length, the electrons cannot shield the electric field. So below this limit, disturbances to charge density come from the ions, while disturbances in electron density are much smaller $n_e^{(1)} \ll Zn_i^{(1)}$.

5.2.4 The energy of ionic acoustic waves

Let us suppose that an ionic acoustic wave is excited with the electric field $E_x = E_0 \cos(\omega_{ait} - kx)$. Let us examine how the other quantities are connected to E_x within the confines of long wavelengths, $k^2 \lambda_{De}^2 \ll 1$. For electronic and ionic velocities, we use the equations: (4.34) and (4.35). Bearing in mind that $\omega_{ai} \ll \omega_{pi}, kv_{Te}$, for the electrons we obtain:

$$n_e^{(1)} = \frac{en_e0}{k k_B T_{e0}} E_0 \sin(\omega_{ait} - kx), \quad u_e^{(1)} = \frac{e\omega_{ai}}{k^2 k_B T_{e0}} E_0 \sin(\omega_{ait} - kx). \quad (5.20)$$

For the ions, also bearing in mind that $\omega_{ai} \gg kv_{Ti}$, this gives us:

$$n_i^{(1)} = \frac{Ze k}{m_i \omega_{ai}^2} E_0 \sin(\omega_{ait} - kx), \quad u_i^{(1)} = \frac{Ze}{m_i \omega_{ai}} E_0 \sin(\omega_{ait} - kx). \quad (5.21)$$

Using the dispersion equation (9.42) $\omega_{ai}^2 \simeq k^2 v_s^2$, we can see that the amplitudes of the electronic and ionic disturbances are very similar, $u_i^{(1)} \approx u_e^{(1)}$ and $n_e^{(1)} \approx Zn_i^{(1)}$. So the electric current and charge density are very low.

With their substantial mass, the ions contribute to the kinetic energy of the wave,

$$W_i = \frac{1}{2} n_{i0} m_i \left(u_i^{(1)} \right)^2 = \frac{1}{2} \frac{\omega_{pi}^2}{\omega_{ai}^2} \epsilon_0 E_0^2 \sin^2(\omega_{ait} - kx).$$

Their energy is higher by a factor of $\omega_{pi}^2/\omega_{ai}^2 \simeq 1/k^2 \lambda_{De}^2 \gg 1$ than the energy of the electric field, $W_E = \frac{1}{2} \epsilon_0 E_0^2 \cos^2(\omega_{ait} - kx)$. The contribution of the electrons is linked to the potential energy of the wave. According to the law of thermodynamics, the effect of the pressure force generates a surplus of internal energy, $\delta W = -P \delta V$, where δV is the change in elementary volume. In this case, the pressure is linked to the thermal agitation of the electrons, $P^{(1)} = k_B T_{e0} n_e^{(1)}$ and the change in volume is $\delta V = -n_e^{(1)}/n_{e0}$. So for the potential (internal) energy of the wave, we determine that:

$$W_e = \frac{1}{2} \frac{k_B T_{e0}}{n_{e0}} \left(n_e^{(1)} \right)^2 = \frac{1}{2} \frac{1}{k^2 \lambda_{De}^2} \epsilon_0 E_0^2 \sin^2(\omega_{ait} - kx).$$

By calculating the mean throughout the ionic acoustic wave period, we find that the energy contained in the electrons is equal to that contained in the ions. So this wave represents the oscillations in the kinetic energy of the ions and the pressure of the plasma caused by the thermal agitation of the electrons, while the energy of the electrostatic field is weak, below $k^2 \lambda_{De}^2 \ll 1$. However, within the limit $k^2 \lambda_{De}^2 \ll 1$, the energy of the electrons is weak and the oscillations occur between the kinetic energy of the ions and the electric field.



5.3 Problems

1. On the basis of the phase velocity $v_{ph} = \omega/k$, (5.7), determine the group velocity $v_g = \partial\omega/\partial k$. From this, establish that $v_{ph}v_g = c^2$. Establish the expression of the propagation index $N = c/v_{ph} = kc/\omega$. What can we say about the wave for $\omega_{pe} \gtrsim \omega$?
2. Consider $\omega^2 = n_c e^2 / m_e \epsilon_0$ where n_c is the wave cut-off density, or the critical plasma density. From this, determine the expression of the plasma index according to n_{e0}/n_c . Demonstrate that for $n_{e0} \ll n_c$, the index can be simply expressed as $N \approx 1 - n_{e0}/2n_c$. Show that the electrical permittivity ϵ can be expressed as: $\epsilon = N^2 = 1 - \omega_{pe}^2/\omega^2$. Note that the plasma propagation index is less than 1.
3. Based on the fluid equations for the electrons, and the Poisson's equation, and assuming that the plasma is cold ($T_e = 0$), calculate the plasma frequency by determining the movement of the electrons (assume that the ions are immobile). Compare the average kinetic energy of the electrons and the energy of the electric field.
4. Consider an electric plasma wave moving through a homogeneous plasma with a temperature of $k_B T_e = 100$ eV, electronic density of $n_e = 10^{16} \text{ m}^{-3}$, and frequency of 1.1 GHz. What is the wavelength in cm?
5. A space shuttle returning to earth suffers a communication breakdown due to the fact that a plasma is generated by the shock wave in front of the shuttle. If the radio frequency is 300 MHz, what is the minimum value of n_e during the communication black-out?
6. Calculate the dispersion relation of ionic acoustic waves using the fluid equations. Use the quasi-neutrality condition instead of the Poisson's equation. Compare the kinetic energy of the ions with the energy of the electric field. Comment on the difference with the plasma wave.



HELLENIC
MEDITERRANEAN
UNIVERSITY



universit 
BORDEAUX



Erasmus+

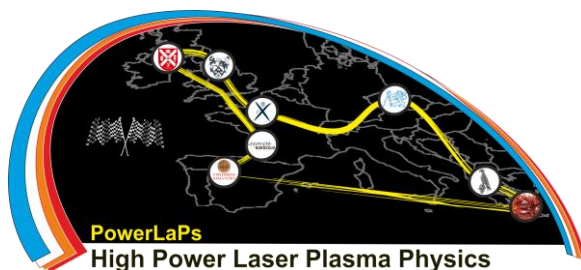
PowerLaPs

Innovative Education & Training in High Power Laser Plasmas

Plasma Physics - Theory and Experiments

Chapter 6: Electromagnetic waves into magnetised plasmas

M. Tatarakis



Erasmus+

HELLENIC
MEDITERRANEAN
UNIVERSITY

6. The propagation of electromagnetic waves into magnetised plasmas

6.1 Magnetised plasma

Both the z-pinch and laser produced plasmas are magnetised. The z-pinch because of the current which flows in it and generates an azimuthal magnetic field and the laser produced plasmas due to currents generated in the blow off plasma. Waves propagating in a magnetised plasma are important because they determine the plasma characteristics and can also be used as diagnostic purposes. In order to understand the propagation of an electromagnetic wave in a magnetised plasma we start from Maxwell's equations:

$$\nabla \cdot \mathbf{E} = \frac{\rho_f}{\epsilon_0} \quad (6.1)$$

$$\nabla \cdot \mathbf{B} = 0 \quad (6.2)$$

$$\nabla \times \mathbf{E} = -\frac{\partial \mathbf{B}}{\partial t} \quad (6.3)$$

$$\nabla \times \mathbf{B} = \mu_0 \left(\mathbf{j}_f + \epsilon_0 \frac{\partial \mathbf{E}}{\partial t} \right) \quad (6.4)$$

where \mathbf{E} and \mathbf{B} are the electric and magnetic field vectors respectively, ϵ_0 and μ_0 are the permittivity and permeability of free space respectively, \mathbf{j}_f is the free electric current density and ρ_f is the free volume charge density.

The important equations for our purpose are the (6.3) and (6.4) where all the electromagnetic properties of the plasma appear explicitly in the current density \mathbf{j} . To eliminate \mathbf{B} we take the $\nabla \times$ of equation (6.3) and the $\partial/\partial t$ of equation (6.4) and find:

$$\nabla \times \nabla \times \mathbf{E} = -\frac{\partial}{\partial t} \left[\mu_0 \mathbf{j} + \epsilon_0 \mu_0 \frac{\partial \mathbf{E}}{\partial t} \right] \quad (6.5)$$

In order to proceed we need to assume that the current is a linear function of the electric field which means that if a variation \mathbf{E}_1 of the electric field gives rise to a current \mathbf{j}_1 and similarly

a variation \mathbf{E}_2 to a current \mathbf{j}_2 , then a variation of $\mathbf{E}_1 + \mathbf{E}_2$ gives rise to a current $\mathbf{j}_1 + \mathbf{j}_2$. We also assume that the plasma is homogeneous in space and time. This means that the dielectric constant $\boldsymbol{\epsilon}$ and the electric conductivity $\boldsymbol{\sigma}$ are independent of the position \mathbf{r} and time t . Generally, a plasma is an anisotropic medium, thus the conductivity $\boldsymbol{\sigma}$ is a tensor. Because of the above assumptions it is possible to Fourier analyse the electric field and the current so that,

$$\mathbf{E}(\mathbf{r}, t) = \int \mathbf{E}(\mathbf{k}, t) e^{i(\mathbf{k} \cdot \mathbf{r} - \omega t)} d^3 \mathbf{k} d\omega$$

$$\mathbf{j}(\mathbf{r}, t) = \int \mathbf{j}(\mathbf{k}, t) e^{i(\mathbf{k} \cdot \mathbf{r} - \omega t)} d^3 \mathbf{k} d\omega$$

Each Fourier mode can be treated separately since each satisfies equation (6.5). In order to have a closed system of equations, we need to know how the electromagnetic field influences the current. The assumption of linearity mentioned above allows us to write the relationship between the current density and the electric field for each Fourier mode as $\mathbf{j}(\mathbf{k}, \omega) = \boldsymbol{\sigma}(\mathbf{k}, \omega) \cdot \mathbf{E}(\mathbf{k}, \omega)$ or $\mathbf{j}_r = s_{rs} \mathbf{E}_s$. This is usually referred to as the Ohm's law.

The wave equation (6.5) now becomes for each Fourier mode,

$$\mathbf{k} \times (\mathbf{k} \times \mathbf{E}) = -i\omega(\boldsymbol{\mu}_0 \boldsymbol{\sigma} \cdot \mathbf{E} - \epsilon_0 \boldsymbol{\mu}_0 i\omega \mathbf{E}) \quad (6.6)$$

Noting that $\mathbf{k} \times (\mathbf{k} \times \mathbf{E}) = (\mathbf{k} \cdot \mathbf{E})\mathbf{E} - (\mathbf{k} \cdot \mathbf{k})\mathbf{E}$ equation (6.6) can be written as,

$$\left(\mathbf{k}\mathbf{k} - k^2 \mathbf{1} + \frac{\omega^2}{c^2} \boldsymbol{\epsilon} \right) \cdot \mathbf{E} = 0 \quad (6.7)$$

where $\mathbf{1}$ is the unit matrix and $\boldsymbol{\epsilon}$ is the dielectric tensor,

$$\boldsymbol{\epsilon} = \left(\mathbf{1} + \frac{i}{\omega \epsilon_0} \boldsymbol{\sigma} \right) \quad (6.8)$$

From equation (6.7) three homogeneous equations, one for each coordinate can be written. In order to derive a non-zero solution from these equations, the determinant of the matrix of coefficients must be equal to zero,

$$\det\left(\mathbf{k}\mathbf{k} - k^2\mathbf{1} + \frac{\omega^2}{c^2}\boldsymbol{\varepsilon}\right) = 0 \quad (6.9)$$

Equation (6.9) is the dispersion relation.

The plasma conductivity tensor must be calculated and hence the permittivity. For this purpose, the **cold plasma approximation** is used where the thermal motions of electrons and ions are considered to be negligible ($T_e=T_i=0$). So, the electrons and ions are taken to be at rest except for motions induced by the waves. Collisions are neglected as well.

We assume a uniform external static magnetic field \mathbf{B}_0 . The equation of motion is:

$$m_e \frac{\partial \mathbf{v}}{\partial t} = -e(\mathbf{E} + \mathbf{v} \times \mathbf{B}_0) \quad (6.10)$$

where the second order term involving $\mathbf{v} \times \mathbf{B}$ and the term $\mathbf{v} \cdot \nabla \mathbf{v}$ are neglected since we are treating fluctuations only in the linear approximation.

Because of the cold plasma approximation the velocity is harmonic in time for a single Fourier wave mode. Therefore,

$$\mathbf{v}(\mathbf{r}, t) = \mathbf{v}(\mathbf{r})e^{-i\omega t} \quad (6.11)$$

For convenience we choose \mathbf{B}_0 to be in the z direction, $\mathbf{B}_0=(0,0,B_0)$ as shown in Figure 6.1. Then on considering Fourier components equation (6.10) becomes,

$$\begin{aligned}
 -m_e i\omega v_x &= -eE_x - eB_0 v_y \\
 -m_e i\omega v_y &= -eE_y + eB_0 v_x \\
 -m_e i\omega v_z &= -eE_z
 \end{aligned} \tag{6.12}$$

If we solve for v_x , v_y , v_z we have:

$$\begin{aligned}
 v_x &= \frac{-ie}{\omega m_e} \frac{1}{\left(1 - \frac{\Omega^2}{\omega^2}\right)} \left[E_x - i \frac{\Omega}{\omega} E_y \right] \\
 v_y &= \frac{-ie}{\omega m_e} \frac{1}{\left(1 - \frac{\Omega^2}{\omega^2}\right)} \left[i \frac{\Omega}{\omega} E_x + E_y \right] \\
 v_z &= \frac{-ie}{\omega m_e} E_z
 \end{aligned} \tag{6.13}$$

where $\Omega = eB_0/m_e$ is the electron cyclotron frequency. Writing current as $\mathbf{j} = -en_e \mathbf{v} = \boldsymbol{\sigma} \mathbf{E}$ the conductivity tensor is:

$$\boldsymbol{\sigma} = \frac{in_e e^2}{m_e \omega} \frac{1}{1 - \frac{\Omega^2}{\omega^2}} \begin{bmatrix} 1 & \frac{-i\Omega}{\omega} & 0 \\ \frac{i\Omega}{\omega} & 1 & 0 \\ 0 & 0 & 1 - \frac{\Omega^2}{\omega^2} \end{bmatrix} \tag{6.14}$$

This is the electron current conductivity. The ions can be treated in exactly the same way and an identical equation is obtained with the ion mass, charge and density parameters instead of the electron ones. Then $\boldsymbol{\sigma}_{\text{tot}} = \boldsymbol{\sigma}_e + \boldsymbol{\sigma}_i$.

Having the conductivity tensor, the dielectric tensor can be found from equation (6.8). So,

$$\boldsymbol{\varepsilon} = \begin{bmatrix} 1 - \frac{\omega_{pe}^2}{\omega^2 - \Omega^2} & \frac{i\omega_{pe}^2\Omega}{\omega(\omega^2 - \Omega^2)} & 0 \\ \frac{-i\omega_{pe}^2\Omega}{\omega(\omega^2 - \Omega^2)} & 1 - \frac{\omega_{pe}^2}{\omega^2 - \Omega^2} & 0 \\ 0 & 0 & 1 - \frac{\omega_{pe}^2}{\omega^2} \end{bmatrix} \quad (6.15)$$

where $\omega_{pe} = \sqrt{\frac{n_e e^2}{\varepsilon_0 m_e}}$ is the electron plasma frequency. In general, if we want to consider and

the ion contribution for the dielectric tensor we just add the same terms but with the ions parameters and we have,

$$\begin{aligned} \varepsilon_{11} = \varepsilon_{22} &= 1 - \sum_s \frac{\omega_{ps}^2}{\omega^2 - \Omega_s^2} \\ \varepsilon_{12} = -\varepsilon_{21} &= -i \sum_s \frac{\omega_{ps}^2 \Omega_s}{\omega(\omega^2 - \Omega_s^2)} \\ \varepsilon_{33} &= 1 - \sum_s \frac{\omega_{ps}^2}{\omega^2} \end{aligned} \quad (6.16)$$

where the index s indicates the species of the plasma ($s=e$ for electrons and $s=i$ for ions). Because $m_i \gg m_e$ the ion contribution is small provided the frequency is high enough.

Now that the dielectric tensor is known we can solve equation 6.9 to find the characteristic waves which can propagate in the plasma. Without loss of generality, we orient the system of coordinates so that $k_x=0$, which means $\mathbf{k} = k(0, \sin q, \cos q)$, where q is the angle between \mathbf{k} and \mathbf{B}_0 as shown in figure 6.1.

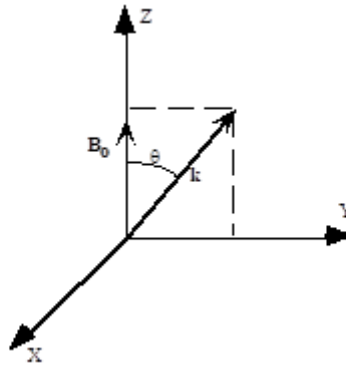


Figure 6.1 Coordinate system for wave propagation in plasma

We also define the non-dimensional quantities $\alpha = \frac{\omega_{pe}^2}{\omega^2}$, $\beta = \frac{\Omega}{\omega}$ and the refractive index $\eta = \frac{kc}{\omega}$. Then by solving equation (6.9) the determinant becomes:

$$\begin{vmatrix} -k^2 + \frac{\omega^2}{c^2} \varepsilon_{11} & \frac{\omega^2}{c^2} \varepsilon_{12} & \frac{\omega^2}{c^2} \varepsilon_{13} \\ \frac{\omega^2}{c^2} \varepsilon_{12} & -k^2 + k^2 \sin^2 \theta + \frac{\omega^2}{c^2} \varepsilon_{22} & k^2 \sin \theta \cos \theta + \frac{\omega^2}{c^2} \varepsilon_{23} \\ \frac{\omega^2}{c^2} \varepsilon_{31} & k^2 \sin \theta \cos \theta + \frac{\omega^2}{c^2} \varepsilon_{32} & -k^2 + k^2 \cos^2 \theta + \frac{\omega^2}{c^2} \varepsilon_{33} \end{vmatrix} = 0 \quad (6.17)$$

By substituting the dielectric elements from equation (6.15) and using the non-dimensional quantities defined above the determinant becomes,

$$\begin{vmatrix} -\eta^2 + 1 - \frac{\alpha}{1 - \beta^2} & \frac{i\alpha\beta}{1 - \beta^2} & 0 \\ -\frac{i\alpha\beta}{1 - \beta^2} & -\eta^2 \cos^2 \theta + 1 - \frac{\alpha}{1 - \beta^2} & \eta^2 \sin \theta \cos \theta \\ 0 & \eta^2 \sin \theta \cos \theta & -\eta^2 \sin^2 \theta + 1 - \alpha \end{vmatrix} = 0 \quad (6.18)$$

We see that in the cold plasma approximation \mathbf{e} is independent of the direction of the \mathbf{k} , thus this dispersion relation is a quadratic equation for k^2 and therefore for h^2 . Solving equation (6.18) we find,

$$\eta^2 = 1 - \frac{\alpha(1-\alpha)}{1-\alpha - \frac{1}{2}\beta^2 \sin^2 \theta \pm \sqrt{\left[\left(\frac{1}{2}\beta^2 \sin^2 \theta\right)^2 + (1-\alpha)^2 \beta^2 \cos^2 \theta\right]}} \quad (6.19)$$

This is the so called **Appleton-Hartree formula** for the refractive index. In order to understand the properties of the waves that can propagate in the cold plasma some special cases will be discussed.

6.2 Isotropic plasma

Let's consider a plasma without an external magnetic field \mathbf{B}_0 . Then $W=0$ and the dielectric tensor can be written as,

$$\boldsymbol{\varepsilon} = \begin{bmatrix} 1 - \frac{\omega_{pe}^2}{\omega^2} & 0 & 0 \\ 0 & 1 - \frac{\omega_{pe}^2}{\omega^2} & 0 \\ 0 & 0 & 1 - \frac{\omega_{pe}^2}{\omega^2} \end{bmatrix} \quad (6.20)$$

We can see that the dielectric tensor is diagonal with all three elements equal, $\varepsilon_{11} = \varepsilon_{22} = \varepsilon_{33} = 1 - \frac{\omega_{pe}^2}{\omega^2} = \varepsilon$. Thus the plasma is isotropic. Using equation (6.20) to find the dispersion relation from equation (6.9) we obtain, assuming, without loss of generality, that \mathbf{k} is along the z-axis,

$$\begin{vmatrix} -k^2 + \frac{\omega^2}{c^2} \varepsilon & 0 & 0 \\ 0 & -k^2 + \frac{\omega^2}{c^2} \varepsilon & 0 \\ 0 & 0 & \frac{\omega^2}{c^2} \varepsilon \end{vmatrix} = 0 \quad (6.21)$$

The solutions can easily be found:

$$-k^2 + \frac{\omega^2}{c^2} \varepsilon = 0 \quad \mathbf{E} \text{ transverse} \quad (6.22)$$

$$\frac{\omega^2}{c^2} \varepsilon = 0 \quad \mathbf{E} \text{ longitudinal} \quad (6.23)$$

There are two different modes of wave propagation. The transverse mode has a dispersion relation which can be written as $\eta \equiv \frac{kc}{\omega} = \varepsilon^{1/2}$ and is the familiar expression of simple optics.

The longitudinal mode, for which the electric field is parallel to the wave vector is governed by the dispersion relation $\omega^2 = \omega_{pe}^2$. This mode corresponds to plasma oscillations.

The transverse mode is governed by the dispersion equation $\omega^2 = \omega_{pe}^2 + c^2 k^2$. Such waves can propagate only if the frequency is higher than the plasma frequency. This mode has a "cut-off" at $\omega = \omega_{pe}$. From the third equation of Maxwell it can be seen that this mode involves both an electric and magnetic field which are orthogonal to each other and to the wave vector \mathbf{k} . Thus, the transverse mode represents an electromagnetic wave. From equation (22) it can be seen that if $\omega > \omega_{pe}$, $k = \pm c^{-1}(\omega^2 - \omega_{pe}^2)^{1/2}$. Hence the propagation vector is real and the wave can propagate. If $\omega < \omega_{pe}$, $k = \pm ic^{-1}(\omega_{pe}^2 - \omega^2)^{1/2}$ and the propagation vector is imaginary. This means that the wave amplitude decreases exponentially. Such a wave is known as an evanescent wave.

6.3 Propagation normal to the magnetic field

We now consider propagation normal to the magnetic field, thus $q=p/2$. The Appleton-Hartree formula gives,

$$k^2 c^2 = \omega^2 - \omega_{pe}^2 \quad \text{or} \quad k^2 c^2 = \omega^2 - \frac{\omega_{pe}^2 (\omega^2 - \omega_{pe}^2)}{\omega^2 - \omega_{pe}^2 - \Omega^2} \quad (6.24)$$

which are the dispersion relations for propagation of electromagnetic waves normal to the magnetic field. The characteristic polarisations of the electric field are respectively:

$$E_1 = E_2 = 0, E_3 \neq 0 \quad \text{and} \quad \frac{E_1}{E_2} = -i \frac{\omega (\omega^2 - \omega_{pe}^2 - \Omega^2)}{\omega_{pe}^2 \Omega}, E_3 = 0 \quad (6.25)$$

respectively. The dispersion relation corresponding to $E_3 \neq 0$ is seen to be identical to the dispersion relation for electromagnetic waves in a non-magnetised plasma. So the magnetic field has no effect on the dispersion relation. This is because in the present case the electric field is parallel to the magnetic field and the electrons are free to move parallel to the magnetic field. The dispersion relation corresponding to $E_3 = 0$ is the more interesting case and is shown in figure 6.2. The cut-off frequencies can be found:

$$\begin{aligned} \omega_1 &= -\frac{1}{2} \Omega + \left(\omega_{pe}^2 + \frac{1}{4} \Omega^2 \right)^{1/2} \\ \omega_2 &= \frac{1}{2} \Omega + \left(\omega_{pe}^2 + \frac{1}{4} \Omega^2 \right)^{1/2} \end{aligned} \quad (6.26)$$

At $\omega = \omega_h = \left(\omega_{pe}^2 + \Omega^2 \right)^{1/2}$, there is a resonance. This frequency is known as "upper hybrid frequency". The electromagnetic waves can propagate normal to the magnetic field for $\omega_1 < \omega < \omega_h$, and $\omega > \omega_2$.

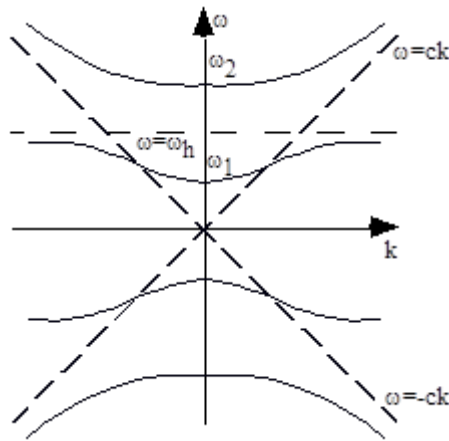


Figure 6.2 Dispersion relation for EM waves propagating transverse to the magnetic field

6.4 Parallel propagation

In this case $q=0$ so $\mathbf{k}=(0,0,k)$ and the wave propagates parallel to the magnetic field. From equation 6.19 the solutions for this case are:

$\eta^2 = 1 - \frac{\alpha(1-\alpha)}{(1-\alpha)(1\pm\beta)}$. So for $\alpha \neq 0 \Rightarrow \omega^2 \neq \omega_{pe}^2$, $\eta^2 = 1 - \frac{\alpha}{1\pm\beta}$ or the dispersion relation

$$\omega^2 \left(1 - \frac{\omega_{pe}^2}{\omega(\omega \pm \Omega)} \right) = c^2 k^2 \quad (6.27)$$

The wave equation (6.7) becomes,

$$\begin{pmatrix} -\frac{k^2 c^2}{\omega^2} + 1 - \frac{\omega_{pe}^2}{\omega^2 - \Omega^2} & \frac{i\omega_{pe}^2 \Omega}{\omega(\omega^2 - \Omega^2)} & 0 \\ -\frac{i\omega_{pe}^2 \Omega}{\omega(\omega^2 - \Omega^2)} & -\frac{k^2 c^2}{\omega^2} + 1 - \frac{\omega_{pe}^2}{\omega^2 - \Omega^2} & 0 \\ 0 & 0 & 1 - \frac{\omega_{pe}^2}{\omega^2} \end{pmatrix} \begin{pmatrix} E_1 \\ E_2 \\ E_3 \end{pmatrix} = 0 \quad (6.28)$$

Because $\omega^2 \neq \omega_{pe}^2$ it can be seen from equation (6.28) that $E_3=0$ so the dispersion relation (6.27) describes transverse waves.

If $\omega^2 = \omega_{pe}^2$ then $E_3 \neq 0$ and we have the longitudinal electrostatic wave, that is, plasma oscillations.

We now see from (6.28) that for the transverse wave, E_1 and E_2 have the same absolute magnitude but they are different in phase by 90 degrees,

$$\frac{E_1}{E_2} = \mp i \quad (6.29)$$

that is, circularly polarised waves with left and right handed \mathbf{E} rotation respectively with respect to the direction of the magnetic field.

Let us examine the dispersion relation (6.27) for the case that $\omega_{pe} = 2\Omega$. The ω - k diagram is shown in figure (6.3).

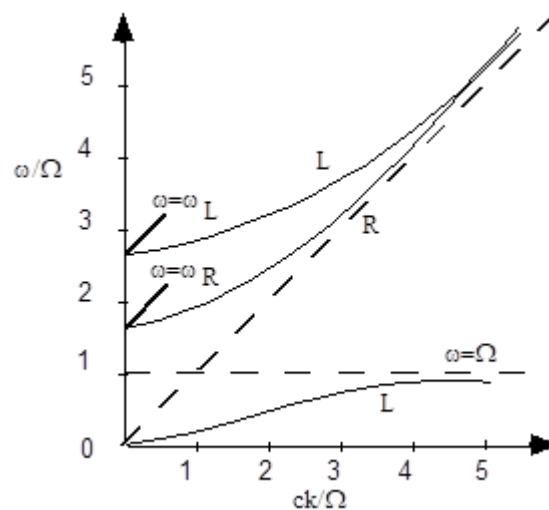


Figure 6.3 Dispersion relation for $\omega_{pe}=2\Omega$ for parallel propagation

where ω_R and ω_L are the cut-off frequencies for the right-hand and left-hand circular polarised modes respectively. At $\omega = \Omega$ there is a resonance as it can be seen from equation (6.27) for the L-mode which is due to the synchronism of the electromagnetic wave and the electron cyclotron frequency. Furthermore the wave can not propagate in the range $\Omega < \omega < \omega_L$.

6.5 Faraday rotation

Consider a linearly polarised transverse wave propagating along the direction of the magnetic field. This wave can be decomposed into two counter rotating circularly polarised waves which are characterised by the propagation vectors given by equation (6.27) or,

$$k_{\pm} = \frac{\omega}{c} \left[1 - \frac{\omega_{pe}^2}{\omega(\omega \pm \Omega)} \right]^{1/2} \quad (6.30)$$

where only the positive signs have been kept because the wave propagates along the positive z-direction and the "+" corresponds to the right hand circular polarised wave.

Since $k_+ \neq k_-$, there will be a progressive phase change between the two components as the wave propagates. The combined wave is still linearly polarised, but the polarisation of the \mathbf{E} vector varies with position. It was shown above that for parallel propagation ($q=0$) there are two modes for the transverse electromagnetic wave propagating into the magnetised plasma. For the right-hand circular polarisation $E_1/E_2=+i$ and for the left-hand one $E_1/E_2=-i$, while the index of refraction for these two modes is given from equation (6.30). If the amplitude of each circularly polarised mode is E_0 then the x and y component of the linearly polarised wave can be synthesised from the circular polarised ones as follows:

$$\begin{aligned} E_1 &= E_0 \left[\cos(k_+ z - \omega t) + \cos(k_- z - \omega t) \right] \\ E_2 &= E_0 \left[\cos(k_+ z - \omega t) - \cos(k_- z - \omega t) \right] \end{aligned} \quad (6.31)$$

and using the appropriate trigonometric formulas can alternatively be written as:

$$\begin{aligned}
 E_1 &= 2E_o \cos\left[\frac{k_+ + k_-}{2} z - \omega t\right] \cos\left[\frac{k_+ - k_-}{2} z\right] \\
 E_2 &= 2E_o \cos\left[\frac{k_+ + k_-}{2} z - \omega t\right] \sin\left[\frac{k_+ - k_-}{2} z\right]
 \end{aligned}
 \tag{6.32}$$

If ϕ is the angle that the electric vector makes with the x-axis then $\frac{E_2}{E_1} = \tan\phi$ and from

$$(6.29) \text{ we see that } \phi = \frac{k_+ - k_-}{2} z.$$

Therefore,

$$\frac{d\phi}{dz} = \frac{1}{2}(k_+ - k_-) = \frac{1}{2} \frac{\omega}{c} \left\{ \sqrt{1 - \frac{\omega_{pe}^2}{\omega(\omega + \Omega)}} - \sqrt{1 - \frac{\omega_{pe}^2}{\omega(\omega - \Omega)}} \right\}
 \tag{6.33}$$

If $\Omega \ll \omega$ ($b \ll 1$) which is a condition normally valid for laboratory plasmas, we can approximate the square roots using Taylor's series so that,

$$\sqrt{1 - \frac{\omega_{pe}^2}{\omega^2} \frac{1}{1 \pm \frac{\Omega}{\omega}}} \approx \sqrt{1 - \frac{\omega_{pe}^2}{\omega^2}} \pm \frac{\Omega}{2\omega} \frac{\omega_{pe}^2}{\omega^2 \sqrt{1 - \frac{\omega_{pe}^2}{\omega^2}}}.$$

Thus, equation (6.33) becomes:

$$\frac{d\phi}{dz} = \frac{e^3 \lambda^2}{8\pi^2 m_e^2 \epsilon_o c^3} \frac{n_e B_o}{\sqrt{1 - \frac{n_e}{n_c}}}, \text{ hence the total rotation of the plane of polarisation along the path}$$

of propagation of the wave can be expressed as:

$$\phi = \frac{e^3 \lambda^2}{8\pi^2 m_e^2 \epsilon_0 c^3} \int \frac{n_e B_0}{\sqrt{1 - \frac{n_e}{n_c}}} dz \quad (6.34)$$

and it has also taken in account that $1 - \frac{\omega_{pe}^2}{\omega^2} = 1 - \frac{n_e}{n_c}$ and $\omega_{pe}^2 = \frac{n_e e^2}{\epsilon_0 m_e}$, where $n_c \equiv \frac{\omega^2 m_e \epsilon_0}{e^2}$

is the critical density and l is the wavelength, $\lambda = \frac{2\pi c}{\omega}$.

6.6 Rotation for propagation at a general angle q

The refractive index for propagation at a general q to the magnetic field has already been obtained above and is given by the Appleton-Hartree formula (6.19). For considering the Faraday rotation the characteristic polarisation for the components of the electric field perpendicular to the direction of propagation is required. This requires solving equation (6.7) for \mathbf{E} . It is possible to continue the analysis using the present coordinate system. By eliminating k and E_3 from equation (6.7) the ratio E_2/E_1 can be found and provided that $b \ll 1$ then $E_1/E_2 \approx \mp i$. However for expressing the rotation of the wave polarisation is easier to consider a coordinate system in which the propagation vector \mathbf{k} , is along the z axis and taking the x axis perpendicular to \mathbf{B} as shown in Figure (6.2). Starting with the general equation for propagation (6.7) with the \mathbf{k} vector in the z direction and arbitrary dielectric tensor, eliminating E_3 and k , the equation for the polarisation, $\rho = E_1/E_2$ is obtained in the general form:

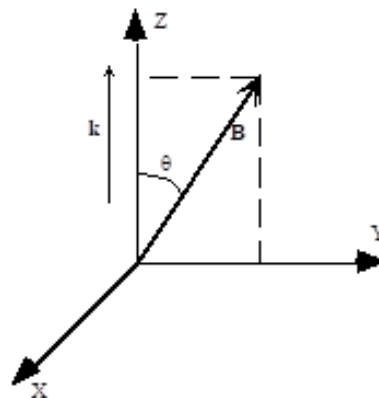


Figure 6.4 Coordinate system to study the polarisation effects

$$\begin{aligned}
 & -(\varepsilon_{21}\varepsilon_{33} - \varepsilon_{31}\varepsilon_{23})\rho^2 + (\varepsilon_{11}\varepsilon_{33} - \varepsilon_{22}\varepsilon_{33} + \varepsilon_{32}\varepsilon_{23} - \varepsilon_{31}\varepsilon_{13})\rho + \\
 & (\varepsilon_{12}\varepsilon_{33} - \varepsilon_{32}\varepsilon_{13}) = 0
 \end{aligned} \tag{6.35}$$

The dielectric tensor for this coordinate system can be found following the same algebra as that for dielectric tensor (6.15) and can be written as,

$$\varepsilon = \begin{bmatrix} 1 - \frac{\alpha}{1 - \beta^2} & \frac{i\alpha\beta\cos\theta}{1 - \beta^2} & -\frac{i\alpha\beta\sin\theta}{1 - \beta^2} \\ -\frac{i\alpha\beta\cos\theta}{1 - \beta^2} & 1 - \frac{\alpha(1 - \beta^2\sin^2\theta)}{1 - \beta^2} & \frac{\alpha\beta^2\cos\theta\sin\theta}{1 - \beta^2} \\ \frac{i\alpha\beta\cos\theta}{1 - \beta^2} & \frac{\alpha\beta^2\cos\theta\sin\theta}{1 - \beta^2} & 1 - \frac{\alpha(1 - \beta^2\sin^2\theta)}{1 - \beta^2} \end{bmatrix} \tag{6.36}$$

It can be seen that the angle between the \mathbf{B} and \mathbf{k} appears explicitly in the dielectric tensor whereas using the former coordinate system the angle appeared after solving the wave equation. However, the disadvantage of this system is that there are no zeros in the dielectric matrix, thus the algebra is harder if the question is to find the dispersion relation only. Therefore the present coordinate system is used only for purposes where polarisation effects are important as opposed to the former one which is practiced when the dispersion relation equation needs to be derived.

Using the matrix elements from (6.36) and the general polarisation equation (6.35) it is found

for r , $\rho^2 + \frac{i\beta\sin^2\theta}{\cos\theta(1-\alpha)}\rho + 1 = 0$ and solving this we find:

$$\frac{E_1}{E_2} = -\frac{i\beta\sin^2\theta}{1(1-\alpha)\cos\theta} \pm i \left[1 + \frac{\beta^2\sin^4\theta}{4(1-\alpha)^2\cos^2\theta} \right]^{1/2}.$$

If $b\sec\theta \ll 1$ and $1-a$ not small the above equation can be written as $E_1/E_2 \approx \mp i$. Consequently, the result is that for $W \ll w$, at all angles not close to perpendicular the characteristic waves are circular. So the previous analysis can be applied, thus,

$$\phi = \frac{k_+ - k_-}{2} z = \frac{\omega}{c} \frac{\eta_+ - \eta_-}{2} z .$$

The Appleton-Hartree formula gives the index of refraction for general propagation. Retaining only first order terms in the assumed small b , can be written:

$$\eta^2 = 1 - \alpha \pm \alpha \beta \cos \theta \quad (6.37)$$

Substituting in the equation for the rotation angle f we obtain, $\phi \approx \frac{1}{2} \frac{\omega}{c} \left[\frac{\alpha \beta \cos \theta}{(1 - \alpha)^{1/2}} \right] z$, so the

total rotation along the path of propagation is $\phi \approx \frac{1}{2c} \int_{\ell} \frac{\omega_{pe}^2 \Omega \cos \theta}{\omega^2 \sqrt{1 - \frac{\omega_{pe}^2}{\omega^2}}} dz$ which alternatively

can be written:

$$\phi \approx \frac{e^3 \lambda^2}{8\pi^2 m_e^2 \epsilon_0 c^3} \int_{\ell} \frac{n_e \mathbf{B} \cdot d\ell}{\sqrt{1 - \frac{n_e}{n_c}}} \quad (6.38)$$

where the dz has been replaced with the more general $d\ell$. Furthermore for $\frac{n_e}{n_c} \ll 1$ the rotation angle can be approximated to,

$$\phi \approx \frac{e^3 \lambda^2}{8\pi^2 m_e^2 \epsilon_0 c^3} \int_{\ell} n_e \mathbf{B} \cdot d\ell \quad (6.39)$$

Within the limit of the approximations applied, this is a general formula for the Faraday rotation angle for an electromagnetic wave propagating into a magnetised plasma at any angle



to the direction of the magnetic field. Thus, it is proportional to the parallel component of the magnetic field, the plasma electron density and the square of the wavelength.

The above analysis for the propagation of electromagnetic waves in magnetised plasmas is based in the cold plasma approximation which of course is not the case for a real plasma. However, the waves which come out from the cold plasma theory retain their essential features in a hot plasma for most frequencies, so they play an important role in the study of wave propagation in a plasma, even if it is at a very high temperature.

6.7 Nonuniform media and the WKB approximation

In reality, no laboratory plasma satisfies the condition of being uniform throughout all space. If the plasma does not vary very much over scale lengths of the order of the wavelength, then the wave would behave locally like the homogeneous plasma solution. The wavelengths used in optical plasma diagnostics are very much less than the electron density scale lengths and the plasma may be considered as homogeneous layers and therefore the homogeneous wave equation is valid in each layer. The type of approximation which treats the inhomogeneous plasma as a slowly varying medium is generally known as the WKB approximation (Wentzel, Kramers, Brillouin, Jeffreys) or more simply geometric optics approximation. In this approximation the wave amplitude for a given frequency ω is written in the form:

$$\mathbf{E} = e^{i[\int \mathbf{k} \cdot d\mathbf{l} - \omega t]} \quad (6.40)$$

where l is the distance along the plasma layer considered as homogeneous and \mathbf{k} is the solution of the homogeneous dispersion relation for the given ω . In order for this solution to be a good approximation the fractional variation of \mathbf{k} in one wavelength of the wave must be small or similarly the refractive index scale length must be very much larger than the wavelength of the propagating wave. This can be written as:

$$\frac{|\nabla \mathbf{k}|}{k^2} \ll 1 \text{ or } \frac{\eta^2}{|\nabla \eta|} \gg \lambda \quad (6.41)$$



HELLENIC
MEDITERRANEAN
UNIVERSITY



université
BORDEAUX



Erasmus+

Bibliography

P. A. Sturrock, *An introduction to the theory of Astrophysical, Geophysical and laboratory plasmas*, Cambridge University Press (1994).

I. H. Hutchinson, *Principles of Plasma diagnostics*, Cambridge University Press (1987).

V. L. Ginzburg, *The propagation of Electromagnetic Waves in Plasmas*, New York, Pergamon Press (1964).

R. A. Cairns, *Plasma Physics*, Blackie & Son limited (1985).

F.F.Chen, *Plasma Physics and Controlled Fusion*, Volume 1: Plasma Physics, Plenum Press, New York and London (1990).



HELLENIC
MEDITERRANEAN
UNIVERSITY



université
BORDEAUX



Erasmus+

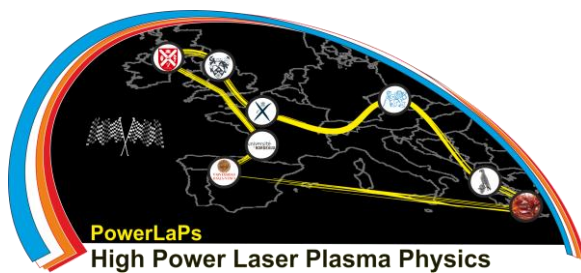
PowerLaPs

Innovative Education & Training in High Power Laser Plasmas

Plasma Physics - Theory and Experiments

Chapter 7: Kinetic description of a plasma

D. Batani, E. d'Humières, J.J. Santos, V.T. Tikhonchuk



Erasmus+

université
de BORDEAUX

7 Kinetic description of a plasma

7.1 Distribution function of particles

The most complete microscopic description of a gas, the N -particles system in a volume V , is given by the description of the coordinates $\vec{r}_i(t)$ and the momenta $\vec{p}_i(t)$ of all particles at all time. This allows us to determine how many particles are in a given domain of momenta (the phase space) and in a given volume of the coordinate space. We introduce a *microscopic distribution function*, $f_{\text{micro}}(t, \vec{r}, \vec{p})$, characterizing the number of particles in a moment t in a volume of the phase space $d^3r \times d^3p$:

$$dN = f_{\text{micro}}(t, \vec{r}, \vec{p}) d^3r d^3p. \quad (7.1)$$

This microscopic distribution function has an exact expression if the positions and momenta of all particles are known. In fact, the function f_{micro} is discontinuous; it is not zero only in the points in the phase space that coincide exactly with the position and the momentum, \vec{r}_i and \vec{p}_i , of one of particles. Therefore, the function f_{micro} can be written as a product of the Dirac delta-functions corresponding to the ensemble of particles:

$$f_{\text{micro}}(t, \vec{r}, \vec{p}) = \sum_{i=1}^N \delta[\vec{r} - \vec{r}_i(t)] \delta[\vec{p} - \vec{p}_i(t)] \quad (7.2)$$

where $\delta(\vec{r}) \equiv \delta(x)\delta(y)\delta(z)$ is the Dirac delta-function in three dimensions. However, such a definition of the distribution function is totally formal. It represents essentially the ensemble of all coordinates and momenta of all particles. Our objective is not to remain at the level of description of discrete particles. We want to introduce a *continuous description* making the void space between the particles disappear. So we make a *spatial average* of the microscopic distribution function obtaining a continuous distribution function:

$$f(t, \vec{r}, \vec{p}) = \langle f_{\text{micro}}(t, \vec{r}, \vec{p}) \rangle_{V_a}. \quad (7.3)$$

This function gives us an approximate description of the exact number of particles in a give volume of the phase space because f_{micro} is different from f . However, this difference $\delta f_{\text{micro}} = f_{\text{micro}} - f$ is a random quantity with a zero average. This random deviation is called a *fluctuation*. The object of the statistical theory is to minimize the fluctuations in order to have the most exact description possible. But we cannot neglect completely the fluctuations: they take in account the correlations between the particles and manifest themselves in the collisional processes.

The choice of the volume V_a of averaging of the distribution function in Eq. (7.3) is not completely arbitrary. It depends on the physical problem that we are dealing with. It is evident that the volume V_a must be sufficiently large compared to the mean volume attributed to each particle $V_a \gg V/N$. If V_a is too small, we may have a very precise spatial resolution, but, because of a very small number of particles N_a in the volume V_a , the average function will be defined with an insufficient precision. It is known from the general statistical theory, the amplitude of fluctuations around the mean value is of the order of $N_a^{-1/2}$. At the same time, the volume V_a must be small enough compared to the total total $V_a \ll V$ in order to describe the system with a sufficient precision.

Practically, in experiments the volume V_a is defined by the spatial resolution of our measurements and in the numerical simulations by the number of macro-particles chosen and by the computer performance. For example, a gas under normal conditions of pressure and temperature has a particle density $n \sim 10^{25} \text{ m}^{-3}$. The mean distance between particles is $d \simeq n^{-1/3} \sim 10 \text{ nm}$. So it would be sufficient to choose the resolution distance $d_a = V_a^{1/3}$ of the order of a micron. Then the

volume V_a contains $N_a \sim 10^7$ particles. Thus, we will be able to measure the mean value with a precision of a few microns and, at the same time, we maintain the fluctuations level under 0.1%.

7.2 Klimontovich equation

We are going to obtain an evolution equation for the distribution function. Let us start with the microscopic function. According to the definition (7.2), the temporal evolution of f_{micro} is due to the movements of all particles. As a consequence, the temporal derivative of the distribution function f_{micro} can be written as:

$$\partial_t f_{\text{micro}} = d_t \sum_{i=1}^N \delta[\vec{r} - \vec{r}_i(t)] \delta[\vec{p} - \vec{p}_i(t)]$$

where $\partial_t = \partial/\partial t$ is the partial temporal derivative, and $d_t = d/dt$ is the total temporal derivative. As the coordinates and the momenta of particles are the quantities depending on time according to the equation of motion, we can write the derivative as follows:

$$\partial_t f_{\text{micro}} = - \sum_{i=1}^N d_t \vec{r}_i \cdot \vec{\nabla} \delta[\vec{r} - \vec{r}_i(t)] \delta[\vec{p} - \vec{p}_i(t)] - \sum_{i=1}^N d_t \vec{p}_i \cdot \partial_{\vec{p}} \delta[\vec{p} - \vec{p}_i(t)] \delta[\vec{r} - \vec{r}_i(t)] \quad (7.4)$$

where $\vec{\nabla} = \partial/\partial \vec{r}$ is the spatial gradient and $\partial_{\vec{p}} = \partial/\partial \vec{p}$ is the partial derivative with respect to the momentum.

Let us consider first the derivative of the particle orbits. The derivative $d_t \vec{r}_i$ is, by definition, the particle velocity, \vec{v}_i . It is related to the momentum: In the classical mechanics $\vec{v}_i = \vec{p}_i/m$, and in the relativistic mechanics $\vec{v}_i = \vec{p}_i/m\gamma$, where the relativistic factor $\gamma = (1 + \vec{p}_i^2/m^2 c^2)^{1/2}$. Finally, the derivative $d_t \vec{p}_i$ is defined by the Newton's law:

$$d_t \vec{p}_i = \vec{F}_i$$

where \vec{F}_i is the force applied to the i -th particle. In the most general case, it depends on time, on the position and on the speed of particle, $\vec{F}_i = \vec{F}_{\text{micro}}(t, \vec{r}_i, \vec{v}_i)$. The subscript of the force recalls that it is of a microscopic origin – it can be produced either by other $j \neq i$ particles or by external sources.

We notice that we can remove now the subscripts of speed \vec{v}_i and of the force F_i in Eq. (7.4) thanks to the specific property of the Dirac delta-function: $a \delta(x - a) = x \delta(x - a)$. So we can pull the velocities and the forces out of the summation and write Eq. (7.4) like an equation for the microscopic distribution function:

$$\partial_t f_{\text{micro}} + \vec{v} \cdot \vec{\nabla} f_{\text{micro}} + \vec{F}_{\text{micro}} \cdot \partial_{\vec{p}} f_{\text{micro}} = 0. \quad (7.5)$$

This is the *Klimontovich kinetic equation*. Although it is a microscopic equation, representing an ensemble of discrete particles, the coordinates and the momenta of individual particles are not formally present. This allows us to develop an equation for the average distribution function.

We recall here that the force \vec{F}_{micro} has in general two components, an internal and an external: $\vec{F}_{\text{micro}} = \vec{F}^{\text{ext}} + \vec{F}^{\text{int}}$. The first one is known, it is normally produced by the sources out of plasma (capacitors, coils, laser beams, etc.). In contrast, the second one is the sum of the forces produced by all particles in plasma. It varies very strongly in space and in time because of a random motion of particles. Therefore, it must be replaced by an average force in the equation for the average distribution function. So we need to establish an equation for the average strength too. Because

that force is of the electromagnetic origin in the case of charged particles (the Lorentz force), we must derive the Maxwell's equations for the mean fields.

The internal, self-consistent force is at the origin of A collective behavior of plasma. We limit our analysis to binary interactions of nearest neighbor particles, and we suppose that the correlations of higher order are negligible. This assumption is valid for the gaseous state where the kinetic energy of charged particles is much higher then the potential energy of their pair-wise interaction.

7.3 Vlasov kinetic equation

To obtain a regular equation for the continuous distribution function we follow the prescription of Eq. (7.3). It means that we have to average the Klimontovich equation (7.5) over a volume V_a as it was explained in the previous section. The averaging of the derivatives does not pose a problem because these operators are applied to average variables, even if the average is made over the positions of individual particles. We have then:

$$\partial_t f + \vec{v} \cdot \vec{\nabla} f + \left\langle \vec{F}_{\text{micro}} \cdot \partial_{\vec{p}} f_{\text{micro}} \right\rangle = 0. \quad (7.6)$$

We notice a problem with the last term: it cannot be easily averaged because it is a *nonlinear* product of two microscopic quantities. To simplify this term we need to introduce an additional hypothesis. This is the *weak correlations hypothesis*: we suppose that the distance between the particles is sufficiently large, so each particle moves as if it is free and there are no other particles around. These free trajectories are regular. They are defined by the average forces, and with the perturbations induced by the movement of other particles are of the second order.

Then, every microscopic quantity can be presented as an average quantity and the corresponding fluctuation. For example,

$$f_{\text{micro}} = f + \delta f_{\text{micro}}, \quad \vec{F}_{\text{micro}} = \vec{F} + \delta \vec{F}_{\text{micro}}. \quad (7.7)$$

If we choose the volume V_a over which we average the microscopic distribution function (7.3), the amplitude of fluctuations, $\delta f_{\text{micro}} \ll f$ will be small, and the mean value will be zero, $\langle \delta f_{\text{micro}} \rangle = 0$. This allows us to develop the last term in Eq. (7.6) in a series of Taylor. Moreover, we have to account for the fact that in a plasma there are several particle species, two at minimum: electrons and ions. So, we define the distribution functions for every species α . At the first order, we obtain a standard form of the kinetic equation:

$$\partial_t f_\alpha + \vec{v} \cdot \vec{\nabla} f_\alpha + \vec{F}_\alpha \cdot \partial_{\vec{p}} f_\alpha = 0. \quad (7.8)$$

The left hand side describes evolution of the average distribution function due to the movement of particles (the second term describes the spatial diffusion) and to the average self-consistent forces (the diffusion in the phase space – the third term). In plasma, this is the Lorentz force that accounts for the self-consistent electric and magnetic fields

$$\vec{F}_\alpha = q_\alpha (\vec{E} + \vec{v} \times \vec{B}). \quad (7.9)$$

This kinetic equation with a self-consistent force is called the *Vlasov equation*. It as been empirically proposed by Anatoly Vlasov in 1945 to give a theoretical explication of plasma oscillations. It is actually the basis of all kinetic models for the particles interacting through the long long range forces: electromagnetic and gravitational.

The Vlasov equation describes evolution of the distribution function in a large scale, larger then the Debye length, and it can be applied to low density plasmas. In contrast it does not accounts for

the fluctuations. The collisional effects become important when the particles come closer to each other. The interaction at short distances, smaller than the Debye length, is the domain where the collisions are important. Therefore, the Vlasov equation can be used under the conditions where the plasma can be considered as collisionless.

7.4 Collision integral

Let us consider now the contribution of the collisional term δf_{micro} in the microscopic distribution function (7.7). We have to account for the fluctuation terms of the second order in Eq. (7.6):

$$\partial_t f_\alpha + \vec{v} \cdot \vec{\nabla} f_\alpha + \vec{F}_\alpha \cdot \partial_{\vec{p}} f_\alpha = - \left\langle \delta \vec{F}_{\text{micro}\alpha} \cdot \partial_{\vec{p}} \sum_{\beta} \delta f_{\text{micro}\beta} \right\rangle \equiv \sum_{\beta} C_{\alpha\beta}. \quad (7.10)$$

Compared to the Vlasov equation, we have a new term in the right hand side called the *collision integral*. To find an explicit form of the collisional integral we need to solve equations for the fluctuations of the electromagnetic field and for the fluctuations of the distribution function. We will discuss the explicit form of the collision integral in the next chapter. Here we just present some general comments.

First of all, the hypothesis of weak fluctuations allows us to account only for pair collisions, between the particles of species α and β in an additive way. That means that Eq. (7.10) considers only binary collisions, while the triple collisions are excluded. Thus, weak correlations correspond to small perturbations of the particle orbits. In each collision, the particle does not change much its direction of propagation and its momentum. So, the right hand side of Eq. (7.10) describes the scattering at small angles.

The general kinetic equation that takes into account the scattering of particles at small angles has been developed by Fokker and Planck in 1917. We will see in the next chapter that Eq. (7.10) is a special case of the Fokker-Planck equation.

We also notice that the collision term is local. There are no operators containing a spatial or a temporal derivative. So the plasma is supposed to be homogeneous and stationary at correlation scale. The spatial scale is defined by the Debye length, $\lambda_{D\alpha}$, by the characteristic speed of particles, that is, its thermal speed, $v_{T\alpha}$. So the characteristic time of a collision is $\lambda_{D\alpha}/v_{T\alpha} = 1/\omega_{p\alpha}$ is the inverse of plasma frequency.

Finally, the collision integral in the form (7.10) satisfies the conservation laws. It preserves the number of particles of each species, the total quantity of motion of the system and its total energy. The mathematical demonstration of these properties is presented in Chapter ??, but it is easy to understand it in a qualitative way. The collisional term in Eq. (7.10) takes into account the Coulomb collisions at small angles. These are elastic collisions – in every collision the number of particles, the momentum and the energy are preserved. So, it is not surprising that the collision integral has the same properties as its microscopic origin.

7.5 Macroscopic field, Maxwell's equations

Kinetic equations (7.8) and (7.10) must be completed with equations for the mean fields, $\vec{E} = \langle \vec{E}_{\text{micro}} \rangle$ and $\vec{B} = \langle \vec{B}_{\text{micro}} \rangle$. The microscopic fields verify the Maxwell's equations:

$$\vec{\nabla} \times \vec{E}_{\text{micro}} = -\partial_t \vec{B}_{\text{micro}}, \quad (7.11)$$

$$\vec{\nabla} \cdot \vec{E}_{\text{micro}} = \epsilon_0^{-1} \rho_{\text{micro}}, \quad (7.12)$$

$$\vec{\nabla} \times \vec{B}_{\text{micro}} = \mu_0 \vec{j}_{\text{micro}} + c^{-2} \partial_t \vec{E}_{\text{micro}}, \quad (7.13)$$

$$\vec{\nabla} \cdot \vec{B}_{\text{micro}} = 0. \quad (7.14)$$

These fields are generated by the particles inside the plasma. The microscopic density

$$\rho_{\text{micro}}(t, \vec{r}) = q \sum_{i=1}^N \delta[\vec{r} - \vec{r}_i(t)]$$

is the total sum of every charge multiplies for the correspondent Dirac delta-function defining the particle position. In the same way, the density of the microscopic current is a sum of all currents produced by particles:

$$\vec{j}_{\text{micro}}(t, \vec{r}) = q \sum_{i=1}^N \vec{v}_i(t) \delta[\vec{r} - \vec{r}_i(t)].$$

We can present these microscopic sources utilizing the microscopic distribution function and making an integral over the momentum:

$$\rho_{\text{micro}}(t, \vec{r}) = \sum_{\alpha} q_{\alpha} \int f_{\text{micro } \alpha}(t, \vec{r}, \vec{p}) d\vec{p}, \quad \vec{j}_{\text{micro}}(t, \vec{r}) = \sum_{\alpha} q_{\alpha} \int f_{\text{micro } \alpha}(t, \vec{r}, \vec{p}) \vec{v} d\vec{p}. \quad (7.15)$$

Here we add also a summation over the particle species. This form of presentation of the sources in the Maxwell's equations allows a direct average. As a consequence, the form of Maxwell's equations is the same as for the microscopic equations:

$$\vec{\nabla} \times \vec{E} = -\partial_t \vec{B}, \quad (7.16)$$

$$\vec{\nabla} \cdot \vec{E} = \epsilon_0^{-1} (\rho + \rho^{\text{ext}}), \quad (7.17)$$

$$\vec{\nabla} \times \vec{B} = \mu_0 (\vec{j} + \vec{j}^{\text{ext}}) + c^{-2} \partial_t \vec{E}, \quad (7.18)$$

$$\vec{\nabla} \cdot \vec{B} = 0. \quad (7.19)$$

Here, ρ^{ext} and \vec{j}^{ext} are the density of charge and the density of external current. We can consider them as known quantities. In contrast, the density of charge $\rho = \sum_{\alpha} \rho_{\alpha}$ and the density of current $\vec{j} = \sum_{\alpha} \vec{j}_{\alpha}$ are internal quantities, produced by the particles. They are the average of microscopic sources (7.15):

$$\rho(t, \vec{r}) = \sum_{\alpha} q_{\alpha} \int f_{\alpha}(t, \vec{r}, \vec{p}) d\vec{p}, \quad \vec{j}(t, \vec{r}) = \sum_{\alpha} q_{\alpha} \int \vec{v} f_{\alpha}(t, \vec{r}, \vec{p}) d\vec{p}. \quad (7.20)$$

Because the electromagnetic field produces a long range force, every particle make its motion in a collective field, created by many neighboring particles. This means that plasma demonstrates a collective behavior, differently from a neutral gas, where the effective radius of the force created by each particle is much smaller to the distance between two particles.

7.6 Macroscopic quantities in a plasma

Every microscopic physical quantity can find a correspondent average as, for example, we already demonstrated for the transition from the microscopic charge density to the mean charge density. For particles of species α we define:

- the density of particles:

$$n_{\alpha}(t, \vec{r}) = \int f_{\alpha}(t, \vec{r}, \vec{p}) d\vec{p}, \quad (7.21)$$

- the vector of mean velocity:

$$\vec{u}_{\alpha}(t, \vec{r}) = \frac{1}{n_{\alpha}(t, \vec{r})} \int \vec{v}_{\alpha} f_{\alpha}(t, \vec{r}, \vec{p}) d\vec{p}, \quad (7.22)$$

- the mean energy:

$$U_\alpha(t, \vec{r}) = \frac{1}{n_\alpha(t, \vec{r})} \int \varepsilon_\alpha f_\alpha(t, \vec{r}, \vec{p}) d\vec{p}, \quad (7.23)$$

where \vec{v}_α and $\varepsilon_\alpha(\vec{p})$ are the speed and the energy of the particle. In the classical mechanics $\vec{v}_\alpha = \vec{p}/m_\alpha$ and $\varepsilon_\alpha = \vec{p}^2/2m_\alpha$. These definitions apply also to the relativistic or quantum plasmas, where the relation of the speed, $\vec{v}_\alpha(\vec{p})$ and the energy of particle, $\varepsilon_\alpha(\vec{p})$, with the momentum are more complicated functions. For example, for the relativistic case, where $p \approx m_\alpha c$, the speed, $\vec{v}_\alpha = \vec{p}/\gamma_\alpha m_\alpha$, and the kinetic energy of particle, $\varepsilon_\alpha = (\gamma_\alpha - 1) m_\alpha c^2$, depend of the relativistic factor $\gamma_\alpha(\vec{p}) = 1/\sqrt{1 - \vec{p}^2/m_\alpha^2 c^2}$.

- the tensor of momentum flux:

$$P_{\alpha ij}(t, \vec{r}) = \int p_i v_j f_\alpha(t, \vec{r}, \vec{p}) d\vec{p}, \quad (7.24)$$

- the vector of energy flux:

$$\vec{\Gamma}_\alpha(t, \vec{r}) = \int \varepsilon_\alpha(\vec{p}) \vec{v} f_\alpha(t, \vec{r}, \vec{p}) d\vec{p}. \quad (7.25)$$

Two last functions describe the *transport processes* of the quantity of motion and of the energy in plasma. It is often interesting to separate the mean motion of particles of the species α with the mean speed \vec{v}_α , and the chaotic (thermal) motion with the relative momentum $\vec{p}' = \vec{p} - m_\alpha \vec{v}_\alpha$. This allows to divide the energy (7.23) and the fluxes (7.24) and (7.25) of all particles into the mean and the chaotic parts. For a classical plasma the energy is

$$U_\alpha = \frac{1}{2} m_\alpha \vec{v}_\alpha^2 + \frac{3}{2} k_B T_\alpha, \quad (7.26)$$

where the temperature T_α is a measure of thermal motion. It is defined by the following equation

$$k_B T_\alpha = \frac{1}{3m_\alpha n_\alpha(t, \vec{r})} \int (\vec{p} - m_\alpha \vec{v}_\alpha)^2 f_\alpha(t, \vec{r}, \vec{p}) d\vec{p}. \quad (7.27)$$

In the same way, the momentum flux $P_{\alpha ij} = m_\alpha n_\alpha u_{\alpha i} u_{\alpha j} + p_{\alpha ij}$ contains a term corresponding to the plasma pressure

$$p_{\alpha ij} = \frac{1}{m_\alpha} \int (\vec{p} - m_\alpha \vec{v}_\alpha)_i (\vec{p} - m_\alpha \vec{v}_\alpha)_j f_\alpha(t, \vec{r}, \vec{p}) d\vec{p}.$$

The energy flux is divided in three terms:

$$\vec{\Gamma}_\alpha = \frac{1}{2} m_\alpha n_\alpha \vec{v}_\alpha^2 \vec{v}_\alpha + \frac{5}{2} n_\alpha k_B T_\alpha \vec{v}_\alpha + \vec{q}_\alpha. \quad (7.28)$$

They describe the convective transport of the enthalpy, $\frac{1}{2} m_\alpha \vec{v}_\alpha^2 + \frac{5}{2} k_B T_\alpha$, and the heat flux:

$$\vec{q}_\alpha(t, \vec{r}) = \frac{1}{2m_\alpha} \int (\vec{p} - m_\alpha \vec{v}_\alpha)^2 (\vec{p} - m_\alpha \vec{v}_\alpha) f_\alpha(t, \vec{r}, \vec{p}) d\vec{p}. \quad (7.29)$$

A quasi-neutral, close to equilibrium plasma has the total charge density close to zero, $\sum \rho_\alpha \approx 0$, and a Maxwellian distribution function on the momentum:

$$F_\alpha(\vec{p}) = \frac{n_\alpha}{(2\pi m_\alpha k_B T_\alpha)^{3/2}} \exp\left(-\frac{(\vec{p} - m_\alpha \vec{v}_\alpha)^2}{2m_\alpha k_B T_\alpha}\right). \quad (7.30)$$



In this case the kinetic pressure is a scalar, $p_{\alpha ij} = p_{\alpha} \delta_{ij}$ and we have the following relation between pressure and temperature: $p_{\alpha} = n_{\alpha} k_B T_{\alpha}$. This is the equation of state of an ideal gas. We define also the thermal speed of particles, $v_{T\alpha} = (k_B T_{\alpha} / m_{\alpha})^{1/2}$. These relations will be utilized later in this course.

Notice a difference between the momentum of the particle \vec{p} and the pressure p_{α} .

Notice that in plasma physics publications we measure the temperature in energy units without writing explicitly the Boltzmann constant k_B .

7.7 Problems

1. Verify the following relation for the Lorentz force:

$$\frac{d}{dt} F[\vec{R}(t)] = \vec{\nabla} F \cdot \frac{d\vec{R}}{dt}.$$

2. Using the Vlasov equation (7.8) show that the equations of Poisson (7.17) and Ampere (7.18) are equivalent in the absence of a magnetic field. Find a relation between the charge density and the density of current.
3. Show that the Vlasov equation (7.8) with the Lorentz force can be written as an equation of continuity in the phase space, \vec{r}, \vec{v} . Give the expressions for the flux in the coordinate space and in the phase space.
4. Show that the collisional term in the Fokker-Planck equation can be written as a divergence in the phase space.
5. Obtain the equation of continuity starting from the Fokker-Planck equation (7.10).
6. Show that for the Maxwellian distribution function (7.30) the mean energy of particles is $U_{\alpha} = \frac{3}{2} k_B T_{\alpha}$. Find an expression for the pressure tensor for this distribution function.
7. Supposing that all electrons have the mean energy of thermal agitation, determine the maximum radius of density fluctuation they can produce. Suppose that the ions are homogeneous and at rest and that the fluctuation is spherical. Determine the amplitude of the electric field and of the electrostatic potential in this fluctuation. What is the probability of this fluctuation?
8. Verify that density and temperature for a Maxwellian distribution function satisfy the general definitions (7.21) and (7.23) for the mean density and the mean speed of particles.
9. Demonstrate relation (7.28) for the energy flux.
10. Show that the Maxwell-Boltzmann distribution function

$$F_{MB}(\vec{r}, p) = \frac{n_0}{(2\pi m k_B T)^{3/2}} \exp\left(-\frac{p^2}{2m k_B T} + \frac{q \Phi}{k_B T}\right)$$

is a solution of a stationary Vlasov equation in the electrostatic potential $\Phi(\vec{r})$. Find the spatial distribution of the particle density. Explain the physical meaning of the constant n_0 .



HELLENIC
MEDITERRANEAN
UNIVERSITY



université
BORDEAUX



Erasmus+

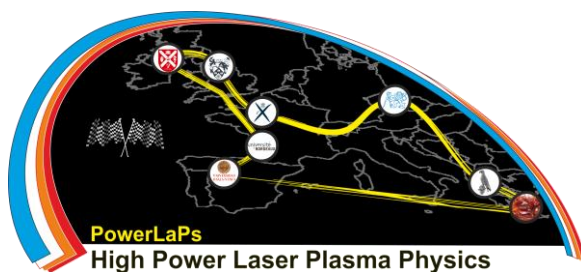
PowerLaPs

Innovative Education & Training in High Power Laser Plasmas

Plasma Physics - Theory and Experiments

Chapter 8: Equilibrium solutions to the Vlasov kinetic equation

D. Batani, E. d'Humières, J.J. Santos, V.T. Tikhonchuk



Erasmus+

université
de BORDEAUX

8 Equilibrium solutions to the Vlasov kinetic equation

8.1 Equilibrium of a homogeneous plasma

At equilibrium, the distribution function of particles is independent on time. In this case the Vlasov equation (7.8) and the Maxwell's equations have the following solutions. Let us consider first the case of a homogeneous plasma, $\vec{\nabla} f_\alpha = 0$. The term $\vec{E} \cdot \partial_{\vec{p}} f_\alpha$ will be zero if the electric field is zero, $\vec{E} = 0$. On the contrary, the term with the magnetic field, $(\vec{v} \wedge \vec{B}) \cdot \partial_{\vec{p}} f_\alpha$, will be zero in two cases: (i) a homogeneous magnetic field and an isotropic distribution function, $f_\alpha(p)$ or (ii) a zero magnetic field, $\vec{B} = 0$.

The Maxwell's equations for a zero electric field and a constant magnetic field are satisfied if the sources are zero, $\rho = 0$ et $\vec{j} = 0$. These condition lead to three important consequences:

- The plasma is electrically neutral: for two species of opposite charges – the ions of a positive charge $q_i = Ze$, and the electrons of a negative charge $q_e = -e$, the neutrality condition reads: $Zn_i = n_e$.
- The electric current in plasma is zero. That condition reads

$$\vec{j} = \sum_{\alpha} q_{\alpha} n_{\alpha} \vec{u}_{\alpha} = q_i n_i (\vec{u}_i - \vec{u}_e) = 0.$$

That means that both species have the same mean velocities, $\vec{u}_i = \vec{u}_e = \vec{u}$. Therefore, in the reference frame moving with this velocity, the distribution functions of both species are isotropic, $f_{\alpha}(\vec{p}) = f_{\alpha}(p)$.

- The distribution function has only one maximum and $\partial_p f_{\alpha} < 0$. This third condition is not evident. It comes from the condition of *stability* of the distribution function with respect to small amplitude perturbations. That problem will be discussed in Sec. 9.9 of this course.

Within these limitations, the particle distributions in a plasma without collisions are arbitrary and depend essentially on the way the plasma is created. For a plasma in equilibrium the distribution function is a Maxwellian function (7.30). This has been shown in the previous section ??.

8.2 Plasma in an external electric potential

Charged particles in an electromagnetic field exhibit a complex movement and their distribution function is not Maxwellian anymore. We consider here a simple case: the distribution function of particles of a charge q and mass m in an external potential $\Phi(x)$. We assume that the particles move just in one direction along the x -axis under the action of the electric field $E_x = -\partial_x \Phi$. The distribution function, $f(p_x, x)$ is a solution to the stationary Vlasov equation

$$v_x \partial_x f - q \partial_x \Phi \partial_{p_x} f = 0. \quad (8.1)$$

We can construct a solution of this partial derivative equation by using the method of characteristics. The total differential of f is: $df = dp_x \partial_{p_x} f + dx \partial_x f$. In order to satisfy the equation (8.1), we should find a line in the phase space x, p_x , where df is zero. Equation (8.1) will take a form of a full differential, if the following relation is satisfied:

$$\frac{dx}{v_x} = -\frac{dp_x}{q \partial_x \Phi}.$$

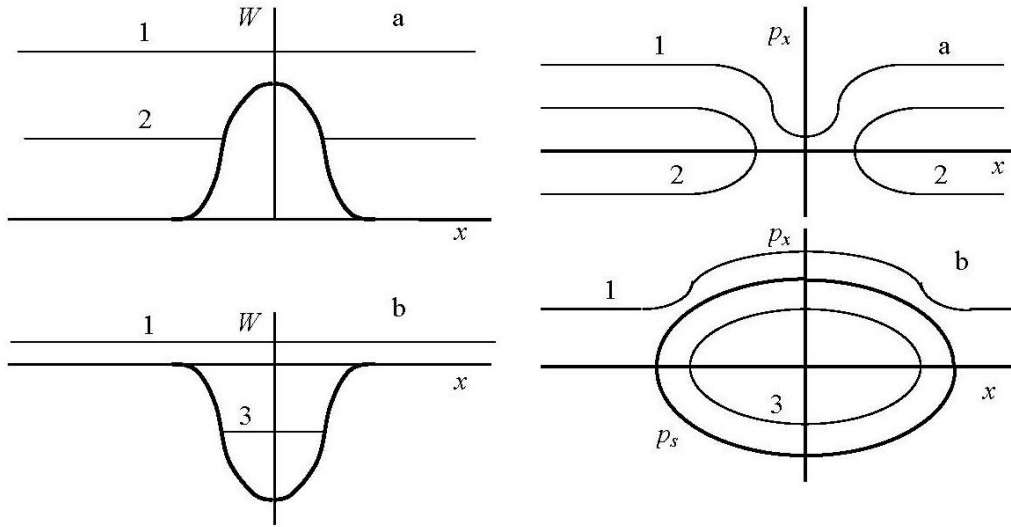


Figure 30: Energy $W(x)$ (left) and the phase space $p_x(x)$ of particles (right) in an electrostatic potential. Left: a) a potential bump: all the particles can go to infinity – the distribution function is defined in a unique way. 1 – transmitted particle. Particle with an energy less than $q\Phi_{\max}$ are reflected (2); b) a potential well: particles with a negative energy are trapped (3). Their distribution function depends on the temporal evolution. Right – trajectories of particles: a) a potential bump – all particles are connected to infinity; b) a potential well: particles with a negative energy are trapped, their trajectories are closed.

We re-write this equation as $p_x dv_x + q d\Phi = 0$ which is a full differential $dW = 0$ of the total energy of particle, $W = p_x^2/2m + q\Phi(x)$. As a consequence, the general solution to the Vlasov equation reads:

$$f(x, p_x) = F[W(x, p_x)]. \quad (8.2)$$

where F is an arbitrary function. This relation comes easily from the conservation of mechanical energy of the particle in a stationary potential. If we assume that for $|x| \rightarrow \infty$ the potential is zero and the distribution function is a Maxwellian function (7.30), the solution to Eq. (8.2) is:

$$f(x, p_x) = F(W) = \frac{n_0}{(2\pi m k_B T)^{1/2}} e^{-W/k_B T} = \frac{n_0}{(2\pi m k_B T)^{1/2}} \exp\left(-\frac{p_x^2}{2m k_B T} - \frac{q\Phi(x)}{k_B T}\right).$$

This is the Maxwell-Boltzmann distribution function.

Knowing f , we can calculate the density of particles from definition(7.21):

$$n(x) = n_0 e^{-q\Phi(x)/k_B T} \quad (8.3)$$

where n_0 is the density of particles in the point x where the potential is zero. Formula (8.3) is often called *Boltzmann distribution*. For a positive potential, $q\Phi > 0$, the density of particles decreases where the potential increases. We can consider this as a partial reflection of particles from the potential bump (see Fig. 30-a).

The case of a potential well, or a negative potential, has to be considered separately. As we see in Fig. 30-b, a particle with a negative energy is trapped and oscillates in the well. The distribution function of these particles is not defined in a unique way. It depends on how the potential has been

created. If, for example, we first created a potential in a empty space and after that launched the particles from infinity, then there are no particles with a negative energy, that is, $f = 0$ for $W < 0$, and no particles are trapped. However, if we created the potential in a plasma, some particles can be trapped.

We consider this latter case supposing the potential is created slowly and thus the particles follow the adiabatic evolution in time. During the time when the potential evolves, the energy of particles is not conserved. According to the classical mechanics, there is another quantity that is conserved: this is the adiabatic invariant – the integral of the momentum between the stopping points:

$$I = 2 \int_{x_1}^{x_2} p_x(x, t) dx \equiv 2 \int_{x_1}^{x_2} \sqrt{2m(W - q\Phi(x, t))} dx \quad (8.4)$$

where $q\Phi < 0$, $W < 0$, $W > q\Phi_{\min}$ et $x_{1,2}$ are the stopping points, $q\Phi(x_{1,2}) = W$.

So, the distribution function of trapped particles must depend on I , but not explicitly on x . Moreover, $F(W)$ must be a continuous function of W , in particular, for the energy $W = 0$, that separates the free and trapped particles. As W changes in time, the only possibility to satisfy this condition is to make $F(W < 0)$ constant: $f_p = F(W < 0) = F(0) = n_0/\sqrt{2\pi m k_B T}$. In contrast, the distribution function of free particles, f_l , with $W > 0$, is a Maxwellian function.

The difference in the behavior of free and trapped particles can be better understood while looking at the orbits of particles in the phase space, p_x, x , presented in Fig. 30, panels c) and d). In the case of a positive potential, the orbits of all the particles are connected to infinity. The distribution function is completely defined for these asymptotic values because they are conserved along the trajectory. In the case of a negative potential, the separatrix, $p_s(x)$, divides the space in free and trapped particles. It is defined by the condition $W_s = 0$, so, $p_s = \sqrt{-2mq\Phi(x)}$. The period of oscillations of the trapped particles depends on their energy. because of that the particles are mix up with time, and the distribution function becomes constant, equal to its value along the separatrix.

Now we can calculate the density of particles $n(x)$ assuming that initially the distribution function was Maxwellian. The formula for the density reads:

$$n(x) = \int_{-\infty}^{\infty} f(x, p_x) dp_x = 2 \int_0^{p_s} f_p dp_x + 2 \int_{p_s}^{\infty} f_l dp_x =$$

$$\frac{2n_0 p_s}{\sqrt{2\pi m k_B T}} + \frac{2n_0}{\sqrt{2\pi m k_B T}} \int_{p_s}^{\infty} e^{-p_x^2/2m k_B T - q\Phi/k_B T} dp_x.$$

We can calculate the last integral in two limits:

- For a weak potential, $|q\Phi| \ll k_B T$, developing the distribution function in a Taylor series, we obtain:

$$n \approx n_0 \left[1 + \frac{-q\Phi}{k_B T} + \frac{4}{3\sqrt{\pi}} \left(\frac{-q\Phi}{k_B T} \right)^{3/2} \right].$$

The difference from the Boltzmann distribution is in the last term.

- For a strong potential, $|q\Phi| \gg k_B T$, the contribution of free particles is negligible, and we find:

$$n \approx 2n_0 \sqrt{\frac{-q\Phi}{\pi k_B T}}.$$

In difference from the Boltzmann distribution, here the density increases as a square root of the potential.

8.3 Plasma in a capacitor

Let us consider a plasma in a capacitor that is characterized by the width L and the potential U . We would like to find the density of particles and the potential inside a capacitor assuming that the temperature T is uniform. The plasma is made of protons ($q_i = e$) and electrons ($q_e = -e$) and the distribution functions of ions and electrons are Maxwellian in the points where the potential is zero.

The electric field in the capacitor: $E = -d_x\Phi$ depends on the electrical potential $\Phi(x)$. The solution of the stationary Vlasov equation (7.8) is constructed similarly as in the previous paragraph. The distribution function depends on the total energy of particles:

$$f_\alpha(x, p_x, p_y, p_z) = F_\alpha[W_\alpha(x, p_x), p_y, p_z]. \quad (8.5)$$

where F_α is in our case a Maxwellian function (7.30):

$$F_\alpha(W_\alpha, p_y, p_z) = \frac{n_{\alpha 0}}{(2\pi k_B T m_\alpha)^{3/2}} \exp\left(-\frac{W_\alpha}{k_B T} - \frac{p_y^2 + p_z^2}{2k_B T m_\alpha}\right).$$

Let us assume first that the potential is known, the density of particles can be calculated according to the definition (7.21):

$$n_\alpha(x) = n_{\alpha 0} \exp\left(-\frac{q_\alpha \Phi(x)}{k_B T}\right) \quad (8.6)$$

where $n_{\alpha 0}$ is the density in $x = -L/2$, where the potential is zero. In this case the potential is a monotone function and there are no trapped particles.

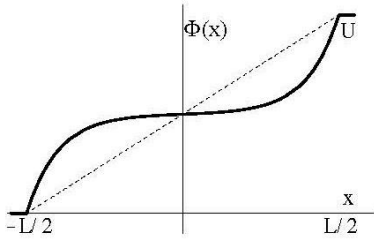


Figure 31: Distribution of the potential in a capacitor in presence (solid line) and in absence of plasma (dotted line). The plasma is in the interval $x \in (-L/2, L/2)$.

The constants $n_{\alpha 0}$ are defined by using the condition of conservation of the total number of particles in the capacitor N_0 . Without an external potential the densities of unperturbed ions and of the electrons are equal: $n_{i0} = n_{e0} = n_0$. (This is the neutrality condition.) Correspondingly, the total number per unity of surface is: $N_0 = n_0 L$. Knowing the potential, we can obtain $n_{\alpha 0}$ by using the condition $N_0 = \int_{-L/2}^{L/2} dx n_\alpha(x)$. To simplify the following calculations, we consider the case $eU \ll k_B T$, where the plasma is sufficiently hot, and we can develop the exponential function in the Boltzmann law into the Taylor series, $e^\phi \approx 1 + \phi$. This allows us to write the density of particles in the potential Φ as:

$$n_\alpha(x) = n_0 \left[1 - \frac{q_\alpha}{k_B T} (\Phi(x) - \bar{\Phi})\right] \quad (8.7)$$

where $\bar{\Phi} = (1/L) \int_{-L/2}^{L/2} dx \Phi(x)$ is the mean potential.

Knowing now the density distribution, we can solve the Poisson equation (7.17) and find the distribution of the potential Φ (figure 31) and of the field E . Introducing the dimensionless potential $\phi = e(\Phi - \bar{\Phi})/k_B T$ and the Debye length $\lambda_D = (k_B T \epsilon_0 / e^2 n_0)^{1/2}$, we can write the Poisson equation (7.17) as:

$$d_x^2 \phi = 2\lambda_D^{-2} \phi.$$

We must solve this equation with the condition that the difference of potential at the borders is U : $\phi(L/2) - \phi(-L/2) = eU/k_B T$. Moreover, because of the symmetry of the problem, the function

$\phi(x)$ is an odd function, $\phi(-x) = -\phi(x)$, and therefore, $\int_{-L/2}^{L/2} dx \phi(x) = 0$. The first integral of the Poisson equation is:

$$(\phi')^2 = 2\lambda_D^{-2}(\phi^2 + \phi_0^2)$$

where ϕ_0 is a constant of integration, that we will determine later. The solution of this equation is:

$$\phi(x) = \phi_0 \sinh[(x + x_0)\sqrt{2}/\lambda_D].$$

The constant is $x_0 = 0$ because the function $\phi(x)$ is an odd function. The other constant ϕ_0 is defined by the condition $\phi(\pm L/2) = \pm eU/2k_B T$. This gives the following formula for the potential ϕ :

$$\phi(x) = \frac{eU}{2k_B T} \frac{\sinh(x\sqrt{2}/\lambda_D)}{\sinh(L/\sqrt{2}\lambda_D)}.$$

Then, we deduce the mean potential $\bar{\Phi}$ utilizing the condition $\Phi(-L/2) = 0$. Finally, we obtain:

$$\bar{\Phi}(x) = \frac{U}{2} + \frac{U}{2} \frac{\sinh(x\sqrt{2}/\lambda_D)}{\sinh(L/\sqrt{2}\lambda_D)}.$$

Taking the derivate of Φ we can calculate the electric field too:

$$E(x) = -\frac{U}{\sqrt{2}\lambda_D} \frac{\cosh(x\sqrt{2}/\lambda_D)}{\sinh(L/\sqrt{2}\lambda_D)}.$$

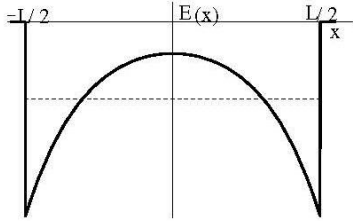


Figure 32: Distribution of the electric field inside a capacitor in presence (solid line) and in absence of plasma (dotted line).

There are two characteristic limits in this formula. If the plasma is of a low density and the Debye length is larger than the capacitor width, $\lambda_D \gg L$, we can develop the hyperbolic function in a Taylor series and $E \approx -U/L$ is a constant as in the case without plasma (dotted line in Fig. 32). However, if $\lambda_D \ll L$, the electric field is localized near the plates of the capacitor in a distance of a few Debye lengths:

$$E(x) \approx -\frac{U}{\sqrt{2}\lambda_D} \exp\left(-\frac{L - 2|x|}{\sqrt{2}\lambda_D}\right).$$

In that case the plasma polarization makes a strong effect. The electric field is enhanced near the plates and is very small inside, Fig. 32. The plasma produces a screening of the electric field in a capacitor. Utilizing (8.7), we can find the density of electrons and ions and demonstrate that indeed, the plasma acts as a dielectric: the density of charge is not zero everywhere. The plasma has a positive charge near the left plate of the capacitor and a negative one near the right plate. However, inside the capacitor, at a distance of a few Debye lengths, the plasma is quasi-neutral.

It is interesting to know how much time the plasma needs to reach this stationary state? In the stationary state, the term with the time derivative in the Vlasov equation (7.8) is very small compared to other two terms: $\partial_t f_\alpha \ll q_\alpha E \partial_p f_\alpha$. Estimating the partial derivative $\partial_p f_\alpha$ as $f_\alpha/m_\alpha v_{T\alpha}$, we can estimate the characteristic relaxation time to the stationary state as $\Delta t_\alpha \approx m_\alpha v_{T\alpha}/|q_\alpha E|$. We see that this time is different for electrons and ions because of the mass difference: $m_i/m_e \sim 1800$. The lighter electrons reach the equilibrium in a time $\sqrt{m_i/m_e} \sim 40$ shorter than the ions. We conclude that the stationary state is established in two steps: first the electrons go to equilibrium, then, later, the ions reach it too.

8.4 Plasma in an external magnetic field

Let us consider here a plasma in an external inhomogeneous magnetic field assuming that the field \vec{B} has the only one component $B_z(x)$. Such a magnetic field can be used to confine the plasma. First we solve the Vlasov equation assuming that the magnetic field is known. Then we calculate an electric current and use the Ampere equation to find the distribution of the magnetic field in plasma.

The stationary Vlasov equation (7.8) in this case can be written as:

$$v_x \partial_x f_\alpha + q_\alpha B_z (v_y \partial_{p_x} f_\alpha - v_x \partial_{p_y} f_\alpha) = 0.$$

We solve it by using the method of characteristics. The equations for the characteristics are:

$$\frac{dv_x}{v_y} = -\frac{dv_y}{v_x} = \omega_{c\alpha}(x) \frac{dx}{v_x}$$

where $\omega_{c\alpha} = q_\alpha B_z / m_\alpha$ is the cyclotron frequency. If the magnetic field is strong enough, the Larmor radius, $v_y / \omega_{c\alpha}$ can be very small with respect to the characteristic length of magnetic field variation, $L = |B_z / d_x B_z|$. In this case we can neglect the dependence of $\omega_{c\alpha}$ on the coordinate x and solve the characteristic equations explicitly: $v_x^2 + v_y^2 = v_\perp^2$ and $x + v_y / \omega_{c\alpha} = X$. Then, we can write the solution of Vlasov equation as:

$$f_\alpha(x, p_x, p_y, p_z) = F_\alpha[X(x, v_y), v_\perp^2, p_z] \quad (8.8)$$

where F in an arbitrary function. Because the Larmor radius $v_y / \omega_{c\alpha}$ is much smaller than the characteristic length of variation of the field we can develop the first argument X in the Taylor series. We obtain then:

$$f_\alpha(x, p_x, p_y, p_z) = \left(1 + \frac{v_y}{\omega_{c\alpha}} \partial_x\right) F_\alpha(x, v_\perp^2, p_z). \quad (8.9)$$

The conditions that have to be satisfied by F_α are following from the conditions of neutrality, $\sum q_\alpha n_\alpha = 0$, and the absence of components x and z of the current: $j_x = j_z = 0$. Using the symmetry of F_α with respect to v_x and v_y , we obtain: for the density $n_\alpha = \int d\vec{p} f_\alpha = \int d\vec{p} F_\alpha$, and for the current $j_{x,z\alpha} = q_\alpha \int d\vec{p} v_{x,z} f_\alpha = q_\alpha \int d\vec{p} v_{x,z} F_\alpha$. The condition $j_x = j_z = 0$ will be satisfied if F_α is a pair function of p_z .

Now we calculate the current in the direction y and inject it in the Ampere equation for the magnetic field:

$$d_x B_z = -\mu_0 j_y = -\mu_0 \sum_\alpha \frac{q_\alpha}{\omega_{c\alpha}} \partial_x \int d\vec{p} v_y^2 F_\alpha(x, v_\perp^2, p_z^2). \quad (8.10)$$

The current j_y is not zero. It is produced by the differential motion of electrons and ions in an inhomogeneous magnetic field. However, this current can be also interpreted as a drift of electrons and ions in mutually perpendicular magnetic and electric fields. The electric field is produced by the gradient of plasma pressure. Indeed, because of the symmetry of function F_α , the integral in the right hand side of Eq. (8.10) is the plasma pressure in the plane perpendicular to the direction of the magnetic field:

$$\sum m_\alpha \int d^3 p v_y^2 F_\alpha = \frac{1}{2} \sum m_\alpha \int d\vec{p} v_\perp^2 F_\alpha = P_\perp.$$

Then, Eq. (8.10) can be written as

$$d_x B_z = -\mu_0 j_y = -\frac{\mu_0}{B_z} \partial_x P_\perp.$$

Integrating it we obtain the equilibrium criterion for a plasma in an external magnetic field:

$$d_x \left(\frac{1}{2\mu_0} B_z^2 + P_\perp \right) = 0. \quad (8.11)$$

The sum of magnetic pressure, $B_z^2/2\mu_0$, and the plasma pressure, P_\perp , is a constant. If the amplitude of the magnetic field increases, the plasma pressure must decrease, and if the temperature is constant, the plasma density decreases. This opens the possibility to confine the plasma in a minimum of the magnetic field. This is the principle of magnetic confinement.

According to Eq. (8.10), the confinement is produced thanks to the electric current produced in plasma. This current goes on the direction of y -axis and it generates a magnetic field that is directed along z -axis, opposite to the external magnetic field. This is a manifestation of the diamagnetic behavior of plasma.

There are other configurations of plasma confinement in the magnetic field. In particular, two configurations are possible in a cylindrically symmetric plasma:

- A θ -pinch – is a plasma cylinder confined by an external magnetic field parallel to the plasma axis. In this case the confinement is produced by an azimuthal current along the plasma surface.
- A Z -pinch – is a plasma cylinder confined by an azimuthal magnetic field created by an axial current in plasma.

8.5 Problems

1. Verify the conservation of the adiabatic invariant utilizing the equation of motion of a particle in a potential $\Phi(x, t)$.
2. Draw the graph of the potential and the electric field in a plasma capacitor for the two cases, $L = 0.3\lambda_D$ and $L = 3\lambda_D$. Calculate the distribution of electron and ion densities in the capacitor. Explain how the plasma polarization contributes to decreasing of the external electric field.
3. Analyze the distribution of the electric field in a capacitor for the intermediate equilibrium assuming immobile ions with a homogeneous density. Calculate the distribution of the electron density in the capacitor.
4. Find the electron distribution function and the electric field in a semi-infinite, isothermal plasma without collisions. Consider the case of cold ions with a constant density $x < 0$. The electrons have a Maxwellian distribution at $x \rightarrow -\infty$ with a temperature T_e .
5. Consider a θ -pinch. The pressure of plasma is constant inside the column, P_0 , and the external magnetic field is B_0 . Calculate the magnetic field inside plasma and give the criterion of confinement. Calculate the intensity of surface current and draw the radial profiles of the pressure, magnetic field and current. How one can realize this configuration?
6. Consider a Z -pinch with a constant plasma temperature. Find an integral condition on the plasma density and electric current that has to be satisfied in the stationary state (the Bennet condition). Calculate the intensity of axial current and draw the radial profile of pressure and of magnetic field supposing that the intensity of current is a constant. How one can realize this configuration?



HELLENIC
MEDITERRANEAN
UNIVERSITY



universit 
BORDEAUX



Erasmus+

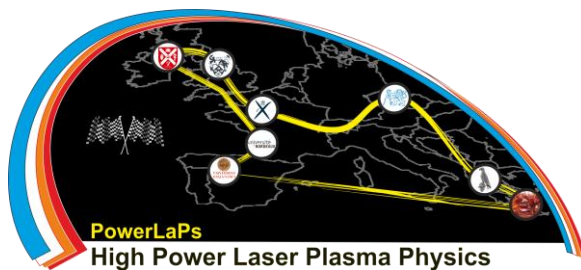
PowerLaPs

Innovative Education & Training in High Power Laser Plasmas

Plasma Physics - Theory and Experiments

Chapter 9: Electromagnetic properties of an isotropic plasma

D. Batani, E. d'Humi res, J.J. Santos, V.T. Tikhonchuk



Erasmus+

universit 
de
BORDEAUX

9 Electromagnetic properties of an isotropic plasma

Plasma is a dielectric medium and therefore it maintains electromagnetic waves – these are periodic motions that correspond to propagation of the electric and magnetic fields coupled to perturbations of the current and electric charge. Various types of waves exist in plasma. In this chapter we restrict ourselves to the simplest case of linear waves in a homogeneous medium. These are low-amplitude waves that can be considered as small perturbations of the initial state. These waves are described by linear equations and they can be analyzed with the universal Fourier method.

Each wave is characterized by two main parameters: a *dispersion*, or a relationship between the frequency of the wave ω and the wave vector \vec{k} , and a *polarization*, which is the direction of the vector of the wave electric field with respect to the direction of the wave vector. In this chapter we show that all the wave properties of the dielectric medium are described by a single tensor, the dielectric permittivity $\epsilon_{ij}(\vec{k}, \omega)$. We will study the general properties of this function before analyzing the particular waves.

9.1 Dispersion equation of electromagnetic waves

The relation between the electric \vec{E} and the magnetic field \vec{B} is described by Maxwell equation: (7.16) – (7.19):

$$\epsilon_0 \vec{\nabla} \cdot \vec{E} = \rho, \quad \partial_t \vec{B} = -\vec{\nabla} \times \vec{E}, \quad (9.1)$$

$$\vec{\nabla} \cdot \vec{B} = 0, \quad c^{-2} \partial_t \vec{E} = -\mu_0 \vec{j} + \vec{\nabla} \times \vec{B} \quad (9.2)$$

where the speed of light is defined as $c^{-2} = \epsilon_0 \mu_0$. We consider here the case where the external sources are absent and the self-consistent sources are linear: the charge density ρ and the current density \vec{j} are linear functions of the electric and magnetic fields. In fact, it is sufficient to consider just one relationship between the electric field \vec{E} and the current \vec{j} , because the other quantities are related by linear equations. The charge density and current are related by the continuity equation

$$\partial_t \rho + \vec{\nabla} \cdot \vec{j} = 0. \quad (9.3)$$

This equation is fundamental because it expresses the law of conservation of electric charge. Electric and magnetic fields are related by the equation of Faraday. Therefore, the relation $\vec{j}(\vec{E})$ contains all the information about the properties of the dielectric medium.

The linear electrodynamics is based on the assumption of a linear relationship between the current and the electric field. This is the Ohm's law. The most general form of this relationship is a convolution tensor:

$$j_i(\vec{r}, t) = \tilde{\sigma}_{ij} \star E_j = \int d\vec{r}' \int dt' \tilde{\sigma}_{ij}(\vec{r} - \vec{r}', t - t') E_j(\vec{r}', t'). \quad (9.4)$$

The conductivity $\tilde{\sigma}_{ij}$ is a tensor because it makes a link between two vectors, \vec{j} and \vec{E} . This relationship is in general non-local and a non-stationary. The only major limitation is the *principle of causality*: at a given moment of time the current can be generated only by the field at precedent times. In addition, $\tilde{\sigma}_{ij}$ it is a real function because the current and the field are real functions.

9.1.1 Isotropic medium with time dispersion

The number of independent components of the tensor of conductivity and the explicit form of spatial and temporal behavior are defined by properties of the medium. Spatial dispersion arises from the

thermal agitation, and it is especially important for low frequency waves. It is necessary to retain the spatial dispersion for longitudinal waves, but not for electromagnetic waves. For an isotropic medium without spatial dispersion the conductivity is a scalar. This is understandable since in this case there is no privileged direction. The only second rank tensor available is the Kronecker symbol, δ_{ij} , so, $\tilde{\sigma}_{ij} = \tilde{\sigma}(t) \delta_{ij}$. The temporal dispersion comes from the finite response time of the particles to the electric field. It is more important for the waves with a period comparable to the characteristic time response of the medium. For example, the periods of oscillations of electrons in atoms or the atoms in molecules. But, outside these resonances, the temporal dispersion is less important and often we can consider $\tilde{\sigma}$ as a constant. In addition, for very short excitation times, which are smaller than all characteristic times, the media response must be very weak.

The Maxwell's equations are linear and having a linear Ohm's law, it is more convenient to analyze them in the Fourier space by making the Fourier transforms in time and in space. In this case the differential operators and the integrals are transformed into algebraic operations and all Fourier components are independent. Suppose that the functions \vec{E} , \vec{B} , \vec{j} and ρ depend on time and on spatial coordinate as $\exp(-i\omega t + i\vec{k} \cdot \vec{r})$. Then, for an isotropic medium without spatial dispersion the Ohm's law takes the form $\vec{j} = \sigma(\omega)\vec{E}$, where $\sigma(\omega)$ is the Fourier transform of the function $\tilde{\sigma}(t)$.

Injecting this relation in the equation of continuity (9.3) we obtain a formula for the charge density induced by the electric field, $\rho = \sigma \vec{k} \cdot \vec{E} / \omega$. We see that only the longitudinal component of field produces the charge separation, while the transverse field induces a divergence-free, purely rotational current.

It may be noted again that, according to the general definition, the current is related to the polarization, $\vec{j} = \partial_t \vec{P}$. In a Fourier space this relation can be written, $\vec{P} = (i\sigma/\omega) \vec{E}$, therefore, the quantity $\chi = i\sigma/\omega$ is the dielectric susceptibility. This allows us to introduce the electric induction, $\vec{D} = \epsilon_0 \vec{E} + \vec{P}$, and the dielectric permittivity (or a dielectric constant) by the definition $\vec{D} = \epsilon_0 \epsilon \vec{E}$, where

$$\epsilon = 1 + i\sigma/\epsilon_0\omega. \quad (9.5)$$

These definitions allow us to simplify the Maxwell's equations. First of all, the Poisson equation can be written, $i\epsilon_0 \epsilon \vec{k} \cdot \vec{E} = \rho^{\text{ext}}$. Where in the real space we have

$$\vec{\nabla} \cdot \vec{D} = \rho^{\text{ext}}. \quad (9.6)$$

Therefore, the longitudinal electric field (electrostatic) can exist without external sources only if the dielectric constant is zero. This can happen only in a medium with time dispersion, therefore, the equation

$$\epsilon(\omega) = 0 \quad (9.7)$$

is the dispersion equation for electrostatic waves.

The electromagnetic waves are described by the Faraday and the Ampere's equations:

$$\omega \vec{B} = \vec{k} \times \vec{E}, \quad -i\omega \epsilon_0 \epsilon \vec{E} + \vec{j}^{\text{ext}} = i\mu_0^{-1} \vec{k} \times \vec{B}. \quad (9.8)$$

In the absence of external sources, taking into account that in this case $\vec{k} \cdot \vec{E} = 0$, we obtain the dispersion equation of electromagnetic waves:

$$\epsilon(\omega) = N^2 \quad (9.9)$$

where $N = ck/\omega$ is the refraction index. We see that these waves also exist in medium without dispersion, where ϵ is a constant, or even in a vacuum, where $\epsilon = 1$. The only limitation is that the dielectric permittivity is positive.

Equations (9.8) can be written in real space as follows:

$$\partial_t \vec{B} = -\vec{\nabla} \times \vec{E}, \quad \partial_t \vec{D} + \vec{j}^{\text{ext}} = \mu_0^{-1} \vec{\nabla} \times \vec{B}. \quad (9.10)$$

This form is useful for analyzing problems with external sources.

9.1.2 Isotropic medium with a spatial dispersion

The conductivity characterizes a response of the medium – the electric current \vec{j} – to the electric field \vec{E} . The response depends on the parameters of medium at equilibrium and on the characteristics of perturbation ω and \vec{k} . In the case of an isotropic medium without spatial dispersion there is no any privileged direction. The only symmetric tensor of the second rank available in this case is the Kronecker tensor δ_{ij} . Therefore, the conductivity is characterized by one scalar function, $\sigma_{ij} = \sigma \delta_{ij}$. In the case of medium with temporal dispersion, σ is a function of the frequency ω .

In the case of an isotropic medium with a spatial dispersion there is one privileged direction – the direction of the wave propagation defined by the wave vector \vec{k} . Therefore, we may build a second rank tensor using the vector \vec{k} and also the Kronecker tensor δ_{ij} . There are only two possible combinations, which are: δ_{ij} and $k_i k_j / k^2$. It is convenient to introduce two elementary independent tensors, $k_i k_j / k^2$ and $\delta_{ij} - k_i k_j / k^2$. The first one characterizes the response to the longitudinal electric field, parallel to the vector \vec{k} . The second tensor is related to the response to the transversal field. Therefore, in a medium with spatial dispersion the conductivity tensor is described by two scalar functions, σ^l et σ^{tr} :

$$\sigma_{ij} = \sigma^l \frac{k_i k_j}{k^2} + \sigma^{tr} \left(\delta_{ij} - \frac{k_i k_j}{k^2} \right). \quad (9.11)$$

According to our discussion in the preceding paragraph, the dielectric permittivity tensor has the same structure:

$$\epsilon_{ij} = \delta_{ij} + \frac{i}{\epsilon_0 \omega} \sigma_{ij} = \epsilon^l \frac{k_i k_j}{k^2} + \epsilon^{tr} \left(\delta_{ij} - \frac{k_i k_j}{k^2} \right) \quad (9.12)$$

where $\epsilon^{l,tr} = 1 + i\sigma^{l,tr}/\epsilon_0\omega$ are the longitudinal and the transverse permittivities. From these equations we see that the charge perturbation is produced by the longitudinal part of the field, $\rho = \sigma^l \vec{k} \cdot \vec{E} / \omega$. Thus, the Poisson equation gives us the following equation for longitudinal waves:

$$\epsilon^l(\vec{k}, \omega) = 0. \quad (9.13)$$

This equation is the generalization of Eq. (9.7) for a medium with spatial dispersion. The electrostatic waves do not exist in vacuum. The transverse part of the dielectric permittivity is involved in the Ampere equation, which can be written in the following form: $\omega \epsilon_0 \epsilon^{tr} \vec{E}_{tr} = c^2 \vec{k} \times \vec{B}$, where \vec{E}_{tr} is the electric field component perpendicular to the vector \vec{k} . Using the Faraday equation we obtain:

$$\epsilon^{tr}(\vec{k}, \omega) = N^2. \quad (9.14)$$

This dispersion equation is similar to Eq. (9.9). The transverse electric field and the magnetic field are coupled, and they are perpendicular to the direction of wave propagation, $\vec{E} \perp \vec{B} \perp \vec{k}$. However, the electric field \vec{E} can have an arbitrary direction in the plane perpendicular to the wave vector. The fact that the dispersion equation (9.14) is the same for both field components in the plane perpendicular to \vec{k} means that the electromagnetic wave is degenerate: two electromagnetic waves with a give \vec{k} have the same frequency $\omega(k)$ but different polarizations.

9.2 General proprieties of the dielectric permittivity

The dielectric permittivity plays an important role in electrodynamics. It describes the wave modes of the system and also the fields excited by external sources. The dielectric permittivity is in general a complex function of the wave vector \vec{k} and of the frequency ω . It has several general properties that can be established without finding explicit expressions for ϵ .

We notice that in the Ohm's law (9.4), the tensor $\tilde{\sigma}_{ij}$ defines a linear relation between the electric field \vec{E} and the current \vec{j} in the real space. By introducing the vectors of polarization $\vec{j} = \partial_t \vec{P}$ and the electric induction, $\vec{D} = \epsilon_0 \vec{E} + \vec{P}$, similar relations can be obtained for \vec{D} in the real space and in the Fourier space:

$$D_i(\vec{r}, t) = \epsilon_0 \tilde{\epsilon}_{ij} \star E_j, \quad \vec{D}_i(\vec{k}, \omega) = \epsilon_0 \epsilon_{ij} E_j. \quad (9.15)$$

where $\tilde{\epsilon}_{ij}$ is the inverse Fourier transform of ϵ_{ij} :

$$\tilde{\epsilon}_{ij}(\vec{r}, t) = (2\pi)^{-4} \int d\vec{k} \int d\omega \epsilon_{ij}(\vec{k}, \omega) e^{-i\omega t + i\vec{k} \cdot \vec{r}}.$$

These two quantities \vec{E} and \vec{D} are real functions in the real space (\vec{r}, t) this implies that $\tilde{\epsilon}_{ij}(\vec{r}, t)$ is a real function. Therefore, the dielectric permittivity owns the following propriety:

$$\epsilon_{ij}(-\vec{k}, -\omega) = \epsilon_{ij}^*(\vec{k}, \omega). \quad (9.16)$$

In addition, according to Eq. (9.11), the tensor ϵ_{ij} is an even function of the vector \vec{k} . Therefore,

$$\epsilon_{ij}(-\vec{k}, \omega) = \epsilon_{ij}(\vec{k}, \omega). \quad (9.17)$$

This relationship is valid for an isotropic plasma without an external magnetic field. If the magnetic field is present, we must reverse its direction while reversing \vec{k} :

$$\epsilon_{ij}(\vec{k}, \omega, \vec{B}) = \epsilon_{ij}(-\vec{k}, \omega, -\vec{B}). \quad (9.18)$$

Finally, for an isotropic plasma, from Eqs. (9.16) and (9.17) we obtain:

$$\epsilon_{ij}(\vec{k}, -\omega) = \epsilon_{ij}^*(\vec{k}, \omega). \quad (9.19)$$

We also note that for perturbations of a very high frequency the plasma has no time to respond, that is to say, it behaves like a vacuum:

$$\lim_{\omega \rightarrow \infty} \epsilon^{l, tr} = 1. \quad (9.20)$$

9.3 General solution of the dispersion equation

The solutions of the dispersion equations (9.13) and (9.14) define the relationships between the frequency and the wavelength, the *eigenmodes*, which may exist in a plasma without external sources. In general, the dielectric permittivity is a complex quantity and, consequently, the solution $\omega(\vec{k}) = \omega' + i\omega''$ is a complex function. The real part ω' defines the period of oscillations, $2\pi/\omega'$, and the imaginary part ω'' defines the temporal variation of wave amplitude. If ω'' is positive, the amplitude grows with time, which is impossible in a stable medium. In this case we say that the plasma is unstable. On the contrary, the negative value of ω'' means that there is a damping. The wave amplitude decreases with time. In this case we call $\gamma = -\omega''$ the *damping rate*.

The criterion of existence of eigenmodes is that they are weakly damped. This means that in the range of existence of the eigenmodes, the imaginary part of ω is much smaller than its real part, $\gamma \ll \omega$. Therefore, the imaginary part of permittivity in these conditions must also be sufficiently small, and we can solve the dispersion equation by using the method of perturbations. In the case of longitudinal waves (9.13), we separate the real and the imaginary part of ϵ^l and of the frequency. Thus, the dispersion equation reads:

$$\text{Re } \epsilon^l(k, \omega' + i\omega'') + i \text{Im } \epsilon^l(k, \omega' + i\omega'') = 0.$$

We find the solution of this equation by developing the real part in the Taylor series, $\text{Re } \epsilon^l(k, \omega') + i\omega'' \partial_\omega \text{Re } \epsilon^l$. In addition, for a small imaginary part, we may neglect ω'' . With these simplifications, the real part of the dispersion equation becomes $\text{Re } \epsilon^l(k, \omega') = 0$. The imaginary part of this equation gives an expression for ω'' :

$$\omega'' = -\gamma = -\frac{\text{Im } \epsilon^l(k, \omega')}{\partial_\omega \text{Re } \epsilon^l}. \quad (9.21)$$

Similarly, we can deduce from Eq. (9.14) that the damping rate of electromagnetic waves is defined as follows:

$$\omega'' = -\gamma = -\frac{\omega' \text{Im } \epsilon^{tr}(k, \omega')}{\omega' \partial_\omega (\text{Re } \epsilon^{tr}) + 2N^2}. \quad (9.22)$$

Knowing the spectrum of eigenmodes we can define two important variables: the phase velocity

$$\vec{v}_{ph}(\vec{k}) = \omega \vec{k} / k^2 \quad (9.23)$$

and the group velocity

$$\vec{v}_g(\vec{k}) = \partial\omega / \partial\vec{k}. \quad (9.24)$$

The first one is important for the interaction of the wave with the particles: a particle with a speed $\vec{v} \simeq \vec{v}_{ph}$ sees a constant electric field of the wave, and it can easily gain or lose energy. This is the physical basis of collisionless wave damping. The group velocity characterizes the rate of energy transport in the wave. One can also say that it is a speed of propagation of the information in space.

9.4 Linearized Vlasov equation

We consider linear waves, where the characteristic amplitude of the potential perturbation in plasma is smaller than the mean kinetic energy of particles, $e\Phi \ll k_B T$. In this case, the distribution function can be considered as a sum of a stationary function $f_{\alpha 0}(p)$ and a small non-stationary and inhomogeneous perturbation, $\delta f_\alpha(t, \vec{r}, \vec{p})$. Electric and magnetic fields should also be considered as perturbations as they do not exist in the equilibrium state. By injecting function $f_{\alpha 0} + \delta f_\alpha$ in the Vlasov equation (7.8) and considering the linear terms of the order of the perturbation δf , we obtain a linearized Vlasov equation. In Fourier space this equation reads:

$$-i\omega \delta f_\alpha + i\vec{k} \cdot \vec{v} \delta f_\alpha + q_\alpha (\vec{E} + \vec{v} \times \vec{B}) \cdot \partial_{\vec{p}} f_{\alpha 0} = 0. \quad (9.25)$$

In an isotropic plasma the distribution function $f_{\alpha 0}$ depends only on the modulus of the momentum vector. Therefore, its derivative $\partial_{\vec{p}} f_{\alpha 0}$ is directed along the velocity vector \vec{v} , and its scalar product with the Lorentz force, $\vec{v} \times \vec{B}$ is zero. Then, from Eq. (9.25) one obtains an expression for the perturbed distribution function:

$$\delta f_\alpha = -\frac{iq_\alpha}{\omega - \vec{k} \cdot \vec{v}} \vec{E} \cdot \partial_{\vec{p}} f_{\alpha 0}. \quad (9.26)$$

We must pay attention to the domain where the Fourier variables are defined because the denominator $\omega - \vec{k} \cdot \vec{v}$ may be equal to zero. The spatial coordinates are homogeneous, there is no privileged direction, and we can consider \vec{k} as a real vector. On the contrary, we must differentiate between the past and the future time. According to the general definition of the conductivity and the dielectric permittivity, Eqs. (9.4) and (9.5), the electric current and the electric induction at the time t are related to the electric fields at the preceding times, $t' < t$. Therefore, the current should be zero if $t \rightarrow -\infty$. This is another formulation of the *principle of causality*. In Fourier space it corresponds to a specific behavior of all quantities depending on the variable ω . The contour of integration in the inverse Fourier transform should be chosen in such a way that the causality principle is fulfilled automatically.

Formally, we consider all physical quantities as analytic functions in the complex space ω in the upper half-plane, $\omega > 0$. This ensures that, while making the inverse Fourier transform, all perturbations will be zero for $t \rightarrow -\infty$. In other words, the frequency ω formally should always be considered as having a positive complex part, in other words, the integration contours must always pass below the pole $\omega = \vec{k} \cdot \vec{v}$.

We can justify this choice in a different way. Taking into account collisions in the kinetic equation (9.25), we can model them with the term $-\nu_\alpha \delta f_\alpha$ on the right hand side, see Sec. ???. A positive frequency of collisions, $\nu_\alpha > 0$, assures relaxation of any perturbation to an equilibrium. Making a Fourier transform, we obtain an imaginary term in the denominator of Eq. (9.26) : $\omega + i\nu_\alpha - \vec{k} \cdot \vec{v}$. In the limit $\nu_\alpha \rightarrow 0$ this corresponds to the same definition of singularity, that is to say, that the contour of integration over the velocities goes below the pole $\omega = \vec{k} \cdot \vec{v}$.

Using the perturbed distribution function (9.26), we can calculate the current that is proportional to the electric field

$$\vec{j} = -i \sum_{\alpha} q_{\alpha}^2 \int d\vec{p} \frac{\vec{v}}{\omega + i\nu_{\alpha} - \vec{k} \cdot \vec{v}} \vec{E} \cdot \partial_{\vec{p}} f_{\alpha 0}. \quad (9.27)$$

The coefficient of proportionality between the current and the electric field is the electrical conductivity tensor. According to the definition (9.12), the dielectric permittivity of an isotropic collisional plasma is:

$$\epsilon_{ij} = \delta_{ij} + \sum_{\alpha} \frac{q_{\alpha}^2}{\epsilon_0 \omega} \int d\vec{p} \frac{v_i}{\omega + i\nu_{\alpha} - \vec{k} \cdot \vec{v}} \partial_{p_j} f_{\alpha 0}. \quad (9.28)$$

The positive imaginary term in the denominator of this expression means that the pole $\omega + i\nu_{\alpha} - \vec{k} \cdot \vec{v} = 0$ is situated above the integration contour over the velocity component parallel to the wave vector, which goes along the real axis.

The dielectric permittivity tensor, according to the general analysis of Sec. 9.1.2, contains only two independent components: the longitudinal and the transverse part. This can be demonstrated explicitly by considering Eq. (9.28). Choosing the wave vector direction along z -axis, the derivative of an isotropic distribution function can be presented as: $\partial_{p_j} f_{\alpha 0} = v_j \partial_{\varepsilon} f_{\alpha 0}$, where ε is the energy of the particle. So the integral term in Eq. (9.28) has the following structure:

$$G_{ij} = \int d\vec{p} \frac{v_i v_j}{\omega + i\nu_{\alpha} - k v_z} \partial_{\varepsilon} f_{\alpha 0}.$$

First, we see that the components outside the diagonal ($i \neq j$) equal to zero, because they are integrals of an odd function. Among three diagonal components, the terms G_{xx} and G_{yy} are equal because of symmetry of plasma in the plane perpendicular to the wave vector. So there are only two independent components, $G^{tr} = G_{xx} = G_{yy}$, and $G^l = G_{zz}$.

In an invariant manner, the longitudinal part is obtained by multiplying Eq. (9.28) by the tensor $k_i k_j / k^2$. This gives the longitudinal part of plasma dielectric permittivity:

$$\epsilon^l(\vec{k}, \omega) = 1 + \sum_{\alpha} \delta \epsilon_{\alpha}^l(\vec{k}, \omega) \quad \text{where} \quad \delta \epsilon_{\alpha}^l = \frac{q_{\alpha}^2}{k^2 \epsilon_0 \omega} \int d\vec{p} \frac{\vec{k} \cdot \vec{v}}{\omega + i\nu_{\alpha} - \vec{k} \cdot \vec{v}} \vec{k} \cdot \partial_{\vec{p}} f_{\alpha 0}. \quad (9.29)$$

This formula can be simplified. We write the fraction $\vec{k} \cdot \vec{v} / (\omega + i\nu_{\alpha} - \vec{k} \cdot \vec{v})$ as

$$-1 + \frac{\omega + i\nu_{\alpha}}{\omega + i\nu_{\alpha} - \vec{k} \cdot \vec{v}}$$

and we observe that the first term is zero after the integration. Therefore, the longitudinal part of dielectric permittivity reads

$$\delta \epsilon_{\alpha}^l = \frac{q_{\alpha}^2}{k^2 \epsilon_0} \left(1 + i \frac{\nu_{\alpha}}{\omega}\right) \int \frac{d\vec{p}}{\omega + i\nu_{\alpha} - \vec{k} \cdot \vec{v}} \vec{k} \cdot \partial_{\vec{p}} f_{\alpha 0}. \quad (9.30)$$

To obtain the transverse part of permittivity we multiply Eq. (9.28) by the tensor $\frac{1}{2}(\delta_{ij} - k_i k_j / k^2)$ thus obtaining:

$$\epsilon^{tr}(\vec{k}, \omega) = 1 + \sum_{\alpha} \frac{q_{\alpha}^2}{2k^2 \epsilon_0 \omega} \int \frac{d\vec{p}}{\omega + i\nu_{\alpha} - \vec{k} \cdot \vec{v}} (\vec{k} \times \vec{v} \times \vec{k}) \cdot \partial_{\vec{p}} f_{\alpha 0}.$$

Integrating by parts, we obtain a simpler form

$$\epsilon^{tr}(\vec{k}, \omega) = 1 - \sum_{\alpha} \frac{q_{\alpha}^2}{m_{\alpha} \epsilon_0 \omega} \int \frac{f_{\alpha 0}}{\omega + i\nu_{\alpha} - \vec{k} \cdot \vec{v}} d\vec{p}. \quad (9.31)$$

In the following sections we will use these forms to study the plasma eigenmodes.

9.5 Kinetics of electromagnetic waves

9.5.1 Dispersion of electromagnetic waves

Electromagnetic waves exist in the domain of high frequencies. Ions, due to their high inertia are not involved in this process. Formally we can put $m_i \rightarrow \infty$ and the dispersion equation becomes $1 + \delta \epsilon_e^{tr}(\vec{k}, \omega) = N^2$. Moreover, the phase velocity ω/k of high frequency electromagnetic waves is much greater than the electron thermal velocity $\omega/k \gg v_{Te}$. Thus, in the non-relativistic case we can completely neglect the term $\vec{k} \cdot \vec{v}$ in the denominator of Eq. (9.31). Then, the integral over momentum can be performed easily, $\int f_{e0} d\vec{p} = n_{e0}$, and the expression for the transverse permittivity takes the following form:

$$\epsilon^{tr}(\omega) = 1 - \frac{\omega_{pe}^2}{\omega(\omega + i\nu_e)}. \quad (9.32)$$

where $\omega_{pe} = (e^2 n_{e0} / \epsilon_0 m_e)^{1/2}$ is the electron plasma frequency. Under these conditions the transverse dielectric permittivity depends only on the frequency ω . So the plasma behaves as a medium with time dispersion but with no spatial dispersion. Taking the real part of the dispersion equation and assuming that $\nu_e \ll \omega_{pe}$, we obtain the spectrum of electromagnetic waves:

$$\omega_{em}^2 \simeq \omega_{pe}^2 + k^2 c^2. \quad (9.33)$$

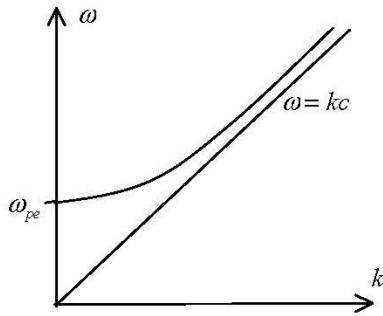


Figure 33: Dispersion curve of a plane electromagnetic wave: the line asymptotic $\omega = kc$ corresponds to the electromagnetic wave in a vacuum.

density is zero, because for a transverse wave the electric field is strictly perpendicular to the wave vector, $\vec{E} \perp \vec{k}$. This means that the *electromagnetic waves are not accompanied by density perturbations*.

Damping of electromagnetic waves is only due to electron-ion collisions. Taking the imaginary part of the dispersion equation, according to Eq. (9.22) we find:

$$-\text{Im } \omega_{em} = \gamma_{em} = \frac{1}{2} \frac{\nu_e i \omega_{pe}^2}{\omega_{em}^2}. \quad (9.34)$$

The electromagnetic wave does not interact with particles resonantly, because its phase velocity is always greater than the speed of light.

9.5.2 Energy of electromagnetic waves

The energy of electromagnetic waves is composed of three terms: the energy of electric field, the energy of magnetic field and the energy of electron motion in these fields. Assuming that the wave has a linear polarization, the wave electric field reads

$$\vec{E}(t, \vec{r}) = \vec{E}_0 \cos(\omega_{em} t - \vec{k} \cdot \vec{r})$$

where $\omega_{em}(\vec{k})$ is given by Eq. (9.33) and the amplitude vector \vec{E}_0 is perpendicular to the wave vector \vec{k} . The expression for the magnetic field follows from the Faraday equation:

$$\vec{B}(t, \vec{r}) = \frac{\vec{k}}{\omega_{em}} \times \vec{E}_0 \cos(\omega_{em} t - \vec{k} \cdot \vec{r}).$$

Averaging over the wave period, $2\pi/\omega_{em}$, we obtain the density of electric energy

$$W_E = \frac{1}{2} \epsilon_0 \langle \vec{E}^2 \rangle = \frac{1}{4} \epsilon_0 \vec{E}_0^2$$

and the density of magnetic energy,

$$W_B = \frac{1}{2\mu_0} \langle \vec{B}^2 \rangle = \frac{1}{4} \epsilon_0 \frac{k^2 c^2}{\omega_{em}^2} \vec{E}_0^2.$$

The dispersion curve is presented in Fig. 33. In the limit of very small wavelengths, $k \gg \omega_{pe}/c$, this mode corresponds to the electromagnetic wave in vacuum. In this case the frequency of the wave is higher to the one of the plasma and so the influence of the plasma is negligible. The plasma contribution becomes more important when the wave frequency approaches ω_{pe} . The current induced in plasma by the wave electric field, according to the principle of Le Chatelet, reduces the displacement current. Because of that the group velocity is reduced. The electromagnetic wave ceases to exist for $\omega < \omega_{pe}$. Because the plasma frequency depends on the electron density, we deduce the critical density (or density cutoff) $n_c = m_e \omega / \epsilon_0 e^2$ from the equation $\omega = \omega_{pe}$. The electromagnetic wave can not penetrate into the plasma beyond the critical density.

Another interesting propriety of electromagnetic waves comes from the kinetic equation (9.26). By integrating δf_e over the momentum we find that the perturbation of the

Using the equation of dispersion, we see that the magnetic energy is smaller than the electrical energy by a factor $k^2 c^2 / \omega_{em}^2 = 1 - \omega_{pe}^2 / \omega_{em}^2$.

We need to account also for the energy of plasma electrons that oscillate in the wave field. According to the linearized equation of electron motion (4.2), $\partial_t \vec{u}_e = -(e/m_e) \vec{E}$, the electron velocity is:

$$\vec{u}_e(t, \vec{r}) = -\frac{e \vec{E}_0}{m_e \omega_{em}} \sin(\omega_{em} t - \vec{k} \cdot \vec{r}).$$

Consequently, the average kinetic energy of electrons is:

$$W_e = \frac{1}{2} n_e m_e \langle \vec{u}_e^2 \rangle = \frac{1}{4} \frac{e^2 n_e}{m_e \omega_{em}^2} \vec{E}_0^2 = \frac{1}{4} \frac{\omega_{pe}^2}{\omega_{em}^2} \epsilon_0 \vec{E}_0^2.$$

Addition of three terms gives the total energy of electromagnetic wave, $W_{tot} = W_E + W_B + W_e = \frac{1}{2} \epsilon_0 \vec{E}_0^2$. The presence of plasma has no effect on the expression for the total energy of electromagnetic wave. This is the same expression as in vacuum, but this energy is distributed differently. The energy of electric field does not change, but some of the magnetic field energy is converted into the energy of plasma current.

The energy W_{tot} is transported into the plasma with the group velocity $\vec{v}_g = \vec{k} c^2 / \omega_{em}$. The energy flux of the wave is given by the Poynting vector, $\vec{S} = \vec{v}_g W_{tot}$. The factor γ_{em} / v_g defines the coefficient of spatial damping of an electromagnetic wave. Therefore, the wave intensity decreases exponentially over the distance $L_d = v_g / 2 \gamma_{em}$. If the electromagnetic wave propagates in a stationary inhomogeneous plasma, its Poynting vector is conserved. However, as the plasma density increases, the group velocity decreases. That means that the energy density of electromagnetic wave increases as the wave enters in a denser plasma.

9.6 Langmuir waves

Langmuir waves are longitudinal plasma waves of a high frequency. They were discovered by Tonks and Langmuir in 1926. The effect of the spatial dispersion of these waves was calculated by Vlasov in 1938 and Bohm and Gross in 1949. Ions are not involved in this process because of their high inertia. As for electromagnetic waves, we can formally put $m_i \rightarrow \infty$ and the dispersion equation of Langmuir waves reads: $1 + \delta \epsilon_e^l(\vec{k}, \omega) = 0$. Moreover, because of the assumption of high frequency, the Langmuir wave phase velocity ω/k is greater than the electron thermal velocity, $\omega/k \gg v_{Te}$.

These two assumptions allow to simplify the expression of the electronic susceptibility. First, we perform an integration in Eq. (9.30) by parts

$$\delta \epsilon_e^l(\vec{k}, \omega) = \frac{e^2}{k^2 \epsilon_0} \left(1 + i \frac{\nu_e}{\omega}\right) \int \frac{\vec{k} \cdot \partial_{\vec{p}} f_{e0}}{\omega + i \nu_e - \vec{k} \cdot \vec{v}} d\vec{p} = -\frac{e^2}{m_e \epsilon_0} \left(1 + i \frac{\nu_e}{\omega}\right) \int \frac{f_{e0}}{(\omega + i \nu_e - \vec{k} \cdot \vec{v})^2} d\vec{p}.$$

Then we develop the denominator in a Taylor series assuming that $k v / \omega \ll 1$ and $\nu_e / \omega \ll 1$:

$$\frac{1 + i \nu_e / \omega}{(\omega + i \nu_e - \vec{k} \cdot \vec{v})^2} \approx \frac{1}{\omega^2} \left(1 + 2 \frac{\vec{k} \cdot \vec{v}}{\omega} + 3 \frac{(\vec{k} \cdot \vec{v})^2}{\omega^2} - i \frac{\nu_e}{\omega}\right).$$

The integrals $\int f_{e0} d\vec{p} = n_{e0}$ and $\int (\vec{k} \cdot \vec{v})^2 f_{e0} d\vec{p} = n_{e0} k^2 v_{Te}^2$ can be calculated explicitly. Then the expression of the permittivity takes the following form:

$$\delta \epsilon_e^l(\vec{k}, \omega) = -\frac{\omega_{pe}^2}{\omega^2} \left(1 + 3 \frac{k^2 v_{Te}^2}{\omega^2} - i \frac{\nu_e}{\omega}\right) \quad (9.35)$$

In the limit of a cold, $v_{Te} \rightarrow 0$, et collision-less, $\nu_e = 0$, plasma we find the formula of the electrical permittivity in the fluid model, $\delta\epsilon_e = -\omega_{pe}^2/\omega^2$. Here there is no dependence on k . Therefore, the dependence of ϵ on k – the *spatial dispersion* – is a kinetic effect produced by the thermal agitation of particles.

The formula (9.35) is obtained with the assumption, $k^2 v_{Te}^2 \ll \omega^2$. This allows us to solve the dispersion equation $\epsilon^l = 0$ by using the method of perturbations. First, we neglect the thermal term and solve the equation $1 - \omega_{pe}^2/\omega^2 = 0$. The solution to this equation is $\omega^2 = \omega_{pe}^2$. Then we put this expression for ω in $\delta\epsilon_e^l$ and solve a more complete equation:

$$1 - \frac{\omega_{pe}^2}{\omega^2} \left(1 + 3 \frac{k^2 v_{Te}^2}{\omega_{pe}^2} - i \frac{\nu_e}{\omega} \right) = 0.$$

The solution to this equation gives the dispersion relation for the electron (Langmuir) plasma waves:

$$\omega_{ep}(k) = \pm \omega_{pe} \left(1 + \frac{3}{2} k^2 \lambda_{De}^2 \right) - \frac{i}{2} \nu_e \quad (9.36)$$

where $\lambda_{De} = v_{Te}/\omega_{pe}$ is the electron Debye length. Two signs in this expression correspond to two waves traveling in opposite directions along the vector \vec{k} . The frequency in Eq. (9.36) is a function of k , see Fig. 34. This is an effect of spatial dispersion. We will see later that Langmuir waves exist only in the limit $k\lambda_{De} \ll 1$ and they are strongly damped for shorter wavelengths.

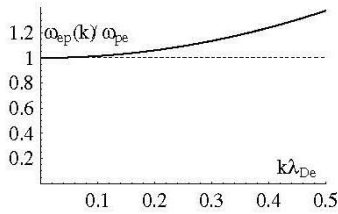


Figure 34: Dispersion curve for the Langmuir wave. The dotted line shows the electron plasma frequency

Langmuir waves are oscillations of the electric charge and electron density. Using the Poisson equation (7.17), we find a relation between the perturbation of electron density δn_e and the electric field E :

$$e\delta n_e = i\epsilon_0 \vec{k} \cdot \vec{E}.$$

The same relationship can be obtained from Eq. (9.26) by using the dispersion law (9.36). The factor i indicates that the maximum density is offset by a quarter period in space relative to the maximum field. This wave exists only in plasma and can not be emitted in vacuum. The group velocity of the plasma waves, $\vec{v}_g = 3\vec{k}\lambda_{De}v_{Te}$, is very small compared to the thermal velocity of electrons and also compared to its phase velocity. Therefore these waves are not able to carry the energy over long distances, they just accumulate energy locally and transfer it to the particles.

The energy of these waves is shared between electric field and particles. According to the course of electrodynamics, the electrostatic energy of a wave of amplitude \vec{E}_0 is given by the following formula:

$$\bar{W}_E = \frac{\epsilon_0}{4} \partial_\omega(\omega \text{Re } \epsilon^l) |\vec{E}_0|^2 \quad (9.37)$$

where the factor $\partial_\omega(\omega \text{Re } \epsilon^l)$ takes into account the energy of particle motion in the wave. This factor is 2 for plasma waves. So half of the energy is stored in the form of kinetic energy of electrons. This energy can be explicitly calculated from Eq. (9.26) in the limit $\omega/k \gg v_{Te}$. The average electron velocity reads:

$$\vec{v}_e = n_{e0}^{-1} \int d\vec{p} \vec{v} \delta f_e \approx \frac{ie}{n_{e0}\omega} \int d\vec{p} \vec{v} \vec{E} \cdot \partial_{\vec{p}} f_{e0} = \frac{ie}{m_e\omega} \vec{E}.$$

It is a quarter period in advance of the electric field. Then the average kinetic energy is:

$$\frac{1}{4}n_e m_e \langle \vec{u}_e \cdot \vec{u}_e^* \rangle = \frac{e^2 n_e}{4m_e \omega^2} \langle \vec{E} \cdot \vec{E}^* \rangle \approx \frac{1}{4} \epsilon_0 \langle |\vec{E}|^2 \rangle = \frac{1}{8} \epsilon_0 E_0^2.$$

Plasma waves correspond to oscillations of energy between the energy of the electric field and the kinetic energy of the electrons. The plasma wave damping will be further considered in Sec. 9.9. It comes from two effects: the electron-ion collisions and the resonant interaction between the electrons and the wave:

$$\gamma_{ep} = \frac{1}{2} \nu_e + \sqrt{\frac{\pi}{8}} \frac{\omega_{pe}}{k^3 \lambda_{De}^3} \exp\left(-\frac{3}{2} - \frac{1}{2k^2 \lambda_{De}^2}\right). \quad (9.38)$$

In particular, the second term is called *Landau damping*. It dominates for large wave numbers and prevents the existence of plasma waves with the wave lengths shorter than the Debye length.

9.7 Ion acoustic waves

Ion acoustic waves are low frequency oscillations of plasma density, $\omega \ll \omega_{pe}$. Their phase velocity lies in the range $v_{Te} \gg \omega/k \gg v_{Ti}$. They have also been discovered by Tonks and Langmuir in 1926. In this case two contributions in the dielectric permittivity are equally important – from the ions and the electrons. The ion susceptibility, $\delta\epsilon_i$, is calculated in the same way that the electron susceptibility for Langmuir waves, because the wave phase velocity is greater than the thermal velocity of the ions. According to Eq. (9.35), we find:

$$\delta\epsilon_i^l(k, \omega) = -\frac{\omega_{pi}^2}{\omega^2} \left(1 + 3\frac{k^2 v_{Ti}^2}{\omega^2} - i\frac{\nu_i}{\omega}\right) \quad (9.39)$$

where $\omega_{pi} = \sqrt{Z^2 e^2 n_{i0} / m_i \epsilon_0}$ is the ion plasma frequency. In calculation of the electron susceptibility, $\delta\epsilon_e$, we can neglect the frequency ω in the integral $\delta\epsilon_e^l$ and, using the following propriety of the Maxwellian function $\partial_{\vec{p}} f_{e0} = -\vec{v} f_{e0} / k_B T_e$, we obtain:

$$\delta\epsilon_e^l = \frac{e^2}{k^2 \epsilon_0} \int \frac{\vec{k} \cdot \partial_{\vec{p}} f_{e0}}{\omega - \vec{k} \cdot \vec{v}} d\vec{p} \approx \frac{e^2}{k^2 k_B T_e \epsilon_0} \int f_{e0} d\vec{p} = \frac{1}{k^2 \lambda_{De}^2}.$$

Finally, the dispersion equation for ion acoustic waves can be written as:

$$1 + \frac{1}{k^2 \lambda_{De}^2} - \frac{\omega_{pi}^2}{\omega^2} \left(1 + 3\frac{k^2 v_{Ti}^2}{\omega^2} - i\frac{\nu_i}{\omega}\right) = 0. \quad (9.40)$$

To solve this equation we use the same technique as it was used in Sec. 9.6 for solving Eq.(9.35). The thermal and collisional terms in the ion susceptibility are small. They can be neglected in first approximation, to obtain an approximate solution, $\omega^2 \approx k^2 c_s^2 / (1 + k^2 \lambda_{De}^2)$, where $c_s = \sqrt{Z k_B T_e / m_i}$ is the ion acoustic speed already introduced in Sec. ???. By injecting this solution into the ion susceptibility with thermal correction, we find a more complete solution:

$$\omega_{ai}^2(k) = \frac{k^2 c_s^2}{1 + k^2 \lambda_{De}^2} + 3k^2 v_{Ti}^2. \quad (9.41)$$

The frequency of ion acoustic wave as a function of the wavenumber is shown in Fig. 35.

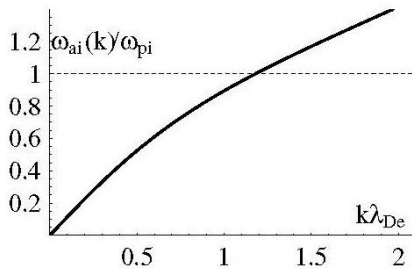


Figure 35: The dispersion curve of the ion acoustic wave for $ZT_e/T_i = 10$. Dotted line indicates the ion plasma frequency.

There are two important limits in this dispersion. The limit of long wavelengths, $k^2\lambda_{De}^2 \ll 1$, is corresponding to the quasi-linear dispersion,

$$\omega_{ai}(k) \approx \pm |k|v_s \left(1 - \frac{1}{2}k^2\lambda_{De}^2\right) \quad (9.42)$$

where $v_s = \sqrt{c_s^2 + 3v_{Ti}^2}$. This recalls the dispersion of an acoustic wave in a neutral medium, and the speed v_s is the speed of sound. In this limit the dispersion is weak. The phase velocity is almost equal to the group velocity and these waves are propagated without deformation of their shape.

The ion acoustic wave in the limit $k^2\lambda_{De}^2 \ll 1$ corresponds to almost neutral oscillations of density associated with a very weak electric field. This can be shown as follows. The electric field is obtained from the Poisson equation

$$i\epsilon_0 kE = Z\epsilon\delta n_i - \epsilon\delta n_e. \quad (9.43)$$

At the same time, by integrating Eq. (9.26) written for electrons over the momentum, one can show that the electric field is $\epsilon_0 E = iek\lambda_{De}^2\delta n_e$. Therefore, the term in the left hand side of Eq. (9.43) is much smaller than each of terms in the right hand side. Therefore, $Z\delta n_i \approx \delta n_e$. This is the condition of quasi-neutrality. The electric field in the ion acoustic waves is a factor $k^2\lambda_{De}^2$ smaller than for the Langmuir waves of same amplitude of density perturbation.

There is a significant difference between the neutral acoustic waves and ion acoustic waves in plasma. The condition of existence of these ion acoustic waves is $v_s \gg v_{Ti}$. This condition can only be satisfied in a non-isothermal plasma where $ZT_e \gg 3T_i$. The ion acoustic waves do not exist in a plasma in thermal equilibrium where $T_i \simeq T_e$.

The spectrum (9.41) extends to the domain of shorter wavelength, $k^2\lambda_{De}^2 \gtrsim 1$, see Fig. 35. However, in the limit $k^2\lambda_{De}^2 \gg 1$, the nature of this wave is different, and it is then called ion plasma wave. In this limit the spectrum is:

$$\omega_{ai}(k) = \pm \omega_{pi} \left(1 + \frac{3}{2}k^2\lambda_{Di}^2 - \frac{1}{2k^2\lambda_{De}^2}\right). \quad (9.44)$$

It is similar to the spectrum of Langmuir waves (9.36). In addition, from Eq. (9.26) we find that in this limit the perturbation of ion density is much larger than the electron density perturbation, $Z\delta n_i \gg \delta n_e$. Moreover, the relationship between δn_i and E is the same as for Langmuir waves. It is concluded that the ion plasma waves in the limit $k\lambda_{De} \gg 1$ are also perturbation of the charge density associated with the ions.

The spectra of Langmuir plasma waves and ion acoustic waves can be deduced also in the two fluid hydrodynamic equations described in Sec. ???. Nevertheless the kinetic approach is more consistent. It helps to avoid mistakes and to get more complete results. In particular, the hydrodynamic model must take into account the fact that the equations of state for electrons and ions are different as they correspond to the high and low frequencies. In the limit of high frequency, $\omega \gg kv_{T\alpha}$, particles behave as an ideal gas in one dimension, which corresponds to the adiabatic index $\gamma_\alpha = 3$. This is because the particle motion in the plane perpendicular to the vector \vec{k} is not perturbed. We conclude this from the kinetic analysis, but in the hydrodynamic theory we must postulate it.

On the contrary, in the limit of low frequencies, $\omega \ll kv_{T\alpha}$, particles behave as an isothermal ideal gas, which corresponds to the adiabatic index $\gamma_\alpha = 1$. This can be explained using the kinetic theory: the phase velocity in this case is lower than the thermal velocity and the particles can easily reach an equilibrium before the wave phase changes. The kinetic theory also allows to analyze more complex systems with distribution functions non-isotropic and non-Maxwellian.

Damping of ion acoustic waves is considered in Sec. 9.9. It comes from two effects: the ion-ion collisions and the resonant interaction between the wave and the electrons and the ions. In the weakly collisional limit, where the frequency of ion-ion collisions is much smaller than the wave frequency, $\nu_{ii} \ll \omega_{ai}$, the damping rate reads:

$$\gamma_{ai} = \frac{1}{2} \nu_{ii} \frac{v_{Ti}^2}{c_s^2} + \sqrt{\frac{\pi}{8}} k v_s \left[\frac{\omega_{pi}}{\omega_{pe}} + \left(\frac{v_s}{v_{Ti}} \right)^3 e^{-v_s^2/2v_{Ti}^2} \right]. \quad (9.45)$$

In particular, the last term is due to the Landau damping on ions. This term depends on the relative temperatures of electrons and ions, T_e/T_i , and the condition of weak damping can be satisfied only in highly non-isothermal plasmas, $T_i/T_e \ll Z$.

9.8 Imaginary part of the dielectric permittivity

The real part of the dielectric permittivity was calculated in Sec. 9.6 and 9.7. The imaginary part of dielectric permittivity comes from two effects: (i) collisions between particles, which are trying to destroy the coherence of their motion in the wave, and (ii) a resonant interaction between the wave and the particles. The collisional damping can be calculated directly from Eqs. (9.35) and (9.40). Here, we consider the non-collisional effects.

In the previous calculation we have neglected the contribution of resonant particles. It comes formally from the pole $\omega = \vec{k} \cdot \vec{v}$ that corresponds to the particles having the velocity equal to the wave phase velocity. To account this singularity we recall that, according to the principle of causality, the frequency ω has to be considered as sitting in the upper part of the complex plane. Therefore, the contour of integration over the particle velocity must pass below the pole.

Assuming that the vector \vec{k} is directed along the z -axis, let us first integrate the expressions for the dielectric permittivity (9.30) and (9.31) over the momenta in the perpendicular plane. Introducing the distribution function in one dimension $F_{\alpha 0}(p_z) = \int f_{\alpha 0} dp_x dp_y$, we have:

$$\delta\epsilon_\alpha^l = \frac{q_\alpha^2}{k\epsilon_0} \int \frac{\partial_{p_z} F_{\alpha 0}}{\omega - kv_z} dp_z, \quad \delta\epsilon_\alpha^{tr} = -\frac{q_\alpha^2}{\epsilon_0\omega} \int \frac{F_{\alpha 0} dp_z}{\omega - kv_z}. \quad (9.46)$$

The contour of integration is plotted in Fig. 36. It makes a half turn below the pole. Formally, this half-turn can be presented as a half of residue of this pole:

$$\frac{1}{\omega - kv_z} = \frac{\mathcal{P}}{\omega - kv_z} - i\pi\delta(\omega - kv_z)$$

where $\delta(x)$ is the Dirac function and \mathcal{P} means the principal part (in the sense of Cauchy) of the integral. The second term in this formula contributes to the imaginary part of permittivity:

$$\text{Im} \delta\epsilon_\alpha^l(k, \omega) = -\frac{\pi q_\alpha^2}{k^2 \epsilon_0} \partial_p F_{\alpha 0} \Big|_{v=\omega/k}, \quad (9.47)$$

$$\text{Im} \delta\epsilon_\alpha^{tr}(k, \omega) = \frac{\pi q_\alpha^2}{k\omega\epsilon_0} F_{\alpha 0} \Big|_{v=\omega/k}. \quad (9.48)$$

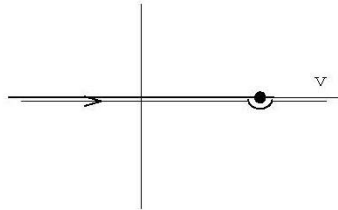


Figure 36: Contour of integration in the formula for the dielectric permittivity over velocity component parallel the wave vector. The pole $v_z = \omega/k$ is marked by a black dot.

We see from these expression that the imaginary part comes from the resonant particles, which propagate with a velocity equal to the phase velocity of the wave. If there is no resonant particles and no collisions, the dielectric permittivity is real. The general condition of the plasma stability requires that $\text{Im}\epsilon$ is positive quantity. This implies that $\partial_v f_{\alpha 0}$ is negative for $v > 0$ and positive for $v < 0$. This is the third criterion of equilibrium that has been postulated in Sec. 8.1.

The imaginary part of the longitudinal permittivity produces a non-collisional damping of electron plasma and ion acoustic waves. The imaginary part of the transverse permittivity does not lead to the damping of electromagnetic waves in a homogeneous plasma, due to the fact that its phase velocity is higher than the light velocity in vacuum, $\omega/k > c$. But, there is a resonant absorption of electromagnetic waves at the edge of an overdense plasma, where $|\omega| \ll \omega_{pe}$. This corresponds to the *anomalous skin effect*.

9.9 Landau damping of plasma waves

Using formula (9.47), we can calculate the imaginary part of longitudinal susceptibility for the Maxwellian distribution function (7.30):

$$\text{Im} \delta\epsilon_{\alpha}^l(k, \omega) = \sqrt{\frac{\pi}{2}} \frac{\omega \omega_{p\alpha}^2}{k^3 v_{T\alpha}^3} \exp\left(-\frac{\omega^2}{2k^2 v_{T\alpha}^2}\right). \quad (9.49)$$

Injecting this formula in the general expression for the wave damping (9.36) and recalling that $\partial_{\omega}(\omega\epsilon) = 2$ for the Langmuir waves, we find:

$$\gamma_{epw} = \sqrt{\frac{\pi}{8}} \frac{\omega_{pe}}{k^3 \lambda_{De}^3} \exp\left(-\frac{3}{2} - \frac{1}{2k^2 \lambda_{De}^2}\right). \quad (9.50)$$

This is the formula for the Landau damping of Langmuir waves. We see that the damping does not exist in the limit of very large wavelengths, $k \rightarrow 0$, because there is no resonant particles at very high phase velocities. The damping is increasing strongly with k and for $k\lambda_{De} \sim 0.4$, it becomes comparable to the frequency, see Fig. 37. For larger values of k , Eq. (9.50) is no longer valid, and Langmuir waves do not exist, because the phase velocity becomes comparable to the thermal velocity of electrons, and the waves are very strongly damped.

Both electrons and ions contribution to Landau damping of ion acoustic waves. It can be calculated in two limits.

In the limit $k\lambda_{De} \ll 1$, the dispersion relation is given by Eq. (9.41), the derivative of the dielectric permittivity can be calculated explicitly, $\partial_{\omega}(\omega\epsilon) \approx 2/k^2 \lambda_{De}^2$, and, using Eqs. (9.21) and (9.47), we find:

$$\gamma_{epw} = \sqrt{\frac{\pi}{8}} k v_s \left[\frac{\omega_{pi}}{\omega_{pe}} + \left(\frac{v_s}{v_{Ti}}\right)^3 e^{-v_s^2/2v_{Ti}^2} \right]. \quad (9.51)$$

The first term in brackets, describes the damping on electrons, the second – on ions. In this limit, the ratio between γ and the frequency $k v_s$ is a constant, which depends on relative temperatures of the electrons and ions, ZT_e/T_i , and the electron-ion mass ratio. The formula (9.51) is valid for $ZT_e/T_i > 4$. For smaller temperature ratio, the ion acoustic waves no longer exist due to a strong damping. In the limit of ion plasma waves, $k\lambda_{De} \gg 1$, the damping increases strongly with k , and

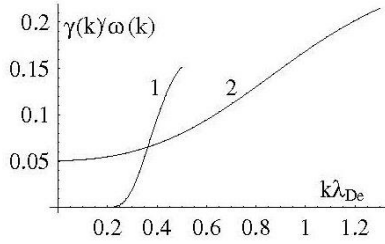


Figure 37: Dependence of damping of plasma waves (1) and ion acoustic waves (2) on the wave number. The damping is normalized by the corresponding wave frequency. It was considered $ZT_e/T_i = 10$.

the waves does not exist for $k\lambda_{D_i} > 0.4$. A typical curve of damping of the ion acoustic wave for a Maxwellian plasma is plotted in Fig. 37.

9.10 Qualitative interpretation of Landau damping

The phenomenon of non-collisional damping was discovered theoretically by Lev Landau in 1946 and since that time has been the subject of many discussions. The main question is: how in a completely reversible system can be produced such an effect as the irreversible wave damping? To better understand this mechanism, we should analyze the role played by individual resonant particles. The purpose of this section is to calculate directly the interaction between waves and particles and to evaluate the energy balance.

We consider a longitudinal wave with the electric field, $E(t, z) = E_0 \sin(\omega t - kz)$, and we write the equations of motion of a particle of mass m and charge q in this wave:

$$d_t z = v_z, \quad m d_t v_z = q E_0 \sin(\omega t - kz). \quad (9.52)$$

As we are interested in the resonant particles, we place ourselves in the reference frame that moves with the phase velocity $v_{ph} = \omega/k$:

$$z = v_{ph} t + Z, \quad v_z = v_{ph} + V.$$

Then the dynamic equations read:

$$d_t Z = V, \quad m d_t V = -q E_0 \sin kZ.$$

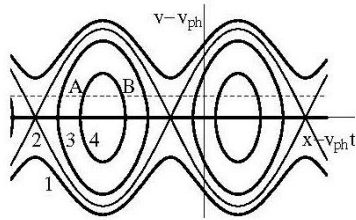


Figure 38: Particle orbits in the resonant reference frame the phase velocity: 1 to 1 free particle, 2 - the separatrix, 3,4 - trapped particles. Particles with positive speeds propagate to the right and those with negative speeds to the left.

In this reference frame the time does not explicitly appears in the equations, and we can calculate the first integral of this system. Assuming that at the initial moment of time, $t = 0$, a particle was at the position $Z = Z_0$ with the speed $V = V_0$, we find

$$\frac{1}{2} m V^2 + \frac{q}{k} E_0 \cos kZ = \frac{1}{2} m V_0^2 + \frac{q}{k} E_0 \cos kZ_0. \quad (9.53)$$

This is the law of energy conservation. The particle having the speed V_0 in the point Z_0 performs a periodic movement. It can takes an energy from the field or, on the contrary, releases energy to the field, but the total energy is conserved. In addition, if the average is performed over the initial coordinate of particle, its energy remains unchanged. It is instructive to consider the phase plot by representing the dependence of the particle velocity on its position, $V(Z)$. According to Eq. (9.53), the trajectory of each particle depends on the value of the parameter $2qE_0/kmV_0^2$, which is the ratio of the wave electric potential, qE_0/k , and the initial kinetic energy of particle. If this parameter is small, the particle is almost free, its speed does not vary much and the frequency of oscillations is high, $\omega_b \approx kV_0$. It increases as we consider the particles far away from the resonance.

In contrast, if the parameter $2qE_0/kmV_0^2 > 1$, the trajectory of the particle is finite, we can say that the particle is trapped in the wave. It performs oscillations around the minimum of potential. $Z_m = 2\pi/k$. The frequency of these oscillations near the bottom of potential is $\omega_b \approx \sqrt{qkE_0/m}$. It is a function of the wave amplitude E_0 . This is essential for our analysis, because we consider the case of a linear wave whose amplitude is very small (formally we consider the limit $E_0 \rightarrow 0$). Then, the period of particle oscillations is infinitely long. Typical trajectories of particles near

the resonance are plotted in Fig. 38. Curve 2 represents the separatrix between free and trapped particles.

From the analysis done above, we conclude:

- if we consider a wave of finite amplitude for a sufficiently long time, much longer than the period of oscillations of the particles, the phenomenon of Landau damping does not exist. The particles retain their average energy and the wave does not damped;
- if we consider a wave of very low amplitude, there are still particles that do not have the time to do a full revolution in the phase space. We will see later that they earn the wave energy. Therefore, the wave loses energy, this is the physical process that explains the Landau damping.

To determine the damping qualitatively, we consider two trapped particles A and B, see Fig. 38, which have the same trajectory and at a given time the same speed v (the dotted line in Fig. 38) close to the phase velocity. During the interval Δt , the particle A gains a speed Δv and an energy $\Delta w = mv\Delta v$. In contrast, the particle B reduces its speed and loses same energy Δw . The number of particles in the point A is $F(v) dv$. So the energy gained by the particles in the point A is

$$dW_+ = \Delta w F(v) dv .$$

The energy lost by the particles sitting initially at the point B is:

$$dW_- = \Delta w F(v + \Delta v) dv .$$

These two quantities are not equal because the numbers of particles with velocities v and $v + \Delta v$ are not equal. Therefore, the net energy gain is:

$$\Delta W = dW_+ - dW_- \approx -\Delta w \Delta v \partial_v F(v) = -m v (\Delta v)^2 \partial_v F(v) .$$

In order to calculate the total energy exchange between the field and the particles in the interval Δt , we must average this expression over all trajectories and integrate over all initial velocities:

$$\Delta W_{\text{tot}} = -m \int v \langle (\Delta v)^2 \rangle \partial_v F(v) dv . \quad (9.54)$$

The average of $(\Delta v)^2$ is a positive quantity. So, the sign of ΔW_{tot} depends just on the sign of the derivate of the distribution function. This is in complete agreement with the formula of Landau damping (9.47).

To determine the coefficient in the formula of Landau damping we must calculate the gain in velocity of the particles during the time Δt from the equation of motion (9.52) in the laboratory frame. We use the method of perturbations. First, we neglect the electric field and determine the trajectory $z_1(t) = z_0 + v_z \Delta t$, where z_0 is the initial coordinate. Then, we inject this solution into the equation of motion and we calculate the gain in velocity due to the electric field:

$$\Delta v = \frac{q}{m} \frac{E_0}{kv_z - \omega} [\cos(kz_0 + (kv - \omega)\Delta t) - \cos(kz_0)] .$$

Then, we calculate the average $(\Delta v)^2$ by considering that the initial coordinate z_0 is a random variable in the interval $(0, 2\pi/k)$:

$$\langle (\Delta v)^2 \rangle = \frac{k}{2\pi} \int (\Delta v)^2 dz_0 = \frac{2q^2}{m^2} \frac{E_0^2}{(kv_z - \omega)^2} \sin^2(kv_z - \omega) \frac{\Delta t}{2} .$$

Injecting this expression in Eq. (9.54), we find the energy absorbed by the particles per unit time, $\Delta W_{\text{tot}}/\Delta t$. Due to the energy conservation, this is the energy lost by the wave. , the we can define the imaginary part of dielectric permittivity:

$$\text{Im } \epsilon^l = \frac{\Delta W_{\text{tot}}/\Delta t}{\omega \epsilon_0 E_0^2/2}.$$

We still need to calculate the integral over the velocities in Eq. (9.54). It extends over the velocities near the phase velocity of the wave. Thus, we introduce a new variable $\xi = (kv - \omega)\Delta t/2$. We can take out of the integral the velocity v and the derivate of the distribution function, $\partial_v F(v)$, as they vary slowly compared to $\langle (\Delta v)^2 \rangle$. This leads to the following expression:

$$\text{Im } \epsilon = -\frac{q^2}{m \epsilon_0 k^2} \partial_v F(v) |_{v=v_{ph}} \int_{-\infty}^{\infty} \frac{\sin^2 \xi}{\xi^2} d\xi.$$

The last integral is just a numerical coefficient in the expression for the imaginary part of permittivity. Its value is π , and thus we find formula (9.47) without making any assumption about the analytical proprieties of the distribution function in the complex plane. This analysis confirms the physical explanation of the phenomenon of Landau damping.

9.11 Problems

1. Calculate the contribution of ions in the dispersion relation of Langmuir waves. Explain why this contribution is small. Calculate the group velocities and the phase velocities for Langmuir waves.
2. Derive the formulas for the dielectric permittivity tensor of an isotropic and ultra-relativistic plasma, assuming that the distribution function is $f_0(p) \propto \exp(-cp/k_B T)$.
3. Using the formula for the dielectric permittivity of the previous problem, calculate the spectrum of Langmuir waves in a ultra-relativistic plasma, where the electron temperature $k_B T_e$ is much greater then $m_e c^2$. The electron distribution function in this case is $f_{e0}(p) \propto \exp(-cp/k_B T_e)$.
4. Consider a strongly degenerate plasma with the electron temperature T_e t much lower than the Fermi temperature T_F . (This case corresponds to electrons in metals and semiconductors.) The distribution function of electrons in this case is

$$f_{e0}(p) \propto \begin{cases} 1 & \text{si } p < p_F, \\ 0 & \text{si } p > p_F \end{cases}$$

where $T_F = p_F^2/2m_e k_B$. Find the relation between the Fermi momentum p_F and the electron density. Calculate the spectrum of Langmuir waves in such a plasma. Compare the result with the spectrum of Langmuir waves in an ultra-relativistic case $k_B T_e \gg m_e c^2$.

5. Find the dispersion relation for plasma and ion acoustic waves from the fluid model (4.1) et (4.2). Choose the adiabatic indexes in the equations of state for electrons and ions according to the wave phase velocities. Explain the choice.
6. Show that the relation, $\tilde{E} = i Z e k \lambda_{De}^2 \epsilon_0 \delta \tilde{n}_i$, can be obtained from Eq. (9.26) written for the ions.



7. Calculate the energy density of ion acoustic wave in the limit $k\lambda_{De} \ll 1$. Compare the energy contributions associated with the field and the particles. How is the energy distributed between the electrons and the ions?
8. Calculate the dispersion and the damping of Langmuir waves in a plasma with cold ions and the following distribution function of electrons: $f_e(\vec{v}) \propto (v_0^2 + v^2)^{-2}$ (distribution of Lorentz).
9. Find the trajectories of free and trapped particles by considering approximate solutions of the system (9.53) in the two limits: $2qE_0/kmv_0^2 \gg 1$ and $2qE_0/kmv_0^2 \ll 1$. Calculate the time required to perform a full oscillation.



HELLENIC
MEDITERRANEAN
UNIVERSITY



universit 
BORDEAUX



UNIVERSIT 
BOLOGNENSIS



UNIVERSIT 
COIMBRENSE



UNIVERSITY
of York



Queen's University
Belfast



Erasmus+

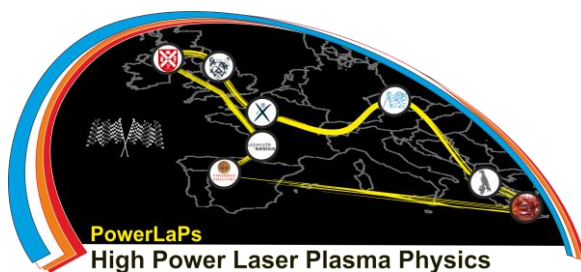
PowerLaPs

Innovative Education & Training in High Power Laser Plasmas

Plasma Physics - Theory and Experiments

Chapter 10: Instabilities of a non-equilibrium plasma

D. Batani, E. d'Humi res, J.J. Santos, V.T. Tikhonchuk



Erasmus+

universit 
de BORDEAUX

10 Instabilities of a non-equilibrium plasma

In previous chapters we considered stable plasmas, where small perturbations propagate in form of damped waves. But this is not always the case. Often the velocity distribution of particles is not Maxwellian and waves become unstable. Then an initial perturbation will be increasing in time or in space. Here we give some examples of instabilities induced by particle motion. First we consider a charged particle propagating in a plasma with a given speed \vec{u} . We show that it loses its energy by exciting the Langmuir and ion acoustic waves, and thus the energy of these waves grows in time. Then we consider a group of particles propagating through a plasma with a given distribution in velocities. We find that these particles may emit plasma waves coherently, and that the growth rate of these waves is given by the formula of Landau damping, but in this case with an opposite sign. Finally, we consider the stabilizing processes, which stop the growth and produce a non-linear saturation of unstable waves.

10.1 Radiative losses of a charged particle in plasma

Landau damping is an example of a more general phenomenon of resonant interaction between waves and particles propagating with a velocity close to the phase velocity of the wave. Here we consider another effect where a particle loses energy by exciting waves in a plasma. This process is similar to the Cherenkov effect of emission of electromagnetic waves by a particle that propagates at a speed higher than the speed of light in that medium.

Let us consider a particle of a charge q propagating with the speed \vec{u} in a homogeneous plasma in a thermodynamic equilibrium. We want to calculate the electric and the magnetic fields created by this charge. Recall that in the limit $\vec{u} = 0$ this charge creates a screened electrostatic field: $\vec{E} = -\vec{\nabla}\Phi$ and

$$\Phi(r) = \frac{q}{4\pi\epsilon_0 r} e^{-r/\lambda_{De}}$$

where the screening (Debye) length depends on the plasma temperature and density. The field created by a moving charge may be deduced from Maxwell equations (7.16) – (7.19) with the external charge density $\rho^{\text{ext}} = q\delta(\vec{r} - \vec{u}t)$ and the external current $\vec{j}^{\text{ext}} = q\vec{u}\delta(\vec{r} - \vec{u}t)$. The self-consistent current and charge density depend on the perturbation of distribution function of plasma particles induced by our test (external) particle.

Assuming that the perturbation is sufficiently small, we can use the linear theory. Equations (9.8) describe the Fourier components of electric and magnetic fields induced by the external current $\vec{j}^{\text{ext}}(\vec{k}, \omega) = 2\pi q\vec{u}\delta(\omega - \vec{k} \cdot \vec{u})$. The resolution of these equations gives the following result for the electric field:

$$\vec{E}(\vec{k}, \omega) = -\frac{2\pi iq}{k^2\epsilon_0\omega} \left[\frac{\vec{k}\omega}{\epsilon^l(\vec{k}, \omega)} - \frac{\vec{k} \times (\vec{u} \times \vec{k})}{k^2 c^2/\omega^2 - \epsilon^{tr}(\vec{k}, \omega)} \right] \delta(\omega - \vec{k} \cdot \vec{u}). \quad (10.1)$$

The first term in square brackets describes the effect of dynamic Debye screening. In the limit $\omega \rightarrow 0$ it reduces to the electrostatic screening. The second term describes excitation of the transverse electromagnetic field by a moving charge.

The quantity we are interested to is the energy lost by particle per unity of time, \dot{W} . Knowing the field \vec{E} , we can calculate the work done by the electric field on the current. According to the law of energy conservation, the rate of energy loss is equal to the work done by the electric field with the opposite sign:

$$\dot{W} = - \int d\vec{r} \vec{j}^{\text{ext}} \cdot \vec{E} \equiv -q\vec{u} \cdot \vec{E}(\vec{u}t, t).$$

The coordinate $\vec{r} = \vec{u}t$ in the argument of electric field corresponds to the position of particle.

In order to calculate the electric field in the position of particle, we perform the inverse Fourier transform of Eq. (10.1). Injecting then this field in the expression for \dot{W} we have:

$$\dot{W} = \frac{iq^2}{\epsilon_0} \int \frac{d\vec{k}}{(2\pi)^3} \frac{\vec{k} \cdot \vec{u}}{k^2} \left[\frac{1}{\epsilon^l(\vec{k}, \vec{k} \cdot \vec{u})} - \frac{(\vec{k} \times \vec{u})^2}{k^2 c^2 - (\vec{k} \cdot \vec{u})^2 \epsilon^{tr}(\vec{k}, \vec{k} \cdot \vec{u})} \right]. \quad (10.2)$$

Two terms in the square brackets describe the energy losses associated with the emission of electrostatic and electromagnetic waves. As the real part of the dielectric permittivity is an even function of the wave vector, the energy loss depends on the imaginary part of dielectric permittivity. Otherwise, the integrand in Eq. (10.2) would be odd, which would mean that the integral is zero.

While considering the imaginary part of ϵ , we note that it is small compared to the real part and that so the significant contribution may come only from the points where the real part is close to zero. Therefore, the radiative losses are associated with excitation of the plasma eigenmodes given by the solution of the dispersion equations:

$$\text{Re } \epsilon^l(\vec{k}, \vec{k} \cdot \vec{u}) = 0 \quad \text{and} \quad (\vec{k} \cdot \vec{u})^2 \text{Re } \epsilon^{tr}(\vec{k}, \vec{k} \cdot \vec{u}) = k^2 c^2. \quad (10.3)$$

The first equation corresponds to excitation of the electrostatic modes – the electron plasma waves and ion acoustic waves. According to the assumption that the imaginary part of dielectric permittivity is small, we simplify the calculation of the integral by taking the limit $\text{Im } \epsilon^l \rightarrow 0$. Using the definition of the Dirac delta function, $\pi \delta(x) = \lim_{s \rightarrow 0} s/(x^2 + s^2)$, we can present the imaginary part of the first term in the integral (10.2) as

$$\text{Im} \frac{1}{\epsilon^l(\vec{k}, \omega)} = \pi \text{sign } \omega \delta[\text{Re } \epsilon^l(\vec{k}, \omega)].$$

Here, the sign of $\omega = \vec{k} \cdot \vec{u}$ takes into account the fact that the imaginary part of permittivity is an odd function.

The second dispersion equation is the same as Eq. (9.14), it describes the excitation of electromagnetic waves. According to Sec. 9.5.1, the frequencies of these waves are such that $\omega > kc$. However, in the case of Eq. (10.3) we are looking for solutions such that $\omega = \vec{k} \cdot \vec{u}$. The ratio $\vec{k} \cdot \vec{u}/k \leq u$ is always smaller than c . Therefore, the solution to the dispersion equation for electromagnetic wave does not belong to the domain of integration. Thus the second term in the integral (10.2) is zero. Qualitatively, this is explained by the fact that particles in plasma do not interact with electromagnetic waves. This is different from the case of a neutral medium (dielectric), where fast particles may emit the electromagnetic waves. This process is called the *Cherenkov effect*. The difference comes from the fact that in a plasma the transverse permittivity (9.32) is smaller than 1, $\epsilon^{tr} = 1 - \omega_{pe}^2/\omega^2$. In contrast, the dielectric permittivity of a dielectric can be greater than 1. Therefore, the phase velocity of electromagnetic waves is lower than c , which gives a possibility to have a resonant interaction with the particles.

Taking into account the previous analysis, Eq. (10.2) can be written as:

$$\dot{W} = -\frac{q^2}{8\pi^2\epsilon_0} \int d\vec{k} \frac{|\vec{k} \cdot \vec{u}|}{k^2} \delta[\text{Re } \epsilon^l(\vec{k}, \vec{k} \cdot \vec{u})]. \quad (10.4)$$

Here, the Dirac delta function takes into account all eigenmodes, that is the Langmuir and ion acoustic waves. According to one of the properties of the Dirac delta function, we have:

$$\delta[\phi(x)] = \sum_i |d_x \phi|^{-1} \delta(x - x_i)$$

where x_i are the zeros of this function: $\phi(x_i) = 0$. In our case, the points that contribute to the integral (10.4) are the solutions of equations

$$(\vec{k} \cdot \vec{u})^2 = \omega_i^2(k)$$

where $\omega_i(k)$ are the frequencies of the electrostatic waves which were discussed in Secs. 9.6 and 9.7. We see that the test particle can excite waves with the phase velocity lower than u , because it is the necessary condition to have a solution of equation $\text{Re } \epsilon^l(\vec{k}, \vec{k} \cdot \vec{u}) = 0$.

We can go further by considering two limits: a slow particle $u \ll v_{Te}$ and a fast particle $u \gg v_{Te}$. If the particle is slow, that is, its speed is smaller than the electron thermal velocity, $u \ll v_{Te}$, it may interact with the ion acoustic waves. Then, Eq. (10.4) reads:

$$\dot{W} = -\frac{q^2}{8\pi^2\epsilon_0} \int d\vec{k} \frac{|\omega_{ai}(k)|}{k^2 |\partial_\omega \text{Re } \epsilon^l|} \delta[(\vec{k} \cdot \vec{u})^2 - \omega_{ai}^2(k)] \quad (10.5)$$

where the derivative $\partial_\omega \text{Re } \epsilon^l$ is calculated for $\omega = \omega_{ai}(k)$. One can verify that the largest contribution in the integral (10.5) comes from the greatest possible k , that means that we may limit ourselves to consideration of ion plasma waves (9.44) which exist in the domain $\lambda_{De}^{-1} < k < \lambda_{Di}^{-1}$. Then, we have the following approximate expressions: $\vec{k} \cdot \vec{u} \approx \pm \omega_{pi}$ and $|\partial_\omega \text{Re } \epsilon^l| \approx 2/\omega_{pi}$. Using these expressions in (10.5) we see that the radiative losses appear if the particle speed $u \gtrsim \omega_{pi} \lambda_{Di}$. Then the losses decrease as the speed increases:

$$\dot{W} \approx -\frac{q^2 \omega_{pi}^2}{8\pi^2 \epsilon_0 u} \ln \frac{\lambda_{De}}{\lambda_{Di}}$$

Higher radiation losses occur for particles with the speeds above the electron thermal velocity, where the excitation of Langmuir waves becomes possible.

10.2 Instability of an electron beam in plasma

The physical and mathematical analysis of the imaginary part of dielectric permittivity presented Sec. 9.9 shows that the sign of Landau damping depends on the shape of distribution function of particles. Stable distributions functions correspond to a decreasing number of particles with the energy. However, under certain conditions it is possible to find a situation where the distribution function is not monotonic. Then the damping rate $\gamma < 0$ is negative, and the amplitude of plasma waves increases with time exponentially, $E_p \propto \exp(-\gamma t)$. That means that plasma is unstable. As the energy of unstable waves grows rapidly, very quickly the linear approach is no longer valid. Theory and modeling of nonlinear effects in plasma or *nonlinear plasma theory* is a broad field that covers important applications. Linear analysis remains always necessary because it defines the conditions of instability, the thresholds and the growth rates.

An example of an unstable plasma is a Maxwellian plasma where a beam of fast electrons is injected. Assume that the electrons of plasma have a density n_e and a temperature T_e . The beam electrons have a much lower density, $n_b \ll n_e$, a mean velocity u_b and a temperature T_b . We are interested here in excitation of Langmuir waves. Therefore, the beam velocity is supposed to be higher than the electron thermal velocity. The ions are assumed to be immobile. They constitute a stationary background to ensure the electrical neutrality, $Zn_i = n_e + n_b$. Using the Maxwellian distributions for the plasma and beam electrons in Eq. (9.29), the real part of dielectric permittivity in the domain $\omega \gg kv_{Te}, kv_{Tb}$ reads:

$$\text{Re } \epsilon^l(\vec{k}, \omega) = 1 - \frac{\omega_{pe}^2}{\omega^2} \left(1 + 3 \frac{k^2 v_{Te}^2}{\omega^2} \right) - \frac{\omega_{pb}^2}{(\omega - \vec{k} \cdot \vec{u}_b)^2} \left(1 + 3 \frac{k^2 v_{Tb}^2}{(\omega - \vec{k} \cdot \vec{u}_b)^2} \right). \quad (10.6)$$

The beam contribution has a form similar to the main plasma with only difference that the frequency is Doppler-shifted, $\omega \rightarrow \omega - \vec{k} \cdot \vec{u}_b$ as the beam propagates with the velocity \vec{u}_b in the laboratory reference frame. In the imaginary part we have also two terms:

$$\text{Im } \delta \epsilon^l(\vec{k}, \omega) = \sqrt{\frac{\pi}{2}} \frac{\omega \omega_{pe}^2}{k^3 v_{Te}^3} \exp\left(-\frac{\omega^2}{2k^2 v_{Te}^2}\right) + \sqrt{\frac{\pi}{2}} \frac{(\omega - \vec{k} \cdot \vec{u}_b) \omega_{pb}^2}{k^3 v_{Tb}^3} \exp\left(-\frac{(\omega - \vec{k} \cdot \vec{u}_b)^2}{2k^2 v_{Tb}^2}\right). \quad (10.7)$$

The second term comes from the electrons of the beam. We see that this term can be negative if $\omega < \vec{k} \cdot \vec{u}_b$, which leads to the development of the instability.

We can obtain explicit formulas for the growth rate in the case where the beam has a very low density, $n_b \ll n_e$, and a very high velocity, $u_b \gg v_{Te}$. We can neglect then the beam contribution in the real part (10.6) and find the standard expression for the Langmuir mode frequency $\omega \approx \omega_{pe}$. According to our assumptions, in the imaginary part (10.7) we can neglect the contribution of plasma since electrons are cold. From this we have:

$$\gamma = \sqrt{\frac{\pi}{8}} (\omega_{pe} - \vec{k} \cdot \vec{u}_b) \frac{\omega_{pe} \omega_{pb}^2}{k^3 v_{Tb}^3} \exp\left(-\frac{(\omega_{pe} - \vec{k} \cdot \vec{u}_b)^2}{2k^2 v_{Tb}^2}\right). \quad (10.8)$$

The damping becomes negative for $k > \omega_{pe}/u_b$, that is to say, for waves with a phase velocity smaller than the velocity of beam. The growth rate becomes maximum for $ku_b - \omega_{pe} \sim kv_{Tb}$. This gives us the following estimate:

$$\gamma_{\max} \simeq \frac{\omega_{pb}^2}{\omega_{pe}} \frac{u_b^2}{v_{Tb}^2}.$$

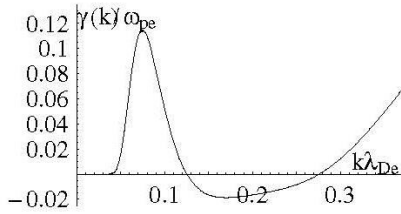


Figure 39: Dependence of the Langmuir wave damping on the wavenumber for an electron beam with parameters: $u_b = 8v_{Te}$, $n_b = 0.03n_e$ et $T_b = 2T_e$. The unstable waves are excited in the interval $k\lambda_{De} \in (0.13 - 0.27)$.

A typical dependence of the growth rate of the beam-plasma instability on the wave vector is presented in Fig. 39. The unstable plasma waves have a phase velocity lower than the average speed of the beam. In this case the electrons of the beam transfer their energy to the waves. This is a process of deceleration of the beam by radiative losses similar to the radiation losses considered in the previous section 10.1.

This process of beam instability is also similar to the Cherenkov effect, but instead of electromagnetic radiation produced by a particle propagating in a medium with a speed greater than the phase velocity of electromagnetic waves, in our case we obtain a coherent emission of electrostatic waves by the beam particles.

This is a *kinetic instability*, because it comes from the imaginary part of permittivity and is associated with the resonant particles of the beam. It can be seen from Eq. (10.8), that the growth rate increases when the temperature of the beam decreases or the beam density increases. The formula (10.8) is valid if $\gamma_{\max} \ll kv_{Tb} \sim \omega_{pe}v_{Tb}/u_b$, which gives the limit for the temperature of the beam: $v_{tb} \gg u_b(n_b/n_e)^{1/3}$.

10.3 Instability of a mono-energetic beam

In the opposite case of a cold beam, $v_{tb} < u_b(n_b/n_e)^{1/3}$ the instability still exists, but it takes place in the hydrodynamics regime, when all particles in the beam emit the wave coherently. In this

case we cannot neglect the contribution of the beam in the real part of permittivity (10.6). On the contrary, the thermal effects are not important in this limit. Correspondingly, we have the following dispersion equation:

$$1 - \frac{\omega_{pe}^2}{\omega^2} - \frac{\omega_{pb}^2}{(\omega - \vec{k} \cdot \vec{u}_b)^2} = 0. \quad (10.9)$$

This is a fourth order algebraic equation for ω , that can have complex roots. We solve it in the limit of a low density beam, $n_b \ll n_e$. From the previous solution, we can assume that the unstable solution corresponds to a frequency close to ω_{pe} and to a phase velocity close to u_b . Therefore, we assume that $\omega = \omega_{pe} + \delta\omega$ and $k = \omega_{pe}/u_b$ in Eq. (10.9). Developing this equation in a series of $\delta\omega$ assuming that the frequency correction is small, $\delta\omega \ll \omega_{pe}$, we deduce a cubic equation, $2\delta\omega^3 = \omega_{pe}\omega_{pb}^2$, that has a complex root with a positive imaginary part,

$$\delta\omega = \frac{-1 + i\sqrt{3}}{2^{4/3}} \omega_{pe} \left(\frac{n_b}{n_e}\right)^{1/3}. \quad (10.10)$$

This unstable root, $\text{Im } \delta\omega > 0$, corresponds to a *hydrodynamic instability* as we did not consider here the kinetic effects that are contained in the imaginary part of permittivity. We note that for this unstable root, the derivative of dielectric permittivity is negative, $\partial_\omega \epsilon(\vec{k}, \omega) < 0$. This means that the energy of the wave (9.37) is negative. We can say that this is an instability of a negative energy wave. It has a growth rate higher than the kinetic instability considered above.

This instability corresponds to the excitation of Langmuir waves by a beam of electrons. It is called a *Buneman instability*. Other types of instabilities are also known. For example, in a hot plasma, where $u_b < v_{Te}$ the ion acoustic waves become unstable if the following condition is verified: $\vec{k} \cdot \vec{u}_b = kc_s$.

10.4 Nonlinear saturation of instabilities

10.4.1 Mono-mode saturation, particle trapping

The exponential growth of the amplitude of unstable waves occurs for a limited time when it may be considered as a small perturbation. After this time, the growing wave amplitude becomes too strong and we must take into account its interaction with other particles and waves. It is said, that the instability enters a nonlinear stage, where the amplitude of wave grows slower than the exponential or it becomes constant. A nonlinear behavior of instabilities is a very complicated phenomenon and it is difficult to describe it analytically in general. The numerical simulations are often used to study the plasma in the nonlinear stage.

Powerful computers provide a detailed analysis of the nonlinear behavior of plasma. However, it is still useful to have some qualitative ideas about possible nonlinear states and estimates the amplitude of the saturated wave. The results of non-linear plasma theory for large amplitude waves depend strongly on the excitation conditions. Here we discuss two examples: the first one corresponds to a regular regime and the second example – to a turbulent regime. Let us consider first the hydrodynamic instability (10.10) where the non-linear saturation occurred through the trapping of beam particles in the wave.

We recall that the frequency of a wave is defined in an accurate manner only if the amplitude is constant. In the case where the amplitude increases or decreases with the growth rate γ , the wave possesses a spectral width $\Delta\omega \sim |\gamma|$. Therefore, if a wave amplitude increases with the growth rate (10.10), its phase velocity is defined with a precision $\Delta v_{ph} \sim u_b(n_b/n_e)^{1/3}$, which is much greater than the thermal velocity of the beam, v_{tb} . Therefore, all electrons in the beam interact with a single coherent wave.

In the linear model we consider the evolution of the wave assuming that the beam distribution is given. The dominant nonlinear effect is a modulation of the electron beam density and velocity by the wave electric field. According to the analysis of Sec. 9.10, the electrons can be trapped in the wave if it has a finite amplitude. The conservation of energy in the beam reference frame allows us to write a relation between the electron energy loss and the wave field amplitude: $e\Phi \simeq \frac{1}{2}m_e\Delta u_b^2$, where $\Phi \sim E/k$ is the wave potential and $k = \omega_{pe}/u_b$ is its wave vector. The wave growth stops when the beam electrons are falling out of the resonance, that is, $\Delta u_b \gtrsim \Delta v_{ph}$. Then the criterion of saturation reads:

$$eE_{\text{sat}}u_b/\omega_{pe} \simeq \frac{1}{2}m_e u_b^2 (n_b/n_e)^{2/3}. \quad (10.11)$$

This qualitative estimate gives us the wave energy at saturation and consequently the energy lost by the beam:

$$W_E \simeq \frac{1}{2}\epsilon_0 E_{\text{sat}}^2 \simeq \frac{1}{2}m_e u_b^2 n_b (n_b/n_e)^{1/3}. \quad (10.12)$$

Recalling that $n_b \ll n_e$, we see that the energy density of a plasma waves is lower than the energy density of the beam. One can interpret this instability saturation in a different way. The trapping of electrons in the wave produces a broadening of the electron energy distribution in the beam. Because the electrons are trapped in all possible phases, the initially mono-energetic electron beam distribution function is transformed into a plateau in the interval $\pm\sqrt{e\Phi_{\text{sat}}/m_e} \simeq \Delta v_{ph}$. So the beam distribution function obtains an effective temperature with a thermal velocity of the order of Δv_{ph} . This beam does not verify the criterion of hydrodynamic instability and therefore, the growth stops. In reality, it does not stop completely, but the hydrodynamic instability is transformed in the kinetic instability with a smaller growth rate.

10.4.2 Multi-mode saturation, a quasi-linear theory

The saturation of the kinetic instability occurs differently. According to our analysis in Sec. 10.3, the growth rate of kinetic instability $\gamma \simeq \omega_{pe}n_b v_{Tb}^2/n_e u_b^2$ is smaller than for the hydrodynamic instability, while the width of the spectrum of excited waves, $\Delta k \simeq \omega_{pe}v_{Tb}/u_b^2$, is larger, so that $\Delta k \gg \gamma/u_b$. Therefore, the plasma beam excites simultaneously several modes with different wavelengths. The phases of these waves are not correlated and constitute a broad turbulent spectrum.

The interaction of electrons with several incoherent waves takes a stochastic character. The chaotic motion of an electron is made of an addition of the electric fields of several waves with slightly different frequencies and phases. Then, instead of a regular oscillatory motion in one wave, the electron motion in incoherent waves takes a character of diffusion. The evolution of the average distribution function of electrons in the field of many incoherent waves is described by a *quasi-linear theory*. The total electric field of plasma waves having a wave number k is presented in the form of a Fourier spectrum:

$$E(x, t) = \frac{1}{2\pi} \int dk E_k(t) \exp\left(-i \int^t \omega_k(t) dt + ikx\right).$$

For sake of simplicity, we consider here a one-dimensional situation of a homogeneous plasma of a length L . The time dependence of the amplitude E_k is described by the imaginary part of mode frequency, $\text{Im}\omega_k$. It is the solution of the dispersion equation, $\epsilon^l(k, \omega) = 0$. However, in the quasi-linear theory, ϵ^l depends on the electron distribution function that is described by the Vlasov equation.

Thus, in difference from the linear theory, here, the distribution function evolves in time and the mode growth rate also changes with time. At first glance it may be considered contradictory

as, according to the linear theory, the dielectric permittivity depends on the frequency, but not on time. However, here we are considering the average distribution function, which is approximately constant at the plasma wave period but it varies in time scale comparable to the wave amplitude growth time. Consequently, we need to derive from the standard Vlasov equation a new quasi-linear equation for a slowly varying part of the electron distribution function.

Such an equation is derived by using the perturbation method. The distribution function of electrons is represented as a slowly varying part $f_0(t, v)$ and the fast varying components

$$f_e(t, x, v) = f_0(t, v) + \delta f_0(t, v) = f_0(t, v) + \frac{1}{2\pi} \int dk f_k(t, v) \exp \left(-i \int^t \omega_k(t) dt + ikx \right). \quad (10.13)$$

The oscillating components f_k are small compared to f_0 . They describe the linear electron response to each plasma mode. Differently from the linear model, here we assume that the function f_0 is not stationary, but may vary over time slowly.

This is the main hypothesis of the quasi-linear theory – the *separation of two time scales*: the short time is of the order of the wave period, $\Delta t_f \simeq 2\pi/\omega_k \simeq 2\pi/\omega_{pe}$, and the long time scale is of the order of the wave rise time, $\Delta t_l \simeq 1/\gamma_k$. First of all, we obtain equations for the oscillating components of the distribution function. Inserting Eq. (10.13) in the Vlasov equation we linearize it considering the long time as a parameter. Then, for components $f_k(v)$ we obtain the following equation:

$$-i \omega_k f_k + i k v f_k + q_e E_k \partial_p f_0 = 0. \quad (10.14)$$

This equation is similar to Eq. (9.25) except that the function f_0 , the electric field E_k , and the wave frequency ω_k vary now in the slow time scale. Injecting the solution of this equation in the Poisson equation, we obtain the dispersion equation $\epsilon^l(t, \omega, k) = 0$, depending on time. Its solution gives us the wave frequency $\omega_k(t)$ and the growth rate, $\gamma_k(t)$. Differently from Eq. (10.8), the distribution function in this equation is an arbitrary function. Correspondingly, the wave growth rate depends also on time:

$$\gamma_k(t) = -\omega_{pe} \frac{\pi e^2 m_e}{2k^2 \epsilon_0} \partial_p f_0 |_{v=\omega_k/k}. \quad (10.15)$$

Knowing the instantaneous growth rate, we can describe the evolution in time of the energy of each wave mode (9.37),

$$\bar{W}_k = \frac{1}{2} \epsilon_0 \partial_\omega (\omega \operatorname{Re} \epsilon^l) |\vec{E}_k|^2.$$

The mode amplitude $E_k(t)$ varies in time as $\propto \exp[-\int^t \gamma_k(t') dt']$. Correspondingly, variation in time of the mode energy satisfies the following differential equation:

$$\partial_t \bar{W}_k = -2\gamma_k \bar{W}_k. \quad (10.16)$$

As the modes are incoherent, the total plasma wave energy is just a sum of all unstable modes, that is

$$\bar{W}_E = \frac{1}{2\pi L} \int dk \bar{W}_k. \quad (10.17)$$

This expression for the energy density can be obtained explicitly by averaging the energy density of the electric field over the plasma length L :

$$\begin{aligned} \bar{W}_E &= \frac{\epsilon_0}{2L} \partial_\omega (\omega \operatorname{Re} \epsilon^l) \int dx E^2(x, t) = \\ &= \frac{\epsilon_0}{2(2\pi)^2 L} \int dx \int dk \int dk' E_k E_{k'} \exp \left(-i \int^t \omega_k dt' - i \int^t \omega_{k'} dt' + ikx + ik'x \right). \end{aligned}$$

First of all, we calculate the integral over the coordinate x : $\int dx \exp i(k+k')x = 2\pi \delta(k+k')$. Here we need to take into account that $E_{-k} = E_k^*$, because the electric field $E(x, t)$ is a real quantity and the wave frequency is an odd function, $\omega_{-k} = -\omega_k$. Then, integrating over k' , we obtain the formula (10.17).

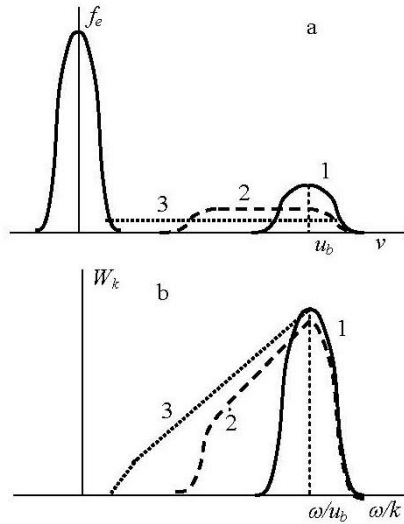


Figure 40: Evolution of the distribution function of the electrons (a) and of the wave spectrum (b) in the quasi-linear relaxation: 1 - in the linear phase, 2 - during relaxation, 3 - after the saturation.

Now we can derive the equation for the average distribution function f_0 . Inserting the distribution function (10.13) in the Vlasov equation and averaging it over the plasma length we obtain:

$$\partial_t f_0 = \frac{e}{L} \int dx E(x, t) \partial_p \delta f(t, x, v).$$

Similarly as in the previous formula for \bar{W}_E , the interference between modes can be neglected. Retaining the coherent contribution of modes with $k+k' = 0$, the equation for f_0 takes the following form:

$$\partial_t f_0 = \frac{ie^2}{2\pi L} \partial_p \int dk \frac{|E_k|^2}{\omega - kv} \partial_p f_0. \quad (10.18)$$

Similarly as in the calculation of Landau damping in Sec. 9.9, we present the denominator in this equation as the sum of the principal part and the residue,

$$\frac{1}{\omega - kv} = \mathcal{P} \frac{1}{\omega - kv} - i\pi \delta(\omega - kv).$$

The imaginary part of this integral is an odd function and its contribution is zero. Thus only the pole contribution $\omega - kv = 0$ remains. That corresponds to the resonance interaction of a particle with the velocity v with the wave mode having the same phase velocity. The equation for the average distribution function takes finally the following form:

$$\partial_t f_0 = \partial_p \left(\frac{e^2}{\epsilon_0 L v} \bar{W}_{\omega/v} \partial_p f_0 \right). \quad (10.19)$$

This is a diffusion equation in the phase space. The diffusion coefficient is proportional to the spectral energy of the waves \bar{W}_k with the resonant wave number $k = \omega/v$.

The system of two equations for the spectral intensity of the waves (10.16) and for the average distribution function (10.19) describes the evolution of plasma in the long time scale in the case of excitation of several modes with non-correlated phases.. Each of these equations is linear, but with coefficients depend to the other function. Therefore, this is a *quasi-linear* system.

Let us consider qualitatively the evolution of distribution function in the case of the kinetic instability of an electron beam. First, the growth rate (10.15) is positive in the range of velocities (v_1, v_2) where the derivative $\partial_p f_0$ is positive. In the corresponding interval of wave numbers $(\omega_1/v_1, \omega_2/v_2)$ the spectral intensity of the wave grows exponentially. According to Eq. (10.19) it is causing a diffusion of the distribution function in the velocity space. Similarly to the diffusion in the real space, the diffusion in the phase space leads to flatering of the distribution function. Therefore, the derivative of the distribution function in the domain of diffusion decreases with time, and the instability growth rate decreases correspondingly. Thus, the quasi-linear diffusion leads to saturation of the kinetic instability.



The diffusion stops when the distribution function is constant in the velocity interval corresponding the wave numbers where the energy density \bar{W}_k is non-zero. A constant distribution function corresponds to a zero growth rate. However, as it can be seen in Fig. 40, stabilization of the modes in the initially unstable domain of wave numbers leads to destabilization of the waves with smaller phase velocities. Therefore, the process of growing of the waves and of particle diffusion continue until all domains of positive derivatives f_0 will be eliminated. The initial electron beam distribution widens towards smaller velocities producing general slowing of the beam electrons. Upon the saturation, the distribution function of the beam is a plateau between the thermal velocity of the plasma electrons and the initial beam velocity u_b .

As we can see, the quasi-linear evolution ends up with a stable but non-Maxwellian distribution function. Further relaxation to the thermal equilibrium takes place in a longer time scale due to the electron-electron collisions. In contrary, the collisional effects are not important in the quasilinear time scale where the collective effects of wave-particle interaction play a dominant role.

10.5 Problems

1. Using the expression for the energy loss rate (10.5), calculate the radiative losses of a fast particle having the velocity $u \gg v_{Te}$.
2. Find the condition of instability in a plasma with a current of electrons. Consider the case where the average velocity of the electrons u_e is in the range $v_{Te} \gg u_e \gg v_{Ti}$ and $ZT_e \gg T_i$.
3. Show that the maximum growth rate of instability of a beam of the electrons in the kinetic regime is given by the following formula: $\max |\gamma| = \omega_{pe}(n_b/n_e)u_b^2/v_{Tb}^2$. Taking into account the Landau damping of the electrons of the plasma, find the wave number k_* where $\gamma(k_*) = 0$.
4. Consider a homogeneous plasma of electrons and positrons have the density n and the temperature T . Calculate the longitudinal dielectric permittivity for high frequency waves, $\omega \gg kv_T$. Find the frequency of plasma wave and the Landau damping rate. Find the relative velocity of the electron and positron component where these waves become unstable. Calculate the maximum growth rate of this instability of inter-penetrating electron and positron beams and the wave vector corresponding to the maximum growth for the case of a cold plasmas, $v_T \rightarrow 0$.



HELLENIC
MEDITERRANEAN
UNIVERSITY



université
BORDEAUX



Erasmus+

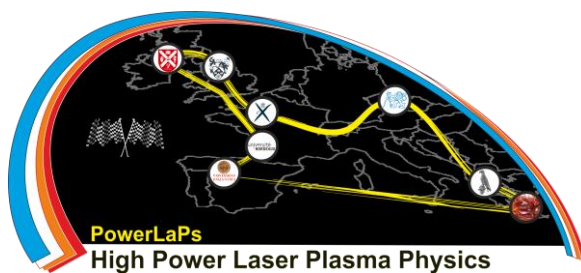
PowerLaPs

Innovative Education & Training in High Power Laser Plasmas

Plasma Physics - Theory and Experiments

Chapter 11: Plasmas and Radiation

D. Batani



Erasmus+

université
de BORDEAUX

11. Plasmas and Radiation

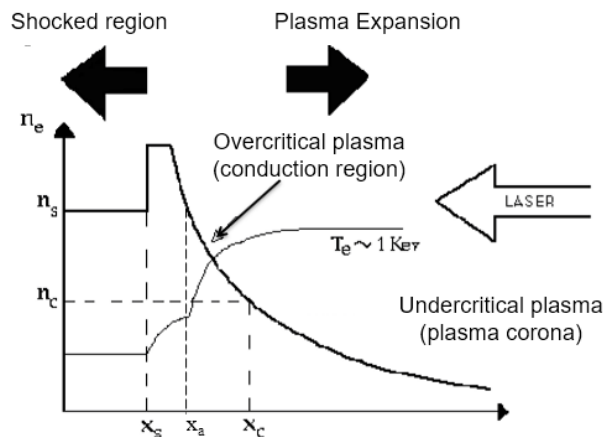
11.1 Radiative properties of plasmas

The radiative properties of plasmas may be summarized to:

- Radiation emission from plasmas (bound-bound, recombination, bremsstrahlung, with some remarks on H-like and He-like spectra)
- Line broadening mechanisms
- Equilibrium in a plasma (Maxwell, Boltzmann, Saha)
- Photon absorption and opacity (in particular collisional absorption)
- Equation of radiative transfer and blackbody limit

11.2 Laser-Plasma profile in the ns regime

The ns regime is dominated by hydrodynamics:



and has the characteristics:

Critical density

$$\omega_L^2 = \omega_p^2 + c^2 k^2 \quad n = \sqrt{1 - \frac{\omega_L^2}{\omega_p^2}} = \sqrt{1 - \frac{n_e}{n_{cr}}} \quad n_{cr} = \frac{1.1 \times 10^{21} \text{ cm}^{-3}}{\lambda(\mu\text{m})^2}$$

Energy balance at critical density: Absorbed flux \approx Energy flux carried away by thermal electrons

$$\alpha I_L = n_e v_e T_e$$

$$n_e \approx n_{cr} = 10^{21} / \lambda^2 \quad v_e \propto T_e^{1/2}$$

electron thermal velocity
(NRL Plasma formulary)

$$v_{Te} = (kT_e/m_e)^{1/2}$$

$$= 4.19 \times 10^7 T_e^{1/2} \text{ cm/sec}$$

Coronal temperature

$$T_e (eV) = 10^{-6} \left(I_L (W / cm^2) \lambda^2 (\mu m) \right)^{2/3}$$

Ablation (Shock) Pressure

$$P = n_e T_e$$

$$P (MBar) \approx 10 \left(\frac{I_L / 10^{14} (W / cm^2)}{\lambda^2 (\mu m)} \right)^{2/3}$$

Conduction zone

11.3 Equilibrium (and types of equilibrium) in a plasma

Free electrons are in equilibrium when they have a Maxwellian distribution of velocities:

$$\begin{aligned} dN &= \sqrt{\frac{2}{\pi}} \left(\frac{m}{T} \right)^3 v^2 \exp(-mv^2 / 2T) dv \\ &= \sqrt{\frac{4}{\pi T^3}} E^{1/2} \exp(-E / T) dE \end{aligned}$$

Clearly this cannot be applied to the relativistic regime since it implies $v > c$.

$$E^{1/2} dE = \left(\frac{1}{2} mv^2 \right)^{1/2} mvdv = \sqrt{\frac{m^3}{2}} v^2 dv$$

Where E is the kinetic energy of electrons.

The electron-electron collision time is:

$$\tau_{ee} (\text{sec}) = 1.7 \times 10^4 \frac{T_e^{3/2} (eV)}{\log \Lambda n_e (cm^{-3})} \approx 1.7 \times 10^3 \frac{T_e^{3/2} (eV)}{n_e (cm^{-3})}$$

$$\left[\tau_{ei} (\text{sec}) = \frac{1}{v_{ei}} \approx 3 \times 10^4 \frac{T_e^{3/2} (eV)}{n_e (cm^{-3})} \right]$$

$$T_e \approx 1keV \quad n_e \approx 10^{21} cm^{-3} \Rightarrow \tau_{ee} \approx 0.1ps$$

Coulomb collisions, Spitzer's model, Λ Coulomb logarithm.

Bound electrons are distributed on the electronic levels of atoms (ions) in agreement with Boltzman's statistics:

$$n(E_i) \gg g_i \exp(-E_i / T)$$

where g_i is the density of states.

Planckian distribution of photons (black body emission). Number of photons per unit volume and frequency:

$$dN(\nu) = \frac{8\pi\nu^2}{c^3} \frac{1}{\exp(h\nu / T) - 1} d\nu$$

$$E_{ph} = h\nu$$

Energy per unit volume per unit frequency:

$$u_p(\nu) = \frac{8\pi h\nu^3}{c^3} \frac{1}{\exp(h\nu / T) - 1}$$

Radiation emission from the surface of a black body:

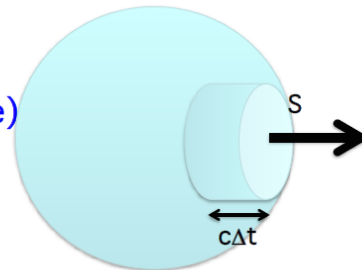
Energy density (per unit frequency)

$$u_p(\nu) = \frac{8\pi h\nu^3}{c^3} \frac{1}{\exp(h\nu / T) - 1} \quad (J / m^3) / (\Delta\nu)$$

Energy flux from surface (per unit frequency, time, and unit solid angle)

$$B_p(\nu) = \frac{u_p(\nu)c}{4\pi} =$$

$$\frac{2h\nu^3}{c^2} \frac{1}{\exp(h\nu / T) - 1} \quad (W / m^2) / (\Delta\nu\Omega)$$



But photons, in the more general case of a grey body, follow Kirchoff's law

$$\frac{e(n)}{a(n)} = B_p(n)$$

$\alpha(\nu)$ absorptivity: proportion of incident radiation absorbed, a blackbody has $\alpha(\nu) = 1$ at all wavelengths

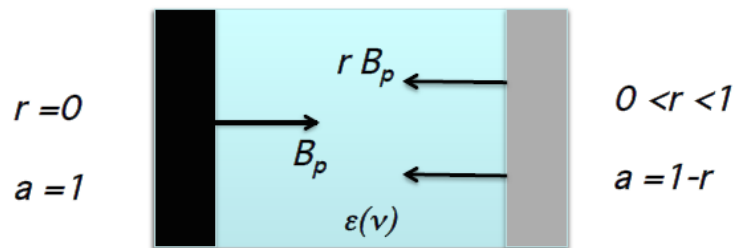
$\epsilon(\nu)$ emissivity

At equilibrium, there is a direct link between emission and absorption ("opacity" problem)

Kirchoff's law

Thermal equilibrium: $T_{\text{blackbody}} = T_{\text{GreyBody}}$ (2nd law of thermodynamics),
 r reflectivity, a absorptivity, $\varepsilon(\nu)$ grey body emission $B_p(\nu)$ blackbody emission

$B_p(\nu)$ and $\varepsilon(\nu)$ units of W/m^2 , a without dimensions



Between the body the radiation is exactly balanced

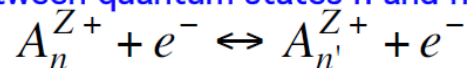
$$B_p(\nu) = \varepsilon(\nu) + r B_p$$

$$\Rightarrow \frac{\varepsilon(\nu)}{B_p(\nu)} = 1 - r \equiv a \quad \Rightarrow \varepsilon(\nu) = a B_p(\nu)$$

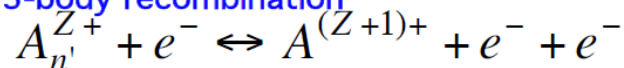
What is the equilibrium for ions?

Atomic processes in a plasma:

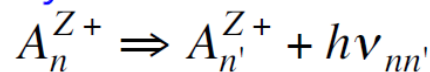
Collisional excitation (between quantum states n and n')



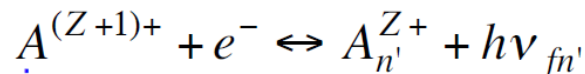
Collisional ionization and 3-body recombination



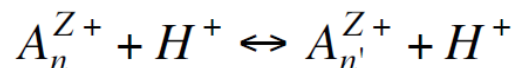
Spontaneous radiative decay



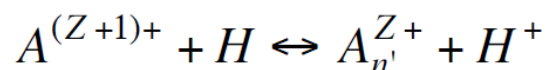
Radiative recombination



Collisional excitation from ions



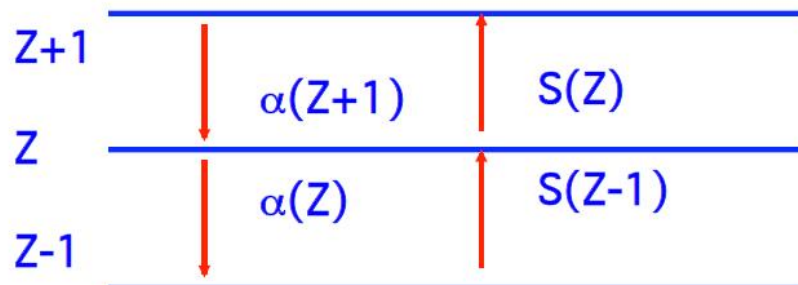
Charge exchange



Ionization equilibrium in a plasma

$$\frac{dN(Z)}{dt} = N_e \left[-S(Z)N(Z) - \alpha(Z)N(Z) + S(Z-1)N(Z-1) + \alpha(Z+1)N(Z+1) \right]$$

Here $S(Z)$ is the ionization rate. The recombination rate $\alpha(Z)$ has the form $\alpha(Z) = \alpha_r(Z) + N_e \alpha_3(Z)$, where α_r and α_3 are the radiative and three-body recombination rates, respectively.



Ionization from ion ground state, averaged over Maxwellian electron distribution, for $0.02 \lesssim T_e/E_\infty^Z \lesssim 100$ (Ref. 35):

$$(12) \quad S(Z) = 10^{-5} \frac{(T_e/E_\infty^Z)^{1/2}}{(E_\infty^Z)^{3/2} (6.0 + T_e/E_\infty^Z)} \exp\left(-\frac{E_\infty^Z}{T_e}\right) \text{ cm}^3/\text{sec},$$

Due to the exponential term, there is no significant ionization if $T \ll E_\infty^Z$, the ionization energy of the considered ion. Usually $T \approx 0.1 E_\infty^Z$ is enough to get significant ionization

Collisional (three-body) recombination rate for singly ionized plasma:³⁸

$$(15) \quad \alpha_3 = 8.75 \times 10^{-27} T_e^{-4.5} \text{ cm}^6/\text{sec}.$$

Electron-ion radiative recombination rate ($e + N(Z) \rightarrow N(Z - 1) + h\nu$)
for $T_e/Z^2 \lesssim 400$ eV (Ref. 37):

$$(13) \quad \alpha_r(Z) = 5.2 \times 10^{-14} Z \left(\frac{E_\infty^Z}{T_e} \right)^{1/2} \left[0.43 + \frac{1}{2} \ln(E_\infty^Z/T_e) + 0.469(E_\infty^Z/T_e)^{-1/3} \right] \text{ cm}^3/\text{sec.}$$

For $1 \text{ eV} < T_e/Z^2 < 15 \text{ eV}$, this becomes approximately³⁵

$$(14) \quad \alpha_r(Z) = 2.7 \times 10^{-13} Z^2 T_e^{-1/2} \text{ cm}^3/\text{sec.}$$

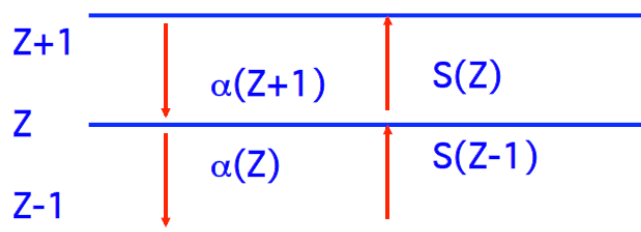
In stationary conditions (equilibrium)

$$\frac{dN(Z)}{dt} = n_e [-S(Z)N(Z) - \alpha(Z)N(Z) + S(Z-1)N(Z-1) + \alpha(Z+1)N(Z+1)] = 0$$

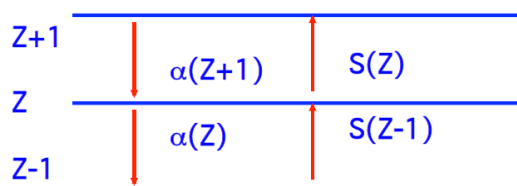
$$\frac{dN(0)}{dt} = n_e [-S(0)N(0) + \alpha(1)N(1)] = 0$$

$$\frac{dN(Z_{\max})}{dt} = n_e [-\alpha(Z_{\max})N(Z_{\max}) + S(Z_{\max} - 1)N(Z_{\max} - 1)] = 0$$

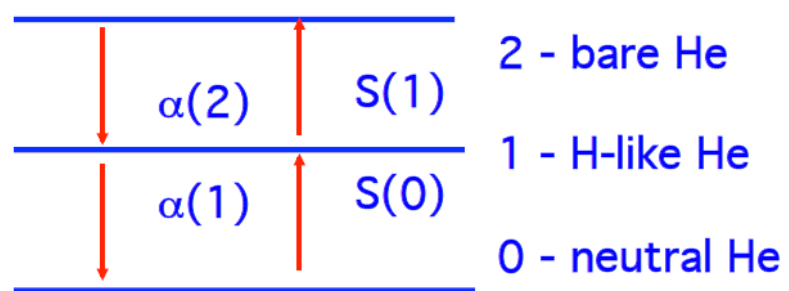
$$\sum_{0, Z_{\max}} N(Z) = N_{\text{tot}} = \text{const}$$



$$\frac{N(Z+1)}{N(Z)} = \frac{S(Z)}{\alpha(Z+1)} = \frac{S(Z)}{\alpha_r(Z+1) + n_e \alpha_3(Z+1)}$$



Example for helium



$$\frac{dN_0}{dt} = n_e [-S(0)N_0 + \alpha(1)N_1] = 0 \quad (1)$$

$$\frac{dN_1}{dt} = n_e [-S(1)N_1 - \alpha(1)N_1 + S(0)N_0 + \alpha(2)N_2] = 0 \quad (2)$$

$$\frac{dN_2}{dt} = n_e [-\alpha(2)N_2 + S(1)N_1] = 0 \quad (3)$$

From (1)

$$n_e [-S(0)N_0 + \alpha(1)N_1] = 0 \Rightarrow \frac{N_1}{N_0} = \frac{S(0)}{\alpha(1)}$$

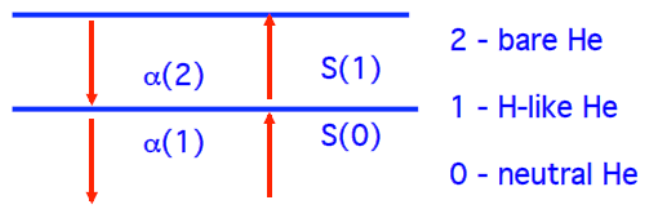
And from (3)

$$n_e [-\alpha(2)N_2 + S(1)N_1] = 0 \Rightarrow \frac{N_2}{N_1} = \frac{S(1)}{\alpha(2)}$$

Also notice that

$$N_0 + N_1 + N_2 = N_{tot} = \text{const}$$

$$n_e = N_1 + 2N_2$$



At very high densities

$$\frac{N(Z+1)}{N(Z)} \approx \frac{S(Z)}{n_e \alpha_3(Z+1)}$$

This is Saha's distribution (or Saha-Boltzman distribution).

Physical meaning of Saha's law:

$$\frac{N(Z+1)}{N(Z)} \gg \frac{S(Z)}{n_e a_3(Z+1)}$$

Ions recombine mainly due to collisions. Radiative de-ionization become negligible. At high densities (or long plasmas) the emitted photons are re-absorbed before they scape the plasma, therefore they do not contribute to recombination

Notion of "optically thick" plasma.

Saha's distribution.

In a steady state at high electron density,

$$(18) \quad \frac{N_e N^*(Z)}{N^*(Z-1)} = \frac{S(Z-1)}{\alpha_3},$$

Saha equilibrium:³⁹

$$(17) \quad \frac{N_e N_1^*(Z)}{N_n^*(Z-1)} = 6.0 \times 10^{21} \frac{g_1^Z T_e^{3/2}}{g_n^{Z-1}} \exp\left(-\frac{E_\infty^Z(n,l)}{T_e}\right) \text{ cm}^{-3},$$

where g_n^Z is the statistical weight for level n of charge state Z and $E_\infty^Z(n,l)$ is the ionization energy of the neutral atom initially in level (n,l) , given by Eq. (2).

At very low densities

$$\frac{N(Z+1)}{N(Z)} = \frac{S(Z)}{\alpha(Z+1)} = \frac{S(Z)}{\alpha_r(Z+1)}$$

This is called "Coronal equilibrium" CE (typical of the low-density corona of the sun)

$$\frac{N(j+1)}{N(j)} = 7.2 \cdot 10^{-12} T^{-3/4} I_j^{11/4} \exp\left(-\frac{I_j}{T}\right)$$

Physical meaning of “Coronal equilibrium”

The low density of the plasma or its short extension imply that as soon as a photon is emitted it escapes from the plasma and therefore cannot be re-absorbed and re-ionize other atoms. Notion of “**optically thin**” plasma

The low density of the plasma also implies that collisions are rare events. So not much possibility of getting electrons in excited states.

However radiative de-excitation (which is dominant over collisional de-excitation) is preferentially towards the ground state which is therefore overpopulated

Rate for spontaneous decay $n \rightarrow m$ (Einstein A coefficient)³⁴

$$(6) \quad A_{nm} = 4.3 \times 10^7 (g_m / g_n) f_{mn} (\Delta E_{nm})^2 \text{ sec}^{-1}.$$

At intermediate densities

$$\frac{N(Z+1)}{N(Z)} = \frac{S(Z)}{\alpha(Z+1)} = \frac{S(Z)}{\alpha_r(Z+1) + n_e \alpha_3(Z+1)}$$

This is called “Collisional Radiative Equilibrium” CRE

Conditions of validity for Saha distribution

$$\begin{aligned} n_e (\text{cm}^{-3}) &\geq 7 \times 10^{18} Z^7 n^{-17/2} (T / E_Z^\infty)^{1/2} \\ &\approx 1.7 \times 10^{14} T (\text{eV})^{1/2} \left(E_{Z_{\max}}^\infty \right)^3 \end{aligned}$$

(n principal quantum number)

Corona model is applicable if

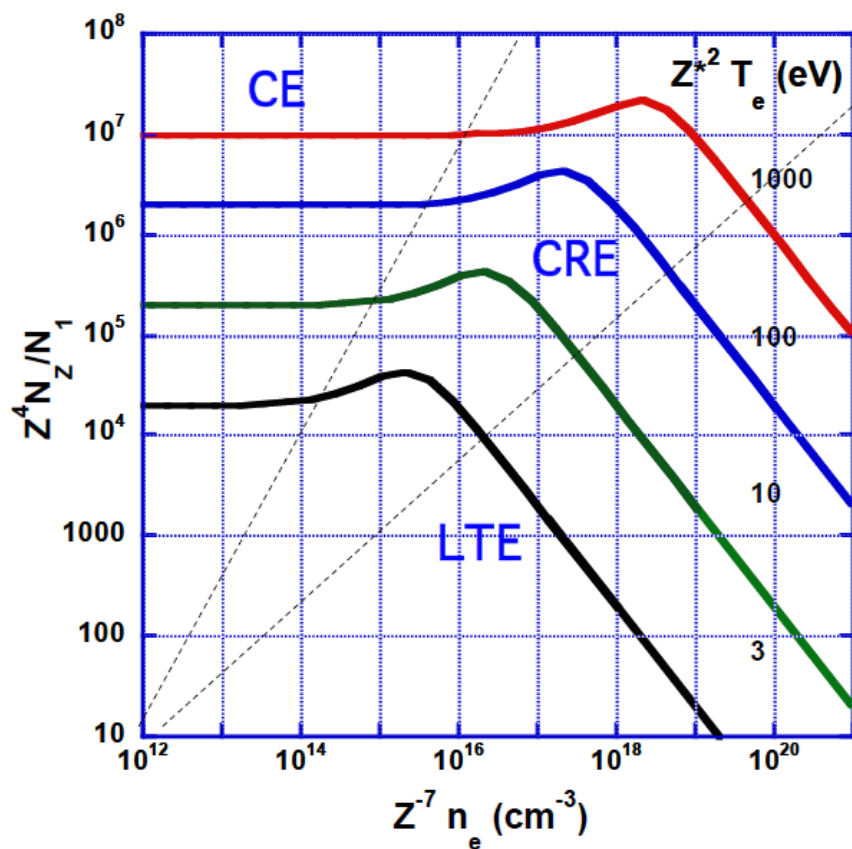
$$n_e (\text{cm}^{-3}) < 10^{16} T (\text{eV})^{7/2}$$

In CE ionization degree is independent on electron density:

$$\frac{N(Z+1)}{N(Z)} \approx \frac{S(Z)}{\alpha_r(Z+1)}$$

On the contrary in Saha equilibrium, ionization decreases when electron density increases (more collisions bringing to recombination)

$$\frac{N(Z+1)}{N(Z)} \approx \frac{S(Z)}{n_e \alpha_3(Z+1)}$$

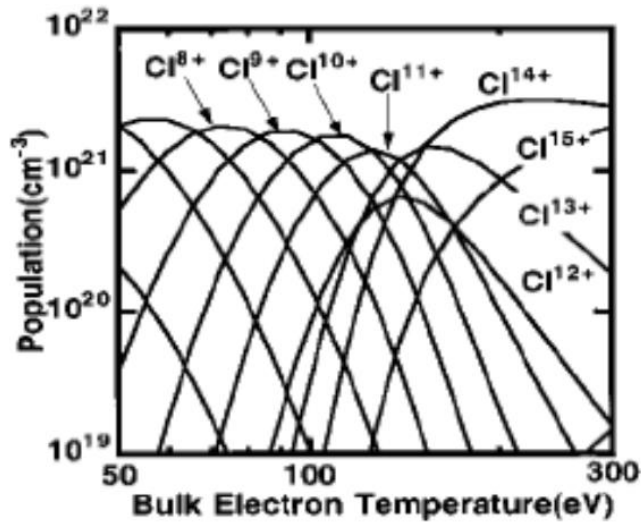


Ionization states

Thermal effects produce a Saha-like distribution of ionization states. This is related to EOS.

With short pulses field and tunnel ionization may also be important

Usually 3 ionization states dominate in the plasma



Average ionization degree in a plasma

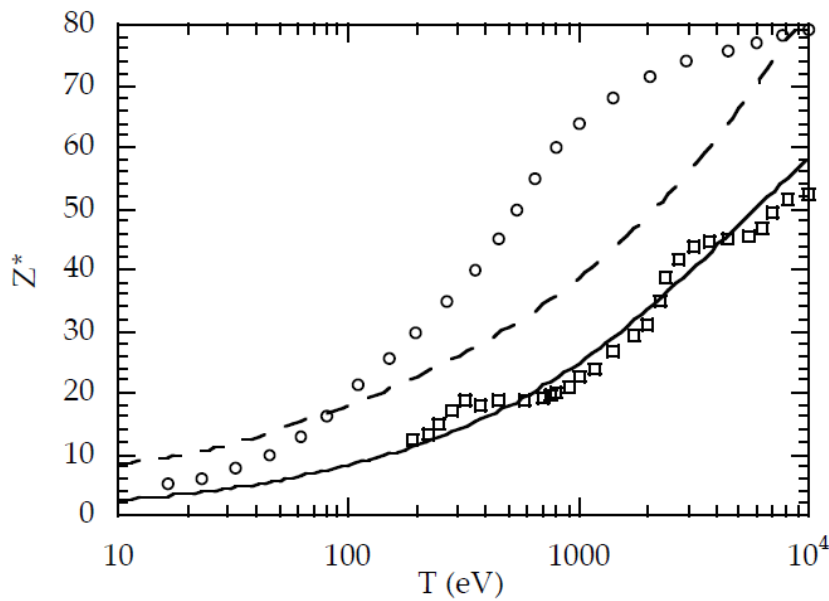
In CE ionization degree is independent on electron density

$$Z^* = 26 \left(\frac{T \text{ (KeV)}}{1 + (26/Z)^2 T \text{ (KeV)}} \right)^{1/2}$$

In CRE the dependence is not big

$$Z^* = \text{Min} \left(Z, \frac{2}{3} (AT_e \text{ (eV)})^{1/3} \right)$$

Such formulas need to be corrected because at $T=0$ Z^* =average number of electrons per atom in the conduction band (e.g. $Z^*=3$ for Al). This result is obtained by Quantum models of plasmas at high density and low temperature (e.g. Thomas-Fermi model).

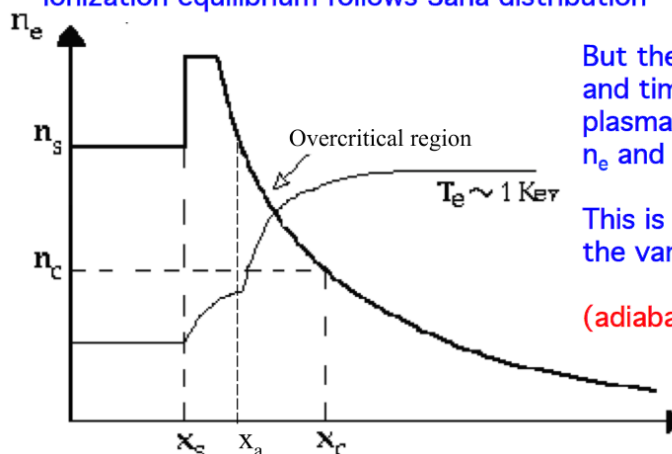


Average ionization degree for gold at density $\rho = 0.1 \text{ g/cm}^3$ vs. temperature. Squares: coronal limit, Circles: Thomas Fermi model, Dashed line: CRE formula, Continuous Line: CE formula

Types of equilibrium in a plasma

- Free electrons follow Maxwell distribution
- Ionization equilibrium:
 - Low densities - CE
- Intermediate densities - CRE
- High density - Saha distribution
- The high density case corresponds to LOCAL THERMODYNAMIC EQUILIBRIUM (LTE)

In LTE we have that:
 Free electrons follow Maxwell distribution
 Bound electrons follow Boltzman distribution
 Ionization equilibrium follows Saha distribution



But they follow the space and time evolution of the plasma parameters n_e and T_e

This is possible ONLY if the variations are slow

(adiabatic approximation)



In the low density case (CE) photons escape the plasma as they are emitted: the spectrum emitted by the plasma exactly reflects that of individual atoms (ions).

We can “see” inside the plasma

In the high density case, photons are reabsorbed and remitted many times before they can escape. Therefore the radiation is strongly affected and tends to become a thermal radiation.

We can only see the surface of the plasma

When the radiation becomes thermal we speak of complete local thermal equilibrium or we say that there is equilibrium between matter and radiation.

In this case the temperature in Planck's formula is the electron temperature

If there is no dependence on position, we have the true “Thermodynamic Equilibrium”

11.4 Equation of radiation transfer

$$\frac{dI}{ds} = j(\omega) - a(\omega)I$$

Between two points along a ray, intensity increases because of (spontaneous) emission and decreases because of absorption. We neglect scattering to simplify the equation. We also neglect stimulated emission.

α → linear absorption coefficient

j → emission of radiation (energy per unit volume, unit time, and unit frequency)

$$\frac{dI}{ds} = j(\omega) - \alpha(\omega)I$$

If there is no emission, we get Lambert-Beer's law for absorption of e.m. radiation in a medium

$$\frac{dI}{ds} = -\alpha(\omega)I$$

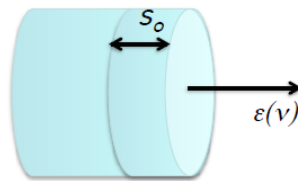
$$I(s) = I_0 \exp(-\alpha(\omega)s) = I_0 \exp(-s / s_0(\omega))$$

Here $s_0 = 1/\alpha$ is the photon mean free path in the medium.

Transmission is

$$T = I / I_0 = \exp(-\alpha s)$$

On average, only the photons emitted within a mean free path s_0 can escape from the surface of the medium (those at larger depths are absorbed before reaching the surface)



This gives a relation between the emission coefficient per unit volume of the material $j(\nu)$ [units W/m^3] and the emissivity of the medium $\varepsilon(\nu)$ [units W/m^2]
(for simplicity here we neglect the per unit frequency and per unit solid angle, so ε and I have the same units)

$$I = \varepsilon = j(\omega)s_0(\omega) \quad \Rightarrow \quad I = \varepsilon = \frac{j(\omega)}{\alpha(\omega)}$$

$$\frac{dI}{ds} = j(\omega) - \alpha(\omega)I \quad \text{W}/\text{cm}^2 \quad \text{W}/\text{cm}^3 \quad 1/\text{cm}$$

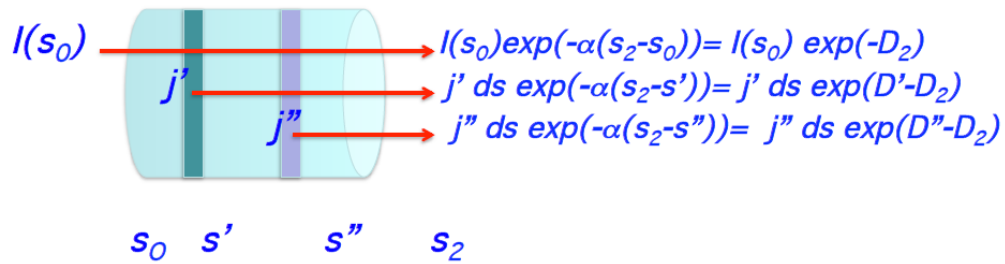
Between two points along a ray, intensity increases because of emission and decreases because of absorption

$$I(s_2) = I(s_1)e^{-(D_2 - D_1)} + \int_{s_1}^{s_2} j(\omega)e^{-(D - D_2)} ds$$

Reabsorption is taken into account.
 $D(s)$ is the optical depth (or optical density)

$$D(s) = \int_{s_0}^s \alpha(\omega) ds$$

Physical interpretation



$$I(s_2) = I(s_0) e^{-D_2} + \int_{s_0}^{s_2} j(\omega) e^{(D - D_2)} ds$$

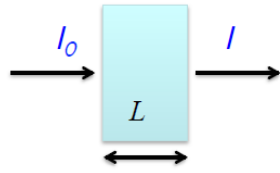
$$D(s) = \int_{s_0}^s \alpha(\omega) ds = \alpha(\omega) L \quad (L = s_2 - s_0)$$

For a uniform plasma slab of thickness L

$$\begin{aligned}
 I(s_2) &= I(s_0) e^{-D_2} + \int_{s_0}^{s_2} j(\omega) e^{(D - D_2)} ds \\
 &= I(s_0) e^{-D_2} + \int_{s_0}^{s_2} (j(\omega) / \alpha(\omega)) e^{(D - D_2)} dD \\
 &= I(s_0) e^{-D_2} + (j / \alpha) [1 - e^{-D_2}]
 \end{aligned}$$

$$D(s) = \int_{s_0}^s \alpha(\omega) ds = \alpha(\omega) L \quad (L = s_2 - s_0)$$

Relation between a absorptivity and α linear absorption coefficient



$$T = I / I_0 = \exp(-\alpha L)$$

Lambert-Beer's law

$$a = 1 - I / I_0$$

$$\Rightarrow a = 1 - e^{-\alpha L}$$

When the optical depth is $\gg 1$ the plasma is said to be optically thick. This means absorptivity is close to unit

$$\alpha L \gg 1 \quad \Rightarrow a \approx 1$$

$$I(s_2) = I(s_0)e^{-D_2} + (j / \alpha) [1 - e^{-D_2}]$$

When the optical depth is $\gg 1$, i.e. the plasma is optically thick then

$$D(s) = \int_{s_0}^s \alpha(\omega) ds \gg 1$$

$$I(s_2) \approx (j / \alpha)$$

as it was "guessed" before

Integral vs. local form of Kirchoff's law

$$\varepsilon(\nu) / a(\nu) = B_p(\nu) \quad \leftarrow$$

But if the optical depth ($\alpha L \gg 1$) is large

$$I = (j / \alpha)$$

Identifying I and ε we get

$$\varepsilon \approx (j / \alpha) = a B_p(\omega)$$

$$a = 1 - \exp(-\alpha L)$$

But $a \approx 1$ from which

$$j(\nu) / \alpha(\nu) = B_p(\nu) \quad \leftarrow$$

The relation

$$j(\nu) / \alpha(\nu) = B_p(\nu)$$

has been obtained for optically thick plasmas but it is always valid (it is "local")

Then the equation of radiation transfer can be written as follows:

$$\begin{aligned} \frac{dI}{ds} &= j(\omega) - \alpha(\omega)I = \\ &= \alpha(\nu) [B_p(\nu) - I] \end{aligned}$$

During propagation the light becomes more and more similar to a black body

In general α however depends on frequency. Let's take the collisional absorption coefficient μ

$$\mu = \alpha = \text{const} \frac{Z^2 n_e n_i \ln(\Lambda)}{n_r T_e^{1/2}} \frac{1 - e^{-h\nu/kT}}{\nu^3} g_{\text{ff}}$$

$$\approx 3.1 \times 10^{-7} \frac{Z n_e^2 \ln(\Lambda)}{n_r \omega^2 T_e^{3/2}}$$

at low frequencies

Then there is a "transition frequency" ω_T which gives an optical depth $D=1$

$$\mu = \alpha = 3.1 \times 10^{-7} \frac{Z n_e^2 \ln(\Lambda)}{n_r \omega^2 T_e^{3/2}}$$

$$D = \alpha(\omega) L = 1$$

$$\omega_T^2 = 3.1 \times 10^{-7} \frac{Z n_e^2 \ln(\Lambda)}{T_e^{3/2}} L \quad [n_r \approx 1]$$

For $\omega \ll \omega_T$, the plasma emits a black body spectrum

At low frequencies, $\omega \ll \omega_T$, the plasma emits a black body spectrum.

The maximum of black body emission is at (Wien's law)

$$\lambda_{\max} (\text{A}) = \frac{2500}{T_e}$$

And Stefan Boltzman's law implies that

$$\sigma T^4 \approx I_L / 2$$

Where $\sigma \approx 10^5$ with T in eV and I_L in W/cm²

If the plasma is thin ($\omega \gg \omega_T$)

$$D(s) = \alpha(\omega)L \ll 1$$

$$I(s_0) \approx 0$$

$$I(s_2) = (j / \alpha) [1 - e^{-D_2}] \approx (j / \alpha) [1 - (1 - D_2)] = jL$$

but

$$j = B_p \alpha$$

$$I(s_2) = jL = B_p \alpha L$$

If we take the limit of high frequencies ($h\nu \gg T$)

$$B_p(\nu) = \frac{2h\nu^3}{c^2} \frac{1}{\exp(h\nu/T) - 1}$$

$$\alpha = \text{const} \frac{Z^2 n_e n_i \ln(\Lambda)}{n_r T_e^{1/2}} \frac{1 - e^{-h\nu/T}}{\nu^3} g_{\text{ff}}$$

$$j = \alpha B_p(\nu) = \frac{2h\nu^3}{c^2} \frac{1}{\exp(h\nu/T) - 1} \frac{Z^2 n_e n_i \ln(\Lambda)}{n_r T_e^{1/2}} \frac{1 - e^{-h\nu/T}}{\nu^3} g_{\text{ff}}$$

$$= \frac{2hZ^2 n_e n_i \ln(\Lambda) g_{\text{ff}}}{n_r T_e^{1/2} c^2} \frac{1 - e^{-h\nu/T}}{e^{h\nu/T} - 1} \approx \text{const} \frac{Z^2 n_e n_i \ln(\Lambda)}{T_e^{1/2}} e^{-h\nu/T}$$

Bremsstrahlung emission

$$(e^{h\nu/T} - 1 \approx e^{h\nu/T} \quad \text{and} \quad 1 - e^{-h\nu/kT} \approx 1)$$

For $\omega \ll \omega_T$, long plasma and low frequency, the plasma emits a black body spectrum.

$$\omega_T^2 = 3.1 \times 10^{-7} \frac{Z n_e^2 \ln(\Lambda)}{T_e^{3/2}} L$$

It is a surface emission. We cannot see inside the plasma, photons are reabsorbed, we only see the surface

$$I(s_2) \approx (j / \alpha) = B_p(\nu)$$

Since photons are reabsorbed and density is high, we are likely in LTE conditions

For $\omega \gg \omega_T$, thin plasma and high frequency, we see the inner part of the plasma. It is a volume emission.

At high frequencies bremsstrahlung-like emission

$$I(s_2) \approx jL = j_o \exp(-hv / kT)$$

Photons escape from the plasma and density is low. We are likely in CE conditions

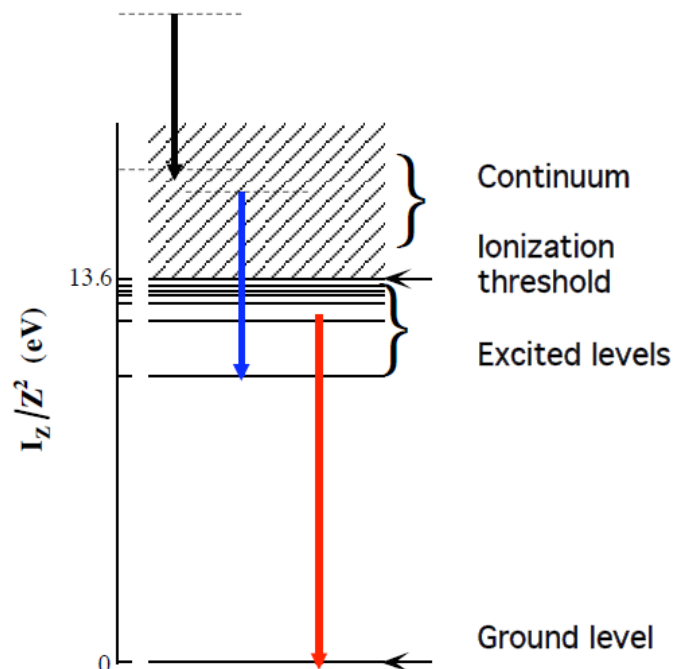
11.5 Radiation emission from plasmas

Three types of emission:

Free-Free emission (continuum) or “bremsstrahlung”

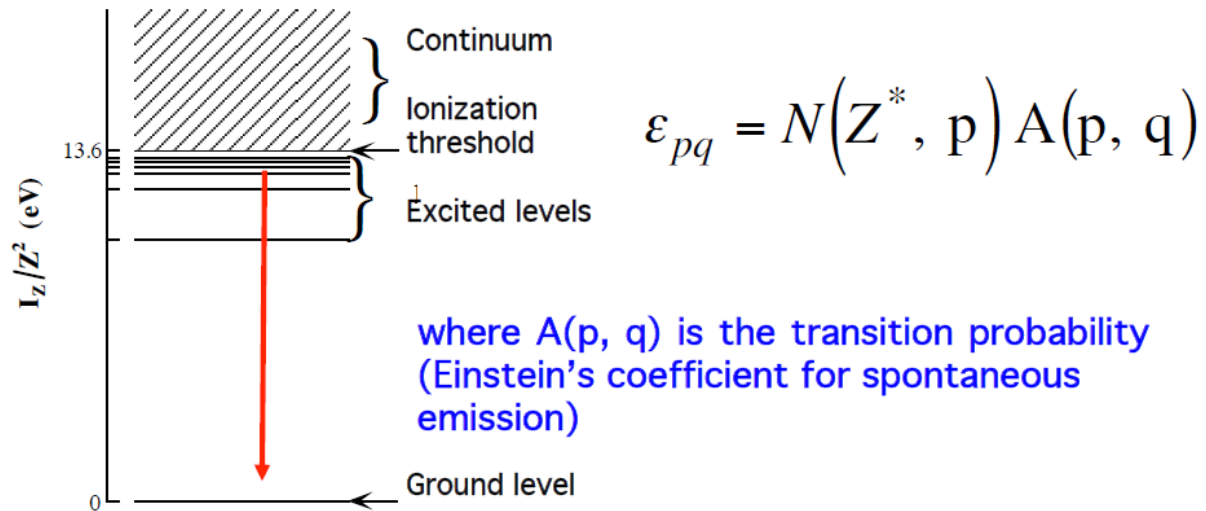
Free-Bound emission
(continuum)

Bound bound emission
(lines)



Line emission

The emissivity of a spectral line arising from a $p \rightarrow q$ transition for an ion with charge Z^* is related to the electronic population $N(Z^*, p)$ of the upper level p



(here ϵ is in term of number of emitted photons per unit time. To get the real emissivity one must multiply by the photon energy corresponding to the transition)

The problem of line emission is to find the population on each level.

$$\epsilon_{pq} = N(Z^*, p) A(p, q)$$

$$\frac{dN(Z^*, p)}{dt} = -N(Z^*, p) A(p) + R_r(p) - N(Z^*, p) C(p) + R_c(p)$$

$$A(p) = \sum A(p, p')$$

Where the first term $-NA$ gives the depletion towards the lower levels due to radiative decay, R represents the population increase of the level due to radiative processes (absorption), $-NC$ represents collisional depletion towards lower levels, and the fourth term the collisional increase in population.

In stationary conditions

$$\epsilon_{Z^*, pq} = \frac{A(p, q)}{A(p) + C(p)} [R_r(p) + R_c(p)]$$

At equilibrium, the population on each bound level follows Boltzmann's distribution

$$\begin{aligned} \varepsilon_{pq} &= N(Z^*, p) A(p, q) = \\ &= \frac{A(p, q)}{A(p) + C(p)} [R_r(p) + R_c(p)] \\ &= g_i \exp(-E_i / T) A(p, q) \end{aligned}$$

Cross section (Bethe approximation) for electron excitation by dipole allowed transition $m \rightarrow n$ (Refs. 32, 33):

$$(3) \quad \sigma_{mn} = 2.36 \times 10^{-13} \frac{f_{mn} g(n, m)}{\epsilon \Delta E_{nm}} \text{ cm}^2,$$

where f_{mn} is the oscillator strength, $g(n, m)$ is the Gaunt factor, ϵ is the incident electron energy, and $\Delta E_{nm} = E_n - E_m$.

Electron excitation rate averaged over Maxwellian velocity distribution, $X_{mn} = N_e \langle \sigma_{mn} v \rangle$ (Refs. 34, 35):

$$(4) \quad X_{mn} = 1.6 \times 10^{-5} \frac{f_{mn} \langle g(n, m) \rangle N_e}{\Delta E_{nm} T_e^{1/2}} \exp\left(-\frac{\Delta E_{nm}}{T_e}\right) \text{ sec}^{-1},$$

where $\langle g(n, m) \rangle$ denotes the thermal averaged Gaunt factor (generally ~ 1 for atoms, ~ 0.2 for ions).

Rate for spontaneous decay $n \rightarrow m$ (Einstein A coefficient)³⁴

$$(6) \quad A_{nm} = 4.3 \times 10^7 (g_m / g_n) f_{mn} (\Delta E_{nm})^2 \text{ sec}^{-1}.$$

Line emission in CE equilibrium

In coronal equilibrium the ground level is “over-populated”.

The total radiative decay of each level is dominated by the radiative decay towards the ground level

$$\frac{dN(Z^*, p)}{dt} = -N(Z^*, p)A(p) + R_r(p) - N(Z^*, p)C(p) + R_c(p)$$

$$A(p) = \sum A(p, p') \approx A(p, 0)$$

The same applies for collisional excitation

In CE (and CRE) bound electrons do not necessarily follow Boltzman.

In coronal equilibrium:

Intensity emitted per unit volume from the transition $n \rightarrow m$ in an optically thin plasma:

$$(7) \quad I_{nm} = 1.6 \times 10^{-19} A_{nm} N_n \Delta E_{nm} \text{ watt/cm}^3.$$

Condition for steady state in a corona model:

$$(8) \quad N_0 N_e \langle \sigma_{0n} v \rangle = N_n A_{n0},$$

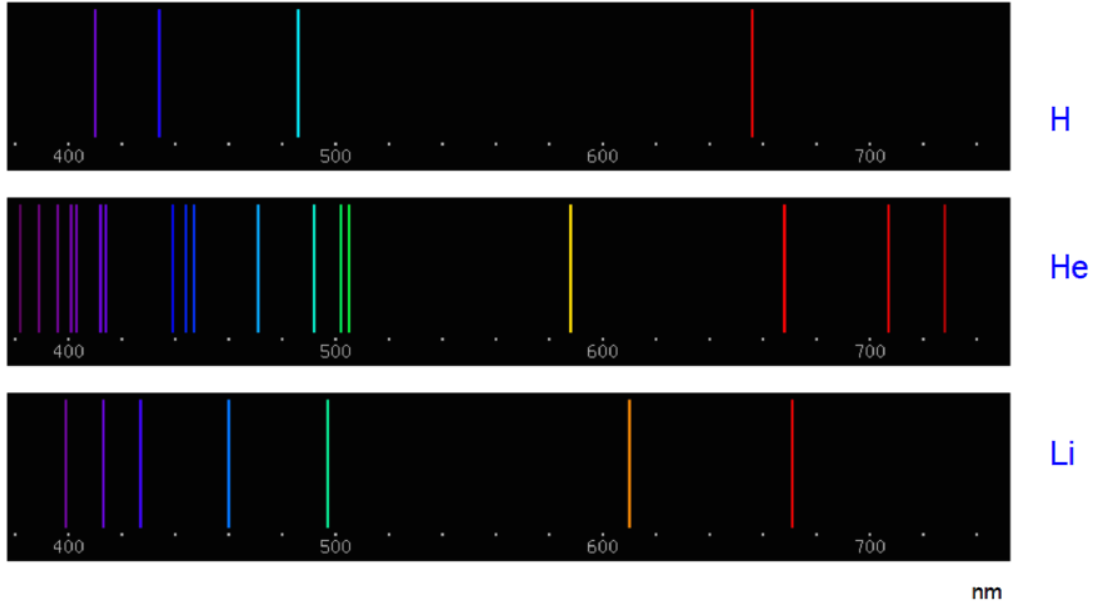
where the ground state is labelled by a zero subscript.

Hence for a transition $n \rightarrow m$ in ions, where $\langle g(n, 0) \rangle \approx 0.2$,

$$(9) \quad I_{nm} = 5.1 \times 10^{-25} \frac{f_{nm} g_m N_e N_0}{g_0 T_e^{1/2}} \left(\frac{\Delta E_{nm}}{\Delta E_{n0}} \right)^3 \exp \left(-\frac{\Delta E_{n0}}{T_e} \right) \frac{\text{watt}}{\text{cm}^3}.$$

Line emission: K-shell spectra

Simple spectra: very good for diagnostic and for generation of quasi-monochromatic sources.



Simple spectra: very good for diagnostic and for generation of quasi-monochromatic sources.

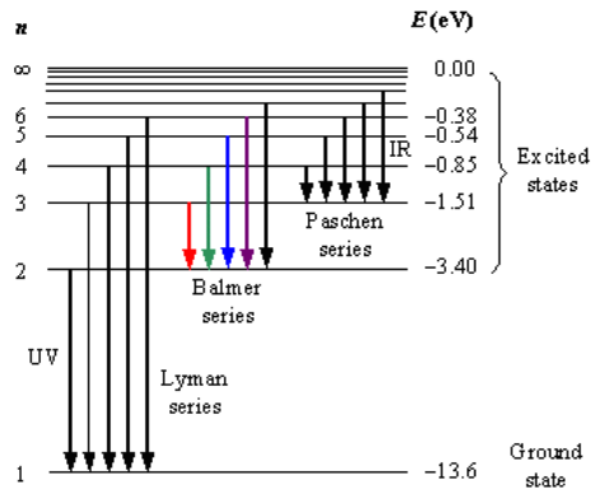
Hydrogen (Bohr's formula):

$$h\nu = E_m - E_n$$

$$E_n = -\frac{I_H Z^2}{n^2} = -\frac{RhcZ^2}{n^2}$$

$$I_H = 13.6\text{eV}$$

For $Z \approx 7$, these lines enter the X-ray domain ($h\nu \approx 1\text{keV}$)



Energy levels of the hydrogen atom with some of the transitions between them that give rise to the spectral lines indicated

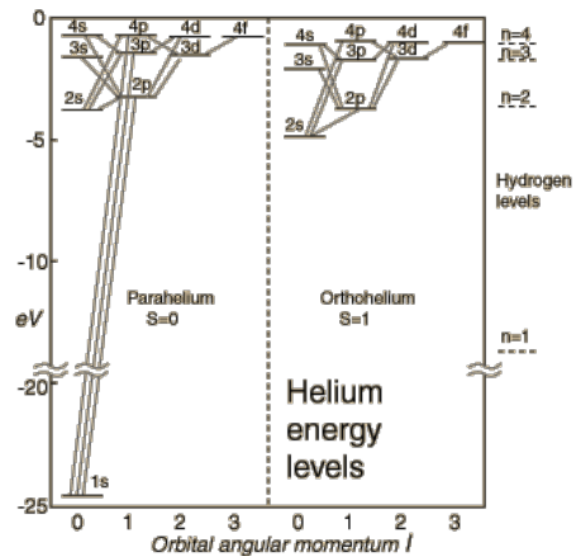
Simple spectra: very good for diagnostic and for generation of quasi-monochromatic sources.

Helium: fundamental state $1s^2$
(the ground level is $1s$ as in Hydrogen)

Alkaline metals, one valence electron
(the ground level is $2s$)

$$E_{n,l} = -\frac{RhcZ^2}{(n - \Delta(n,l))^2}$$

$\Delta(n,l)$ is the "quantum defect". Effect of the Z screening electrons on the effective nuclear charge. At large distance $Z_{\text{eff}}=1$, on the fundamental level $Z_{\text{eff}}=Z$



Line emission: L-shell spectra

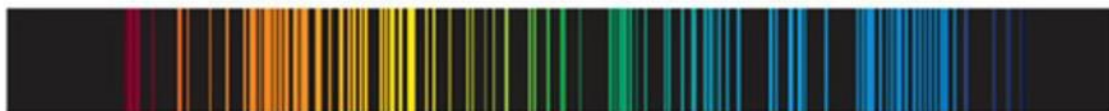
Spectral characterised by «bands» of lines



Hydrogen light spectrum

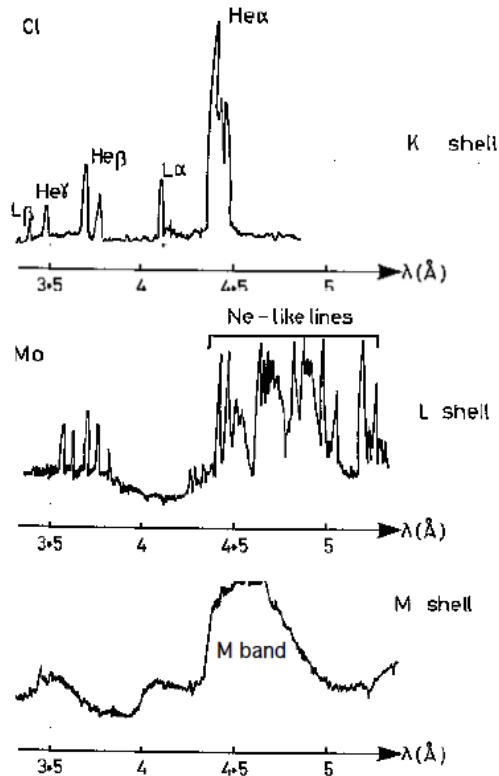


Helium light spectrum



Neon light spectrum

Line emission: K-shell, L-shell, M-shell spectra



Transition from simple spectra with a few lines (K-shell)

To bands of lines (L-shell)

To a quasi continuum (M and N-shell)

The generation of X-rays increases with Z , i.e. with the «shell index»

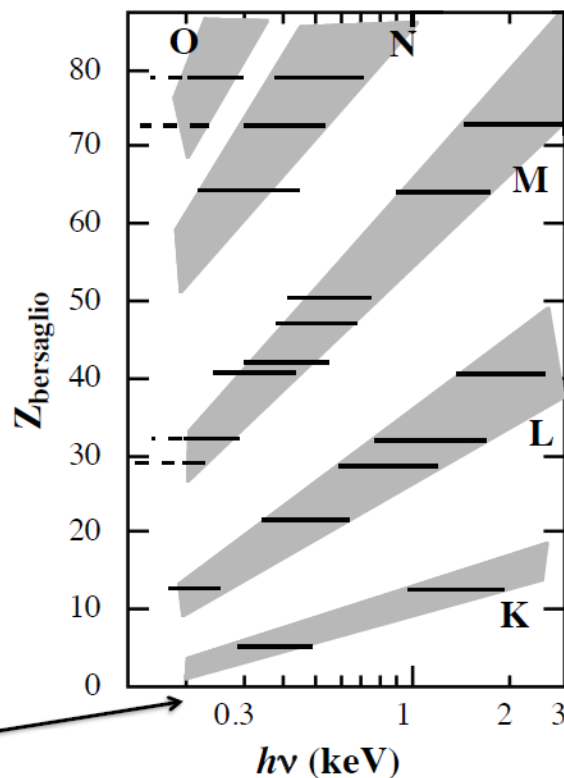
Characteristics of (X-ray) emission from plasmas

Emitted lines vs. Z of target

Scaling with Z^2

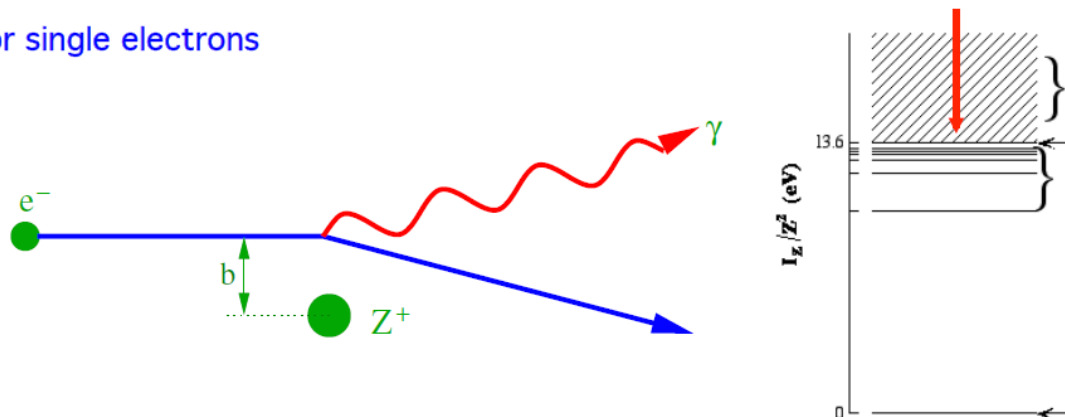
$$h\nu = I_H Z^2 \left(\frac{1}{n^2} - \frac{1}{m^2} \right)$$

Scaling with Z^2



Bremsstrahlung emission

For single electrons



We will follow an approximate derivation. For a more complete treatment see [2] and [1]. We will consider an electron–proton plasma.

Definitions:

- b : impact parameter
- v : velocity of the electron
- n_e : number density of the electrons
- n_p : number density of the protons
- T : temperature of the plasma: $mv^2 \sim kT \rightarrow v \sim (kT/m)^{1/2}$.

Calculation of the spectral power emitted by a single electron

- 1) the electron interacts with the ion only when it passes close to it, hence for a characteristic time $\tau \approx b/v$, corresponding to a characteristic frequency $\omega = 1/\tau \approx v/b$
- 2) The typical acceleration is $a \approx Ze^2/m_e b^2$
- 3) Larmor's formula gives the power emitted during the collision (acceleration) time $P \approx 2e^2 a^2 / 3c^3 = e^6 / m_e^2 c^3 b^4$
- 4) The power per unit frequency will be $P(\omega) = e^6 / m_e^2 c^3 v b^3$
- 5) The impact parameter is estimated from the density of ions $b^3 \approx 1/n_{ion}$

Calculation of plasma emissivity $j(\omega)$

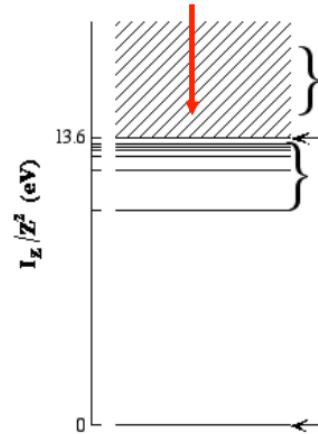
- 1) $P(\omega)$ is multiplied by the density of electrons and dividing by 4π to calculate emissivity per solid angle (isotropic emission)
- 2) This $j(\omega)$ is integrated over the Maxwellian distribution of electrons in the plasma $f(v)dv$

For a Maxwellian population of free electrons the shape of bremsstrahlung emission is exponential. The quantity g_{ff} is the Gaunt factor (which has a quantum origin)

$$\frac{d\varepsilon_{ff}}{d(h\nu)} = 1.5 \times 10^{-32} \frac{n_e}{T_e^{1/2}} g_{ff} \exp(-h\nu/T_e) \sum_i N_i Z_i^2 = J_o(T_e) \exp(-h\nu/T_e)$$

The total power emitted (W/cm³) is

$$P_{ff} = 1.5 \times 10^{-32} n_e T_e^{1/2} \sum_i N_i Z_i^2$$



Attention: the important parameter in plasma emission is not the average ionization degree but the effective ionization degree (higher charges contribute more to emission)

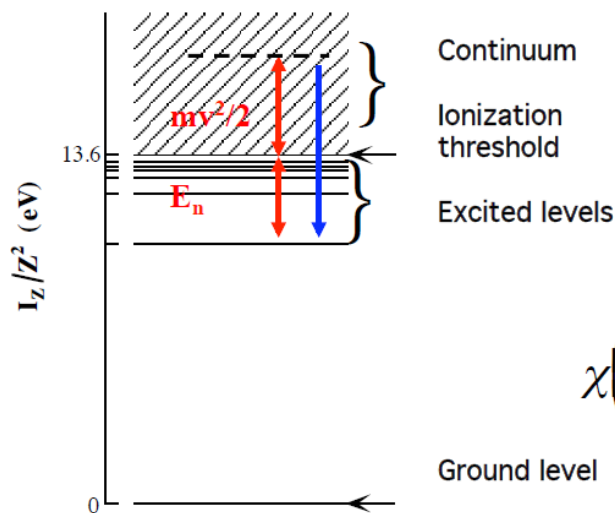
$$\begin{aligned} \frac{d\varepsilon_{ff}}{d(h\nu)} &= 1.5 \times 10^{-32} \frac{n_e}{T_e^{1/2}} g_{ff} \exp(-h\nu/T_e) \sum_i N_i Z_i^2 \\ &= J_o(T_e) \exp(-h\nu/T_e) \end{aligned}$$

$$Z^* = \frac{1}{N_{tot}} \sum N(Z) Z$$

$$Z_{eff} = \frac{1}{N_{tot}} \sum N(Z) Z^2$$

Recombination emission

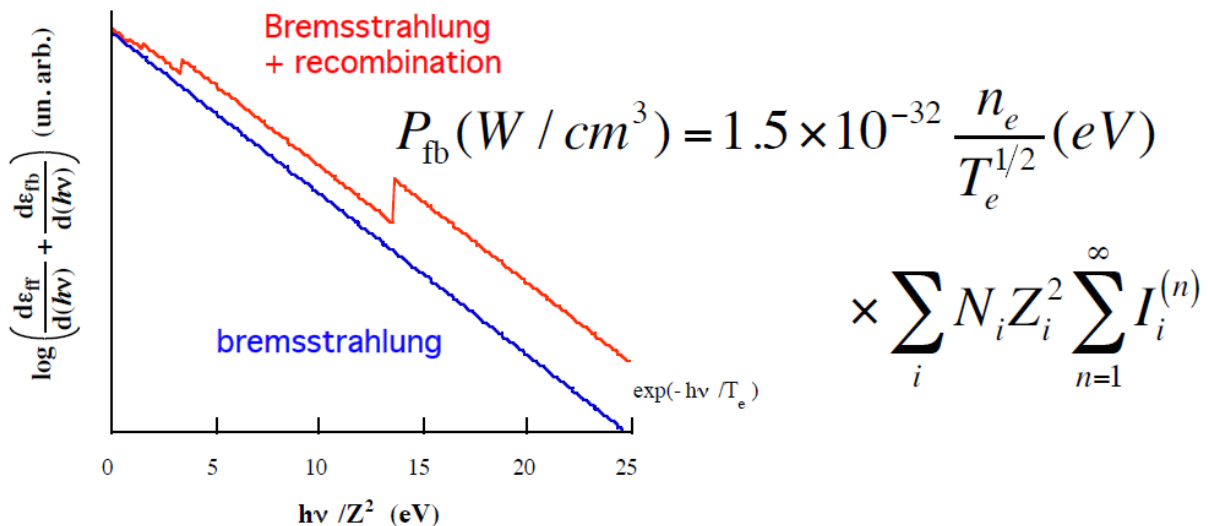
$$\frac{d\varepsilon_{fb}}{d(h\nu)} = 1.5 \times 10^{-32} \frac{n_e}{T_e^{3/2}} \sum_i N_i Z_i^2 \sum_{n=1}^{\infty} \frac{J_i^{(n)}}{n^3} g_{fb}^{(n)} I_i^{(n)} \exp\left[-\frac{(h\nu - I_i^{(n)})}{T_e}\right] \chi(h\nu - I_i^{(n)})$$

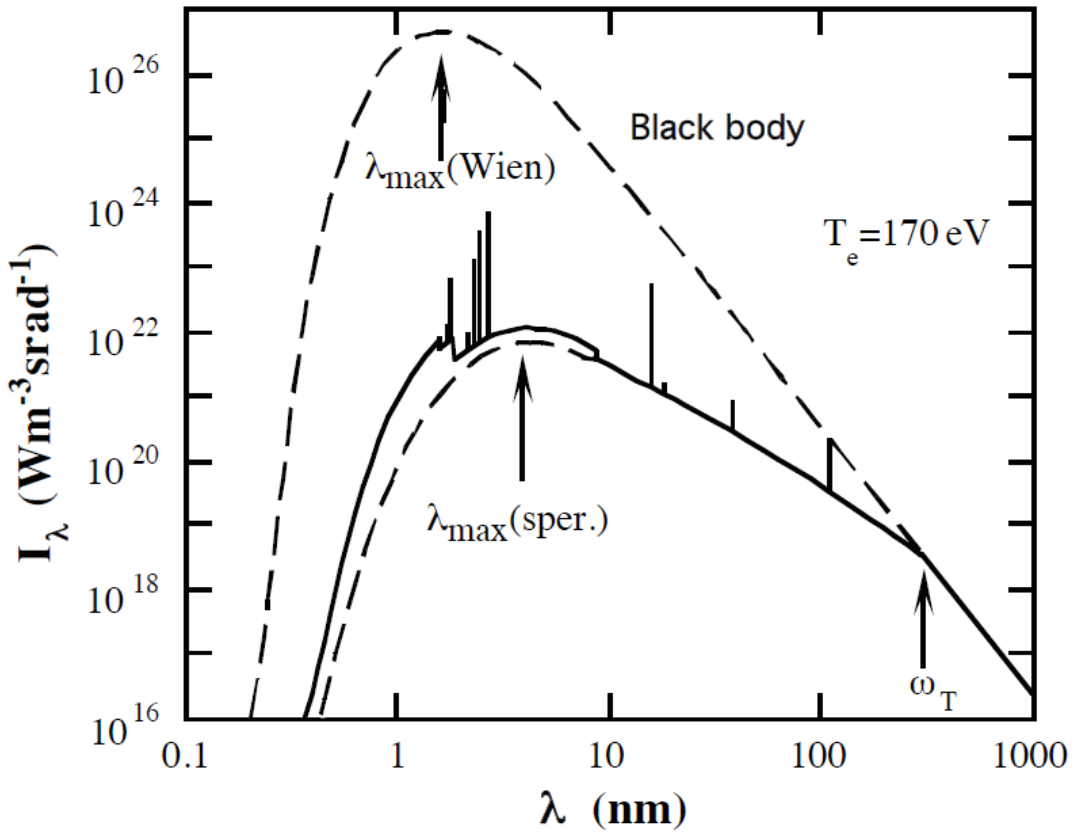


$$h\nu = \frac{1}{2} m_e v_e^2 + E_n^{Z_i}$$

$$\chi(h\nu - I_i^{(n)}) = \begin{cases} 0 & \text{per } h\nu < I_i^{(n)} \\ 1 & \text{per } h\nu \geq I_i^{(n)} \end{cases}$$

A photon is emitted when an ion with charge Z_i captures an electron. Initial states have a continuous distribution implying a continuum spectrum. However spectra are characterized by jumps corresponding to recombination edges





Plasma spectrum

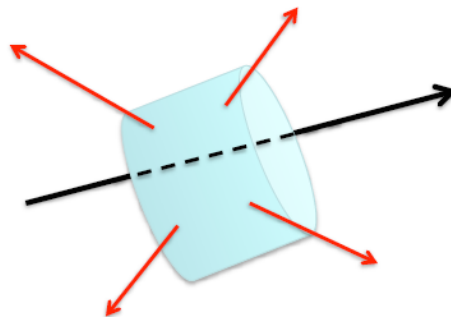
11.6 Radiative hydrodynamics

Hot matter emits radiation. But radiation is absorbed in matter heating it up → matter radiation coupling → radiative hydrodynamics.

From the radiation transfer equation

$$\frac{dI}{ds} = \alpha(\omega)[B_p(\omega) - I(\omega)]$$

the quantity on the right represents the difference between outgoing flux (generation of radiation) and incoming flux (absorption).



The transfer equation can be rewritten in terms of the energy density of radiation

$$\frac{du(\omega)}{dt} = c \alpha(\omega)[u_p(\omega) - u(\omega)]$$

We recall that for black body radiation $B_p(\omega) = \frac{u_p(\omega)c}{4\pi}$)
Then we can define the quantity

$$q = c \int_0^{\infty} \alpha(\omega)[u_p(\omega) - u(\omega)]d\omega$$

q represents the energy lost in a plasma unit volume = difference between emission and absorption.

If $q > 0$ the plasma radiates more energy than it absorbs (radiation cooling). If $q < 0$ the energy loss is negative and the plasma is heated by the excess of absorbed radiation

Divergence of radiation flux

We can also define the radiation flux \underline{S} coming out of a volume in all directions $\underline{\Omega}$

$$\vec{S} = \int I \vec{\Omega} d\vec{\Omega}$$

Applying the theorem of divergence it is possible to see that

$$q = \int_0^{\infty} \nabla \cdot S(\omega) d\omega = \nabla \cdot S$$

Where the divergence of the radiation flux S is:

$$\nabla \cdot S(\omega) = \alpha(\omega)[I_p(\omega) - I(\omega)] = c \alpha(\omega)[u_p(\omega) - u(\omega)]$$

$$\frac{du(\omega)}{dt} = c \alpha(\omega)[u_p(\omega) - u(\omega)]$$

It is analogous to the continuity equation for matter

$$\frac{\partial \rho}{\partial t} = -\nabla \cdot (\rho \vec{v}) \quad \vec{J} = \rho \vec{v}$$

$$\frac{\partial M}{\partial t} = -\int_V \nabla \cdot (\rho \vec{v}) dV = -\int_S \vec{J} \cdot dS$$

Continuity equation for radiation:

$$\frac{du(\omega)}{dt} = -\nabla \cdot S(\omega)$$

$$\nabla \cdot S(\omega) = c \alpha(\omega)[u_p(\omega) - u(\omega)]$$

Energy equation for a fluid (plasma) taking into account the contribution of radiation

$$\frac{\partial}{\partial t} \left(\rho \varepsilon + \frac{\rho u^2}{2} \right) = -\nabla \cdot \left[\rho u \left(\varepsilon + \frac{p}{\rho} + \frac{u^2}{2} \right) \right] - q$$

$$\frac{\partial}{\partial t} \left(\rho \varepsilon + \frac{\rho u^2}{2} \right) = -\nabla \cdot \left[\rho u \left(\varepsilon + \frac{p}{\rho} + \frac{u^2}{2} \right) + S \right]$$

ρ density, p pressure, ε internal energy per unit mass, u fluid velocity

Diffusion Approximation

We can express the flux $S(\omega)$ as a function of $u(\omega)$. From the transfer equation

$$\frac{dI}{ds} = \alpha(\omega) [B_p(\omega) - I(\omega)]$$

In 3D

$$\frac{dI}{ds} = \vec{\Omega} \cdot \nabla I$$

The transfer equation becomes

$$\begin{aligned} \vec{\Omega} \cdot \nabla I &= \alpha(\omega) [B_p(\omega) - I(\omega)] \\ &= c\alpha(\omega) [u_p(\omega) - u(\omega)] \end{aligned}$$

Integrating over all directions

$$\int \vec{\Omega} (\vec{\Omega} \cdot \nabla I) d\vec{\Omega} = \int \vec{\Omega} (c\alpha(\omega)[u_p(\omega) - u(\omega)]) d\vec{\Omega}$$

$$\int \vec{\Omega} u_p(\omega) d\vec{\Omega} = 0 \quad \text{since black body radiation is isotropic.}$$

Then the terms on right and on left respectively become

$$\int \vec{\Omega} (c\alpha(\omega)u(\omega)) d\vec{\Omega} = \alpha(\omega) \int \vec{\Omega} (I(\omega)) d\vec{\Omega} = \alpha(\omega) \vec{S}$$

$$\int \vec{\Omega} (\vec{\Omega} \cdot \nabla I) d\vec{\Omega} = \frac{c}{3} \nabla u(\omega) \quad \text{and finally}$$

$$\vec{S} = -\frac{cl(\omega)}{3} \nabla u(\omega)$$

The expression

$$S(\omega) = -\frac{l_\omega c}{3} \nabla u(\omega)$$

Where $l_\omega = s_o$ is the mean free path of the radiation of frequency ω , represents the “diffusion approximation” of radiation transport. $S(\omega)$ is expressed as a function of the gradient of $u(\omega)$.

Since the black body radiation is isotropic the net flux of this radiation is zero. We can also say that the gradient of $u_p(\omega)$ is zero. Maintaining isotropy requires uniformity of energy density. If this is not uniform the flux will not be zero.

Considering the density of photons $N(\omega)$ at frequency ω one gets

$$S(\omega) = -\frac{l_{\omega}c}{3} \nabla u(\omega)$$

$$u(\omega) = N(\omega)\hbar\omega \qquad S(\omega) = cN(\omega)\hbar\omega = J(\omega)\hbar\omega$$

$$J(\omega) = -D(\omega)\nabla N(\omega) \qquad D(\omega) = \frac{l_{\omega}c}{3}$$

The usual particle diffusion relation between the flux and the density.

In both cases the factor 1/3 comes from the integration over all directions (in 3D)

We can consider that $\nabla u(\omega) \approx \frac{u(\omega)}{x}$

where x is the typical distance over which the radiation density changes. Then

$$S(\omega) = -\frac{l_{\omega}}{x}cu(\omega)$$

In the case of optically thick plasmas, $l_{\omega} \ll x$ and the radiation flux is very small in comparison with $cu(\omega)$. The smaller is $l_{\omega} \ll x$, the smaller the flux and the more exact the diffusion approximation.

The case

$$S(\omega) = -cu(\omega)$$

corresponds to when the photons travels all in the same direction (maximum anisotropy)

In the case of optically thin plasmas, $l_\omega \gg x$ and one would get $S(\omega) > cu(\omega)$.

$$S(\omega) = -\frac{l_\omega}{x} cu(\omega)$$

This means that the diffusion approximation cannot be used with optically thin plasmas

Steady state radiation in an infinite medium of constant temperature would be in thermodynamic equilibrium. The intensity is independent on direction and determined by Planck formula. Photons arriving at any point in space are born in the vicinity of that point at typical distances comparable with the photon mean free path. Photons generated further away are absorbed.

Hence only the immediate vicinity of a point "participates" in establishing the equilibrium radiation. Even if the temperature at farther distance is different from the temperature of this region there is no practical effect at the considered point.

Therefore, in a sufficiently extended optically thick medium the intensity will be very close to the equilibrium value corresponding to the local temperature.

We can get the total radiation flux integrating over frequency ω

$$S = \int S(\omega) d\omega = -\frac{c}{3} \int l_\omega \nabla u(\omega) d\omega$$

In the case of weak anisotropy and slowly varying plasma parameters

$$\int u(\omega) d\omega \approx \int u_p(\omega) d\omega = u_p = \frac{4\sigma T^4}{c}$$

if l was independent on ω we would get

$$S = -\frac{cl}{3} \frac{16\sigma T^3}{c} \nabla T$$

In the general case we can still write $S = -\frac{cl}{3} \frac{16\sigma T^3}{c} \nabla T$

where l is the ‘‘Rosseland mean free path’’ and is averaged over frequencies as follows

$$\begin{aligned}
 l \nabla u_p &= \int l_\omega \nabla u_p(\omega) d\omega \\
 l &= \frac{\int l_\omega \nabla u_p(\omega) d\omega}{\nabla u_p} = \frac{\int l_\omega (du_p(\omega) / dT) d\omega}{du_p / dT} \\
 &= \frac{\int l_\omega (du_p(\omega) / dT) d\omega}{\int (du_p / dT) d\omega}
 \end{aligned}$$

Rosseland mean free path

l is given by $l = \int l_\omega G(u) du$

$$G(u) = \frac{15}{4\pi^4} \frac{u^4 e^{-u}}{(1 - e^{-u})^2} \quad u \equiv \frac{\hbar\omega}{kT}$$

Or, if we consider explicitly the absorption coefficient $\alpha(\omega)$

$$\begin{aligned}
 l &= \int \frac{1}{\alpha(\omega)} G'(u) du \\
 G'(u) &= \frac{15}{4\pi^4} \frac{u^4 e^{-u}}{(1 - e^{-u})^3}
 \end{aligned}$$

Radiation losses from a heated “thick” body

The total energy lost by the body per unit time is the integral over volume of the radiation losses q (variation of energy per unit time and unit volume)

$$Q = \int q \, dV = \int S_o \, dS$$

$$S_o \approx \sigma T_{br}^4 \approx \frac{lc}{x} u_p \approx \frac{l}{x} \sigma T^4$$

This can be used to define a “brightness temperature” T_{br} of the body which is close to the temperature of the surface layer

$$T_{br} \approx \left(\frac{l}{x} \right)^{1/4} T$$

Only if $l \approx x$ then $T_{br} \approx T$

Radiation losses from a heated “thin” body

For an optically thin body $l_\omega \gg x$ which brings to a physical absurd (a body cannot emit more than a blackbody at the same temperature)

In reality if $l_\omega \gg x$ is large almost all photons emerge from the surface and only a fraction $x/l_\omega \ll 1$ of photons are absorbed. The radiation density is x/l_ω of its equilibrium value (so much smaller than the equilibrium value)

Since the body is optically thin in first approximation we can write

$$\begin{aligned} J &= \int J(\omega) \, d\omega = \\ &= c \int \alpha(\omega) u_p(\omega) \, d\omega = c \int \frac{u_p(\omega)}{l_\omega} \, d\omega \end{aligned}$$

if l was independent on ω we would get

$$J = \frac{c}{l} \int u_p(\omega) d\omega = \frac{4\sigma T^4}{l}$$

In general, as in the case of thick plasmas, we can still write

$$J \approx \frac{4\sigma T^4}{l_1}$$

where we have introduced an ‘‘averaged’’ optical mean free path l_1 (Planck’s mean free path)

Planck mean free path

$$\frac{1}{l_1} \int u_p(\omega) d\omega = \int \alpha(\omega) u_p(\omega) d\omega$$

$$\alpha_1 = \frac{1}{l_1} = \frac{\int \alpha(\omega) u_p(\omega) d\omega}{\int u_p(\omega) d\omega} = \int \alpha(\omega) G_1(\omega) d\omega$$

$$G_1(\omega) = \frac{15}{\pi^4} \frac{u^3}{e^u - 1} \quad u = \frac{\hbar\omega}{kT}$$

Planck opacity applies to the case of optically thin bodies,
Rosseland opacity to the case of optically thick bodies

➤ **O1-Annex: Chapter 11 Supplementary educational material.**



HELLENIC
MEDITERRANEAN
UNIVERSITY



UNIVERSITÉ
BORDEAUX



UNIVERSITÀ
BOLOGNA



UNIVERSITY
of York



Queen's University
Belfast



Erasmus+

O1 – Experiments



HELLENIC
MEDITERRANEAN
UNIVERSITY



université
BORDEAUX



Erasmus+

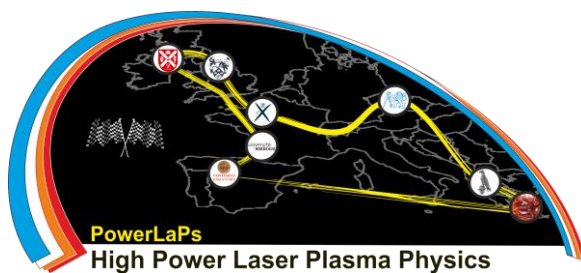
PowerLaPs

Innovative Education & Training in High Power Laser Plasmas

Plasma Physics - Theory and Experiments

EXP 1: FLYCHK

D. Batani, J. Trela

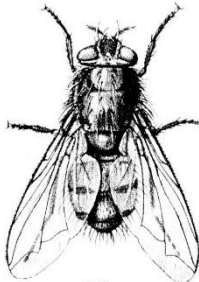


université
de BORDEAUX

1. The FLYCHK code

The How To

For



Fly

Developed by Richard W. Lee and co-workers (original version November 1995)

Los Alamos & NIST

Some notes by D. Batani & J. Trella

1

FLYCHK

FLYCHK is a kinetic code mainly used for X-ray spectroscopy.

It contains information on elements from **helium** to **gold** with detailed information, where appropriate, on the beryllium-like, lithium-like, helium-like and hydrogen-like ion stages.

The code requires the user to specify the **atomic number** and information on the **electron temperature and density** of interest. This information can be provided in a file that contains the time history of the plasma evolution or by specification of a grid of temperatures and densities.

With these inputs the code calculates:

- 1) in a steady-state approximation either non-LTE, or LTE, a set of populations for the ion stages and the detailed levels or
- 2) a time-dependent evolution of the populations.

Starting from this, the code calculates emission or absorption spectra. These are very accurate for K-shell spectra while for L-shell spectra the description is only approximate.

2

Steady-state solution can be in LTE (Local-Thermal Equilibrium) giving Saha's distribution

$$\left(\frac{n_i}{n_{i+1}}\right)^s = 1.66 \times 10^{-22} N_e \frac{g_i}{g_{i+1}} \frac{e^{-U}}{T^{3/2}}$$

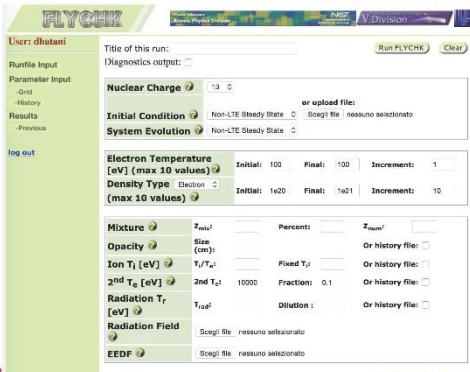
(here $U = I_p/T_e$, T_e is in eV and N_e in cm^{-3}), or in non-LTE but stationary conditions (i.e. for instance coronal equilibrium).

Otherwise time-evolution can be obtained by specifying time-dependent parameters in a « history » file (this can also be the results of a hydrodynamic simulations)

time	ne	te
0.0e-12	1.0e+21	01.00
1.0e-12	1.0e+21	10.00
2.0e-12	1.0e+21	50.00
3.0e-12	1.0e+21	50.00
4.0e-12	1.0e+21	50.00
5.0e-12	1.0e+21	50.00
6.0e-12	1.0e+21	50.00
7.0e-12	1.0e+21	50.00
8.0e-12	1.0e+21	50.00
9.0e-12	1.0e+21	50.00
1.0e-11	1.0e+21	50.00
1.1e-11	1.0e+21	50.00
1.2e-11	1.0e+21	50.00
1.3e-11	1.0e+21	50.00

3

Flychk GRID



4

How to "install" FLYCHK

FLYCHK is a full online simulation tool for atomic population and emission/absorption spectra calculation. Therefore, it does not require a real installation but since it use Java applets, which are considered out-dated, it make it not compatible with most of the web browser. Here are some steps to do to be able to run FLYCHK simulations (for windows 10)

- Install Internet Explorer 11 (it is the only browser supporting Java).
- Install Java
 - Go to <https://java.com/en/download>
 - Click on Free Java Download
 - Agree and Start Free Download
 - Execute and install java
- Configure Java
 - Open Java configuration on the computer
 - Go to security and modify the Exception site list
 - Add <http://nlte.nist.gov> to the exception.

Note that if Java is not supported on recent web browser, it is due to the potential security flaws and it is not advice to use IE11 with Java for regular browsing.

5

How to run FLYCHK /1

There is multiple way to run FLYCHK, depending on the complexity of the problem.

Webpage – History Grid

FLYCHK allows to specify everything directly on the interactive webpage. While it can be very convenient, the inputs must be re-enter at every simulation. And there is no log of the input off line.

In grid mode, only steady state calculation can be done (LTE or non-LTE). The essential parameters to set are the material (z) and the grid point in density (electron, ion or mass) and temperature.

Webpage – History File

In the history webpage, the grid is no longer specified directly but it must be given with a file. This file contains time step (which for steady state calculation are ignored but allows to separate the different simulations).

There is also the possibility to run time dependent simulations. In this case the time depends of what have been specified in the history file is use (if it not specified otherwise on the webpage).

6

How to run FLYCHK / 2

There are multiple ways to run FLYCHK, depending on the complexity of the problem.

Runfile – History Grid
It is also possible to write the key word + value in a file and to upload it directly to FLYCHK. This allows to run the same simulation or slightly different simulation more easily.
Using the grid option for the history keyword, I could not make FLYCHK work...

Runfile – History File
In the case where the keyword history is used with the option file, both files (the file with all keyword + the history file) must be in a .zip archive. Here are the steps for working in this way:
Write keyword and their value in a file named "runfile"
Write the temperature and density in a file named as in the runfile (at keyword history)
Compress both file in .zip (not .rar or other)
From the FLYCHK webpage, upload the archive (the name of archive does not matter).

7

Some topics contained in FLYCHK which will not be described during the theoretical course on Friday...

- Hot electrons
- K-α generation
- Opacity effects
- Line profiles
- Satellite lines
- Continuum Lowering

8

Hot electron propagating in a multilayer target

When an intense laser source interacts with a plasma, non-linear process such as Stimulated Raman Scattering can occur. This process can lead to the production of supra thermal electrons (called Hot Electrons). This HE can travel deep in the solid target and heat it. The understanding of the HE population (temperature, total number) is very important and still not very well known.

A typical set up for the characterization of HE consists of a two-layer target:

- A low Z material in the front for the interaction with the laser (Carbon graphite for example)
- A high Z material in the back for the characterization of the HE (Copper)

Bremsstrahlung radiation
Bremsstrahlung radiation is produced by "collision" of the electrons with ions (Free-Free transition). The spectrum is characterized by the distribution:

$$I_{B\gamma}(T, \nu) = I_0 \exp(-h\nu / kT_e)$$

For a given temperature T and in logarithmic scale, the bremsstrahlung spectrum is a straight line with a slope characteristic of T.

9

K-shell ionization and K-α emission

The Kα emission from the target tracks the fast electron beam transport

A fast electron ionizes the inner shell of an atom in the propagation medium

The atom in the subsequent recombination process emits a photon called Kα photon, the emission is completely isotropic

Is therefore possible, by studying x-ray emission, to get information on the fast electrons propagating into the target

10

Spectrum from an Al-Cu target

X-ray spectrum recorded with a conical crystal spectrometer on the rear side of the target (Al (11 μm)-Cu-Al) at 45° to the equatorial plan. The spectrometer records the Al-Cu lines from 8.4 Å to 7.2 Å on a DEF film. On a typical spectrum, we observe the Cu-Kα doublet (7.7 - 7.72 Å, 5th order) and the Al-Kα lines (8.269 - 8.3396 Å, 1st order).

E. Martinoli, D. Batani, et al. "Fast Electron Transport and Heating of Solid Targets in High Intensity Laser Interaction Measured by Ka Fluorescence" *Physical Review E*, 73, 046402 (2006)

11

Shift of K-α emission vs. ionization degree (i.e. background temperature)

Target heating induces a blue shift of the Kα line (See for example : Akl et al. Phys. Plasmas 14, 023102 2007)

P. Palmeri, G. Boutoux, D. Batani, and P. Quinet «Effects of target heating on experiments using Kα and Kβ diagnostics» *PHYSICAL REVIEW E* 00, 003100 (2015)

12

Influence of fast electrons on spectra

The presence of fast electrons constitutes an additional way of "over-populating" the upper levels by collisional effects. Therefore they can change the spectra sensibly

Cl spectrum from chlorinated plastics (C₉H₇Cl)

13

Line broadening and line shapes

Doppler broadening: Gaussian profile

$$I(\lambda) = \left(\frac{\ln 2}{\pi}\right)^{1/2} \frac{I_0}{\Delta\lambda} \exp\left[-(\ln 2) \frac{(\lambda - \lambda_0)^2}{(\Delta\lambda)^2}\right]$$

$$\frac{\Delta\lambda}{\lambda_0} = \frac{\Delta v}{v_0} = 3.86 \times 10^{-5} \sqrt{\frac{T_i(eV)}{M}}$$

Stark broadening (pressure broadening, collisional broadening): Lorentz profile

$$I(\lambda) = \frac{I_0}{\pi\Delta\lambda} \frac{1}{1 + (\lambda - \lambda_0)^2 / (\Delta\lambda)^2}$$

$$\Delta\lambda(nm) = \lambda_0 \Delta v / v_0 = 0.04 n_{14}^{2/3} [n_{14} = n_e(cm^{-3}) / 10^{14}]$$

14

Line broadening and line shapes

Convolution of Doppler and Stark broadening: Voigt profile

$$I(\nu) = \int I_1(\nu - \nu') I_2(\nu') d\nu'$$

$$\Delta\nu^2 = \Delta\nu_1^2 + \Delta\nu_2^2 \quad (\text{both gaussian})$$

$$\Delta\nu = \Delta\nu_1 + \Delta\nu_2 \quad (\text{both lorentzian})$$

$$\Delta\nu \approx 0.5346\Delta\nu_L + \sqrt{0.2166\Delta\nu_L^2 + \Delta\nu_G^2} \quad (\text{gaussian + lorentzian})$$

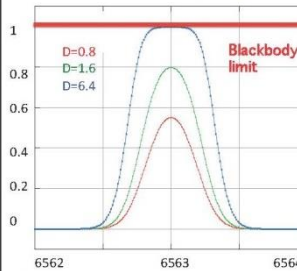
15

Line broadening and line shapes

Opacity broadening

Optically thick lines (absorption)

Need to consider the opacity (α) and the plasma extension (L)



$$I(s_2, \omega) \approx I(s_0, \omega) e^{-D_2} + (j(\omega) / \alpha(\omega)) [1 - e^{-D_2}]$$

$$D(s) = \int_{s_0}^s \alpha(\omega) ds = \alpha(\omega)L$$

Lines can be optically thick at the centre and optically thin at the edges.
Strong lines can be thick as faint ones remain thin

16

Opacity effects /1

When the plasma medium has a finite size the emitted radiation may eventually escape the medium. For spatially uniform plasma of geometrical path length l one must consider the radiation mean free path before absorption and re-emission, $1/\kappa$, where κ is the opacity, and the optical depth is $\tau = \kappa l$, which represents the number of mean free paths.

When radiation has $\tau > 1$ the plasma is called optically thick with the result that the rates of the radiative processes are effectively reduced compared to cases where $\tau \ll 1$, i.e., the optically thin case. FLYCHK treats the effect of finite optical depth using an escape probability formalism where the radiative rates are reduced by an escape probability as a function of optical depth.

$$R_{ij} \equiv n_i (A_{ij} + B_{ij} \bar{J}_{ij}) - n_j B_{ji} \bar{J}_{ij} \equiv n_i A_{ij} \Lambda$$

where

$$\frac{\pi e^2}{mc} f_{ij} = B_{ij} \frac{h\nu_{ij}}{4\pi} \quad \text{and} \quad \bar{J}_{ij} = \int J(\nu) \phi(\nu) d\nu,$$

17

Opacity effects /2

Λ has values that range from zero, when the optical depth is high and the line transition saturates at the local blackbody limit, to unity, when there is no radiation field, i.e., $J_{ij} = 0$. The escape factor depends on the line profile, $\phi(\nu)$, and the optical path length of the plasma. In Flychk, the optical path length is determined by a user specified plasma size, L , and the Doppler line profile

$$\tau_\nu = n_i \frac{\pi e^2}{mc} f_{ij} L \phi(\nu)$$

$$\phi(\nu) = \frac{e^{-(\Delta\nu/\nu_D)^2}}{\sqrt{\pi} \nu_D} \quad (1/\text{Hz}) : \quad \nu_D = 4.63 \times 10^{-5} \nu_{ij} \sqrt{\frac{T_e}{\mu}} \quad (\text{Hz})$$

Finally the escape factor is given by

$$\Lambda = \frac{1}{\tau_0 \sqrt{\pi \ln(\tau_0)}} \quad \text{for } \tau_0 \geq 2.5$$

$$\Lambda = e^{-\tau_0^{1.73}} \quad \text{for } \tau_0 \leq 2.5$$

18

IONIZATION POTENTIAL DEPRESSION

In addition to the ionization and excitation processes, plasma electric fields can effectively reduce the ionization potential of an ion and hence affect the charge state distributions of a plasma. Such "Continuum Lowering" has two limits for low densities (Stewart & Pyatt)

$$\Delta E = \frac{Ze^2}{\lambda_D} \quad \lambda_D(\text{cm}) = 743 \sqrt{\frac{T_e(\text{eV})}{n_i(\text{cm}^{-3})(1+Z^*)}}$$

and for high densities (More)

$$E = \frac{Ze^2}{r_i} \quad r_i(\text{cm}) = \left(0.75 \frac{Z^*}{n_e}\right)^{1/3}$$

21

2. FLYCHK exercises

1) Emission from Al plasma in LTE

Consider a plasma made from Al ($Z=13$) at the electron density $n_e = 10^{19}$, 10^{21} and 10^{22} cm^{-3} and $T_e = 0.5, 1$ and 1.5 keV .

- ❖ Study the mean ionization Z^* as a function of temperature and density. Justify the dependence on density.
- ❖ Study the free-free radiation losses and compare with the formula for bremsstrahlung radiative emission. From NRL (n_e, N_i in cm^{-3} and T_e in eV)

$$P_{ff} (\text{W} / \text{cm}^3) = 1.5 \times 10^{-32} n_e T_e^{1/2} \sum_i N_i Z_i^2$$

- ❖ Choose one value of n_e and T_e and consider the emission spectrum. Compare the slope of the continuum spectrum to the temperature.

Identify the hydrogen-like spectrum and compare to Bohr's formula

$$h\nu = I_{Al} \left(1 - \frac{1}{n^2} \right)$$

where I_{Al} is the ionization potential of hydrogen-like aluminum. Identify the lines as H- α , H- β , H- γ , ... (corresponding respectively $n=2, 3, 4, \dots$) and the ionization threshold H_∞ .

2) LTE vs. non-LTE steady state

From the previous exercise, consider the case $n_e = 10^{19} \text{ cm}^{-3}$ and $T_e = 0.5 \text{ keV}$. Plot the distribution of ionic states in LTE and non-LTE steady state.

Compare the ratio of the density of hydrogenoid to heliumoid ions to what can be obtained from Saha's formula and comment.

3) Hot electron propagating in a multilayer target

Consider Al at density $n_e = 10^{21} \text{ cm}^{-3}$ and $n_e = 10^{23} \text{ cm}^{-3}$ (respectively representing the critical density for $1 \mu\text{m}$ laser and a near-solid density state). Initially, consider the following history file:

```
time ne te
0.0e-12 1.0e+21 01.00
1.0e-12 1.0e+21 10.00
2.0e-12 1.0e+21 50.00
3.0e-12 1.0e+21 50.00
4.0e-12 1.0e+21 50.00
5.0e-12 1.0e+21 50.00
6.0e-12 1.0e+21 50.00
7.0e-12 1.0e+21 50.00
8.0e-12 1.0e+21 50.00
9.0e-12 1.0e+21 50.00
1.0e-11 1.0e+21 50.00
1.1e-11 1.0e+21 50.00
1.2e-11 1.0e+21 50.00
1.3e-11 1.0e+21 50.00
```

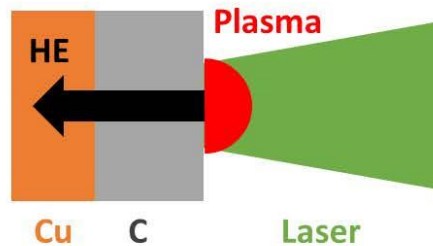
study the evolution of the ionization degree vs. time in the two cases and comment. What happens at different temperatures or different densities?

4) Hot electron propagating in a multilayer target

When an intense laser source interacts with plasma, non-linear process such as Stimulated Raman Scattering can occur. This process can lead to the production of supra thermal electrons (called Hot Electrons). This HE can travel deep in the solid target and heat it.

A typical set up for the characterization of HE consists of a two-layer target:

- A low Z material in the front for the interaction with the laser (Carbon graphite for example)
- A high Z material in the back for the characterization of the HE (Copper)



4.1 = Bremsstrahlung radiation from C

Bremsstrahlung radiation is produced by "collision" of the electrons with ions (Free-Free transition). The spectrum is characterized by the distribution:

$$I_{Br}(T, \nu) \propto \sqrt{T} e^{-\frac{h\nu}{kT}}$$

For a given temperature T and in logarithmic scale, the bremsstrahlung spectrum is a straight line with a slope characteristic of T.

Plasma without HE

Plasma conditions: $n_e = 10^{20} \text{ cm}^{-3}$, $T = 1 \text{ keV}$. Verify the plasma temperature from the spectrum slope.

Plasma with HE

Same plasma condition. HE parameters: $T_h = 40 \text{ keV}$, $\eta_h = 5\%$. Show the emissivity between 1 and 10 keV. Verify the plasma temperatures from the spectrum curve.

Solid C with HE

Solid C conditions: $\rho = 2 \text{ g/cm}^3$, $T = 1 \text{ eV}$. Same HE parameters as Plasma with HE

Show the emissivity between 1 and 10 keV and compare to the previous ones. Comment on the slope and absolute emission.

4.2 = K_α emission of Cu

HE are so energetic that they can knock off an electron from the inner shell (k-shell) of the copper atoms. The ions created this way are not in their fundamental state and they will relax by a chain of bound-bound transition. The most energetic of these bound-bound transition is the one from $2p \rightarrow 1s$ (to check) and is called the K_α line. For copper this line is around 8.2 keV.

Cold K_α

Copper parameters: $\rho = 9 \text{ g/cm}^3$, $T = 1 \text{ eV}$. Same HE parameters as before.

Show the ion distribution and the spectrum around the K_α line of Copper. What is the shape of the line and why? (gaussian, lorentzian, voigt?)

Hot K_α (Steady State)

The copper, with its high density has a good stopping power of the HE and might get warm due to their energy deposition.

Make a history file with constant density of 9 g/cm^3 and a temperature that range from 1eV to 500 eV. Keep the same HE parameters.

Show the spectra obtained and the ion distribution (evolution of mean ion charge?).

How does the K_α line evolve with the temperature and why?



HELLENIC
MEDITERRANEAN
UNIVERSITY



universit 
BORDEAUX



Erasmus+

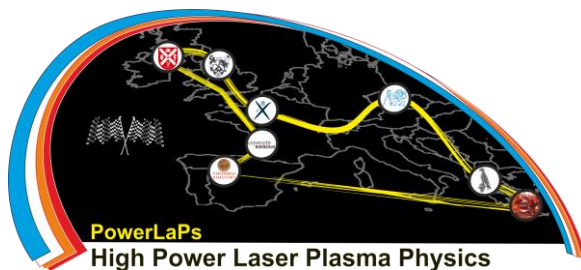
PowerLaPs

Innovative Education & Training in High Power Laser Plasmas

Plasma Physics - Theory and Experiments

EXP 2: Plasma Focus

A. Skoulakis, G. Andrianaki, G. Tazes



Erasmus+

HELLENIC
MEDITERRANEAN
UNIVERSITY



1. Laboratory project aim

The laboratory project aims to make the student familiar with basic experimental and diagnostic techniques used in magnetic compression plasma physics research. The student will learn about techniques for generation of high temperature Z-pinch plasmas and be able to understand the physics underlying the common plasma diagnostics methods. Experimental techniques for generation of Z-pinch plasmas will be exemplified by studying the systems at the “miniature dense plasma focus” magnetically compressed non cylindrical pinch device at CPPL. In addition, the student will gain practical experience of using some diagnostics that are available at CPPL and analyzing real measurement data. Physics concepts underlying the plasma diagnostic methods will be introduced during experimental procedure, using a systematic approach from first principles. A number of plasma diagnostic applications will be introduced in more detail.

After passing the experimental procedure, the student should be able to

- explain the principles and experimental techniques for generation of high temperature Z-pinch type plasmas,
- explain the underlying physics principles and technical features of some commonly used basic plasma diagnostic applications,
- demonstrate the practical usage of some selected plasma diagnostics that are available at CPPL,
- write simple computer codes for acquiring, analyzing and plotting data from some selected plasma diagnostics using a commercial software packages that is commonly used in plasma research,
- perform common data analysis tasks, such as curve fitting, numerical computation and signal filtering using available software routines,
- Present analyzed data in graphic form in short reports, that includes written material that describes the diagnostic setup and the data analysis methods used.

2. Theoretical background

A Dense Plasma Focus (DPF) or Plasma Focus (PF) device is a coaxial-pulsed plasma accelerator that produces very high density and high temperature plasma that lasts for a very short duration. This discharge-based device is not only a source of high density and high temperature plasma but also a rich source of energetic radiations like intense x-rays, EUV, visible light, and energetic particles like neutrons, electrons and also ions depending upon the working condition. In addition, this device exhibits various interesting plasma phenomena such as macro- and micro-instabilities, turbulences etc [1].

There are two types of PF discovered the same year by Mather (USA) [2] and Fillipov (USSR) [3]. For our experiment we are going to use a Mather type Miniature DPF, which was constructed by our group. MPF delivers smaller amounts of energy but is portable and can achieve high repetition rates.

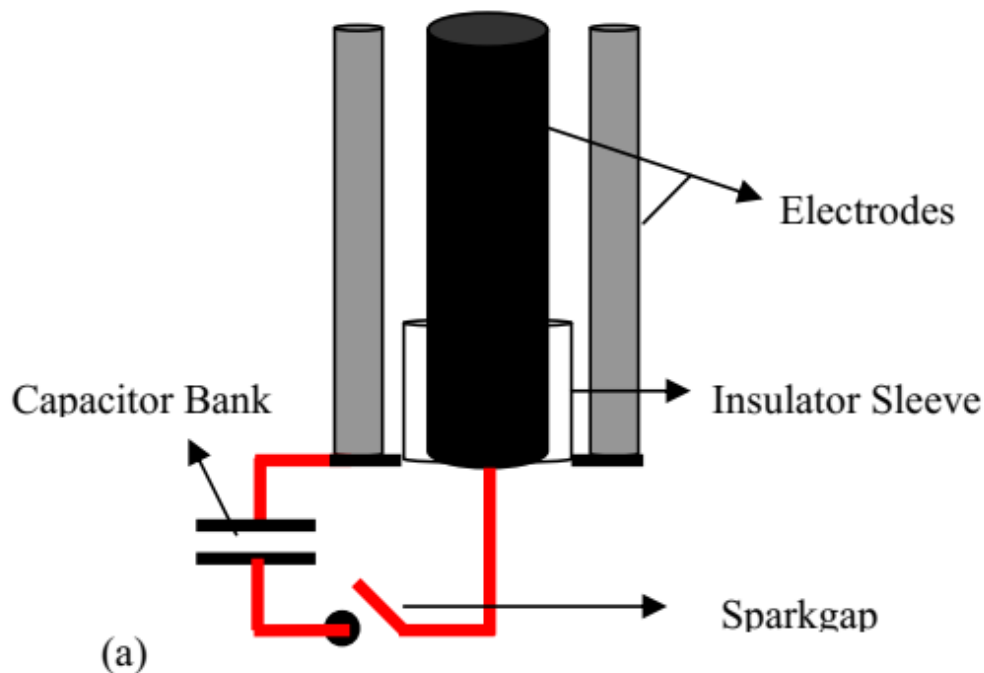


Figure 1: Mather type DPF [1]

3. Operation Principle

A Plasma focus device consists of a fuel chamber which contains two cylindrical coaxial electrodes, separated by an insulator sleeve which covers a part of the inner electrode, as seen in Figure 1. The electrodes are closed in one end, usually the inner one is the anode and the outer is grounded. The chamber is filled with a gas (the gas selection depends on the

application being studied) in the appropriate pressure range. A capacitor bank switched by a spark-gap provides the power and the area between the electrodes acts as an accelerator of the plasma created. So, when a high voltage pulse is applied between the electrodes the dielectric break down of the gas across the insulator takes place and an asymmetric current sheath forms around the insulator. This current sheath moves towards the open end of electrode assembly by $J \times B$ force. During this movement, the current sheath sweeps the gas above it and ultimately compresses the gas at the top of the anode producing hot and dense plasma.

The dynamic processes taking place during the operation of PF device can be classified into three distinct phases, a) breakdown or inverse pinch phase, b) axial acceleration phase and c) radial collapse phase. As seen in Figure 2, the phases can be distinguished in time and space, as they take place successively.

Phases of DPF

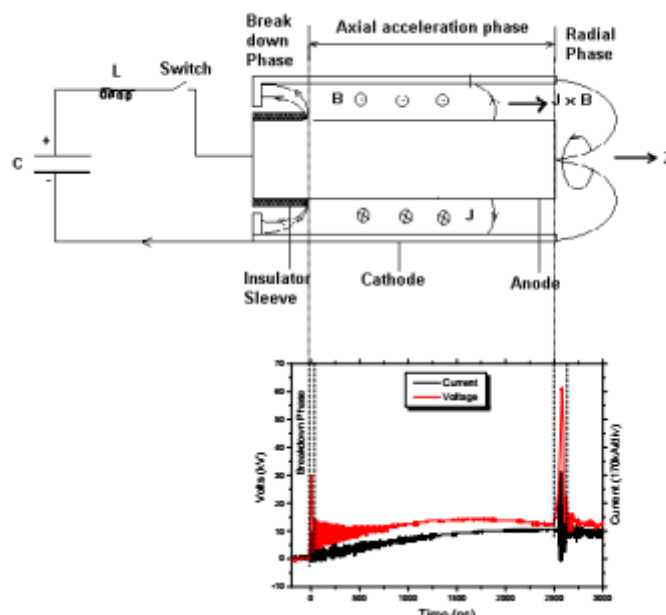


Figure 2: DPF Phases [1]

a) Breakdown or inverse pinch phase: When a high voltage is applied, it is found that the initial breakdown along the insulator surface occurs after the time delay of few nanoseconds [4]. When a high voltage pulse is applied between the electrodes, a high electric field is developed across the insulator. This field accelerates the primary free electrons, initially



present in the working gas, towards the surface of the insulator. Consequently, emission of secondary electrons takes place through collisions, which ionizes a thin gas layer near the insulator surface [5]. A sliding discharge then appears along the insulator surface. When the sliding discharge reaches the closed (bottom) end of the insulator, it generates initial current filaments (plasma configuration) through which the discharge current flows. Due to the interaction of this current with itself induced magnetic field, the current filaments drag away radially from the insulator surface in an inverse pinch manner. When the current filament reaches the inner surface of the outer electrode, its conductance increases substantially and it forms a uniform current sheath. This is the end of the break down phase and the current sheath enters into the axial acceleration phase [1].

b) Axial acceleration phase: Once the current sheath is formed across the insulator sleeve between the anode and the cathode, it starts to accelerate towards the open end of the electrodes along the Z -axis by its own $J \times B$ force. The axial acceleration phase ends when the current sheath reaches the open end of the electrodes and enters in the next phase i.e. the radial collapse phase. The duration of the axial phase is important for the subsequent formation of the hot and dense plasma at the radial compression phase [1].

c) Radial Phase: The radial phase starts when the current sheath reaches at the open end of the central electrode the $J \times B$ force drags the current sheath radially inward. This inward radial force compresses the snowplowed plasma carried by the current sheath on the top of the central electrode. The shape of the current sheath changes to fountain like hollow cylindrical column. This fountain like column is squeezed inwards with azimuthal symmetry. The compressed plasma is further squeezed adiabatically to form a very high density and high temperature plasma column [1].

Based on experimental observations radial phase can be divided in four distinct sub-phases:

- Compression Phase: Plasma under the affect of the magnetic field is compressed.
- Quiescent Phase: After the stagnation, this phase indicates the beginning of the expansion of the plasma column in the axial as well as in the radial direction.
- Unstable Phase: Instabilities like sausage ($m=0$) and king ($m=1$) develop in the plasma.
- Decay Phase: A very large, hot and thin plasma cloud is formed due to the complete breaking of the plasma column [6].

Taking into account a standard geometry of a PF device, the operation of a PF can be controlled by changing the initial voltage applied to the electrodes and the pressure of the gas in the chamber.

4. The miniature plasma focus device

Design and Construction

To design a MPF device [8], one usually starts by determining the energy stored in the capacitor bank that will eventually be transferred to the fuel inside the chamber. Our capacitor bank consists of ten identical capacitors ($C = 200 \text{ nF}$, $V = 30 \text{ kV}$, $L = 15 \text{ nH}$) yielding a total capacitance of $2.0 \text{ }\mu\text{F}$. Depending on their charging voltage, the capacitor bank may provide electrostatic energy ranging from 200 to 400 J. The electric circuit diagram of the assembly is depicted in Figure 3. A high voltage power supply charges the capacitors up to the desired voltage. To trigger the discharge, we use an in-house designed trigger unit that produces a 2.5 kV , $1 \text{ }\mu\text{s}$ impulse that is then transmitted to the pseudo spark switch (PSS) via a pulse shaping circuit [9]. The load of the capacitors is finally carried to the fuel through 4 planar lines in order to reduce the total resistance. The PSS unit is a TDI1-150k/25 type (copper arc thyatron) capable of producing currents well above a hundred kA. Moreover, it has a lifetime of 10^9 shots (for $E \sim 100 \text{ J}$), and therefore, it can operate continuously at a few Hertz for several weeks without undergoing repairs. Yet another advantage of the TDI1-150k/25 type PSS is its reliability of firing practically in 100% of cases with a jitter time less than 4 ns.

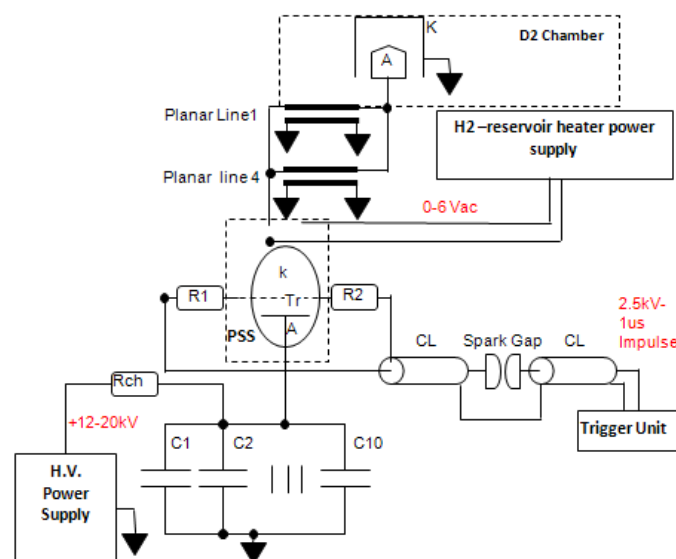


Figure 3: The electric circuit

The assembly is capable of operating at a few Hz without cooling and producing a peak discharge current of $\sim 45\text{--}65$ kA (measured by a Rogowski coil) with a quarter cycle of ~ 260 ns. A key aspect for constructing a fast PF is to keep inductance as low as possible. For small devices, this strongly depends on the connections, and therefore, components must be connected in compact configuration. The external inductance of the assembly, including all electric components and the chamber, is slightly less than 50 nH.

The MPF fuel chamber (see figure 4), consists of a coaxial electrode assembly - a tapered inner electrode that acts as an anode and made of copper of a length 21.6 cm with a 9.5 mm diameter at the closed end and 6.5 mm diameter at the tip, and a solid impermeable cylindrical outer electrode of stainless steel, having inner diameter of 48 mm that acts both as a cathode and the chamber wall. A tapered inner electrode is preferred to have a hole of 3 mm diameter over a solid cylinder because in the latter case the material erosion takes place from the tip due to bombardment of electron beam which contaminates the plasma column. An insulator sleeve of Pyrex glass, with a break down length of 14.6 mm is placed between the anode and the cathode.

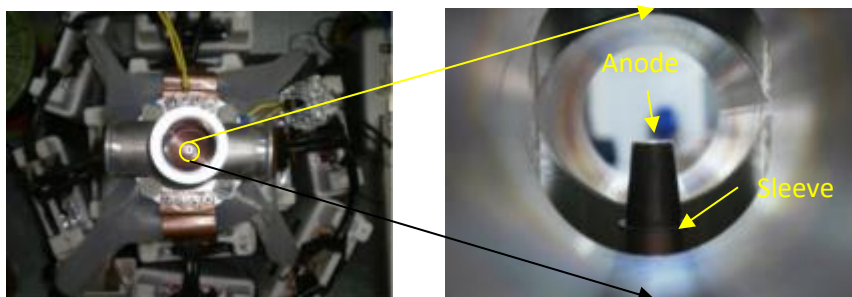


Figure 4: MPF fuel chamber

Current Monitor (Rogowski groove)

In order to verify the generator was performing properly current monitor were used. The monitor consisted of a Rogowski coil (Rogowski groove type) to capture a portion of the current signal within the fuel chamber.

The Rogowski groove placed around a return current wire close to the fuel chamber (fig. 5(a)) and is made up of an annular conductive ring placed around a current conductor (fig. 5(b)). In our case, the registered voltage is solely dependent on dI/dt (the current probe operates in I-dot mode).

Therefore, the registered voltage is:

$$V_{groove} = -L \frac{dI}{dt} \quad (13)$$

Where L is the self-inductance of the rogowski groove.

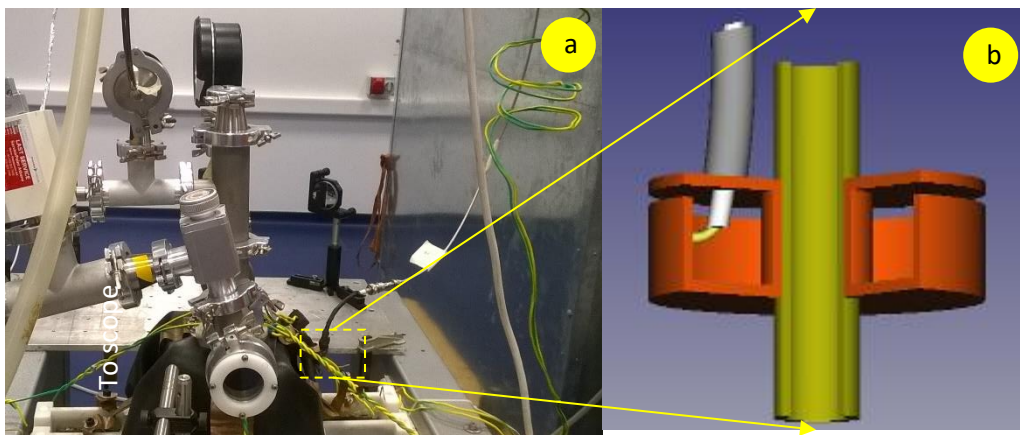


Figure 5: Load Current Monitor (Rogowski groove)

Optical Probing

In order to gain information concerning the refractive index (η) and hence the electron density of a plasma (n_e), an Nd-YAG (Neodymium-doped Yttrium Aluminum Garnet) laser was used to backlight the experiment. Light can only pass through a plasma if the frequency of the plasma ω_p is lower than that of the probe beam ω_{light} . The maximum density which can be probed, known as the critical density n_c , in a compact form is:

$$n_c = 10^{21} \lambda \text{ cm}^{-3} \quad (1)$$

Where λ is in microns.

The refractive index of the plasma is given by:

$$\eta = \sqrt{1 - \frac{n_e}{n_c}} \cong 1 - \frac{n_e}{2n_c} \quad (2)$$

The Nd-YAG laser emits light in the near infra-red ($\lambda=1064$ nm) which then traverses a KDP harmonic generating crystal. This doubles the frequency of the light resulting in a λ of 532nm (green). Substituting this wavelength into equation (1) yields a critical density $n_c=4 \times 10^{21}$ electrons per cubic centimeter.

Interferometry

Interferometry is a very useful technique in order to gain quantitative information regarding the electron density of the plasma. A common interferometric set up is the Mach-Zehnder interferometer. The working principle can be seen in figure 4. The beam splits into two identical collimated beams each one traveling through a different path. The first one will propagate undisturbed, thus stand as reference, while the other will pass through the region of interest experiencing a phase shift relative to the reference beam. The two beams will recombine at the end of their path on a detector. Their interference will result into a pattern of bright and dark fringes.

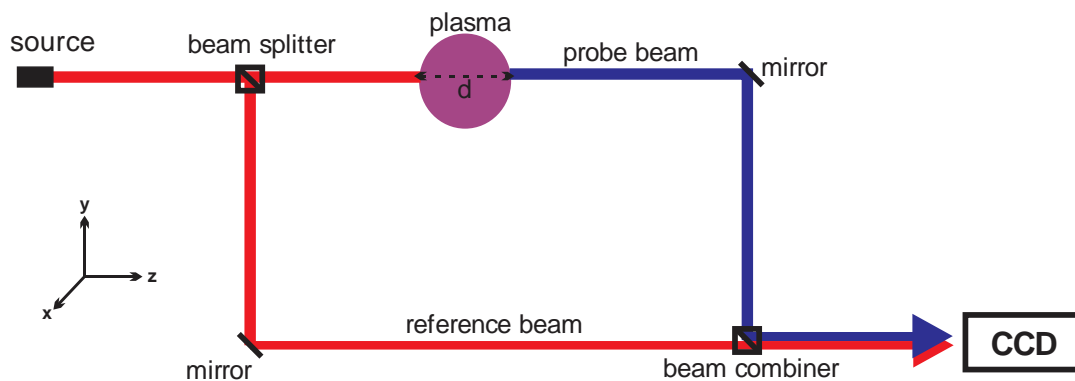


Figure 6: Images showing the propagation of light rays through a shadowgraphy system. Light is focused by a lens and after crossing through the focal point propagates to the image plane.

The refractive index of the plasma will result to a phase shift $\Delta\phi$ of the probe beam. This will lead to a shift of the interference fringes.

$$\Delta\Phi = \Phi_{probe} - \Phi_{ref} = \int_0^{d(x,y)} k_{plasma} dz - \int_0^{d(x,y)} k_0 dz \quad (3)$$

Where $d(x,y)$ is the physical path of propagation inside the plasma as shown in figure 4 $k_0=2\pi/\lambda_0$ is the wavenumber of the laser propagating in air and k_{plasma} while it propagates in plasma.

$$k_{plasma} = \frac{2\pi}{\lambda_{plasma}}, \lambda_{plasma} = \frac{\lambda_0}{\eta}$$

$$\Rightarrow k_{plasma} = \frac{2\pi}{\lambda_0} n \quad (4)$$

Substituting k_0 and k_{plasma} in equation 3

$$\Delta\Phi = \frac{2\pi}{\lambda_0} \int_0^{d(x,y)} \eta dz - \int_0^{d(x,y)} 1 dz = \frac{2\pi}{\lambda_0} \int_0^{d(x,y)} \eta - 1 dz \quad (5)$$

Where η is $n(x,y,z)$. This fringe shift corresponds to the line integral of the refractive index taken along the path through the plasma $\int n_e dl$. One can obtain the formula that connects phase shift to the index of refraction substituting 2 to 5

$$\Delta\Phi = \frac{2\pi}{\lambda_0} \int_0^{d(x,y)} 1 - \frac{n_e}{2n_c} - 1 dz = -\frac{\pi}{\lambda_0 n_c} \int_0^{d(x,y)} n_e dz \quad (6)$$

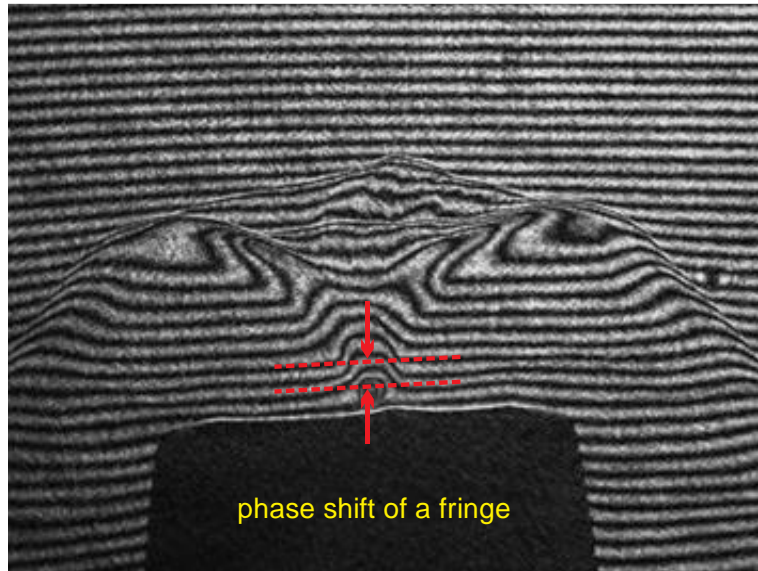


Figure 7: Interferogram of plasma from a plasma focus device taken with a Mach-Zehnder interferometer.

Another useful expression of the equation 6 is as a function of k_0 and ω_0 :

$$\Delta\Phi = -\frac{k_0}{2n_c} \int_0^{d(x,y)} n_e dz = -\frac{\omega_0}{2cn_c} \int_0^{d(x,y)} n_e dz \quad (7)$$

Abel Inversion

Interferometry measures the average value of some quantity along a path through the plasma such as plasma electron density. To deduce local values of this quantity from the available chordal measurements one can use the mathematical properties of the Abel Transformation. This stands only for cylindrically symmetric plasmas, that is, they are independent of θ and z in a cylindrical coordinate system (r, θ, z) . Considering any cylindrically symmetric quantity $f(r)$ like electron plasma density n_e it relates to the phase shift induced to a probe beam $F(y)$ traveling along an optical path:

$$F(y) = \int_{-\sqrt{a^2-y^2}}^{+\sqrt{a^2-y^2}} f(r) dx \quad (8)$$

By changing the x integral into an r integral

$$F(y) = 2 \int_y^a f(r) \frac{r}{\sqrt{r^2-y^2}} dx \quad (9)$$

The inverse transform relates the quantity $f(r)$ to an integral of F , as follows:

$$f(r) = -\frac{1}{\pi} \int_r^a \frac{F(y)}{dy} \frac{dy}{\sqrt{y^2-r^2}} \quad (10)$$

With this formula one can obtain the radial profile of $f(r)$ from measurements of chord integrals $F(y)$. This process is called Abel Inversion.

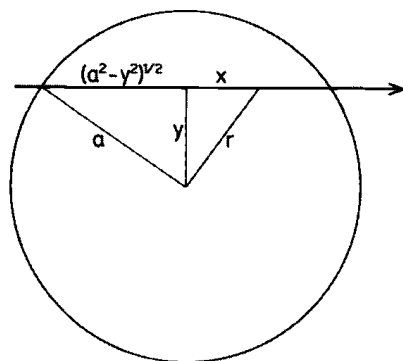


Figure 8: Chordal measurements in a cylinder.

5. Experimental procedure

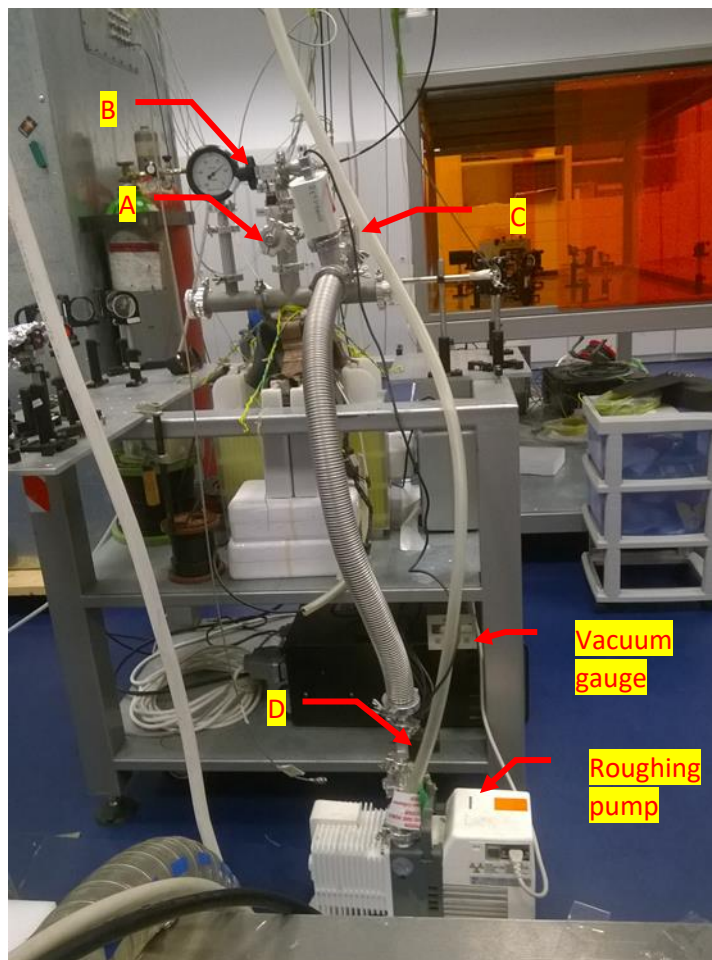
Procedures for the first shot

Setting up vacuum in the chamber (see figure below)

- Open (turn anticlockwise) the A- and C- valves.
- Turn the vacuum gauge on and wait for the pressure to reach a value of 1000 mbar (the reading looks like “-or”).
- Close (turn clockwise) the A- and C- valves.
- Turn on the roughing pump.
- Open (turn anticlockwise) the D- valve and then C- valve.
- Wait for the pressure to reach less than 1×10^{-1} mbar.

Common procedures for each shot

1. Setting up vacuum in the chamber(see figure below)



- Turn on the roughing pump.
- Open (turn anticlockwise) D- valve and then C- valve.
- Wait for the pressure to reach less than 1×10^{-1} mbar.

2. Filling the fuel chamber

- Close C- and D- (turn clockwise) valves.
- Turn off the roughing pump.
- Open (turn slowly anticlockwise) the flow control B-valve to give start for inflow of the gas (in our case the ambient air will be used).
- Wait for the pressure to reach the optimum value and then close (turn quickly clockwise) the flow control B-valve.

3. Capturing the reference image

The active menu that appears on the remote control pad should be "Pk 1".

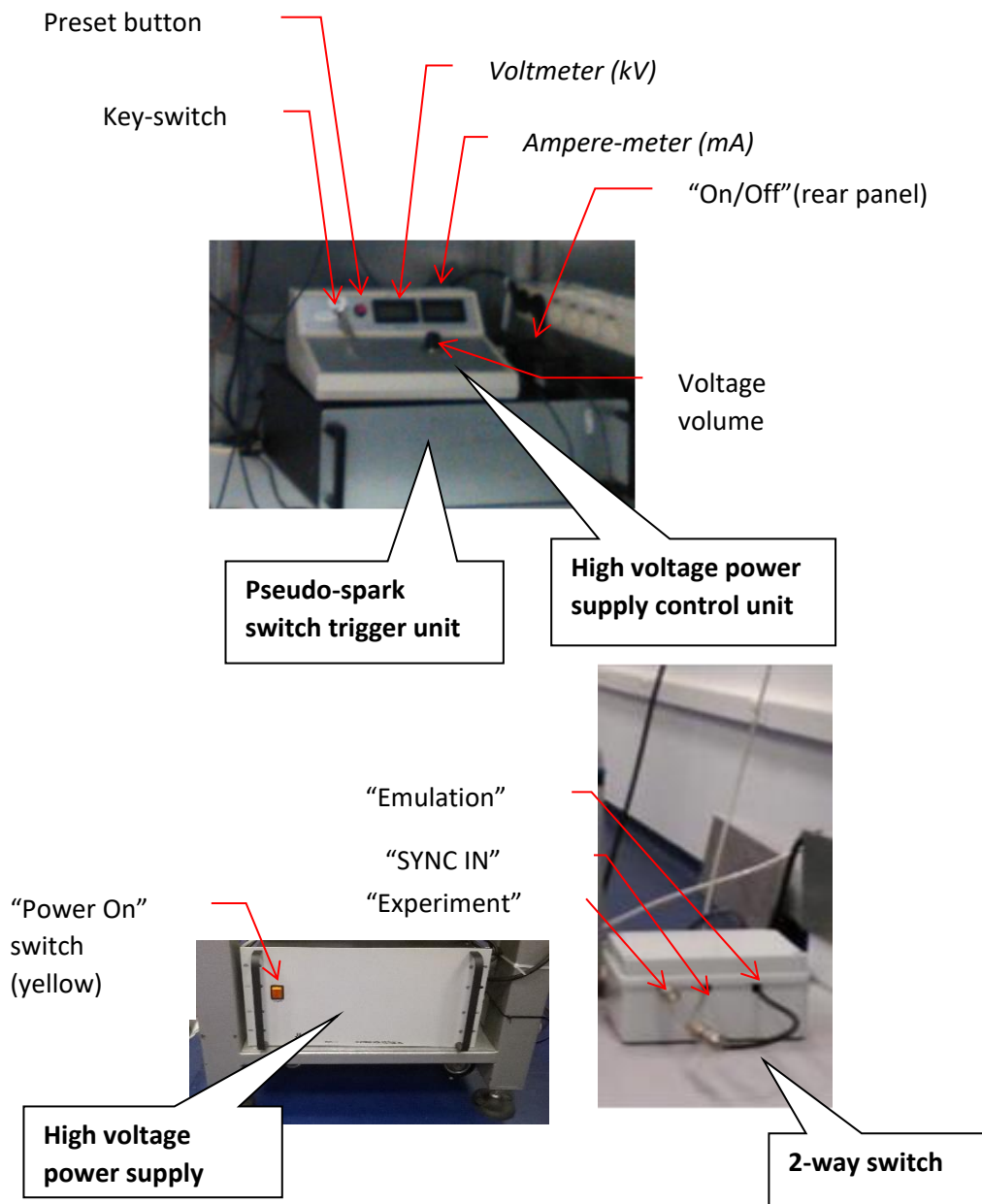
- Press the button "OP" (on the remote control pad) to start laser operation.
- Press and release the button "SEL" (on the remote control pad) 2-3 times to give start and test for pulses packet (single pulse in our case).
- In order to give start for image capture ("Extended shutter" =10,000,000 μ s), press the "single" button "▷ |" (on the virtual control panel of the camera) by using the left click on mouse.
- Press and release the button "SEL" to give start for single pulse and then wait for the capture time interval to expire.
- Press the button "OP" (on the remote control pad) to stop laser operation.
- Save the image as ref_PF_AirXX_VoltYY_shotZZ.BMP, where XX is the absolute pressure of the air inside the fuel chamber, YY is the working voltage and ZZ is the #number of the experimental shot.

a. Firing the pseudo-spark switch

- ✓ **Make sure the fuel chamber is under nominal (1-20 mbars) pressure.**
- ✓ **Make sure the "Power On" switch of the "high voltage power supply (H.V.S.) is turned to "0" position.**
- ✓ **Make sure the Key-switch of the "high voltage power supply (H.V.S) "control unit is turned to "Off" position.**



- ✓ **Make sure the 2-way switch is turned to “emulation” position (SYNC IN cable must be connected together with the “emulation” one).**
 - ✓ **Make sure the predefined output voltage of the H.V.S. is of 12.5 kV by pressing the “preset” button of the H.V.S control unit.**
 - ✓ **Make sure the “Power On” switch of the “Pseudo-spark switch triggering unit” is turned to “Off” position.**
 - ✓ **Make sure the active menu of the “laser remote control pad” looks like “Pk 1”(single shot of one pulse packet).**
-
- Set the oscilloscope to trigger once (single- shot acquisition) by pressing the “single” trigger button.
 - Turn on the H.V.S. by turning the “Power on” switch (yellow) to the “1” position.



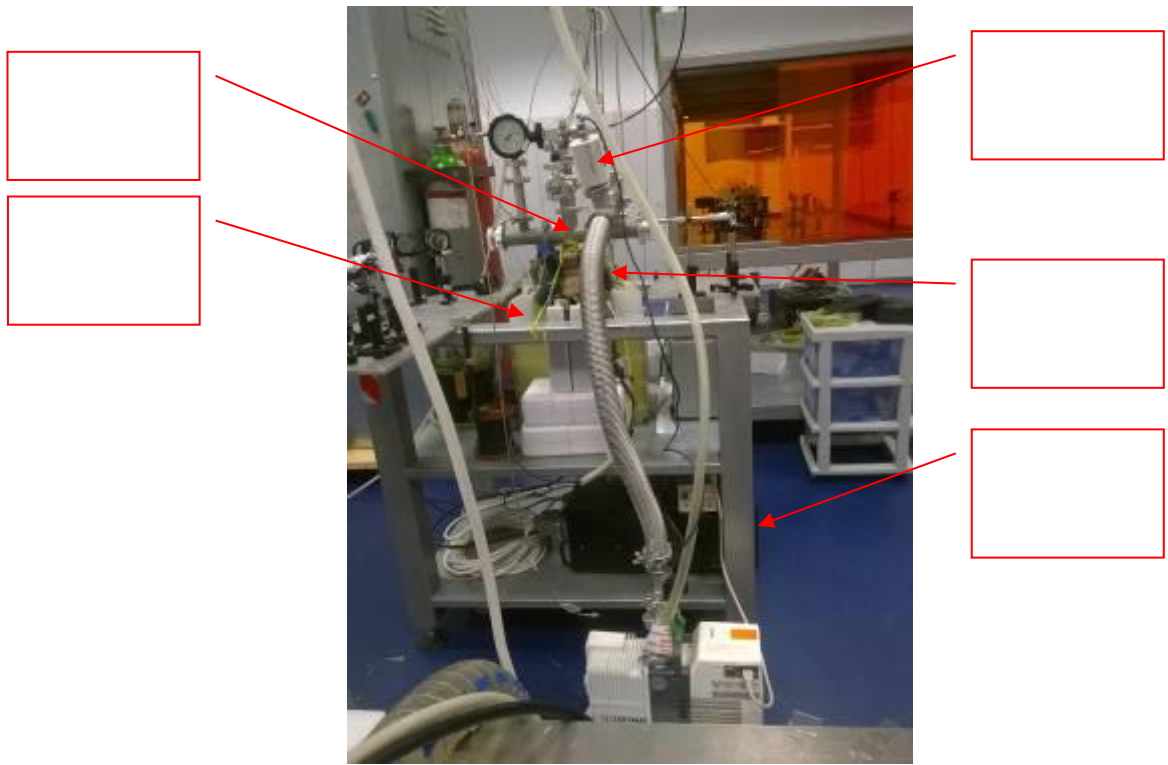
- Press the button "OP" (on the remote control pad) to start laser operation.
- Press and release the button "SEL" (on the remote control pad) 2-3 times to give start and test for pulses packet (single pulse in our case).
- Relay the 2-way switch by changing the connection of the "SYNC IN" cable with "emulation" terminal to with the "experiment" terminal.
- Turn on the "pseudo-spark switch" triggering unit by turning the "Power on" button (rear panel) to the "On" position.



- In order to give start for image capture (“Extended shutter” =10,000,000 μ s), press the single button “▷|” (on the virtual control panel of the CCD camera) by using the left click of the mouse.
- Give start for charging phase by turning the key-switch of the “H.V.S control unit” to the “On” position and wait (charging time interval of about of 2 seconds) for the voltage to reach the nominal value (read on voltmeter) and then terminate the charge by turning the key-switch back to the “Off” position.
- Press and release the button “SEL” (on the remote control pad) to give start for a single pulse. The discharge creates a lightning and a short and absence noise.
- Press the button “OP” (on the remote control pad) to stop laser operation and then wait for the imaging capture time interval to expire.
- Save the image to a file by setting a file name as shot_PF_AirXX_VoltYY_shotZZ.BMP, where XX is the absolute pressure of the air inside the fuel chamber, YY is the working voltage and ZZ is the #number of the experimental shot.
- Turn off the “pseudo-spark switch” triggering unit by turning the “Power on” button (rear panel) back to the “Off” position. .
- Turn off the H.V.S. by turning the “Power on” switch (yellow) back to the “0” position.
- Relay the 2-way switch by changing the connection of the “SYNC IN” cable with “experiment” terminal to with the “emulation” terminal.
- Save all the displayed waveforms into corresponding files for binary and ASCII data format by using a suffix file name as “_PF_AirXX_VoltYY_shotZZ”, where XX is the absolute pressure of the air inside the fuel chamber, YY is the working voltage and ZZ is the #number of the experimental shot.
- Print the screen image to a file by using a file name as “PF_AirXX_VoltYY_shotZZ”.

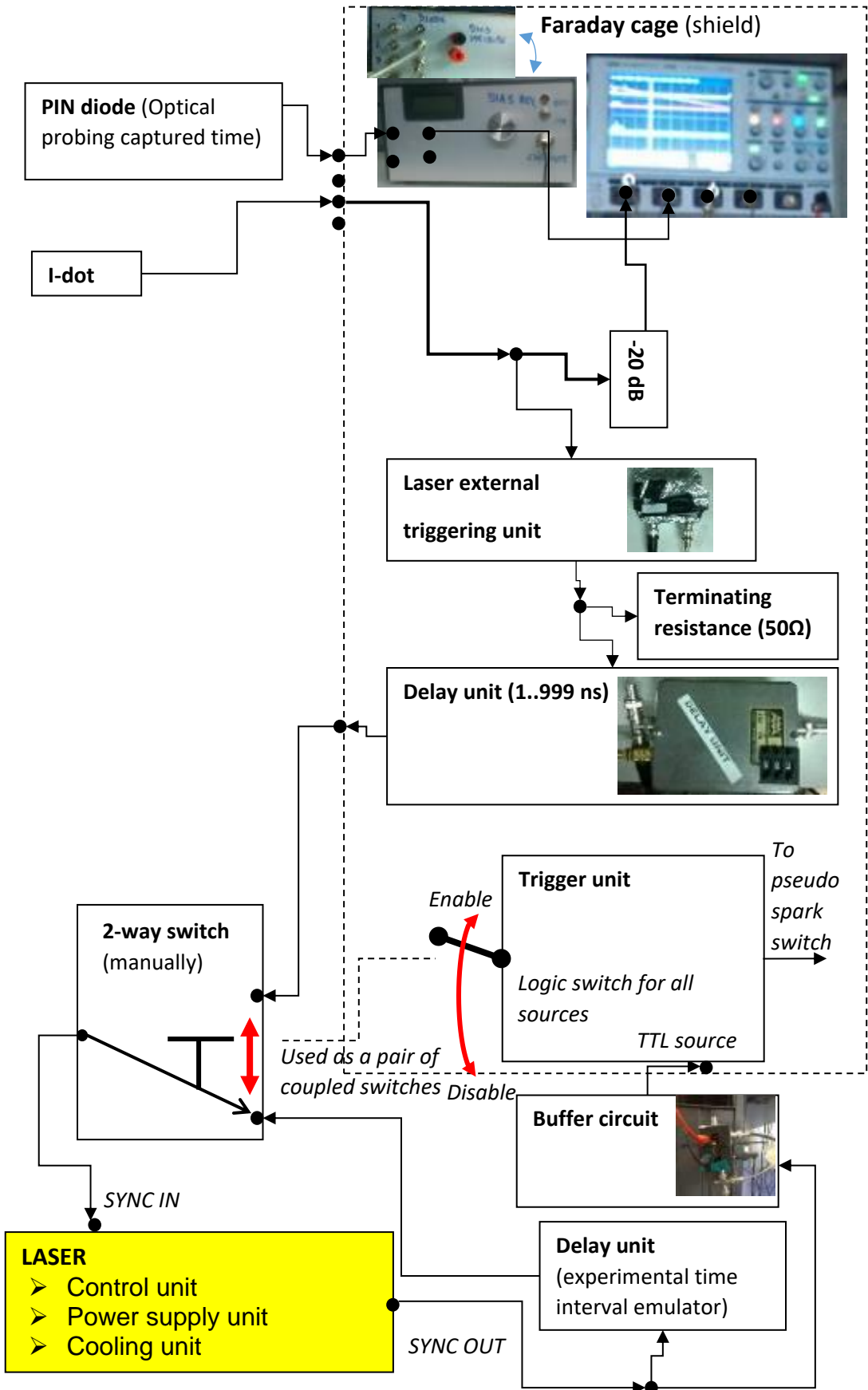
1. Recognize the miniature PF

Recognize some main parts of the PF devise and fill in the corresponding callout frames their names.



2. Recognize the experimental equipment

Recognize the experimental equipment and diagnostics and check their inter-connections by using the wiring diagram that is shown below:

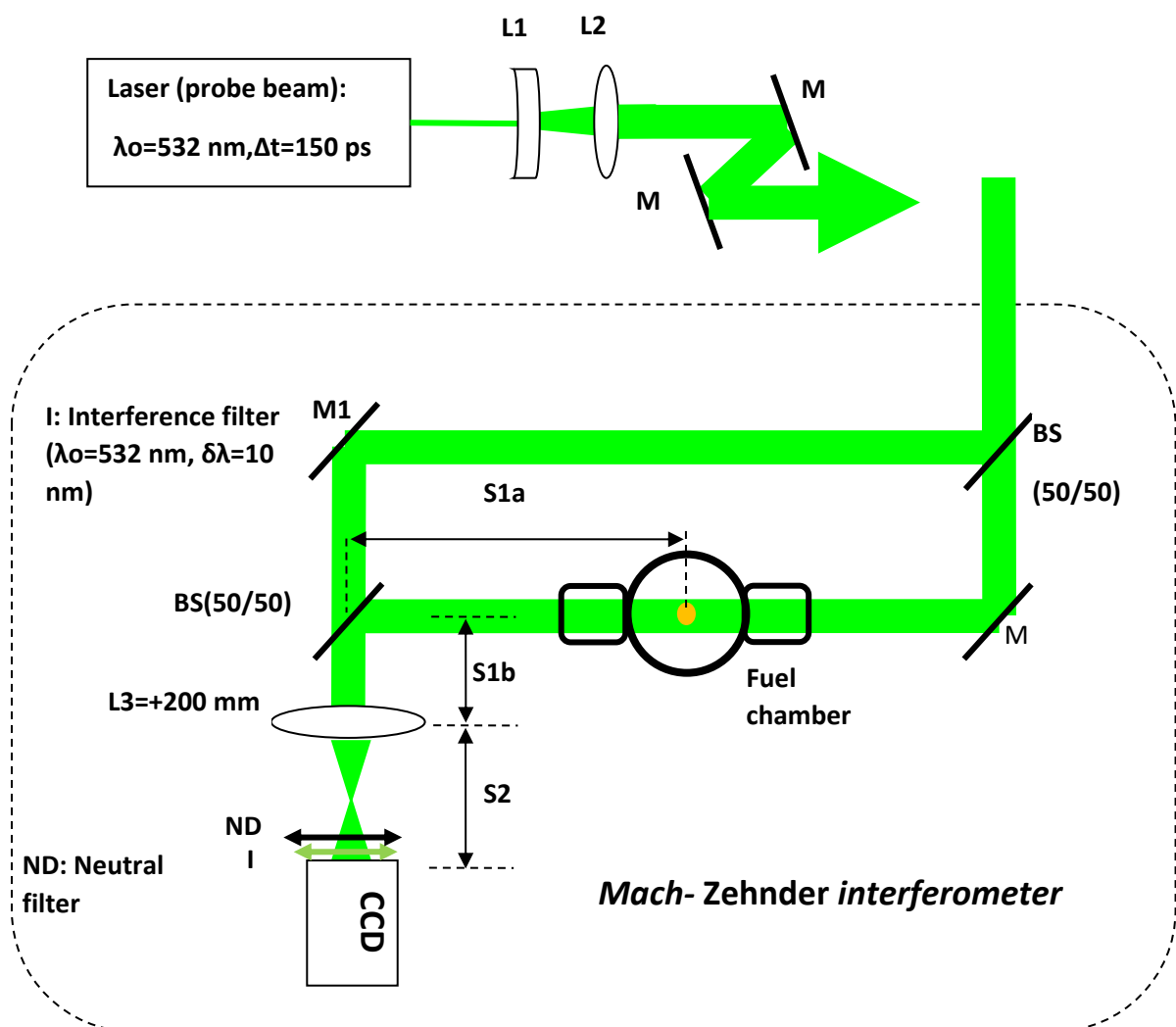


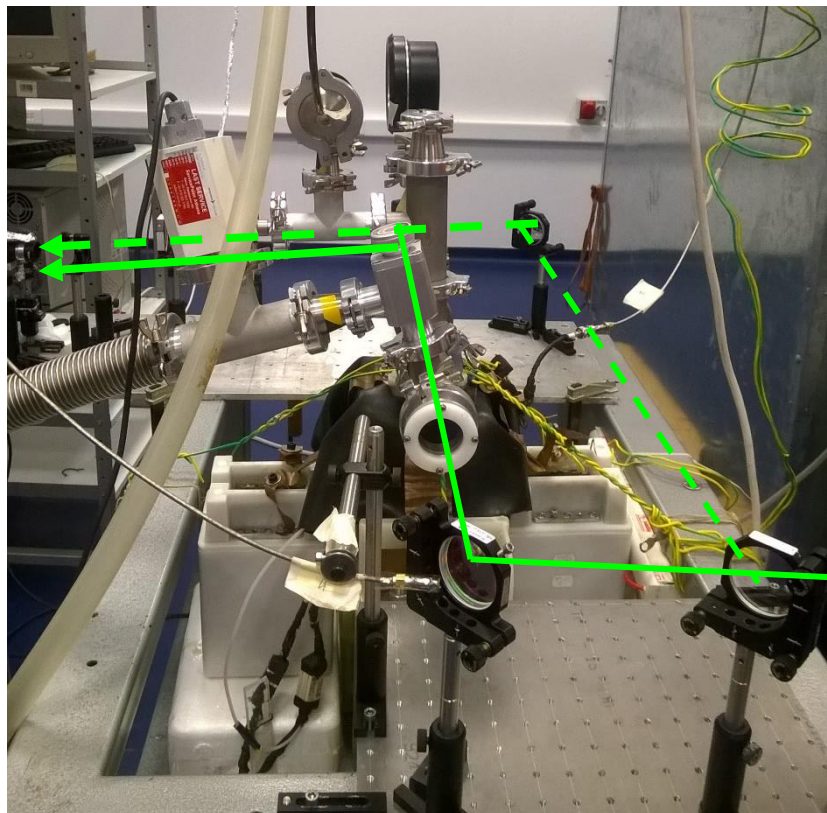
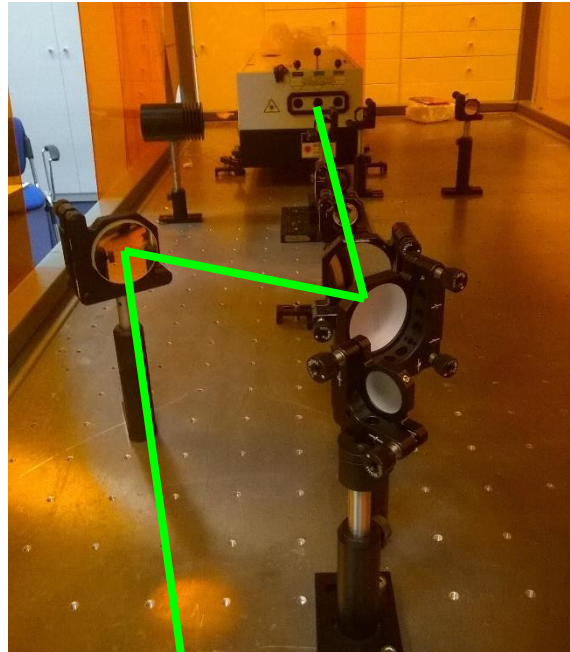
3. Optical probing set-up

For experimental purposes, we have implemented a Mach-Zehnder interferometer that consists (see figures below) of a beam expander & collimator (L1 and L2 lenses), an imaging system (CCD and L3) and a set with various additional optical elements.

M: Mirror (100% reflectivity)

BS: Beam Splitter





- Calculate the magnification (G) of the imaging system (see figure 6), taking into account i) a vertical field of view (FOV) with a length of 15 mm (10 mm will be used



for the height of the plasma column) and ii) the corresponding specifications of CCD (Resolution 1292 (H) × 964 (V), Pixel size 3.75 μm × 3.75 μm).

$$G = \frac{S_2}{S_{1a} + S_{1b}} = \frac{\text{vertical size of the image}}{\text{FOV}}$$

- Then calculate (by using the thin-lens equation) and adjust the imaging system assembly (use the reference beam alone) for a +200 mm focal lens (be careful so that the focus of the laser beam is always in front of the corresponding camera).
- In order to achieve an interferogram with horizontal fringes, adjust the knobs of the Mirror (M1).
- In order to determine the spatial resolution of the imaging system (μm/pixel) use the magnification factor (G) you calculated.

4. Perform shots for 10 different delay times

The setting value of the delay time unit (0...999 ns) should be of 0 ns.

(See *Procedures for the first shot*)

- 1) Set up vacuum in the fuel chamber.

(See *Procedures for the each shot*)

- 2) Fill the fuel chamber with air at pressure of 3 mbar.
- 3) Fire the pseudo-spark switch.
- 4) Increment the setting value of the delay time unit (0...999 ns) by a value of 10 ns.
- 5) Set up vacuum in the fuel chamber.
- 6) Repeat steps 2-5.

6. Experimental results analysis

- 1) Complete the following table

#shot	Rise time of current (10-90%) in ns	Image captured time after the current start in ns	Plasma phase (or sub-phase)
1			
....

- 2) Analyze the interferograms to extract quantitatively information for the: a) overall areal electron density, b) cubic electron density along a straight line (1D) that transverse a



the axis of symmetry at height you choice (Abel inversion), c) plasma sheath rundown velocity during the axial phase, and d) plasma compression velocity during the radial phase.

References

1. Syed Murtaza Hassan, "Development and Studies of Plasma EUV Sources for Lithography" PhD thesis, 2010.
2. Mather JM (1965) Formation of a High-Density Deuterium Plasma Focus, *Phys. Fluids* 8, No. 2, pp. 366-377.
3. Filipov N V, Filipova T I and Vinogradov V P 1962 *Nucl. Fusion (Suppl.)* 2 577.
4. H. Bruzzone, Proc. of 2nd Latin American Workshop on *Plasma Phys. and Controlled Thermonuclear Fusion, Medellin*, 12 (1985) 313.
5. H. Krompholz, W. Neff, F. Ruhl, K. Schonbach and G. Herziger, *Phys. Lett. A*, 77 (1980) 246.
6. [6] Muhammad Shahid Rafique, "Compression Dynamics and Radiation Emission from a Deuterium Plasma Focus", PhD Thesis, 2000.
7. Lee S and Serban A 1996 *IEEE Trans. Plasma Sci.* 24 1101-3.
8. Skoulakis, A., Androulakis, G. C., Clark, E. L., Hassan, S. M., Lee, P., Chatzakis, J. & Tatarakis, M. (2014). A portable pulsed neutron generator. In *International Journal of Modern Physics: Conference Series* (Vol. 27, p. 1460127). The Authors.
9. Chatzakis, J., Hassan, S. M., Clark, E. L., Petridis, C., Lee, P., & Tatarakis, M. (2008). High repetition rate pseudospark trigger generator. *Review of Scientific Instruments*, 79(8), 086103.



HELLENIC
MEDITERRANEAN
UNIVERSITY



universit 
BORDEAUX



UNIVERSITY
of York



Erasmus+

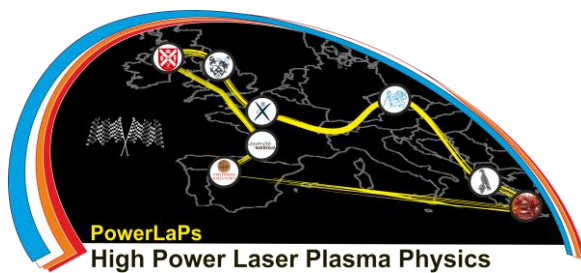
PowerLaPs

Innovative Education & Training in High Power Laser Plasmas

Plasma Physics - Theory and Experiments

EXP 3: Plasma Pinch

A. Skoulakis, G. Andrianaki, G. Tazes



Erasmus+

HELLENIC
MEDITERRANEAN
UNIVERSITY



1. Laboratory project aim

The laboratory project aims to make the student familiar with basic experimental and diagnostic techniques used in magnetic compression plasma physics research. The student will learn techniques capable to generate high temperature Z-pinch plasmas and simultaneously understand the physics underlying the common plasma diagnostics methods. Experimental techniques for generation of Z-pinch plasmas will be exemplified by studying the systems at the “X-pinch” magnetically compressed cylindrical pinch device at CPPL. In addition, the student will gain practical experience of using some diagnostics that are available at CPPL and analyzing real measurement data. The physics concepts that underlie the plasma diagnostic methods will be introduced during the experimental procedure, using a systematic approach from first principles. Moreover, a number of plasma diagnostic applications will be introduced in more detail.

In the end of the experimental procedure, the student should be able to

- explain the principles and experimental techniques for generation of high temperature Z-pinch type plasmas,
- explain the underlying physics principles and technical features of commonly used basic plasma diagnostic applications,
- demonstrate the practical usage of selected plasma diagnostics that are available at CPPL,
- write simple computer codes for acquiring, analyzing and plotting data from some selected plasma diagnostics using a commercial software package that is commonly used in plasma research,
- perform common data analysis tasks, such as curve fitting, numerical computation and signal filtering using available software routines,
- present analyzed data in graphic form in short reports, that includes written material that describes the diagnostic setup and the data analysis methods used.

2. Theoretical background

Over recent decades, various pulsed power generators were developed in order to produce magnetized plasma with magnetic fields in the 100-1000 T range. Such generators able to deliver 1-100 TW of power to a load are established in pulsed power exploding wire experiments, thereby reliably providing an open scientific field for studying High Energy Density Physics (HEDP) [1], with applications such as in inertial confinement fusion [2], laboratory astrophysics [3] and point projection radiography [4].

The X-pinch is a plasma device in which plasmas are produced by using two or more fine wires that are crossed and touch in the middle, in the form of an X. This then forms the load in the anode-cathode gap of a pulsed power generator. Ohmic heating causes the wires to explode into a hot, dense plasma. However since a plasma is very efficient at carrying a current, the current continues to flow and the induced magnetic field around the wires acts to confine the plasma.

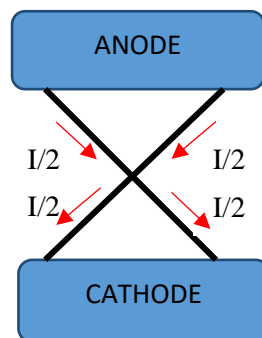


Figure 2.9 Current flow in a 2 wire X-pinch

In a two wire X-pinch the current is divided between the two legs, with the full current (I) only being concentrated at the central crossing point (Figure 2.1). At that point the magnetic pressure that confines the plasma has a maximum value. Typically, a small instability will lead to plasma implosion under the magnetic pressure at the central crossing point, resulting in an intense burst of X-rays that lasts for only a few nanoseconds. The characteristics of the electromagnetic radiation emitted from an X-pinch machine depend on the material and diameter of the wires as well as the electrical characteristics of the generator. Typically, the wires are metallic (10 – 50 μm diameter) and the current characteristics vary from 40 kA to 1 MA with the rise time of 40 ns to a few microseconds. Unlike the Z-pinch (created using a single wire), the X-pinch can produce a predictable single point source almost every time (the instability leading to the pinch will sometimes not occur). The major application of the X-pinch is as a bright-point source of X-ray radiation for a point–projection radiography of plasmas [4-5], biological samples [5-6], and other objects [7]. However, the small size and predictable location of the radiation source(s) within the X-pinch make it attractive for applications such as x-ray backlighting [8] and microlithography [9]. It may also be possible to use the X-pinch for EUV lithography due to the point source of radiation.

Each leg of the X-pinch experiences a local, self-induced magnetic field ($\mathbf{B}_{\text{local}}$), while the configuration as a whole is surrounded by a global magnetic field ($\mathbf{B}_{\text{global}}$). In areas with a dynamically significant $\mathbf{B}_{\text{global}}$, the coronal plasma is accelerated from the wires by the $\mathbf{J} \times \mathbf{B}_{\text{global}}$ force (where \mathbf{J} is the current density) towards the vertical axis of the X at a rate well approximated by an analytical rocket model [10]. The plasma streaming from these wires takes on a quasi-periodic wavelength shape, visible in Figure 2.2. X-ray backlighting data demonstrate that the wire cores remain in their initial positions for the majority of the experiment [11]. The ablation of the wire cores slows once adequate coronal plasma exists for the bulk of the current to shift to the less resistive plasma, but the wire cores ablate until they no longer exist, feeding the coronal plasma throughout the current pulse. Upon arrival at the axis the radial momentum of the streams thermalizes and the axial momentum is conserved, contributing to the formation of plasma jets which propagate bi-directionally towards the electrodes, which are also labeled in Figure 2.2. Almost immediately after the generation of the X-ray pulse, the neck breaks and a gap forms in which the plasma density is several orders of magnitude lower than that in the neck. This process leads to the formation of a mini-diode and the generation of electron and ion beams [12].

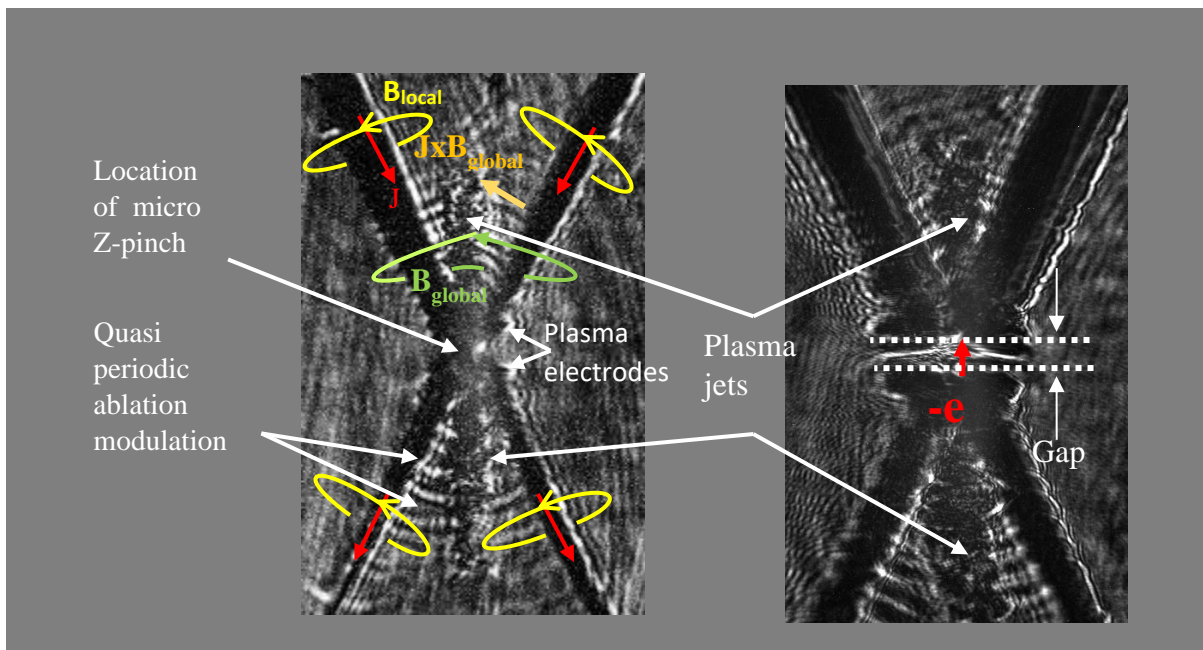


Figure 10.2 Shadowgraphy image of a 5 μm tungsten two-wire X-pinch with identifiable structures labeled. The image were taken 35 ns after the start of the current



3. X-pinch system (apparatus & diagnostics)

3.1 Pulsed power generator

The design and construction of the X-pinch device has been implemented during a funded EU Marie Curie Transfer of Knowledge excellence grant “DAIX” (Development of an Innovative X-ray source) on pulsed power X-pinch plasma devices.

The device is a Capacitive Energy Storage Generator (CESG) type that consists (see Figure 3.1) of a high voltage pulsed power supply (the popular Marx generator), a high voltage & current coaxial cable, a pulse forming line (PFL), a self-breaking spark gap switch (SBS) and a load chamber (vacuum chamber).

The Marx bank is a capacitor bank consisting of four capacitors (0.22 μF , 50 kV, 25 kA) which are charged in parallel and discharged in series. Once the capacitor bank is loaded, a trigger pulse is sent to the spark gap to break the circuit to release the energy. The current flows into the PFL through the coaxial cable which acts as a peak current limiter (<20 kA). The PFL consists of two co-axial cylinders separated by deionized water (1-10 μS) which act as a dielectric. The load chamber is separated from the PFL by a spark gap chamber which is filled with SF_6 (sulfur hexafluoride). The pressure of the SF_6 is adjusted to the optimum value so that the circuit breaks at the desired voltage (160-220 kV). The load chamber is under high vacuum ($< 6 \times 10^{-4}$ mbar), thus ensuring that there is no air plasma generated. Voltage ($V\text{-dot}$) and current (Rogowski groove) monitors are attached at the end of the pulse forming line and at the anode (fit around one of the four current return posts) of the load chamber, respectively. The load chamber has eight viewing ports allowing multiple diagnostics for single shot.

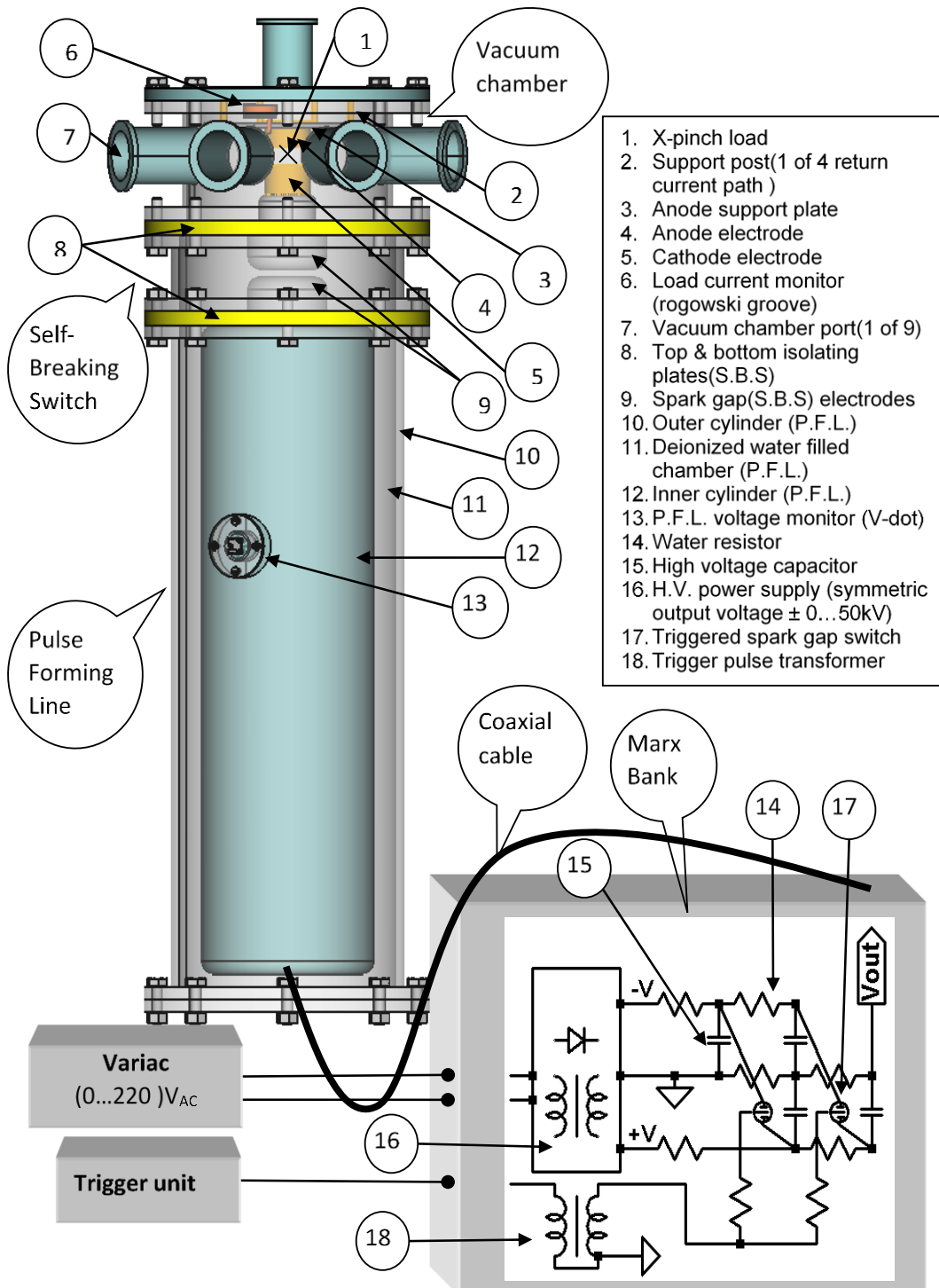


Figure 11.1 Schematic representation of the electrical system involved in pulse compression

3.2 Voltage and Current Monitoring

The generator described above is capable of delivering a peak current of about 45 kA pulse, with a rise time of about 35 ns (10-90%). In order to verify that the generator performs properly, voltage and current monitors are used. The monitors consist of a capacitively coupled probe for monitoring the voltage in the PFL (V_{PFL}) and a Rogowski coil (Rogowski groove type) to capture the current signal within the vacuum chamber.

3.3 PFL Voltage Monitor

The probe (Figure 3.2(b)) is made up of an isolated conducting plate in the outer conductor and is capacitively coupled to the inner conductor of the PFL with a self-capacitance of C_{probe} (Figure 3.2(a)).

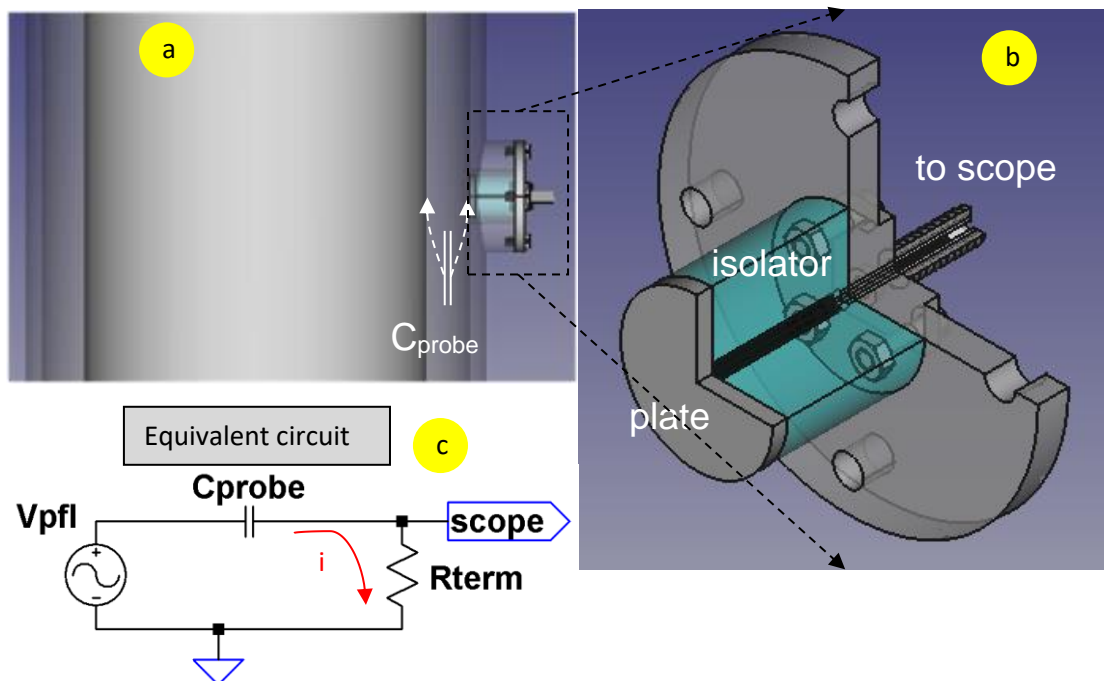


Figure 3.2 Pulse forming line voltage monitor

Assuming the voltage probe can be treated as a parallel plate capacitor due to its relative small size it holds

$$C_{probe} = \frac{A\epsilon_0\epsilon_r}{d} \quad (1)$$

where A is the area of the conducting plate, ϵ_r represents the relative permeability of the dielectric of the PFL (de-ionized water) and d represents the distance between the plates.

The equivalent circuit is given in Figure 3.2(c), where R_{term} is the terminating resistance. The circuit equation can be written as follows:

$$\begin{aligned}
 V_{PFL} &= V_{Cprobe} + V_{scope} \Leftrightarrow \\
 V_{PFL} &= \frac{1}{C_{probe}} \int_0^t i dt' + V_{scope} \Leftrightarrow \\
 V_{PFL} &= \frac{1}{C_{probe} R_{term}} \int_0^t V_{scope} dt' + V_{scope} \quad or \\
 \frac{dV_{PFL}}{dt} &= \frac{V_{scope}}{C_{probe} R_{term}} + \frac{dV_{scope}}{dt}
 \end{aligned} \tag{2}$$

If $V_{scope} \gg C_{probe} R_{term} \frac{dV_{scope}}{dt}$, then from (eq. 2) one can obtain

$$V_{scope} = C_{probe} R_{term} \frac{dV_{PFL}}{dt} \tag{3}$$

Under this condition, the monitor can be used to measure the time derivative of the voltage (*V-dot mode*).

3.4 Load Current Monitor (Rogowski groove)

The current monitoring was performed using a Rogowski groove placed around one of four return current posts close to the load (Figure 3.3(a)) and is made up of an annular conductive ring placed around a current conductor (Figure 3.3(b)).

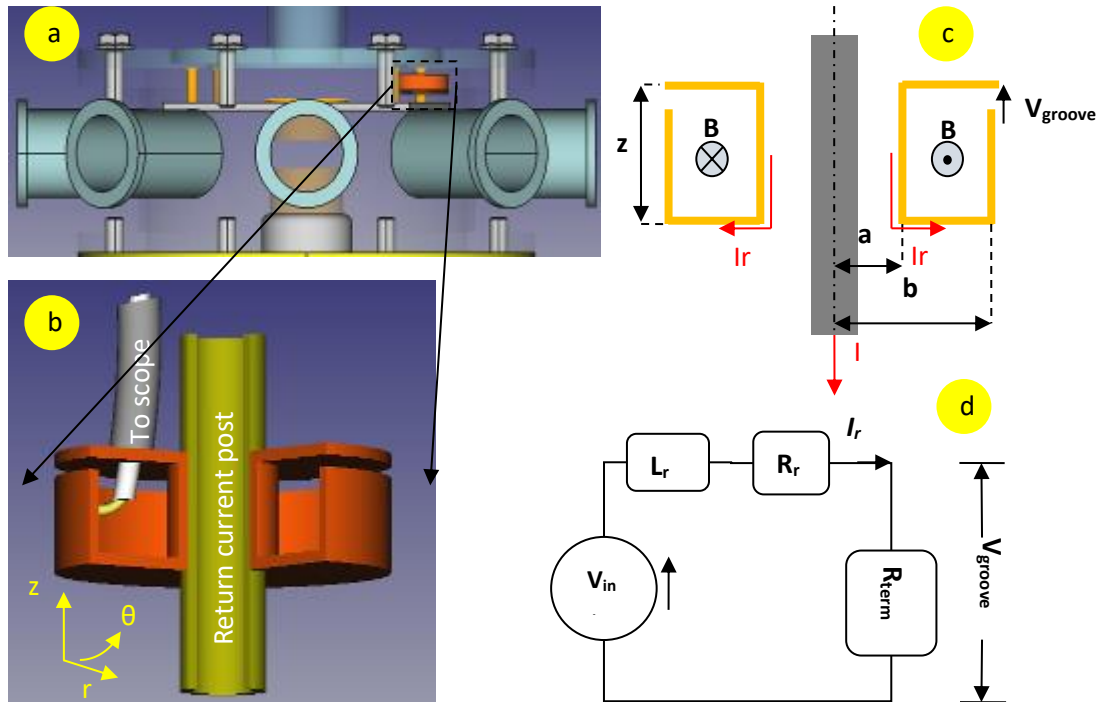


Figure 3.3 Load Current Monitor (Rogowski groove)

Figure 3.3(d) shows the circuit diagram of the probe with its current represented by I_r , inductance represented by L_r , the groove resistance represented by R_r and the terminating resistance represented by R_{term} . The current I_r , driven by the induced voltage (V_{ind}) generates a voltage V_{groove} measured across the terminating resistance R_{term} where $V_{groove} = I_r \times R_{term}$.

In our case the probe acts as a toroidal coil (Rogowski coil) which consists of one winding turn ($N=1$) and has a core with rectangular cross-section (fig. 3.3(c)). The central post carries a current I which gives rise to a magnetic field \mathbf{B}

$$\mathbf{B} = \frac{\mu_0 I}{2\pi r} \hat{\theta} \quad (4)$$

Let Φ denote the magnetic flux through a cross-section (S) of the probe, due the current I . Now, by varying I with time, there will be an induced emf (V_{ind}) associated with the changing magnetic flux in the probe

$$V_{ind} = -N \frac{d\Phi}{dt} = -\frac{d}{dt} \iint_S \mathbf{B} \cdot d\mathbf{s} = -\frac{\mu_0 z}{2\pi} \frac{dI}{dt} \int_a^b \frac{1}{r} dr = -\frac{\mu_0 z \ln\left(\frac{a}{b}\right)}{2\pi} \frac{dI}{dt} = -M \frac{dI}{dt} \quad (5)$$

Where, $M = \frac{\mu_0 z \ln\left(\frac{a}{b}\right)}{2\pi}$ is the mutual inductance of the Rogowski groove.

As the flux changes through the coil, an induced emf (V_{emf}) opposes this change. The self-induced V_{emf} in groove, due to changes in I_r , takes the form

$$V_{emf} = -L_r \frac{dI_r}{dt} \quad (6)$$

According to Ampere's law, the magnetic field B_r is given by ($N=1$)

$$\oint_C \mathbf{B}_r \cdot d\mathbf{l} = B_r \hat{\theta} \oint_C dl = B_r (2\pi r) = N\mu_0 I_r \Leftrightarrow \mathbf{B}_r = \frac{\mu_0 I_r}{2\pi r} \hat{\theta} \quad (7)$$

where I_r and dl are the current located in the bounded surface by 'C' and the line element of path (C) respectively.

The total self-magnetic flux Φ_r through the probe may be obtained by ($N=1$):

$$\Phi_r = N \iint_S \mathbf{B}_r \cdot d\mathbf{s} = \frac{\mu_0 z \ln\left(\frac{a}{b}\right)}{2\pi} I_r = L_r I_r \quad (8)$$

Therefore, the self-inductance is:

$$L_r = \frac{\Phi_r}{I_r} = \frac{\mu_0 z \ln\left(\frac{a}{b}\right)}{2\pi} = M !!! \quad (9)$$

The circuit equation of the current measuring systems of Figure 3.3 (d) is:

$$\begin{aligned} V_{ind} &= -V_{emf} + I_r R_r + V_{groove} \quad \Leftrightarrow \\ V_{ind} &= L_r \frac{dI_r}{dt} + I_r (R_r + R_{term}) \xrightarrow{R_{term} \gg R_r} \\ V_{ind} &= L_r \frac{dI_r}{dt} + I_r R_{term} \end{aligned} \quad (10)$$

In our case, the registered voltage is solely dependent on dI/dt (the current probe operates in I-dot mode). The condition for this mode is

$$\frac{L_r}{R_{term}} \frac{dI_r}{dt} \ll I_r \quad (11)$$

Equation (10) taking into account condition (11) becomes

$$V_{ind} = I_r R_{term} \stackrel{(5)}{\Leftrightarrow} -M \frac{dI}{dt} = I_r R_{term} \quad (12)$$

Therefore, the registered voltage is:

$$V_{groove} = -M \frac{dI}{dt} \quad (13)$$

3.5 Optical Probing

In order to gain information concerning the refractive index (η) and hence the electron density of a plasma (n_e), an Nd-YAG (Neodymium-doped Yttrium Aluminum Garnet) laser was used to backlight the experiment. Light can only pass through a plasma if the frequency of the plasma ω_p is lower than that of the probe beam ω_{light} . The maximum density, which can be probed, known as the critical density n_c , in a compact form is:

$$n_c = 10^{21} \lambda \text{ cm}^{-3} \quad (14)$$

where λ is in microns.

The refractive index of the plasma is given by:

$$\eta = \sqrt{1 - \frac{n_e}{n_c}} \cong 1 - \frac{n_e}{2 n_c} \quad (15)$$

The Nd-YAG laser emits light in the near infrared ($\lambda=1064$ nm) which then traverses a KDP harmonic generating crystal. The frequency of the light is double resulting in a λ of 532 nm (green). Substituting this wavelength into equation (14) yields a critical density $n_c=4 \times 10^{21}$ electrons per cubic centimeter.

3.6 Shadowgraphy

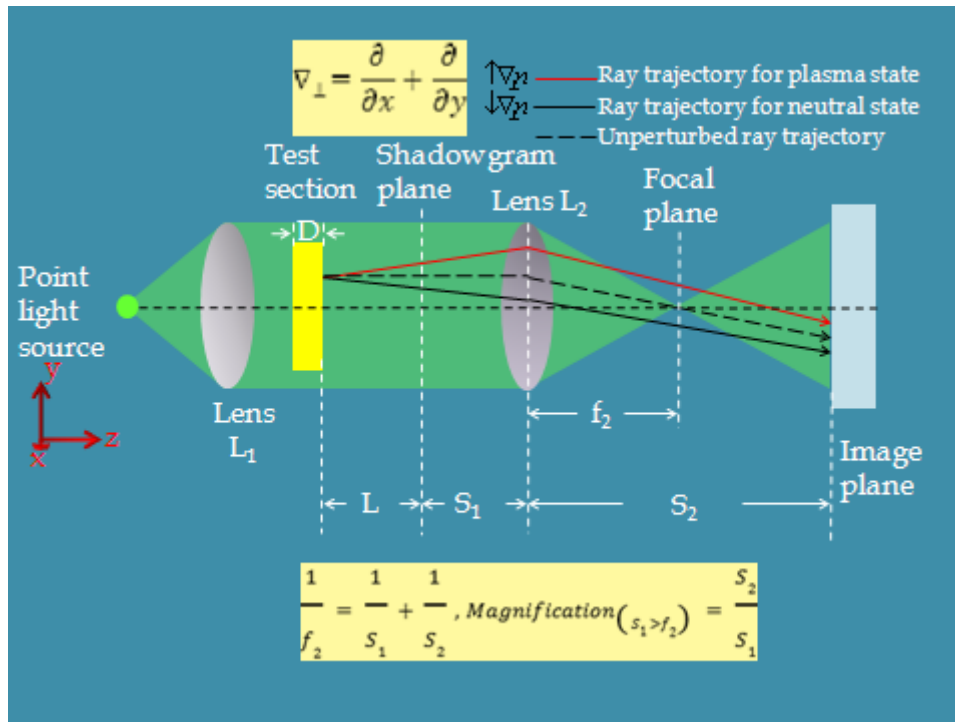


Figure 3.4 Images showing the propagation of light rays through a shadowgraphy system. Light is focused by a lens and after crossing through the focal point propagates to the image plane

In shadowgraphy (Figure 3.4), the light that propagates through regions with large density gradients is diverted significantly, leaving that portion of the image dark. The refracted radiation brightens undisturbed areas of the image, or in the case of very high density gradients, the light will be lost from the system. The intensity variations arise from the second derivative of the refractive index. The intensity incident (I) on the CCD (image plane) compared to the intensity of an undisturbed beam (I_o) will be [13]:

$$\left(\frac{\partial^2}{\partial x^2} + \frac{\partial^2}{\partial y^2} \right) \int_0^D \eta(x,y,z) dz = -\frac{1}{L} \frac{I(x,y) - I_o}{I_o} \quad (16)$$

where x and y are the coordinates orthogonal to the propagation direction of the beam, and L is the distance between the object (test section) and the shadowgram plane (a conjugate plane of the image plane).

3.7 Time-resolved soft x-ray detector

The low cost BPX65-PIN (silicon intrinsic (I) semiconductor between a p-type (P) and an n-type (N) semiconductor regions) (figure 3.5(c)) diodes with a fast response (nanosecond timescale) are chosen for X-ray measurements using our X-pinch source. The BPX65 PIN diodes of the smaller sensitive area (1 mm × 1 mm) are mounted on the SMA female connectors with a variety of filters (Figure 3.5(b)). A set of five filtered BPX65-PIN diodes (fig. 3.5(a)) is designed to measure the x-ray fluence in the range of 1 keV to 10 keV. An illustration of the bias circuit diagram can be seen in Figure 3.5(d).

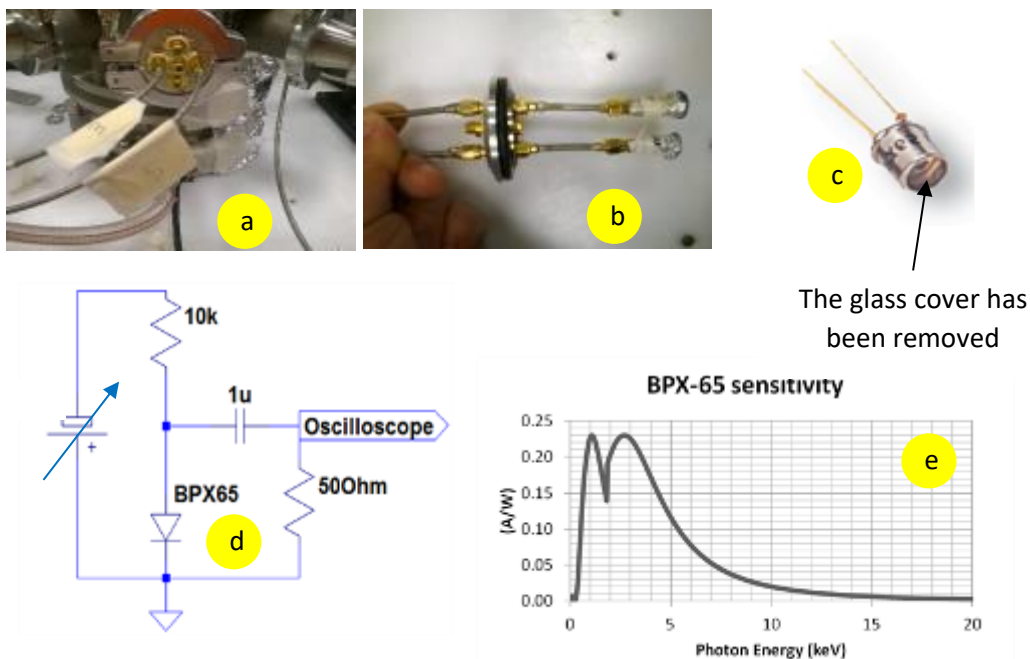


Figure 3.5 Time-resolved soft x-ray detector

A reverse bias is imposed on the diode which causes the intrinsic layer to act as an insulator, stopping current while setting up an electric field across the I layer. As photons are absorbed by the silicon they liberate charge carriers which are accelerated by the electric field, producing a current which is recorded. The transient signal is coupled out through a capacitor along 50 Ω semi-rigid cable to an oscilloscope where the voltage across a 50 Ω termination is measured. A curve of the diode sensitivity can be seen in Figure 3.5(e), the diodes are sensitive for 0.5-15 keV. The use of filter sets in conjunction with PIN diodes can provide spectral resolution to these diagnostics, supplying information concerning the emission characteristics of the central plasma. The detector spectral sensitivity ($S_{(E_f)}$) in the presence of a filter has been calculated by the following equation

$$S_{(E)f} = S_{(E)}e^{-\mu(E)\tau} = S_{(E)}T_{(E)} \quad (17)$$

where $S_{(E)}$ is the sensitivity of the BPX65 diode for the radiation at energy E and $T_{(E)}$, $\mu(E)$ and τ are the transmission coefficient, absorption coefficient and thickness of the filter, respectively

The transmission curve, as well as the detector response convolved with various filters are shown in Figures 3.6(left) and 3.6(right), respectively.

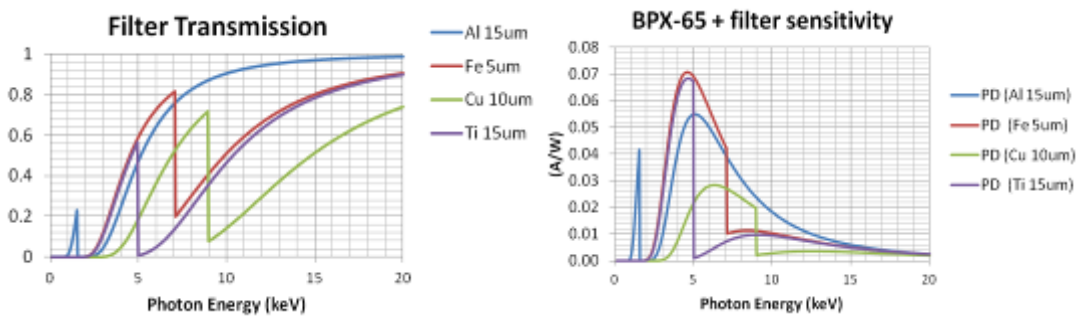


Figure 3.6 Transmission curves of various filters and the plot of BPX65-PIN diode response convolved with that filters

3.8 X-ray Imaging

Pinhole cameras provide spatially resolved, time integrated information regarding radiation from the X-pinch [11, 14]. They show (Figure 3.7) intense radiation from the small micro-pinch source in addition to the large source from energetic electron (electron beams accelerated across “mini-diodes” near the X-pinch crossing point) radiation. The pinhole images directly show a small central spot from the micro-pinch. They also show the main features of the X-pinch limbs on the anode side. No features are observed on the cathode side. This means that electron beam interactions with the plasma or the cooler wire material play a very important role in the X-ray emission.

Anode

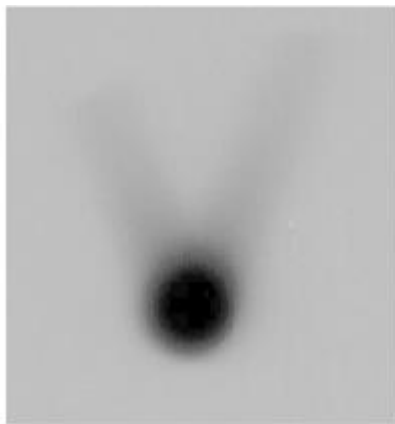


Figure 3.7 A typical time-integrated Pinhole Camera Image of a tungsten two-wire X-pinch

The complicated structure and small dimensions of the emitting regions, which are of the most interest, require the use of high-resolution pinhole cameras having a low luminosity. Due to their small dimensions, the recorded images are difficult to analyse even at a relatively large magnification.

3.8.1 Slit step-wedge (SSW) camera

Another well-known device is a slit most often applied in spectrographs to obtain one-dimensional spatial resolution in the direction perpendicular to the dispersion direction. Devices using a slit turned out to be rather convenient in studies of Z-pinchs due to the axial symmetry of the latter. One such device, namely, a slit camera with step-wedge filters (slit step-wedge (SSW) camera (Figure 3.8)), was designed especially for pinch experiments [11, 15-17]. The use of such a camera made it possible to overcome many difficulties in studying the spatial structure of the pinch.

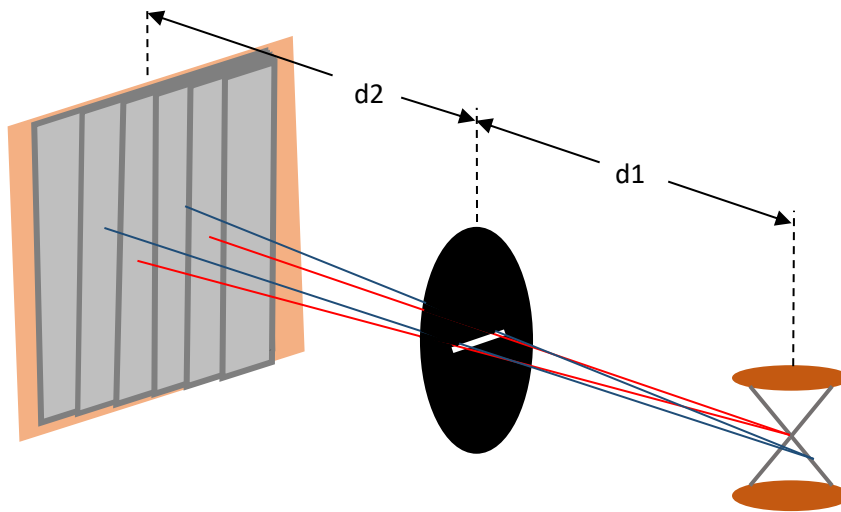


Figure 3.8 Scheme of a slit step-wedge (SSW) camera and scheme of image recording

The SSW camera provides spatial resolution in one dimension, by the use of a slit, taking advantage of the fact that the central part of the X pinch has very little radial extent. The slit is oriented perpendicular to the z-axis to give us spatial resolution along the z-direction. The various filter thickness in the SSW give us an idea regarding the photon energies radiated from different locations along the z-axis. Likewise with a pinhole camera, the SSW camera is able to show a narrow intense spot from the micro-pinch in the centre with more diffuse radiation from energetic electrons. In our case, the image is recorded on one film through a six-step attenuator made of aluminium foil with thicknesses of **15 μm** . The number of layers was chosen to be multiple to 2^n . Due to the sufficiently large step width (on the order of 3 mm), the image dimensions were large enough to perform averaging of the optical density, thereby appreciably improving the signal-to-noise ratio and identify even weak images.

3.8.2 Point projection radiography

Point projection radiography is a technique that is able to capture calibrated areal density maps of a plasma sample [18, 19] (in our case an aluminum wire is used). This begins with a point source of photons such as an X-pinch. These photons are released isotropically and impinge upon a plasma sample. A fraction of the photons that interact with the plasma are absorbed. The resulting non-uniform distribution behind the plasma is collected on a detector. This is illustrated in Figure 3.9.

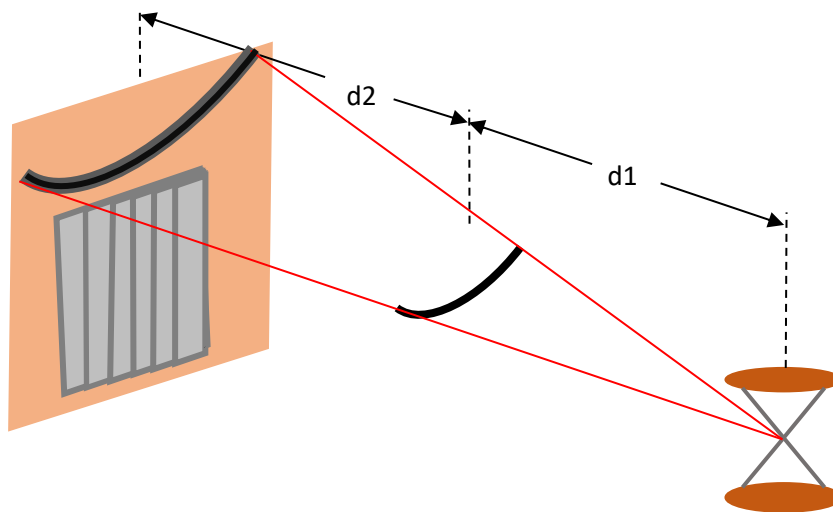


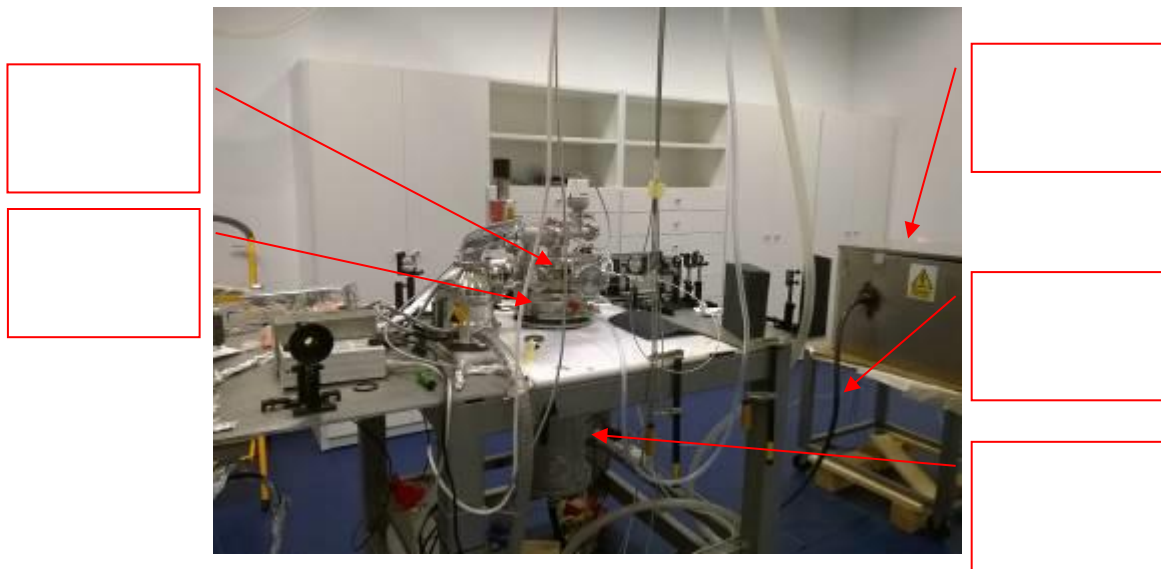
Figure 3.9 Scheme of a Point projection radiography and scheme of image recording

A calibration is obtained by simultaneously imaging a step-wedge (Figure 3.9) made from the same material as the plasma under study. The step wedge is often placed near the detector and far away from the object plasma. When preparing to collect such an image, it is important to ensure that the image of the plasma does not overlap the step-wedge. This will cause errors during the calibration since some steps may receive a higher flux than others. The resolution of a point projection system with a geometry like that shown in Figure 3.9 is primarily determined by the size of the photon source. A finite source size causes the true image of the sample plasma to be blurred. This limits the image resolution to the order of the source size. The hotspot of an X-pinch provides a micron (μm) scale source size [20].

4. Experimental procedure

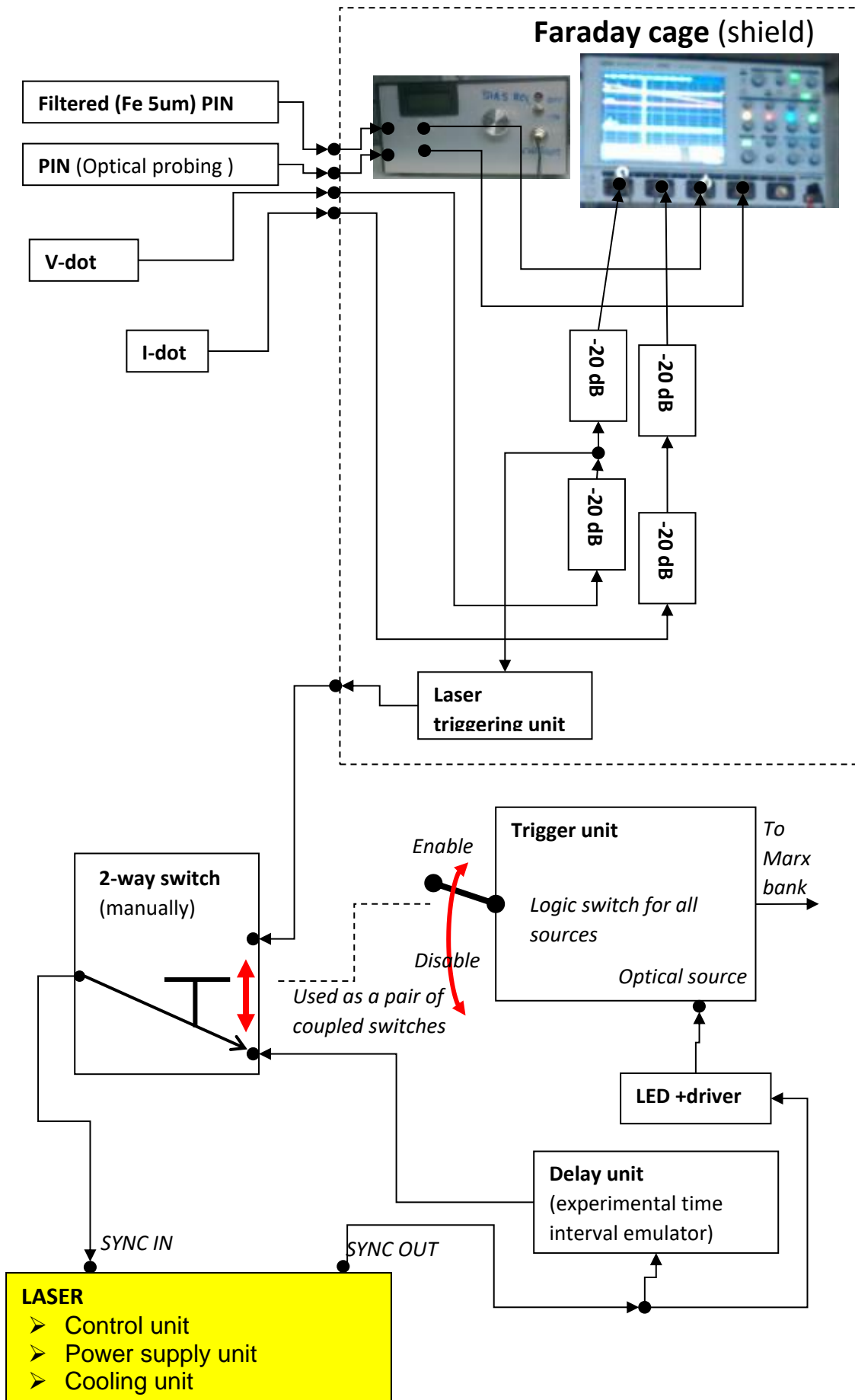
4.1 Recognize the X-pinch system

Recognize some main parts of the X-pinch system and fill in the corresponding callout frames their names.



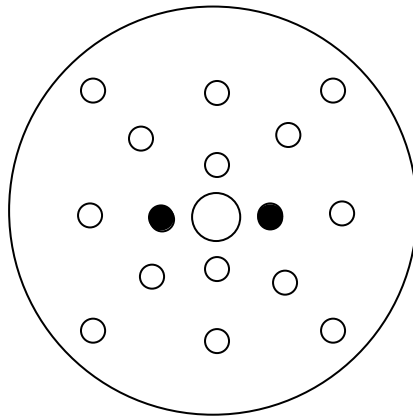
4.2 Recognize the experimental equipment

Recognize the experimental equipment and diagnostics and check their inter-connections by using the wiring diagram that is shown below:

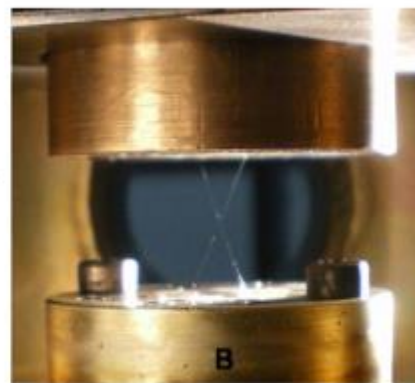
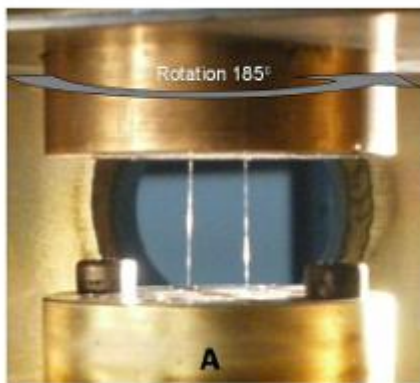


4.3 Create and install an X-pinch load

- Carefully unwind about 10 cm of the tungsten wire.
- Place a fishing weight at each end.
- Introduce the two ends in the anode. Use these holes to get a crossing angle of about 55° :



- Install the anode on the anode plate, the weights should go in the corresponding holes of the cathode.
- Twist the X-pinch of 180° - 190° . Use the port on the top of the chamber to check if the two wires are in contact.

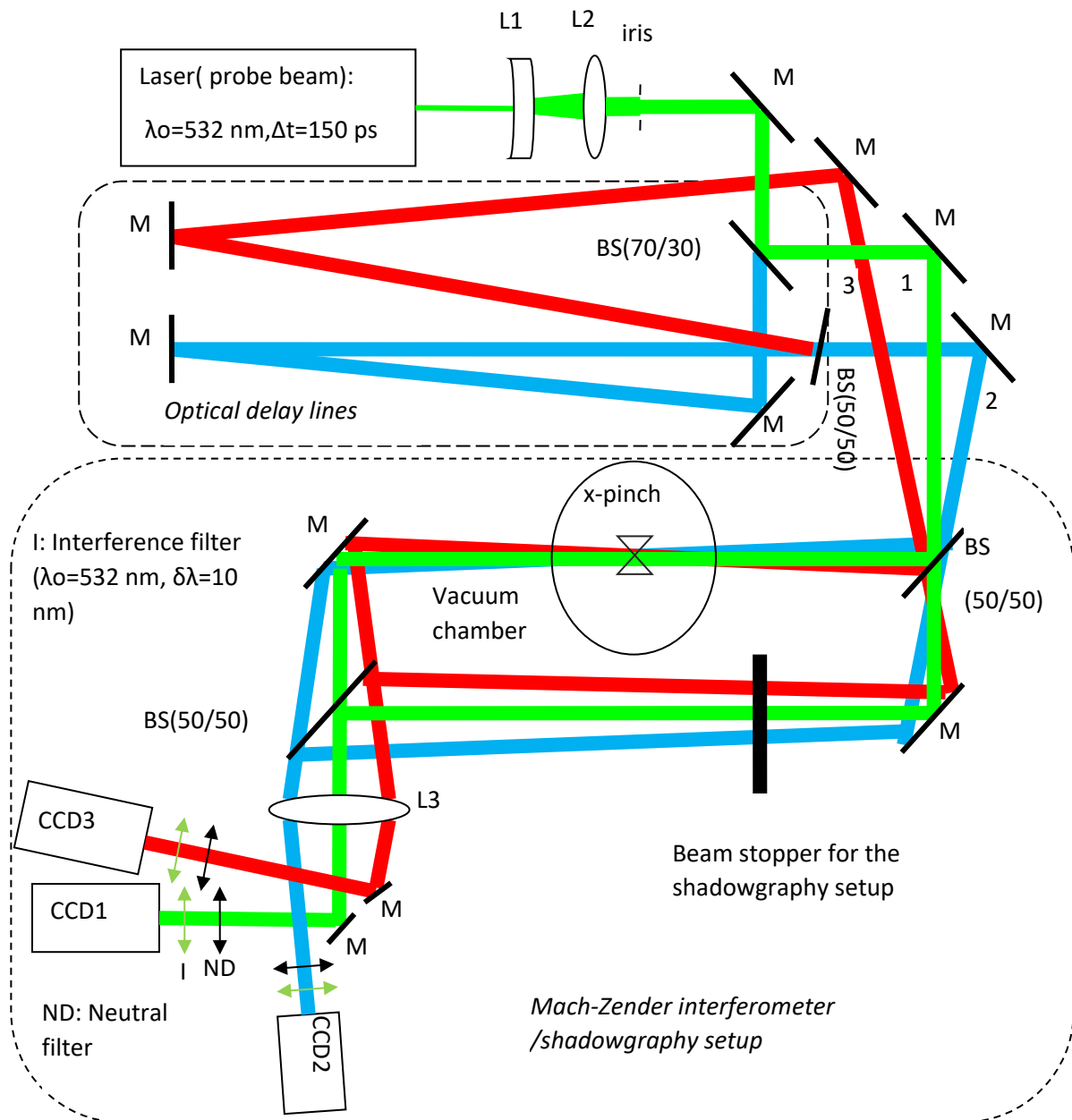


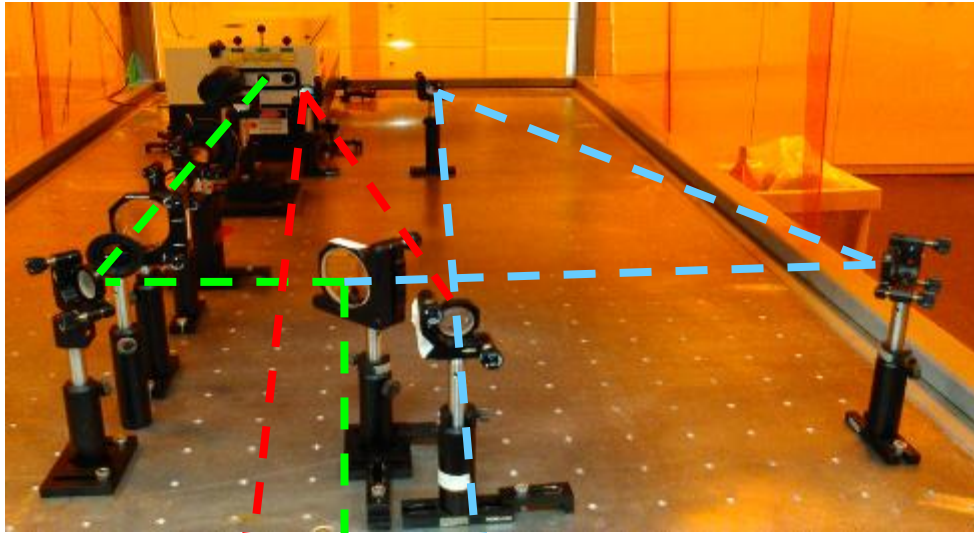
4.4 Optical probing set-up

For experimental purposes, we have implemented a 3-frame Mach-Zender interferometer (or shadowgraphy setup) that consists (see figures below) of a beam expander & a collimator (L1 and L2), a set of two optical delay lines (delay time 7.8 ns & 6.5 ns, respectively), a three-frame imaging system (CCD1..3 and L3) and a set of various additional optical elements.

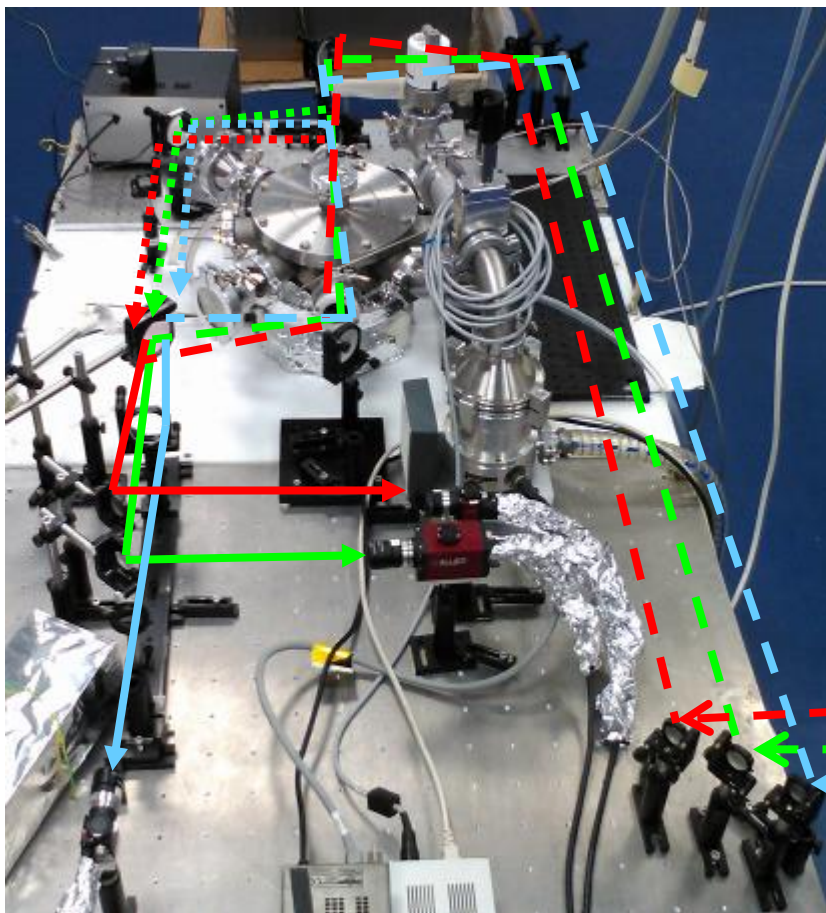
M: Mirror (100% reflectivity)

BS: Beam Splitter





(3) (1) (2)



(3)

(1)

(2)



- Calculate the magnification (G) of the imaging system (see Figure 3.4), taking into account i) a vertical field of view (FOV) with a length of 15 mm (height of the X-pinch load) and ii) the corresponding specifications of CCD (Resolution 1292 (H) × 964 (V), Pixel size $3.75 \mu\text{m} \times 3.75 \mu\text{m}$)

$$G = \frac{S_2}{L + S_1} = \frac{\text{vertical size of the image}}{\text{FOV}}$$

- Then calculate (by using the thin-lens equation) and adjust the imaging system assembly for a +200 mm focal lens (be careful so that the focus of each laser beam is always in front of the corresponding camera).
- In order to achieve a distance (L) of 10mm (see Figure 3.4) move each CCD camera towards [Why?] imaging lens (L3) at a displacement of about $S_{2_old} - G \cdot S_1$.
- In order to determine the spatial resolution of the imaging system ($\mu\text{m}/\text{pixel}$) use the magnification factor (G) you calculated.

4.5 Capture the reference image(s)

The active menu that appears on the remote control pad should be "Pk 1".

- Press the button "OP" (on the remote control pad) to start laser operation.
- Press and release the button "SEL" (on the remote control pad) 2-3 times to give start and test for pulses packet (single pulse in our case).
- In order to give start for image capture ("Extended shutter" = 10,000,000 μs), press the "single" button " $\triangleright |$ " (on the virtual control panel of each camera) by using the left click on mouse. Quickly repeat this procedure for each active CCD camera.
- Press and release the button "SEL" to give start for single pulse and then wait for the capture time interval to expire.
- Press the button "OP" (on the remote control pad) to stop laser operation.
- Save the image(s) as ref_w5um_delayXX_shotYY_55.BMP, where XX is the total optical delay time (0ns, or 7.8ns, or 14.3 ns), YY is the #number of the experimental shot and 55 is the crossing angle.

4.6 Fill the spark gaps of the Marx Bank

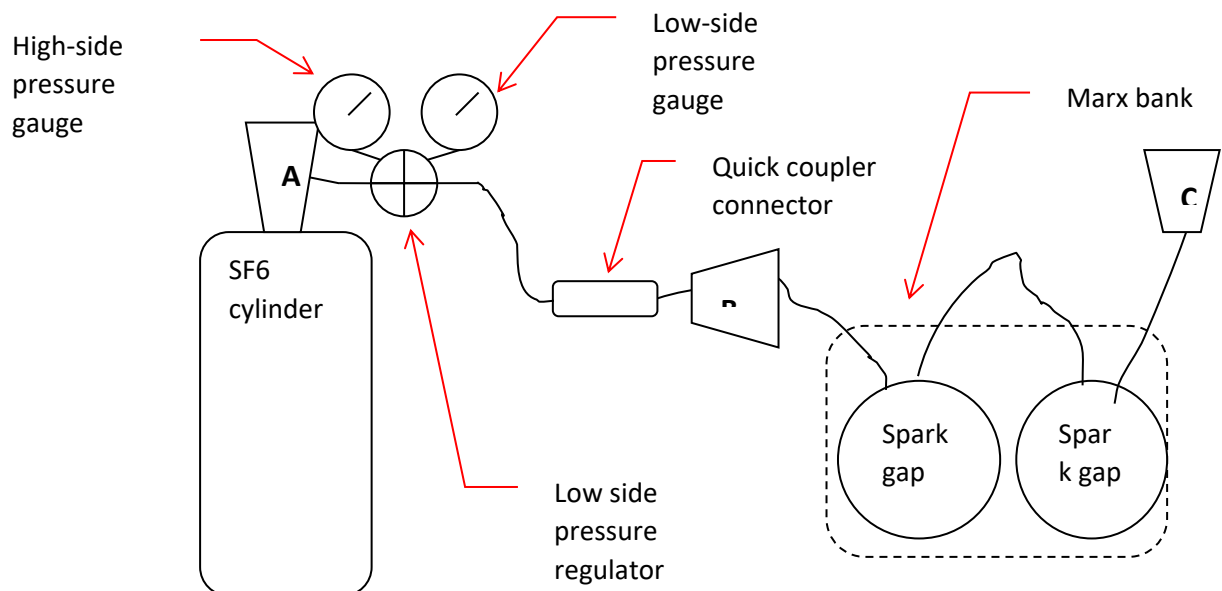
Attention please: Don't turn the valve of the pressure regulator

- Open (turn anticlockwise) the A-valve. B- and C-valves should be already closed (handle of the ball valve must be perpendicular to the hose axis (flow) when closed).

- In order to replace the gas in the spark gaps, open the B- and C-valves (the handle must lie flat in alignment with the flow) and wait for a few seconds. Then close the C-valve.
- Close (turn clockwise) the A-valve. Adjust the gas pressure to a value about 1.3 Bars (read on the low-side pressure gauge) by using the C-valve.
- Close the B-valve and then disconnect the quick coupler connector.

4.7 Fill the self-breaking switch

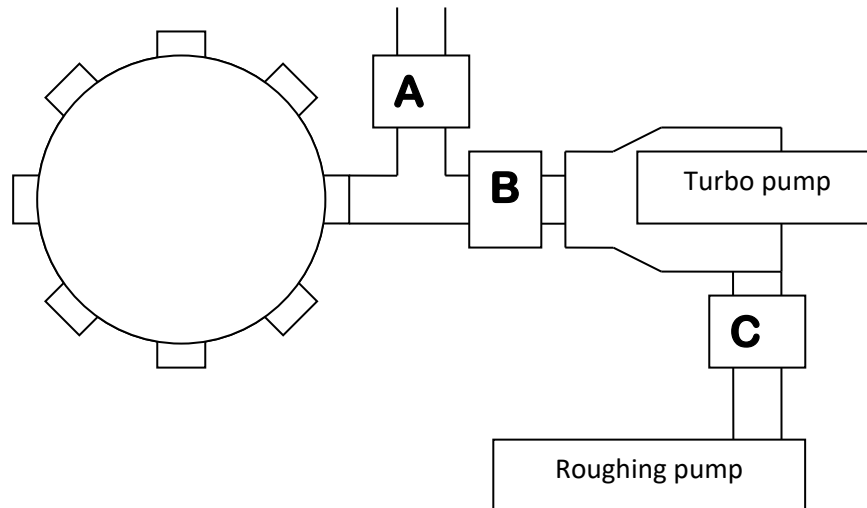
- Use the quick coupler to connect the outlet hose of the SF₆ cylinder together with the inlet hose of the self-breaking switch.
- Repeat all the steps (except the last one) you did for the sub- procedure -5.



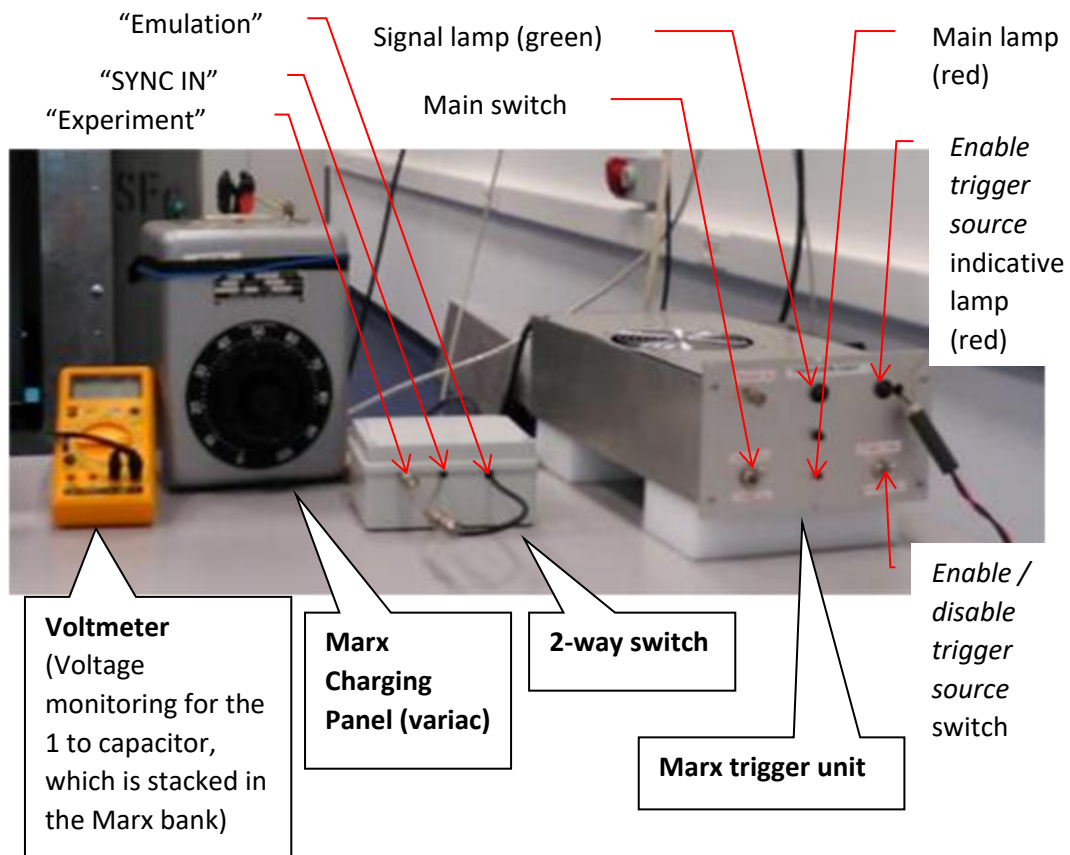
4.8 Set up vacuum in the chamber

- Turn the vacuum gauge on and wait for the warm-up time to be expiring (wait for the pressure to reach a value of 1000 mbar).
- Close the chamber with the joint and the cover. All ports of the chamber must be closed.
- Close (turn clockwise) the A-valve. B- and C-valves should be already closed.
- Turn on the roughing pump.

- Open B- (pull up the black colored piston) and C- (turn anticlockwise) valves.
- Wait for the pressure to reach less than 5×10^{-2} mbar.
- Turn the turbo-molecular pump box on by using the rear switch. Wait for the four lamps to turn off.
- Press the "Start/stop" button. The lamp turns on.
- Wait for the pressure to reach less than 5×10^{-4} mbar.



4.9 Fire the Marx Bank



The active menu that appears on the remote control pad should be "Pk 1".

- Set the oscilloscope to trigger once (single- shot acquisition) by pressing the “single” trigger button.
- Press the button “SEL” together with “ Δ ” (on the remote control pad) to select “Home” menu (display looks like “XX \rightarrow YYYm”, here: XX -amplification level and YYY-reading of energy meter in mJ) and then switch the amplification system of the laser off by simultaneous pressing buttons “ Δ ” and “ ∇ ” (XX-amplification level indicator starts to blink).
- Press the button “OP” (on the remote control pad) to start laser operation.
- Turn the left (main) switch of the Marx trigger unit on (main lamp must turn on with a red color) and wait for the warm-up time to expire (should be five minutes long), then under normal conditions the signal lamp must turn on with a green color.

- Turn slowly and clockwise the turning button of the Marx Charging Panel. The read values on the voltmeter LCD at the right increase. Note that values are divided by a factor of 1/100. So "100 V" indicates a voltage of 10 kV.

When a 34 kV (340 V on the LCD) voltage is reached:

- Switch the amplification system of the laser on by simultaneous pressing buttons "△" and "▽" (XX-amplification level indicator stops to blink), and then press the button "SEL" together with "▽" to select "Single-shots" menu.
- Press and release the button "SEL" (on the remote control pad) 2-3 times to give start and test for pulses packet (single pulse in our case).
- Relay the 2-way switch by changing the connection of the "SYNC IN" cable with "emulation" terminal to with the "experiment" terminal.
- Turn the "enable/disable triggering source" switch of the "Marx trigger" unit into the "Enable" position (the corresponding indicator must be turned on with a red color).
- In order to give start for image capture ("Extended shutter" =10,000,000 μs), press the single button "▷|" (on the virtual control panel of each camera) by using the left click on mouse. Quickly repeat this procedure for each active CCD camera.
- Quickly turn the turning button of the Marx Charging Panel anticlockwise to zero.
- Press and release the button "SEL" (on the remote control pad) to give start for a single pulse. The discharge creates a lightning and a short but intense noise.
- Press the button "OP" (on the remote control pad) to stop laser operation and then wait for the imaging capture time interval to expire.
- Save the image(s) as shot_w5um_delayXX_shotYY_55.BMP, where XX is the total optical delay time (0 ns, or 7.8 ns, or 14.3 ns) and YY is the #number of the experimental shot.
- Turn the "enable/disable triggering source" switch of the "Marx trigger" unit into the "Disable" position (the corresponding indicator must be turned off).
- Turn the left (main) switch of the Marx trigger unit off.
- Relay the 2-way switch by changing the connection of the "SYNC IN" cable with "experiment" terminal to with the "emulation" terminal.
- Save all the displayed waveforms into corresponding files for binary and ASCII data format by using a suffix file name as "_w5um_shotXX_55", where XX is the #number of the experimental shot.
- Print the screen image to a file by using a file name as "w5um_shotXX_55".

5. Experimental results analysis

5.1 Voltage & current monitoring

- I. In order to describe the electrical behavior of the x-pinch device (i.e. PFL charging phase,..) analyze the screen image of the oscilloscope.
- II. Moreover, measure the time interval for each individual phase by using the build-in cursors of the oscilloscope. In addition, determinate the rise time (kA/ns) of the current.
- III. Comment on the shape of the waveforms (i.e. linear, constant rate,...).
- IV. Calculate the peak value of the PFL voltage by using a Cprobe capacitance of 3.5 pF and a terminating resistance of 50Ω.
- V. Calculate the peak value of the total (Note: total current is four times the current flowing through one post) load current by using a Lr self-inductance of 1.5 nH.
- VI. Check the validity of the assumption that the probes measure the time derivative (d/dt) of the signals by setting the d/dt as 4/T, where T should be considered the period of the spectral component with the maximum frequency of each specific signal.

5.2 Optical probing

- I. Use an image processing program (e.g. ImageJ) to measure on the shadowgrams the size (height and width) of selected plasma structures, namely the jets, the legs, the plasma electrodes, the mini-diode (if any), and the central z-pinch column of the x-pinch load. Then, calculate the effective average rate of the plasma expansion (and/or compression) for these above structures.
- II. Analyze the waveform of the PIN diode that measures the optical probing captured time moment in order to determine the timing(after the start of the current) of the shadowgrams were taken.
- III. Calculate the areal electron density along a straight line (1D) that transverse a plasma streamer modulation you choice.

5.3 Time-resolved soft x-ray measurement

- I. Check the waveform of the filtered PIN diode for the proof of a successful pinching, and if any, measure the time that appears after the start of the current.
- II. Determine the energy bins of the x-ray flow measurement.



5.4 X-ray imaging

- I. Study the results obtained using the slit step-wedge camera to identify various emitting regions. Compare the hardness of radiation that emitted from these different regions and comment on the spatial structure of the X-pinch load.
- II. Analyze the results obtained using the point projection radiography to plot the areal density of the step-wedge filter as a function with the optical density of the radiogram as well as the its fitting curve and to determine the averaged (select 5 points) areal density along the axis of symmetry of the test object (Al-wire with a mass density of 2.7 gr/cm^3) using the fitting curve you calculated. Then calculate the diameter of this test object.

References

1. Burdiak, G. C., et al. "Cylindrical liner Z-pinch experiments for fusion research and high-energy-density physics." *Journal of Plasma Physics* 81.3 (2015).
2. "Z-Pinch Inertial Fusion Energy". *Fire.pppl.gov*. Retrieved 2015-06-20.
3. Lebedev, S. V., et al, "Laboratory Astrophysics Experiments with Z-Pinches", the 7th International Conference on Dense Z-Pinches, Alexandria, Virginia, USA (2008).
4. Douglass, J.D., "An Experimental Study of Tungsten Wire-Array Z-Pinch Plasmas Using Time-Gated Point-Projection X-Ray Imaging ". PhD thesis, Cornell University, (2007).
5. Shelkovenko, T. A., S. A. Pikuz, and D. A. Hammer. "A review of projection radiography of plasma and biological objects in X-Pinch radiation." *Plasma Physics Reports* 42.3 (2016): 226-268.
6. Song, Byung Moo, et al. "X pinch x-ray radiation above 8 keV for application to high-resolution radiography of biological specimens." *IEEE Transactions on Nuclear Science* 51.5 (2004): 2514-2519.
7. Beg, F. N., et al. "Compact X-pinch based point x-ray source for phase contrast imaging of inertial confinement fusion capsules." *Applied physics letters* 89.10 (2006): 101502.
8. Aranchuk, Leonid E., Jean Larour, and Alexandre S. Chuvatin. "Experimental study of X-pinch in a submicrosecond regime." *IEEE transactions on plasma science* 33.2 (2005): 990-996.
9. Hammer, D. A., et al. "X-pinch soft x-ray source for microlithography." *Applied physics letters* 57.20 (1990): 2083-2085.
10. Lebedev, S. V., et al. "Effect of discrete wires on the implosion dynamics of wire array Z pinches." *Physics of Plasmas* 8.8 (2001): 3734-3747.
11. Pikuz, S. A., T. A. Shelkovenko, and D. A. Hammer. "X-pinch. Part I." *Plasma Physics Reports* 41.4 (2015): 291-342.
12. Shelkovenko, T. A., et al. "Accelerated electrons and hard X-ray emission from X-pinches." *Plasma physics reports* 34.9 (2008): 754-770.
13. Gopal, Amrutha, Stefano Minardi, and Michael Tatarakis. "Quantitative two-dimensional shadowgraphic method for high-sensitivity density measurement of under-critical laser plasmas." *Optics letters* 32.10 (2007): 1238-1240.
14. Appartaim, R. K., and B. T. Maakuu. "X-pinch x-ray sources driven by a $1 \mu\text{ s}$ capacitor discharge." *Physics of Plasmas* 15.7 (2008): 072703.



15. Song, Byung Moo, et al. "X pinch x-ray radiation above 8 keV for application to high-resolution radiography of biological specimens." *IEEE Transactions on Nuclear Science* 51.5 (2004): 2514-2519.
16. Shelkovenko, T. A., et al. "Electron-beam-generated x rays from X pinches." *Physics of plasmas* 12.3 (2005): 033102.
17. Pikuz, S. A., T. A. Shelkovenko, and D. A. Hammer. "X-pinch. Part II." *Plasma Physics Reports* 41.6 (2015): 445-491.
18. Pikuz, S. A., et al. "Density measurements in exploding wire-initiated plasmas using tungsten wires." *Physics of Plasmas* 6.11 (1999): 4272-4283.
19. Ivanenkov, G. V., et al. "Formation, cascade development, and rupture of the X-pinch neck." *Journal of Experimental and Theoretical Physics* 91.3 (2000): 469-478.
20. Pikuz, S. A., et al. "Spatial, temporal, and spectral characteristics of an X pinch." *Journal of Quantitative Spectroscopy and Radiative Transfer* 71.2-6 (2001): 581-594.



HELLENIC
MEDITERRANEAN
UNIVERSITY



UNIVERSITÉ
BORDEAUX



Erasmus+

O1 – Annex